LATERAL DYNAMICS OF A MOVING WEB

By

JOHN JARVIS SHELTON

Bachelor of Science
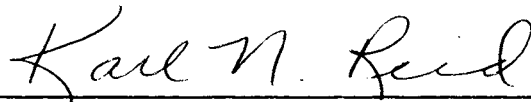University of Oklahoma
Norman, Oklahoma
1957

Master of Science
Oklahoma State University
Stillwater, Oklahoma
1966

Submitted to the faculty of the Graduate College of
the Oklahoma State University
in partial fulfillment of the requirements
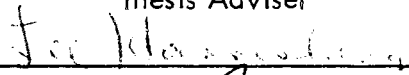for the degree of
DOCTOR OF PHILOSOPHY
July, 1968

LATERAL DYNAMICS OF A MOVING WEB
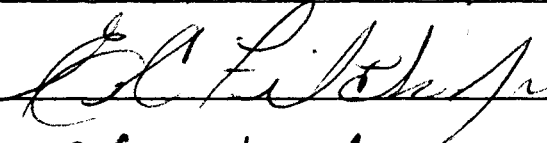
Thesis Approved:

Karl N. Reid
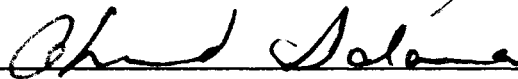Thesis Adviser

Joe Montgomery

E. C. Fitch, Jr.

Ahmed Soliman

N. N. Durham
Dean of the Graduate College

ACKNOWLEDGEMENTS

This thesis, because of its unusual subject matter and the circumstances under which the work was of necessity done, would have been impossible without the close working relationship with my committee. The understanding, encouragement, and direction of the committee members has been indispensible. Dr. Karl Reid particularly spent long hours of conscientious work as the thesis adviser. Dr. E. C. Fitch's encouragement and interest, particularly in the Automatic Controls aspect of the work, has been very helpful. Dr. Lee Harrisberger, despite his demanding schedule, offered advice which contributed a great deal to the final result. Dr. A. E. Salama's early advice and counseling on pertinent subjects of study for the mechanics analysis, as well as his later careful attention to the details of analysis, were indispensible. I sincerely appreciate the efforts of the committee members.

Fellow employees at Fife Corporation who offered support and encouragement are too numerous to mention, but I particularly appreciate the efforts of my supervisor, Bruce Feiertag, for his faith in the work, and his support even under trying circumstances. Others who particularly contributed were Rodney Owen, who finalized the drawings and graphs and not only did the detail design of the web research machine but contributed many important ideas; Donald Branum and Robert Long, both of whom contributed careful craftsmanship and advice without which the research machine would not have been successful; and Martha Denham, who patiently and carefully typed both the rough draft and the final copy. The help of all at Fife is greatly appreciated.

The patience and understanding of Rodessa and David during four difficult years is sincerely appreciated.

iii

TABLE OF CONTENTS

LIST OF TABLES

LIST OF FIGURES

LIST OF SYMBOLS

A	cross–sectional area of the web
A	a constant (Chapter V only)
b	as a subscript, denotes bending without consideration of shear
B	a constant (Chapter V only)
C	a constant
C	distance from pivot to actuator of center-pivoted steering guide
C_1, C_2, C_3, C_4	constants of differential equations, dependent upon KL, or K_eL and nT/AG
D	as a subscript, denotes a condition at the point of departure from the contact area
D	a constant (Chapter V only)
D_1	a roller diameter
E	modulus of elasticity (Young's Modulus)
E_r	reduced modulus
E_t	tangent modulus
f_1, f_2	functions of KL, or K_eL and nT/AG, constants in given derivations
f_4, f_5	functions of K_eL and nT/AG, constants in given derivations
g	acceleration of gravity
g_1, g_2	functions of K_eL and nT/AG, constants in given derivations
G	modulus of elasticity in shear
h_1	function of K_eL and nT/AG, constant in given derivations
i	$\sqrt{-1}$

I	moment of inertia of the web ($tW^3/12$)
K	a parameter, constant for a given operating condition ($T/EI)^{1/2}$
K_c	curvature factor, a function of KL, or K_eL and nT/AG
K_e	a parameter for considering shear deflection, constant for a given operating condition ($K/\sqrt{1 + nT/AG}$)
K_1, K_2	functions of pL and qL, constants in given derivations (Chapter V only)
K_v	the equivalent of K, except for modification to account for the effect of inertia on curvature
L	as a subscript, denotes a condition at the downstream roller
L	the length of a free span of a web
L_1, L_2, L_3	lengths of specific free web spans
m	as a subscript, denotes maximum value (Chapter V only)
M	bending moment in the web
MR_{tr}, MR_{ro}	moment ratios for translation and rotation of the end of the web (comparison of a web with mass to a massless web)
n	a stress-averaging factor, equal to 1.2 for a web
n	a function of web mass per unit length, frequency of vibration, and EI (Chapter V only)
N	shear force normal to the elastic curve of the web
o	as a subscript, denotes a condition at the upstream roller
p	a function of K and n, constant in given derivations (Chapter V only)
q	a function of K and n, constant in given derivations (Chapter V only)
Q	shear force normal to the original web center line
R	radius of curvature
R	roller radius
s	as a subscript denotes the effect of shear only

S	Laplace transform operator
S_1	average tension (T/tW)
t	web thickness
t	time
t	as a subscript, the total effect of bending and shear
T	total (resultant) web tension
T_1, T_2, T_3	time constants of specific web spans
V	velocity of web travel
w	side force on the web per unit length
w	weight of the web per unit length (Chapter V only)
W	web width
W_4	a parameter used for vibration analysis (Chapter V only)
x	distance parallel to the original center line of the web
y	lateral web deflection from its original position
z	lateral position of a roller, or actuator position
β	angle of the arc of lateral slippage
θ	slope of the elastic curve
θ	angle between web and roller (Chapter III only)
θ_r	roller angle
μ	coefficient of friction
π	3.1416
ρ	density (weight per unit volume)
τ	transport time lag
ϕ	an angle
ω	frequency (radians per second)

CHAPTER I

INTRODUCTION

1.1. General Definitions and Background. For this thesis, a "web" is

defined as a strip of material which is either endless or very long in relation to

its width, and very wide in relation to its thickness. This definition includes

products and devices called in various industries by other terms, such as "film",

"belt", "strip", "felt", "foil" and "fabric", although the term "web" is probably

the most widely recognized.

Many materials are partially processed in web form, even though their final

form may require many steps after the web has been cut into small pieces. The

trend is toward further processing in the web form, as exemplified many years ago

in the change from flat plate printing to rotary printing. Such a change, when

successful, usually results in a time saving of several orders of magnitude. There-

fore, the processing of materials processed in web form include paper (both

manufacturing and printing), metal strip, metal foil, plastic films, elastomer sheets

and woven and non-woven fabrics of any kind of fiber.

The above definition of a web includes many endless flat belts used in process

machines. Examples include woven wire, fiberglass and felt belts used in paper-

making machines and a great variety of other manufacturing processes as a carrier

for the product web in its early stages of manufacture. Figure 1.1.1 shows a fabric

printing process which uses a web in the form of an endless belt for processing the

web-type product. Both webs have automatic guides for accurate lateral location.

The schematic representation of the web guide assembly is intended to imply a slider

mechanism on each end of the guide roller, although only one slider assembly is

shown and the connection to the guide roller is not shown. Each slider assembly

may consist, for example, of a block containing linear bushings which slide on

stationary rods.
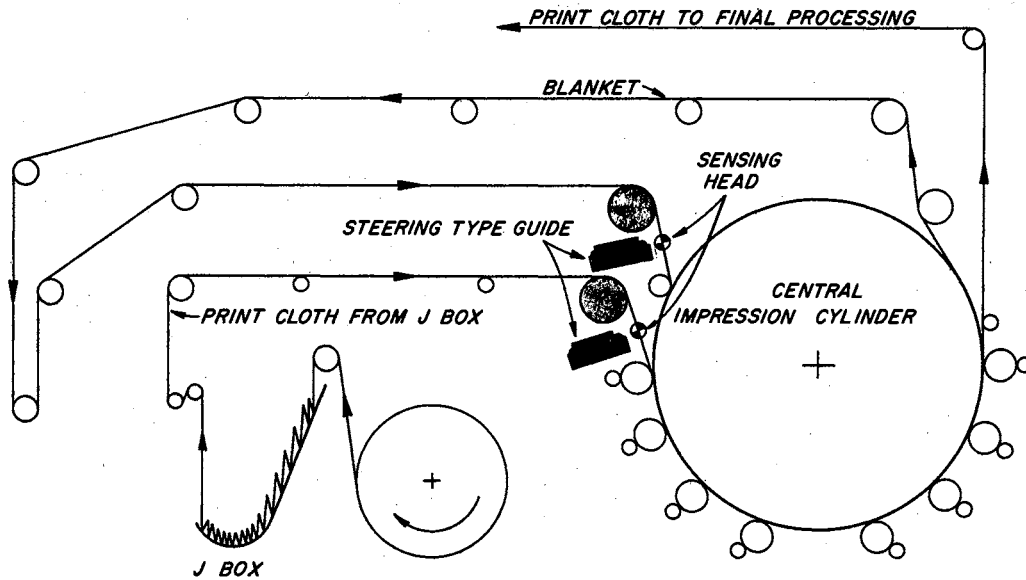
Figure 1.1.1. Cloth Printing Machine With Automatic Web Guides
for Blanket and Cloth

Web guide types may be broadly classified according to their location in

the process line:

(1) Unwind guiding is guiding by shifting the stand which carries an unwind-

ing roll of material which is telescoped or otherwise imperfect, so that the

material is fed off the roll and into the process machine at a fixed point rela-

tive to the machine. Figure 1.1.2 shows a "slitter", a machine for slitting

a web lengthwise into two or more webs, which uses an unwind guide.

(2) Rewind guiding is not actually "guiding" of the web at all, but chasing

of a wandering web by means of a shifting stand which supports the rewinding

roll of material and to which its sensing head is rigidly attached or slaved.
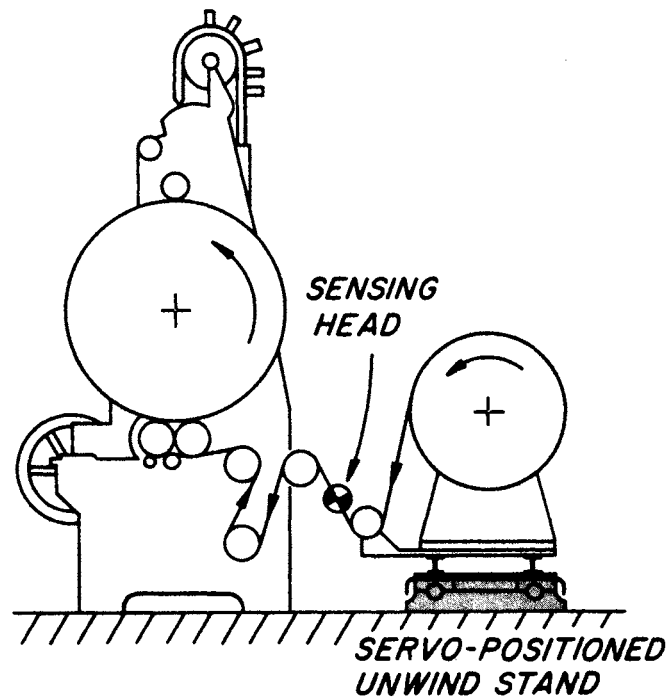
Figure 1.1.2 Shifting Stand for Unwind
Guiding on Slitter.
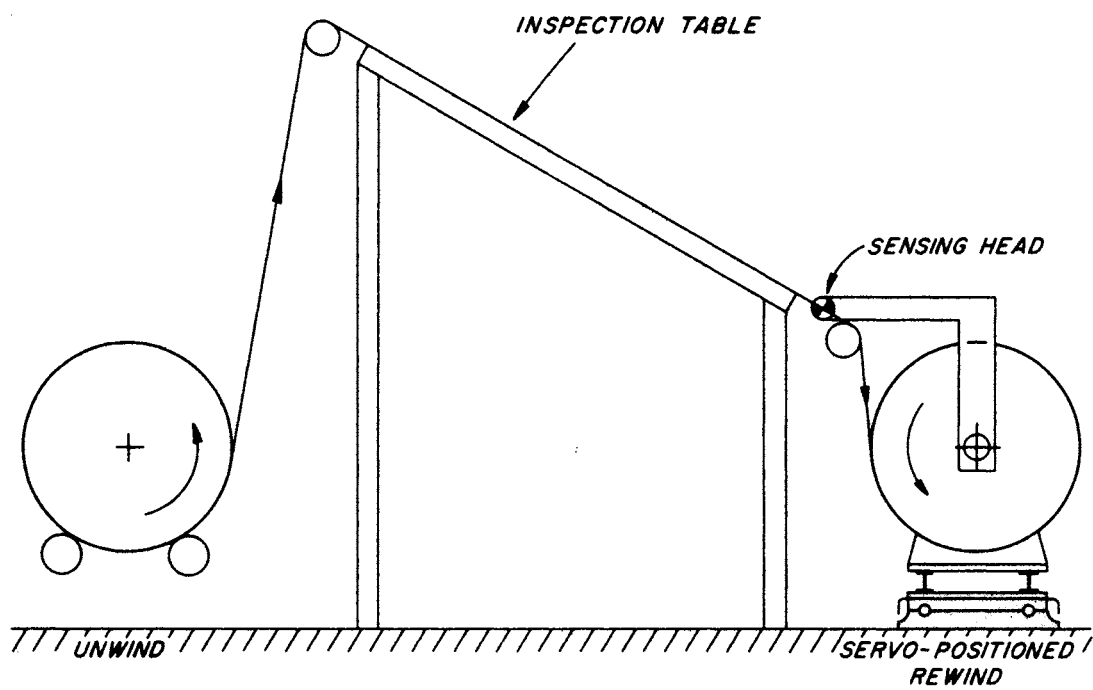
Figure 1.1.3. Shifting Stand for Rewind Guiding
for Textile Inspection Machine.

The result is a smooth edge of the rewound roll of material. Figure 1.1.3 shows a visual inspection machine for textiles which utilizes rewind guiding.

(3) Intermediate guiding is guiding at any point between the unwind and rewind rolls, or at any point along an endless belt.

Unwind or rewind guiding is often necessary because space in the process machine is too limited for an intermediate guide. Figure 1.1.2 shows a very closely coupled machine, on which an intermediate guide could not be readily installed. Particularly in the case of light rolls of material, unwind or rewind guiding may be less complicated and less expensive than intermediate guiding. However, heavy unwind and rewind stands require large, expensive power units, and response is likely to be limited by the dynamics of the positioning device and flexibility of the structure. Another problem often encountered in large rewind guides is difficulty in attaching the sensing head to the stand, because of space limitations. A hydraulic slave system is sometimes used for positioning the sensing head.

A web may need guiding at several points in a process between the unwind and rewind. Obviously, unwind and rewind guiding cannot replace intermediate guiding or vice versa.

Although a web is usually positioned relative to the machine by an intermediate guide, a web guide and perhaps also a servo control can be eliminated in certain laminating operations if one web is allowed to wander and the second web is then positioned relative to the wandering web. Such an installation is shown in Figure 1.1.4.

Intermediate guides may be further classified as servo-controlled and self-powered. Guides for conveyor belts or other strong webs can be successfully powered by the web. Guides which tend to correct errors by their own tendency to shift or deflect when an error occurs have been tried extensively, and have enjoyed a measure of success, particularly in guiding of short endless belts.
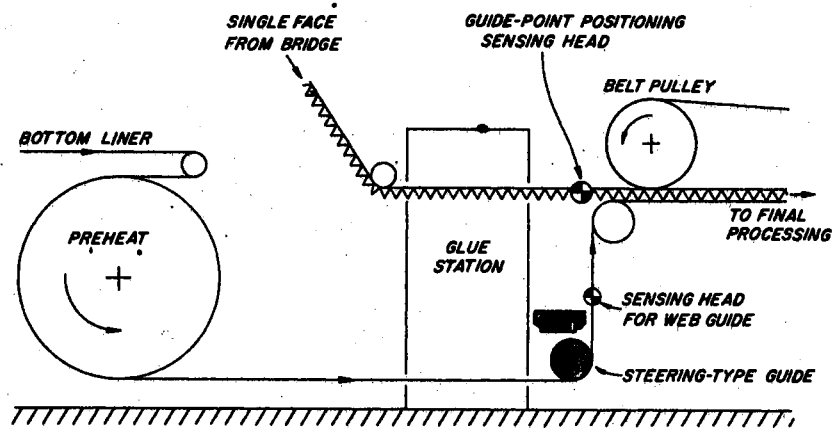
Figure 1.1.4. Positioning One Web With a Command
From Another Web in Glueing of
Corrugated Boxboard.

Angled guides which nip the two edges of the web and which impart their guiding action by varying the nip pressure or by changing the angle of the guide, have been widely applied to textiles. Some edge-nip guides have been powered by the web and some have used external power, such as compressed air. A compressed air-operated edge-nip guide is described in the patent of Snyder, Alexeff and Richards (20).

An interesting intermediate web guide which uses servo-positioned "dead bars" instead of rollers is shown in Figure 1.1.5. Such a guide is described in the patent of Crafts (4). The dead bar guide has the advantage of providing distortion-free guiding with very short entering and exiting spans. The guide causes a great increase in tension unless the web can be floated on a cushion of air. Many textile and paper processes use 45-degree dead bars (turn bars) to change the direction of a web by 90 degrees, as shown in Figure 1.1.6. Intermediate guiding can be accomplished by shifting the turn bar, but the dynamics of such a guide have not been studied.

The most common and most generally satisfactory intermediate web guides are servo-positioned rollers which extend across the entire width of the web. It is advantageous to classify such guides as "steering guides" and "displacement guides". A
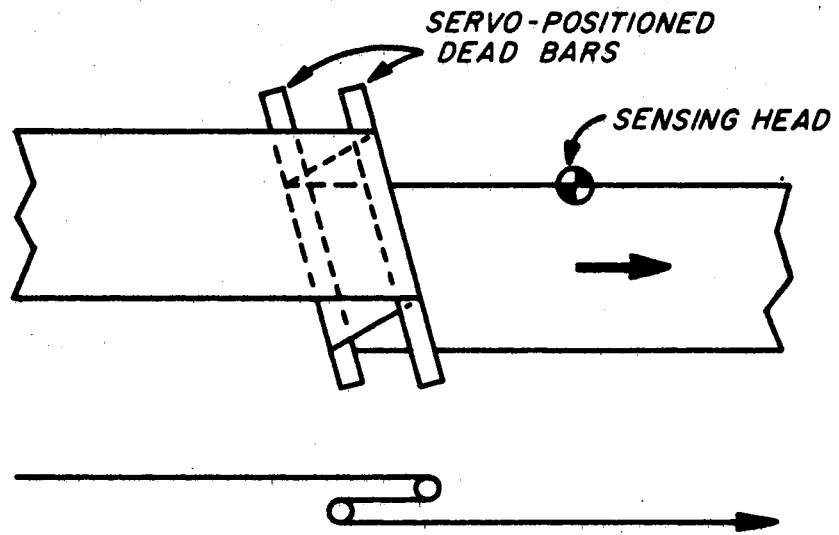
Figure 1.1.5. Dead-bar Web Guide.
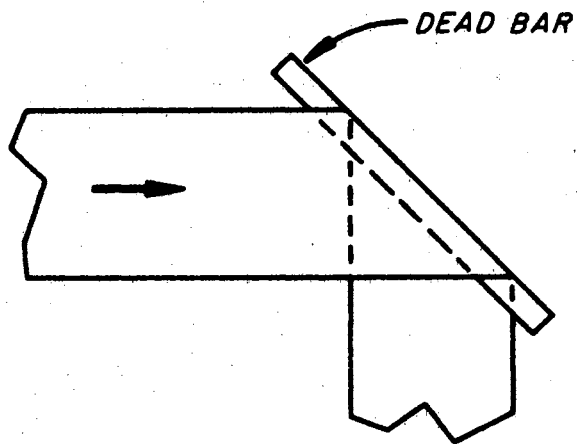
Figure 1.1.6. Dead-bar for Changing
Web Direction.

steering guide as shown in Figure 1.1.7(a) is a shifting roller or set of rollers which imparts its steady-state correction because of non-parallelism between the guide roller or rollers and the previous roller. Its guiding is caused by the tendency of a web to align its entering span perpendicularly to a given roller. The consequent bending of the web can cause yielding, tearing, or wrinkling unless a long entering span is provided. A displacement guide (see Figure 1.1.7 (b)) could be physically identical to a steering guide, but is installed so that the plane of guide motion is perpendicular to the entering span of the web. Therefore, the guide is always paral-lel to the previous roller when viewed into the entering span. The distortion of the web in the entering span is much less severe than for a steering guide; consequently, the entering span can be relatively short.

Unless stated otherwise throughout this thesis, the terms "web guide" and "guide" refer to a servo-controlled cylindrical roller or set of rollers extending across the entire width of the web.

Figure 1.1.8 shows that a web guide may be a combination steering and dis-placement guide. The figure defines the effective spans of steering and displacement. Usually, a guide is predominantly either of the steering or displacement type, because the roller diameter of a guide intended as a steering guide is usually small in relation to the long entering span required, and because the expensive structure required for a displacement guide discourages the usage of displacement guides except where limited space dictates their usage. If a displacement guide were to be installed such that significant steering is accomplished, a long entering span would be required, so that one could have originally used a cheaper steering guide. A guide may some-times be chosen as either the steering or displacement type entirely on the basis of the amount and shape of the space available for the guide.

Figures 1.1.9 and 1.1.10 show process lines on which it was desirable to guide the web as it left an oven, in one case to ensure proper web alignment in the die
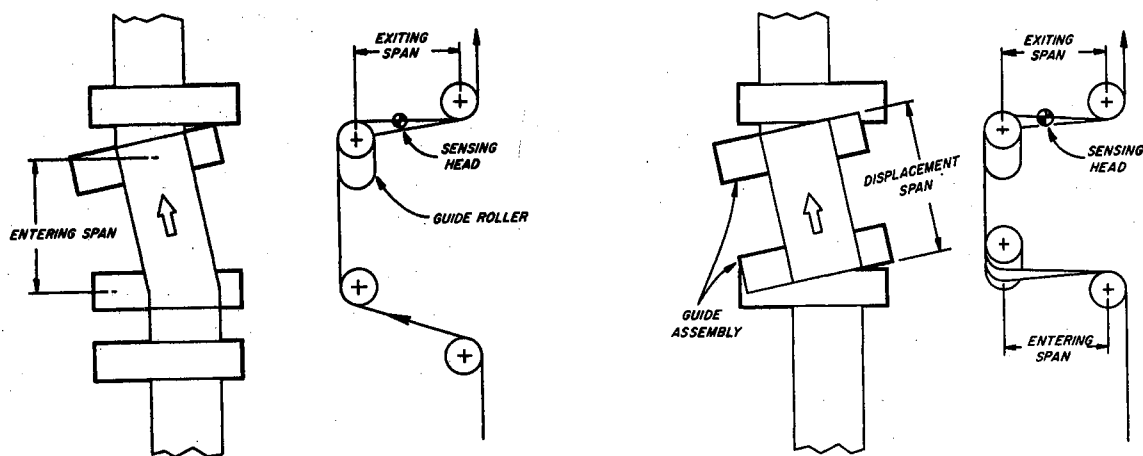
(a) Steering Guide   (b) Displacement Guide

Figure 1.1.7. Basic Types of Servo-Positioned Cylindrical-Roller
Web Guides.
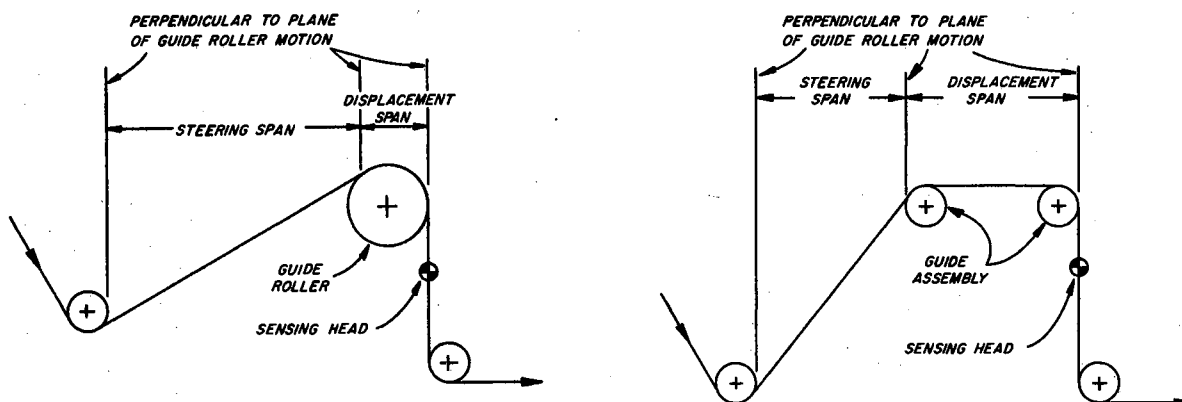
(a) Single Roller   (b) Two-Roller Assembly

Figure 1.1.8. Effective Guiding Spans of Steering and Displacement.
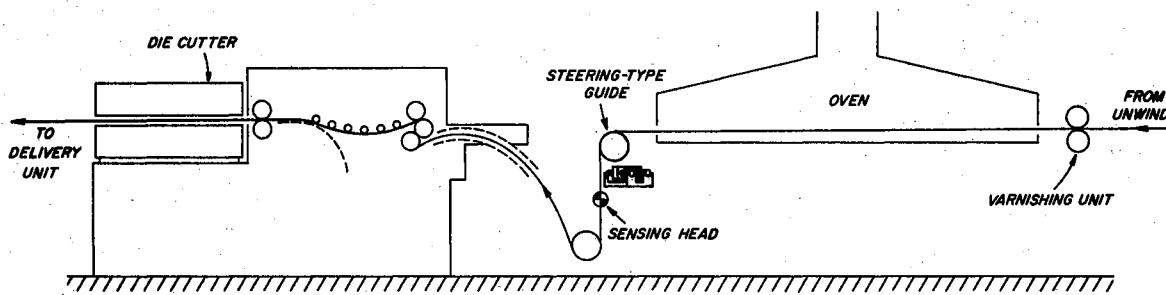
Figure 1.1.9. Die Cutter With Steering Guide at Exit From Oven.
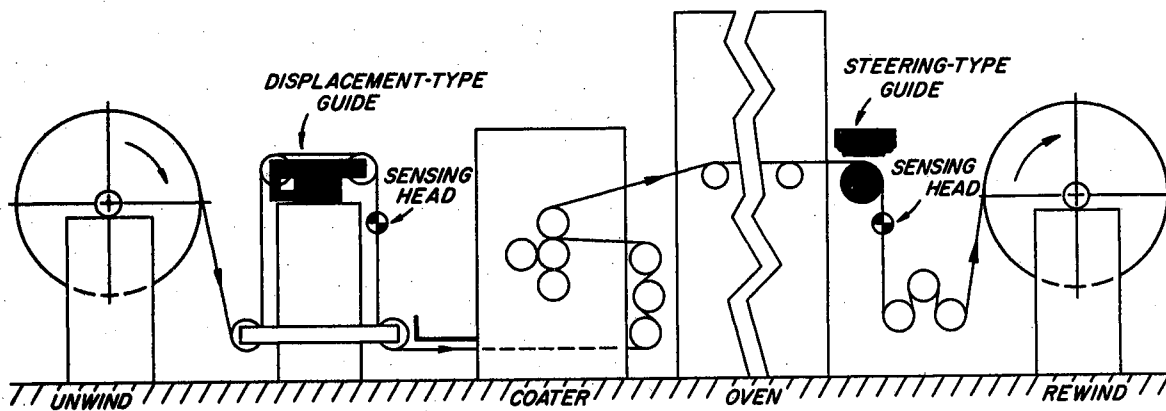
Figure 1.1.10. Web Coating Line With Steering and Displacement Guides.
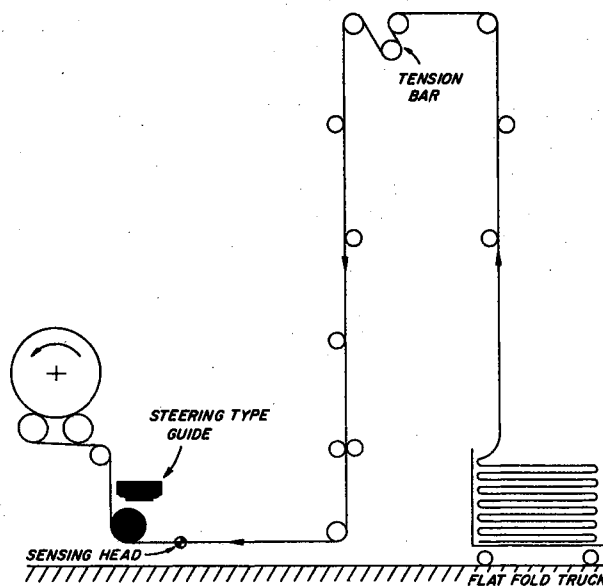
Figure 1.1.11. Textile Rewind Machine With Steering Guide.

cutter and in the other case to ensure a smooth rewound roll of material. Steering-type guides utilized the long span in the ovens for guiding and fed the web down the process line with no excess of rollers and no difficult threading arrangement. Note, however, in Figure 1.1.9 that the guide could not be located near the die cutter. Considerable error could accumulate after the guide before the web reached the die cutter.

Another example of a process in which a steering guide was desirable is shown in Figure 1.1.11. The guide was located as close to the rewinding roll as possible, in order to maximize accuracy. Some complicated rewind stands, with drives, roll changing equipment, and other machinery, do not readily lend themselves to rewind chasing.

Another case of a naturally long, straight web span is shown in Figure 1.1.12. In this case, the polyethylene extrusion tower is tall, and the web simply needs to come back to floor level for slitting of the extruded tube into two sheets and for final windup. The long vertical pass provides plenty of span for steering of the web. The rollers along the vertical pass are wrapped so little by the web that they probably have a negligible effect on the guiding.

Figure 1.1.13 shows part of a machine for manufacture of multiwall paper bags. The multiple steering guide assembly requires little additional space beyond that required for the basic machine, and all six plies are guided at a point close to the start of the manufacturing process.

Displacement-type guides permit the web span on the entering side of the guide to be much shorter than for a steering-type guide. But a displacement guide can seldom merely replace an idler roller in the process line, as was the case for several of the previous steering guide examples. Examples in which limited space necessitates displacement guides include the guide into the coater of Figure 1.1.10, and the guides
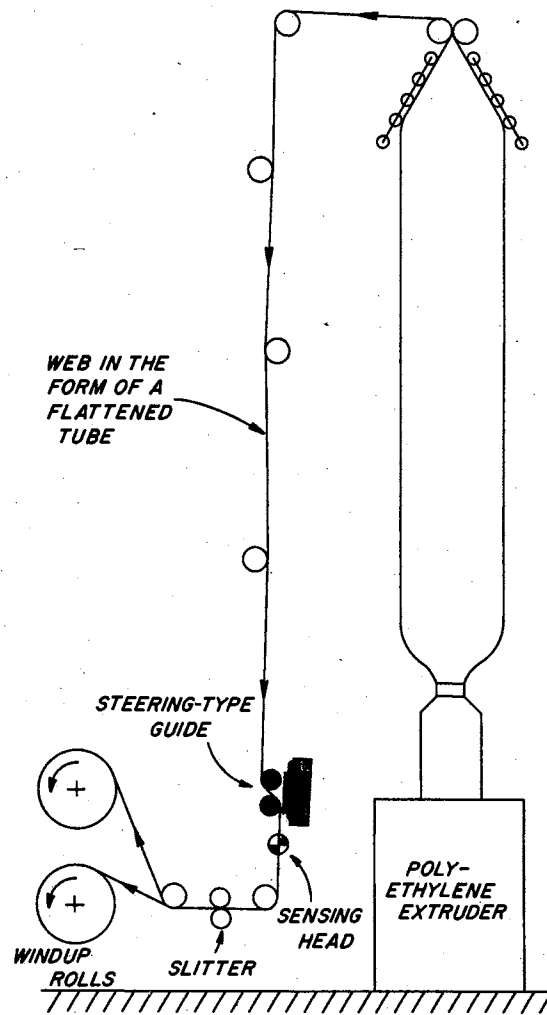
Figure 1.1.12. Polyethylene Extruding Tower
With Steering Guide for Slitter.
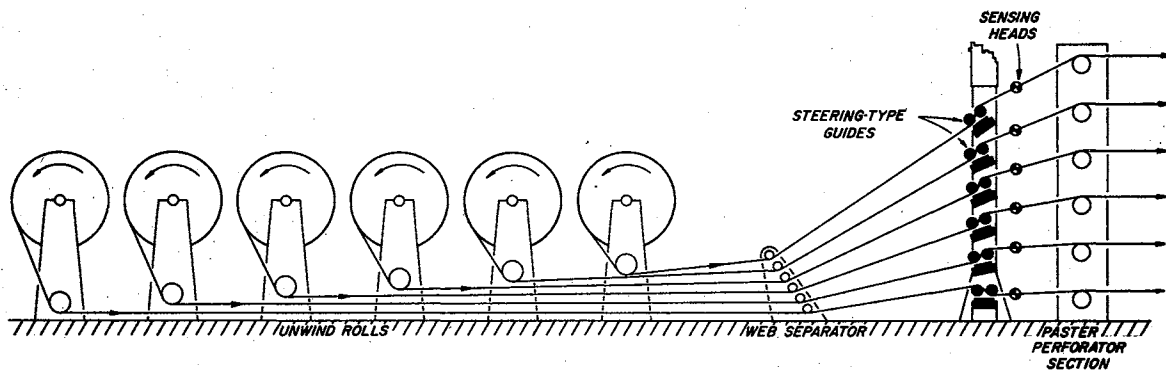
Figure 1.1.13. Steering Guides for Guiding Into Multi-Wall Bag Machine.

on two kinds of business forms presses in Figures 1.1.14 and 1.1.15. A similar space problem is solved with a displacement guide for guiding into printing on a gravure press, as shown in Figure 1.1.16.
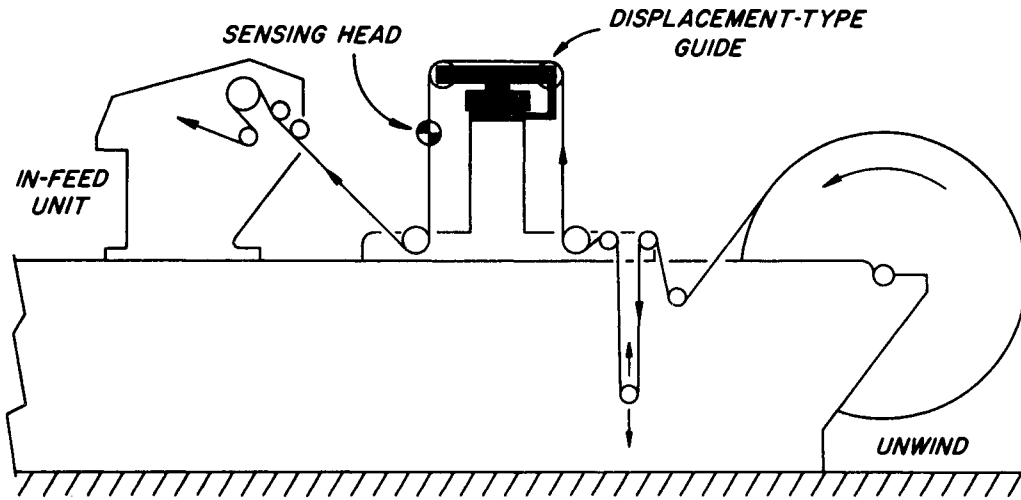
Figure 1.1.14. Business Forms Press With Displacement Guide.
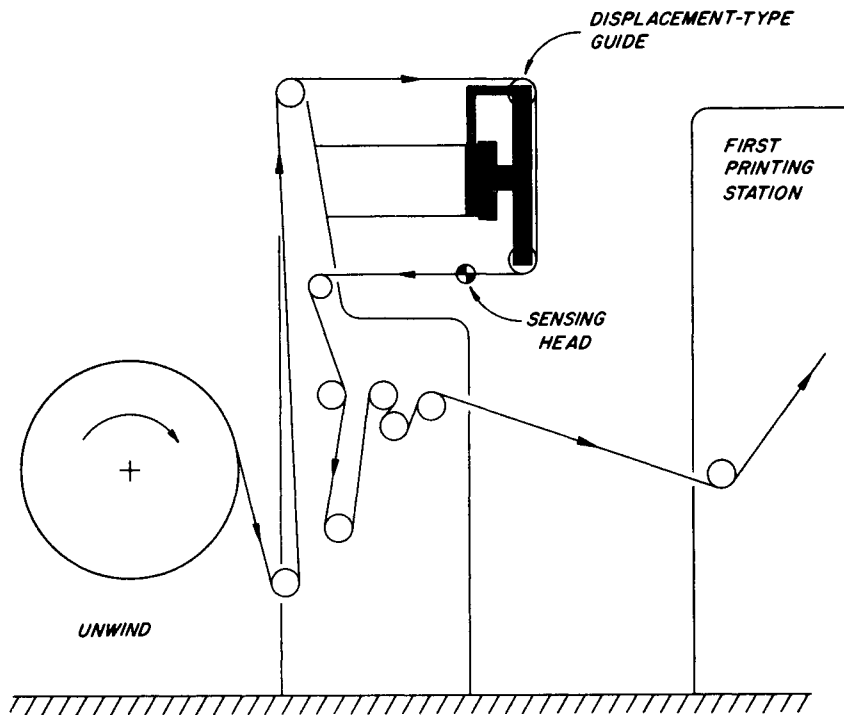
Figure 1.1.15. Business Forms Press With Side-Mounted
Displacement Guide.
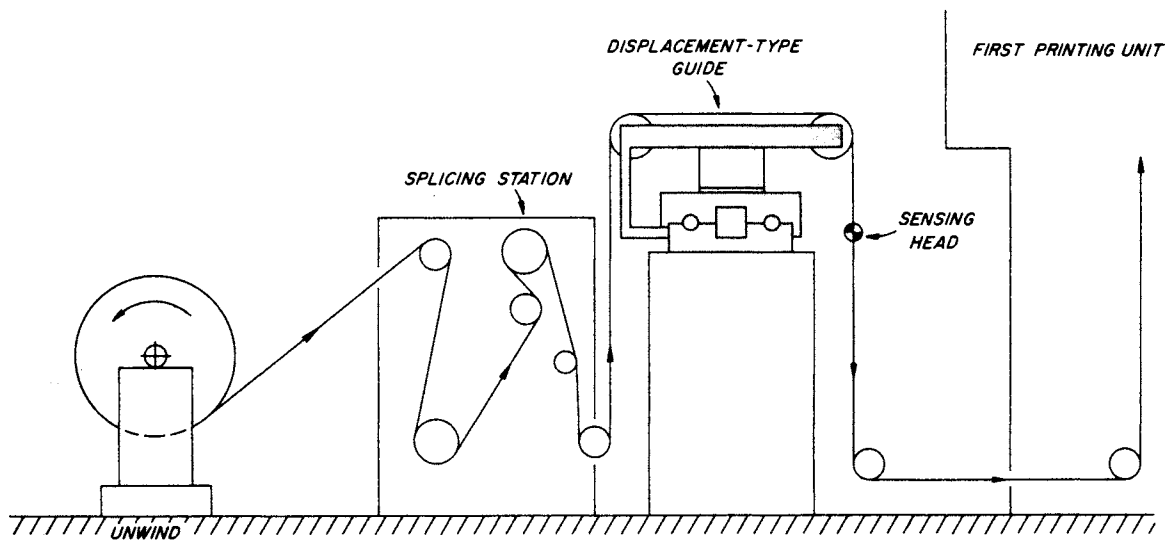
Figure 1.1.16. Gravure Press With Displacement Guide.

Several years ago, the author (18) introduced the terms "static steering factor", "understeering", "neutral steering",and "oversteering" to describe the steady-state behavior of a web guide. The terms seemed particularly appropriate because of the similarity between web steering and automobile steering, for which similar terms are used. However, the word "guiding" should be substituted for "steering" in all the terms if displacement as well as steering guides and combinations thereof are to be included in the definitions. But because this thesis is primarily applicable to steering guides, "steering" will usually be used in the following chapters.

A web processor or web-guide applications engineer would be primarily concerned with the overall static factor; that is, the result of the combination of steering and displacement. The overall static guiding factor is defined as the ratio of steady-state lateral web correction to the lateral displacement of the guide roller, both referenced to the ground, at the point where the web leaves the roller. Therefore, an overall static guiding factor of two means that the steady-state web error corrected by the guide is twice as great as the lateral motion of the guide at the downstream

edge of the contact area between the web and the roller. A static guiding factor greater than unity is overguiding, equal to unity is neutral guiding, and less than unity is underguiding.

For the sake of simplicity and exactness, the following chapters do not consider overall guiding factors. The term "static steering factor" will define the steering factor only in the free span; that is, the ratio between the steady-state displacement of the web as it enters the contact area and the lateral displacement of the roller at the point of entering contact. The difference between this definition and the previous definition is usually insignificant, as web guiding is commonly practiced today.

The "entering span" is the free span of web immediately before the first shifting roller of a guide assembly. The "exiting span" is the free span of web between the last roller on a guide assembly and the next roller, rewind roll, slitter knives, or other process apparatus which grips the web laterally. The "entering roller" is the roller just previous to the entering span, and the "pre-entering span" is the free span of web just previous to the entering roller.

The terms "static" and "steady state" do not mean that the web is not moving longitudinally, but that there is no change in the amount of lateral correction taking place. In other words, the guide is stationary and the web is not moving laterally on the guide. The web is assumed to be moving longitudinally; otherwise, the time constants considered in the dynamic theory would be infinite, and the static condition would not necessarily be the same as the static condition considered in this thesis.

1.2. History and State of the Art of Web Handling Theory. A search of patents, technical catalogs and trade publications revealed very little web handling theory, but provided an interesting history of web guiding practice.

Flat belts which meet the definition of a web have been guided by flanges and yokes for more than a century. Until recent years, strip steel processors depended

upon flanges and edge-contact rollers for intermediate web guiding, but edge damage commonly occurred. Saddle-like plates have been successfully used to "funnel" a highly flexible web into approximate position in applications where the web edge was tough and where a long span was possible where the guiding was desired; final minor corrections were then made with flanges at a point between two rollers.

Crowned pulleys, jointed self-centering rollers, and other self-centering devices have been used with varying degrees of success. It has long been recognized that the centering tendency of a crowned pulley is caused by web curvature, and therefore that a stiff web such as steel cannot usually be guided successfully by a crowned pulley (12). Jointed self-centering devices have been used successfully on endless belts on small duplicating machines, even with wide belts which would be badly distorted by a crowned pulley. A jointed self-centering roller is shown in Figure 1.2.1. Note that the tapered roller halves create centering forces on each side of the web as the roller turns, because of relative lateral motion between the web and the roller. Slow response and other severe problems have limited the success of self-centering devices on continuous webs.
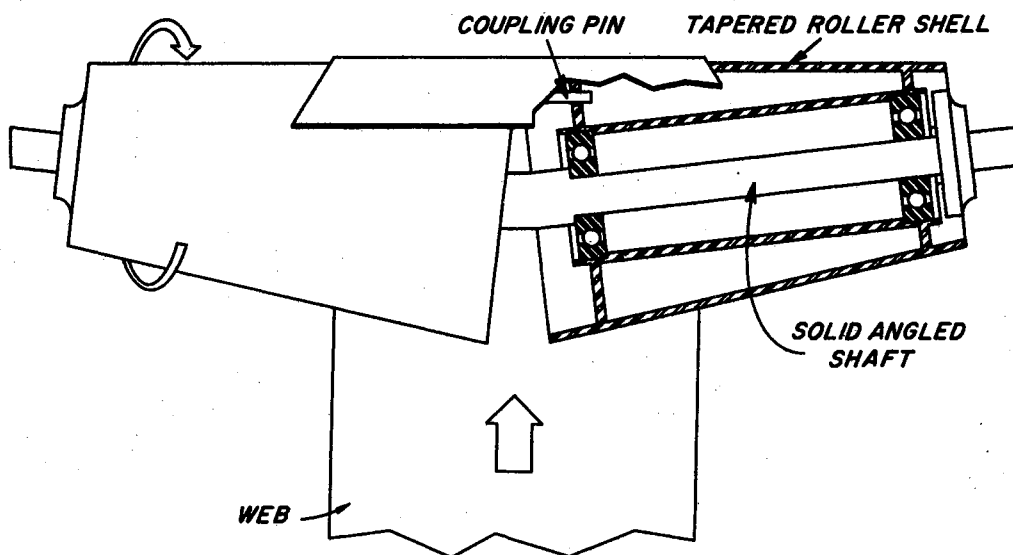
Figure 1.2.1. Jointed Self-Centering Roller.

Lorig (12) in 1950 discussed the steering action of webs on cylindrical, convex, concave, and jointed rollers. His qualitative explanations indicated an understanding of lateral web behavior that few people have achieved, but his paper was completely devoid of quantitative information. He correctly explained that the guiding action of a crowned pulley is caused by web curvature. The amount of curvature or speed of response was not discussed.

According to Amos (2), automatic mill-roll positioners were used first in 1916. The Müller patent of 1934 (15) was for a simple vacuum-piloted hydraulic system for unwind-stand positioning. Servo-controlled intermediate guides apparently date from the Dickhaut patent (6) of 1927, because so-called "Dickhaut guides" were commonly used in the 1940's and 1950's. However, because Dickhaut guides were center-pivoted steering guides (very large overall static steering factor) with a downstream stationary sensing head, no position feedback and no phase lead correction, they continuously hunted at common operating speeds.

Amos (2) reported that "offset-pivoted" web guides (single-pivoted displacement guides) were developed in 1946. However, Markey (14) reported in 1957 that his company, the leader in steel industry guiding, had no displacement guide installations in the steel industry, where the stiff material made steering guides impractical in many applications. Deering (5) and Feiertag (7) revealed that servo-controlled guides, both steering and displacement, have become accepted as a necessity in the steel industry in very recent years, because of higher speeds, thinner strips, and the desire for higher production, less waste, and higher quality.

Stable, accurate servo-controlled steering guides date from the Fife (8) and Wood (24) patents, which were both filed in 1950. Both patents cover guides with mechanisms such that the instant center can be located a distance upstream from the guide. Although the inventors apparently did not understand the fundamental law of web guiding (perpendicularity of the entering span to the guide roller), guides

were installed by trial and error to achieve a reasonably satisfactory static steering factor.

The work of Campbell (3) was more complete .in longitudinal web dynamics (the dynamics of tension and tension control) than in lateral web dynamics. Others, such as Marhauer (13), have made additional contributions to knowledge of tension dynamics. Kouris and his committee (11) found in their study of paper rewind drives that more than fifty processors of paper operated within the same general range of tensile stress, approximately 10 percent of the tensile strength. Continued work in longitudinal web dynamics can be expected to contribute to the knowledge of such parameters as web elasticity, friction, operating tension, and rupture characteristics. Such knowledge is also pertinent to the study of lateral web dynamics.

Some work has been done on the theory of physical properties of webs. Peirce (17) was a pioneer in the derivation of textile properties from models of their weave patterns. Additional work has been done, notably by Adams, Schwarz, and Backer (1). Kellogg and Wangaard (10) developed a correlation between pulp fiber strength, fiber stiffness, sheet density, and sheet properties of paper. A search for analysis or even qualitative understanding of lateral web dynamics reveals an almost unbelievable neglect. An understanding of the static behavior of a web is an essential foundation for a dynamic analysis, but static web analysis has been found to be nonexistent except for the understanding of the static correction of a displacement guide. Web curvature induced by a steering guide has apparently been completely overlooked.

Designers of power transmission belt systems have long recognized that the entering span of a belt must be perpendicular to the axis of rotation of the pulley which it is approaching (9). This fundamental law of web steering was implied by Lorig (12), Campbell (3), Wright (25), and others, but it has not been common knowledge among web processors or builders of web-handling equipment.

The work of Campbell (3) in lateral web dynamics was outstanding but very incomplete. He assumed that a web makes sharp breaks at each roller in a web process line and wrote the corresponding first-order transfer function for web behavior from one roller to the next parallel roller. Later, Sorsen (21) made the same assumption and extended the theory to include a center-pivoted steering roller, but his transfer function for the center-pivoted guide is grossly incorrect. The response of a web on a center-pivoted roller to motion of the roller is a first-order lag, if web curvature is neglected, not an integration as stated by Sorsen.

A large percentage of the first-order dynamic theory of Chapter III of this thesis was done in 1964 and 1965, and was first documented in the unpublished proposal for research for this thesis (19). Some additional results of this thesis, such as the static steering factor concept, were anticipated by the author in References (18) and (19), but certain proposed theories have been discarded. Chapter III, included in this thesis because it has not been published elsewhere and because it provides a foundation for more exact analysis, is far ahead of any published work on web guiding dynamics.

1.3. Important Problems. A knowledge of the lateral static behavior of a web is essential, because one must know if a web will break, wrinkle, or yield under given conditions, and how much correction is accomplished with a given guide displacement.

A knowledge of lateral web dynamics is necessary to accurately predict conditions which could cause web damage, and to ensure optimum stability and accuracy of a web guide control system.

Knowledge of the "critical condition", the condition for which a slack edge occurs, is important, not only to define the domain of linearity, but also because slackness must be avoided when handling some easily damaged materials. However, many steering guides have been successfully installed in situations where a slack

edge often occurs. Therefore, it is desirable to pinpoint the conditions at which a slack edge occurs, and also to analyze the statics and perhaps the dynamics of a web with a slack edge.

Webs often have significant natural curvature (camber), buckles, thickness variations, and other imperfections. Increasing tension usually reduces the effects of imperfections, but tension on a web which has non-symmetrical thickness variations about its center-line causes camber. Figure 1.3.1 shows a web at low tension with buckles due to imperfections, but Figure 1.3.2 shows no buckles in the same web at a higher tension. Camber, though not observable, was probably present with the tension of Figure 1.3.2 because of the non-symmetrical imperfections.

Because camber is a major cause of web errors, there is an urgent need to study the behavior of a naturally cambered web. Such a study would be a great step toward being able to predict the error at a given point downstream from a guide, and thereby to know how many guides are required on a given process line. The accumulated error at a given point downstream from a guide is important in cases wherein it is physically difficult or impossible to locate the guide at the point where guiding is needed, as in Figure 1.1.9.

Long spans of heavy horizontal webs under light tension sag significantly between rollers. Sometimes support rollers break up the span, as shown in Figure 1.3.3, which is a drawing of a steel process line. The entering roller is mounted on a traveling rail car and support rollers are spaced along the rails. Other examples of steering guides with entering spans stabilized or supported by rollers are shown in Figures 1.1.10 and 1.1.12. The effects of the sagging web and the effects of lateral forces of the support rollers on the web would require special study. Other complexities arise from consideration of web velocity and web mass.

Guiding has occasionally been done at the first roller after a free loop, where the tension is only due to the weight of the web. Free-loop guiding analysis

Figure 1.3.1. Web at Low Tension, With Buckles Caused by Imperfections.

Figure 1.3.2. Imperfect Web, With Buckles Eliminated by High Tension.
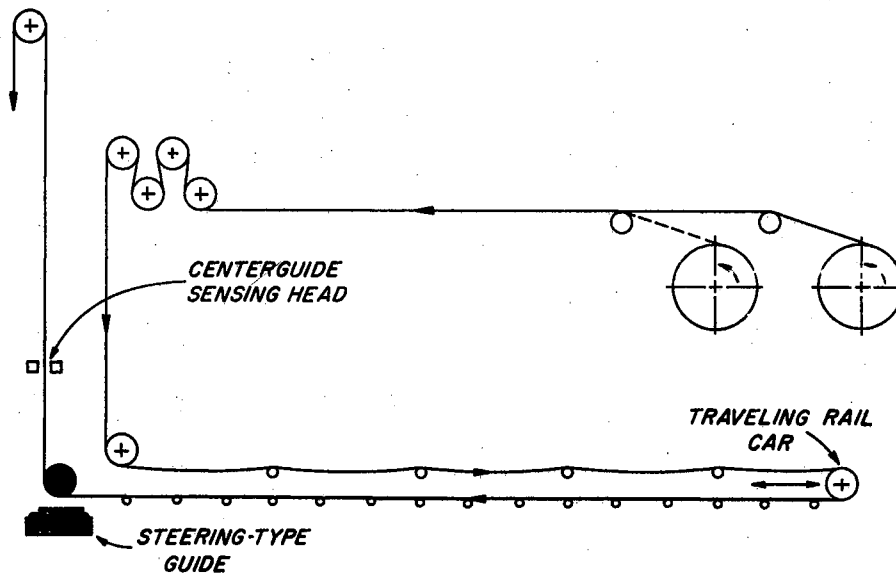
Figure 1.3.3. Steering Guide for Steel Strip With Support Rollers in Entering Span.

would require a derivation and solution of a different differential equation than that for a straight, taut web span.

The side forces required to guide a web are often quite small. The moment in the web at the start of the entering span may be quite large, while the moment just upstream of the entering roller tries to be zero. It is therefore possible to have a situation wherein the web slips circumferentially around the roller at its edges and thereby transfers some moment into its pre-entering span, but enough friction exists near the center of the contact area to locate the web laterally. Such a condition is dangerous if a long pre-entering span exists, because a static instability can result. The stress distribution in and near the contact area needs to be analyzed and experimentally verified, so that the static instability can be avoided.

Unless the entering span is large in comparison to the length of the contact area between the web and the entering roller, an analysis of stresses and strains in the contact area is needed to find the angle of the web at the start of the entering span.

More data than that currently available is needed on materials properties,

particularly of anisotropic materials such as textiles and woven wire. A study similar to the study of Kellogg and Wangaard (10) on paper should be undertaken on felt and other non-woven fabrics, as well as woven wire belts of various weaves. The shear modulus of anisotropic materials varies greatly and is of major importance under certain conditions, and should be included in properties studies of such materials. For homogeneous and isotropic materials the shear modulus is reasonably well defined, always being between one-third and one-half of the Young's modulus.

1.4. Scope of Study. It was necessary to drastically narrow the scope of study from the spectrum of problems discussed in Section 1.3. The thesis is concerned only with the aspect of web guiding judged to be the most useful: The behavior of an initially straight web between parallel or non-parallel cylindrical rollers which extend entirely across the web. The static behavior, the dynamic response of the web to an upstream disturbance, and the dynamic response to a translating and/or rotating guide assembly are studied.

The scope is thus broad enough to apply to unwind and rewind guiding (with the roll of material behaving as a roller), displacement guiding, and steering guiding. However, steering guiding is more complex than the other types because of non-parallelism of rollers, so that most of the examples are of steering guiding.

The thesis generally progresses from simplified cases to more general and more complex cases. As generality is improved, regions of validity of earlier studies are examined.

The static analysis of Chapter II establishes basic techniques of the mechanics analyses of Chapters IV and V. The simplified dynamic analysis method of Chapter III, which neglects materials properties, establishes basic techniques of the web dynamics analyses of Chapters IV and V.

1.5 Assumptions and Justifications. The results of this thesis are limited by several basic assumptions. Most of the common assumptions of beam theory are used,

as well as other assumptions relating specifically to webs.

Except for the study of Section 3.6, it is assumed that the circumferential length of the contact area between the web and the roller is small in relation to the free web span of interest. This assumption is usually valid for a steering guide, but may be incorrect for a single-roller displacement guide, especially if high friction exists and the web has little shear strength.

It is assumed that the correction is small enough that the web edge is never slack. The conditions which assure satisfaction of this assumption are defined in the following chapters.

Web velocity and tension are assumed to be constant, but the results would be valid for cases in which tension and velocity changes occur at low frequencies relative to the important lateral dynamics of the web.

It is assumed that the angle of web wrap or nip pressure and the coefficient of friction between the web and the roller are sufficient to prevent slippage of the web from one span to another. Creep within part of the contact area cannot be prevented, but this assumption specifies that a moment in one span is isolated from the adjacent span, and that lateral breakaway does not occur.

The definition of a web assures that its buckling strength in compression is extremely low. It is assumed that this buckling strength is negligible in comparison to the operating tension. The tension is assumed to be great enough that sagging of the web is very small.

The stress distribution in the web is assumed to be linear. Murphy (16) states that if the radius of curvature divided by the web width is greater than five, linear flexure theory is within 10 percent of the Winkler-Bach curved-beam theory. It is therefore believed that the assumption is satisfactory for current practical applications and operating conditions.

Standard beam-theory assumptions and respective justifications include:

(1) The web is initially straight and uniform. Actual webs are often cambered, but only the position and not the tension distribution is sensed by a servo-controlled guide, in contrast to a self-centering guide, and web error due to camber is automatically corrected.

(2) All deflections are small. This assumption is valid in practical cases, because large deflections would yield, tear or wrinkle thin webs. The maximum correction angle of displacement guides is usually less than five degrees, according to Markey (14). The maximum correction angle of steering guides is usually less than two degrees. The common beam-theory assumption that $(dy/dx)^2$ is small in comparison to unity is valid, as well as the assumption that $\cos (dy/dx) = 1$ and $\sin (dy/dx) = dy/dx$.

(3) The web is homogeneous and uniform. This assumption is never ultimately correct, but is often approximately true. The primary effect on web handling of severe local imperfections is the creation of local buckles and wrinkles, such as those shown in Figure 1.3.1.

(4) A plane section that is normal to the longitudinal axis of the web before deflection remains plane after deflection. Deflection due to shear stresses, if significant, make this assumption invalid, but the approximate method of averaging the shear stresses with the factor "n" as done in this thesis is accepted practice.

Except in Section 2.6, it is assumed that the web is elastic in the range of stresses encountered. This assumption is normally valid for isotropic materials.

CHAPTER II

STATIC BEHAVIOR

An understanding of the static behavior of a web is necessary before its dynamics can be understood. It is necessary that static stability with freedom from wrinkling and tearing be obtained before dynamic behavior is meaningful. Determination of the boundary conditions and subsequent static web analysis lay a foundation for later dynamic analysis and aid in determination of the domain of linear response. This chapter determines the static web shape, stress, and other important measurements.

The two crucial steady-state boundary conditions at the downstream roller are established in this chapter. Later chapters study web dynamics caused by a downstream moment and slope which do not satisfy the static requirements.

The fourth-order differential equations of the elastic curve derived in Sections 2.1 and 2.4 will be solved for specific boundary conditions in the following chapters.

2.1 Elementary Beam Theory Differential Equation and Solution. Except for a velocity effect which will be considered in Section 2.5, the differential equation of the steady-state web elastic curve may be derived from beam theory. The evaluation of the arbitrary constants in the solution depends upon boundary conditions which are justified in Section 2.2. This section is concerned with relatively long free web spans, so that the deflection due to shear stress is negligible. Section 2.4 considers shear deflection.

25

An understanding of all the sign conventions of the mechanics analysis is critically important. The sign conventions shown in Figure 2.1.1 are based on the convention of Timoshenko and Gere (23), and are used for all mechanics analysis.

Equations 2.1.1 through 2.1.5 are essential for establishment of boundary conditions and other derivations. The bending moment is symbolized by M, the normal force by N and the side load per unit length by w in the equations:

$$M = -EIy'' , \qquad\qquad (2.1.1)$$

$$N = -EIy''' \quad \text{(constant I)} , \qquad\qquad (2.1.2)$$
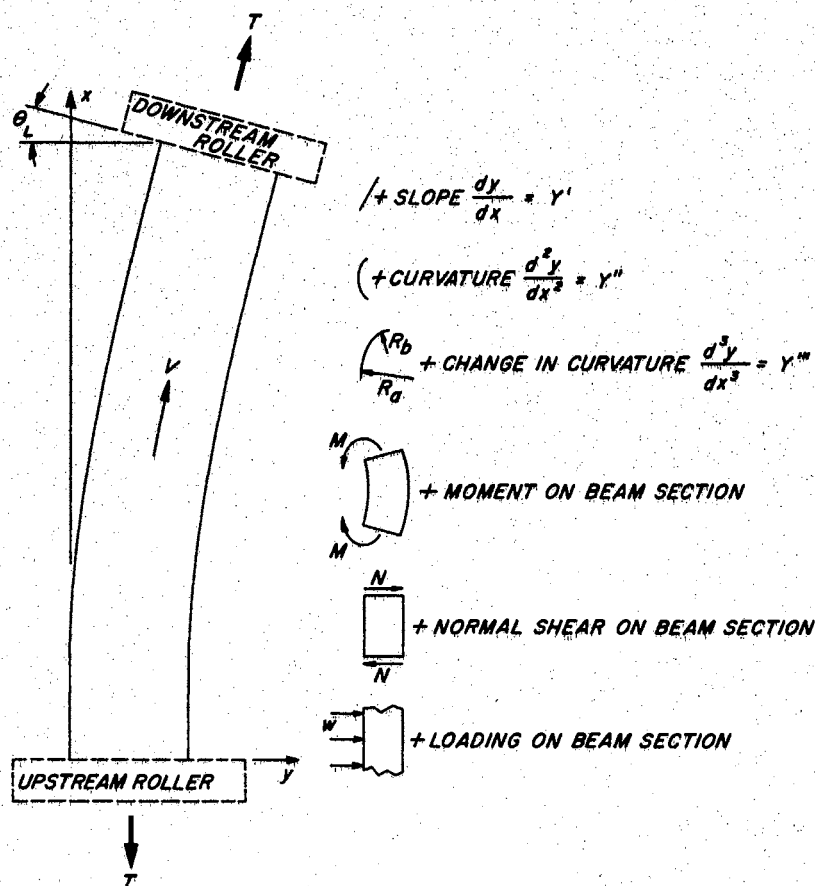
$$N = -E\left[Iy''\right]' \text{(variable I)} , \qquad\qquad (2.1.3)$$

Figure 2.1.1. Sign Conventions for Mechanics Analysis.

$$w = EIy^{iv} \quad \text{(constant I)}, \qquad (2.1.4)$$

and

$$w = E\left[Iy''\right]'' \quad \text{(variable I)}. \qquad (2.1.5)$$

The differential equation of the steady-state elastic web curve in its free span (between rollers) is derived with the aid of Figure 2.1.2, which shows a free web span (a), a horizontal section (b), and a normal section of the web (c). Because all deflections are small, the tension T of (b) and (c) are approximately equal.

If moments are summed about Point 0 of Figure 2.1.2 (b), with clockwise moments positive, it is found that
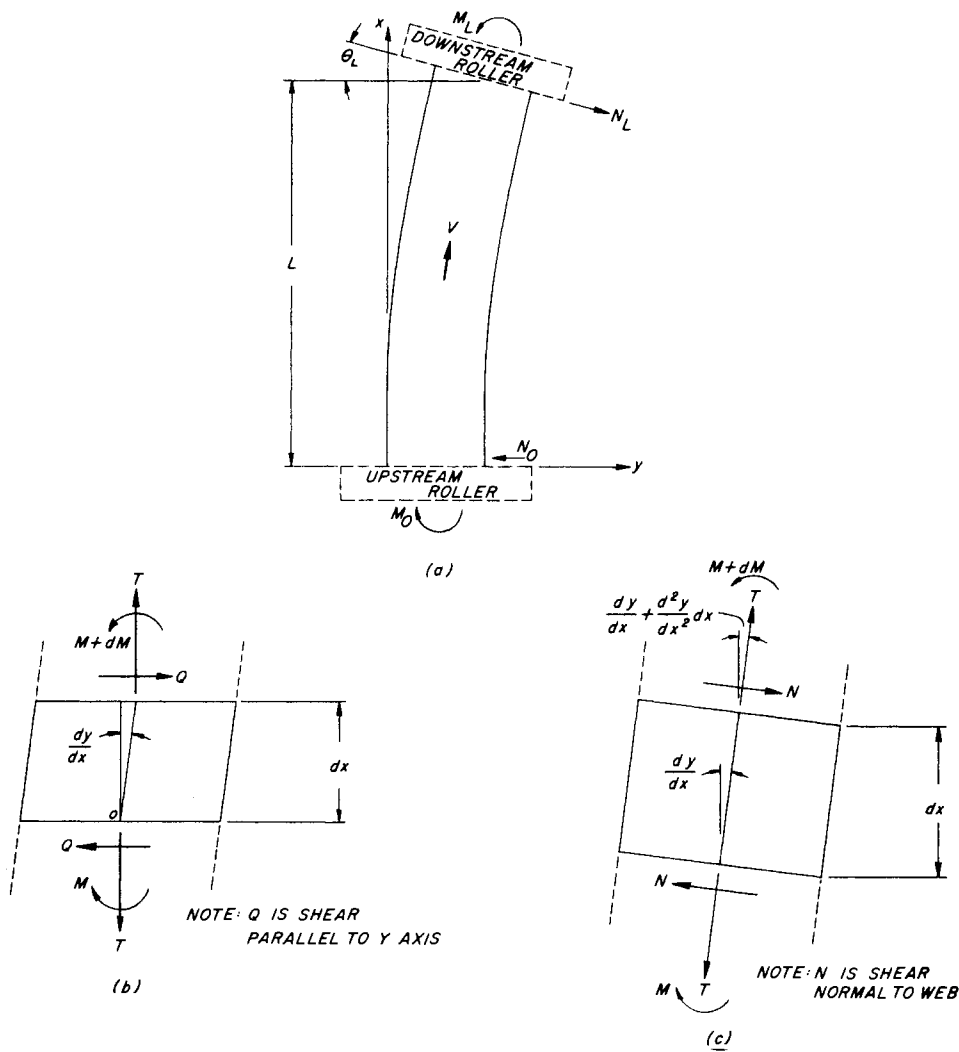
Figure 2.1.2. Freebodies and Symbols for Steady-State Analysis.

$$M + Qdx - (M+dM) - T\frac{dy}{dx}dx = 0$$

or,

$$Q = \frac{dM}{dx} + T\frac{dy}{dx} \quad . \tag{2.1.6}$$

This equation can be combined with the derivative of Equation 2.1.1 to obtain

$$Q = -Ely''' + T\frac{dy}{dx} \quad . \tag{2.1.7}$$

Q is constant because there is no side load assumed in the free span, and EI is a constant because it is assumed that the entire span is taut.

Differentiation of Equation 2.1.7 and division by EI yields the fourth-order differential equation of the elastic curve of a web:

$$y^{iv} - K^2 y'' = 0 \tag{2.1.8}$$

where

$$K^2 = \frac{T}{EI} \quad . \tag{2.1.9}$$

It may be noted from Figure 2.1.2 that

$$N = Q - T\frac{dy}{dx} \quad . \tag{2.1.10}$$

Equation 2.1.8 is a linear ordinary differential equation with constant coefficients. The roots of its characteristic equation are $+K, -K, 0,$ and 0. Therefore, the general solution may be immediately written as:

$$y = C_1 \sinh Kx + C_2 \cosh Kx + C_3 x + C_4 \quad . \tag{2.1.11}$$

Evaluation of the constants in Equation 2.1.11 depends upon four boundary conditions. The static shape of a web between non-parallel rollers appears as shown in Figure 2.1.2 (a). If y is chosen to be zero at $x = 0$, then $C_4 = -C_2$. The second boundary condition, if the friction is assumed sufficient to prevent

circumferential or lateral slippage on the entering roller, is that at $x = 0$, $\frac{dy}{dx} = 0$. This boundary condition establishes that $C_3 = -C_1 K$.

That a web approaches a roller perpendicularly to the roller axis was recognized by Lorig (12), Campbell (3) and Wright (25), and has been experimentally verified in experiments for this thesis. This boundary condition leads to the equation

$$C_1 K \cosh KL + C_2 K \sinh KL + C_3 = \theta_L$$

which may be simplified with the fact that $C_3 = -C_1 K$ and algebraically rearranged to give

$$C_2 = \theta_L/(K \sinh KL) - C_1 (\cosh KL - 1)/\sinh KL.$$

The fourth necessary boundary condition, that the moment on the guide roller is zero in the steady state, is not immediately obvious. Its experimental determination, representing one of the primary contributions of this thesis, is reported in Section 2.2. However, it seems appropriate to digress at this point to give an intuitive proof of this crucial boundary condition.

Imagine that an initially straight and uniform web in its steady state position has a residual negative moment as it makes contact with a roller. The web has a finite radius of curvature, as shown in Figure 2.1.3, which means that the web is longer on one side than the other. If the roller were composed of many short, independent rollers instead of a single body, the roller at the left side of the web would turn fastest, because more length of web is passing over it per unit time. Similarly, the roller on the right end would turn slowest. But both ends of the single roller must turn at the same speed. Thus, because the left side of the web in Figure 2.1.3 would be trying to turn the roller faster and the right side slower, the roller would exert a positive moment on the web until the negative moment was cancelled as a result of the web movement, if the friction forces were sufficient.
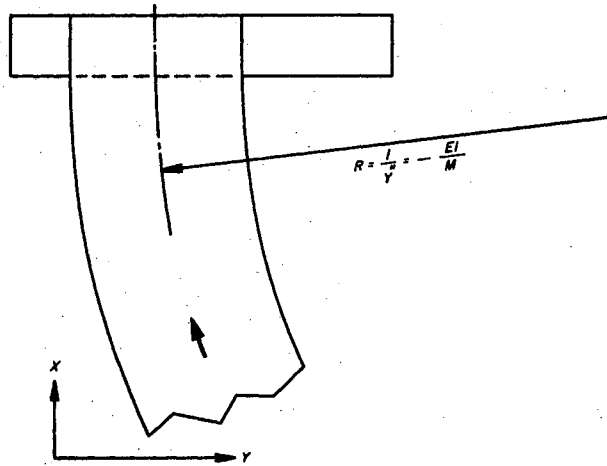
Figure 2.1.3. Web With Moment at Guide Roller.

The initial assumption of a steady-state moment was incorrect, so the steady-state moment at the downstream end of the free span must be zero.

This fourth boundary condition that $M_L = 0$ may be transformed by applying Equation 2.1.1 and dividing by $- EI$ to become $y_L'' = 0$, or

$$K^2 C_1 \sinh KL + K^2 C_2 \cosh KL = 0$$

or
$$C_2 = -C_1 \sinh KL / \cosh KL.$$

The two expressions for C_2 may be equated to solve for C_1, and the other constants can then be evaluated by substitution to obtain:

$$C_1 = -\frac{\theta_L}{K} \frac{\cosh KL}{\cosh KL - 1} \quad , \qquad (2.1.12)$$

$$C_2 = \frac{\theta_L}{K} \frac{\sinh KL}{\cosh KL - 1} \quad , \qquad (2.1.13)$$

$$C_3 = \theta_L \frac{\cosh KL}{\cosh KL - 1} \quad , \qquad (2.1.14)$$

and
$$C_4 = -\frac{\theta_L}{K} \frac{\sinh KL}{\cosh KL - 1} \quad . \qquad (2.1.15)$$

The solution to the differential equation may be non-dimensionalized by dividing by L to obtain:

$$\frac{y}{L} = \theta_L \left[\frac{\cosh KL}{\cosh KL - 1} \left(\frac{x}{L} - \frac{\sinh Kx}{KL} \right) + \frac{1}{KL} \frac{\sinh KL}{\cosh KL - 1} (\cosh Kx - 1) \right] . \qquad (2.1.16)$$

Note that y/L is a linear function of the guide roller angle θ_L. Also, for convenient normalization, $(KL)(x/L)$ may be substituted for Kx.

The curvature factor K_c is $y_L/(L\theta_L)$, or

$$K_c = \frac{y_L}{L\theta_L} = \frac{KL \cosh KL - \sinh KL}{KL(\cosh KL - 1)} . \qquad (2.1.17)$$

The curvature factor varies upward from two-thirds for $KL = 0$ and approaches unity as KL becomes large. A graph of the elastic curves of webs in the range of practical KL values is shown in Figure 2.1.4.

Successive differentiation of Equation 2.1.16, application of Equations 2.1.1 and 2.1.2, and use of the identitites $\cosh^2 KL - \sinh^2 KL = 1$ and $EIK^2 = T$ yields valuable formulas:

$$\frac{dy}{dx} = \theta = \theta_L \left[\frac{\cosh KL}{\cosh KL - 1} (1 - \cosh Kx) + \frac{\sinh KL}{\cosh KL - 1} (\sinh Kx) \right] , \qquad (2.1.18)$$

$$M = -EIy'' = -\frac{TL}{KL} \theta_L \left[\frac{\sinh KL}{\cosh KL - 1} (\cosh Kx) - \frac{\cosh KL}{\cosh KL - 1} (\sinh Kx) \right] , \qquad (2.1.19)$$

$$\text{and } N = -EIy''' = T\theta_L \left[\frac{\cosh KL}{\cosh KL - 1} (\cosh Kx) - \frac{\sinh KL}{\cosh KL - 1} (\sinh Kx) \right] . \qquad (2.1.20)$$

Section 2.2 verifies the validity of the assumed boundary conditions by experimentally showing that the Equation 2.1.20 is correct at $x = L$:

$$\frac{N_L}{T\theta_L} = \frac{1}{\cosh KL - 1} . \qquad (2.1.21)$$
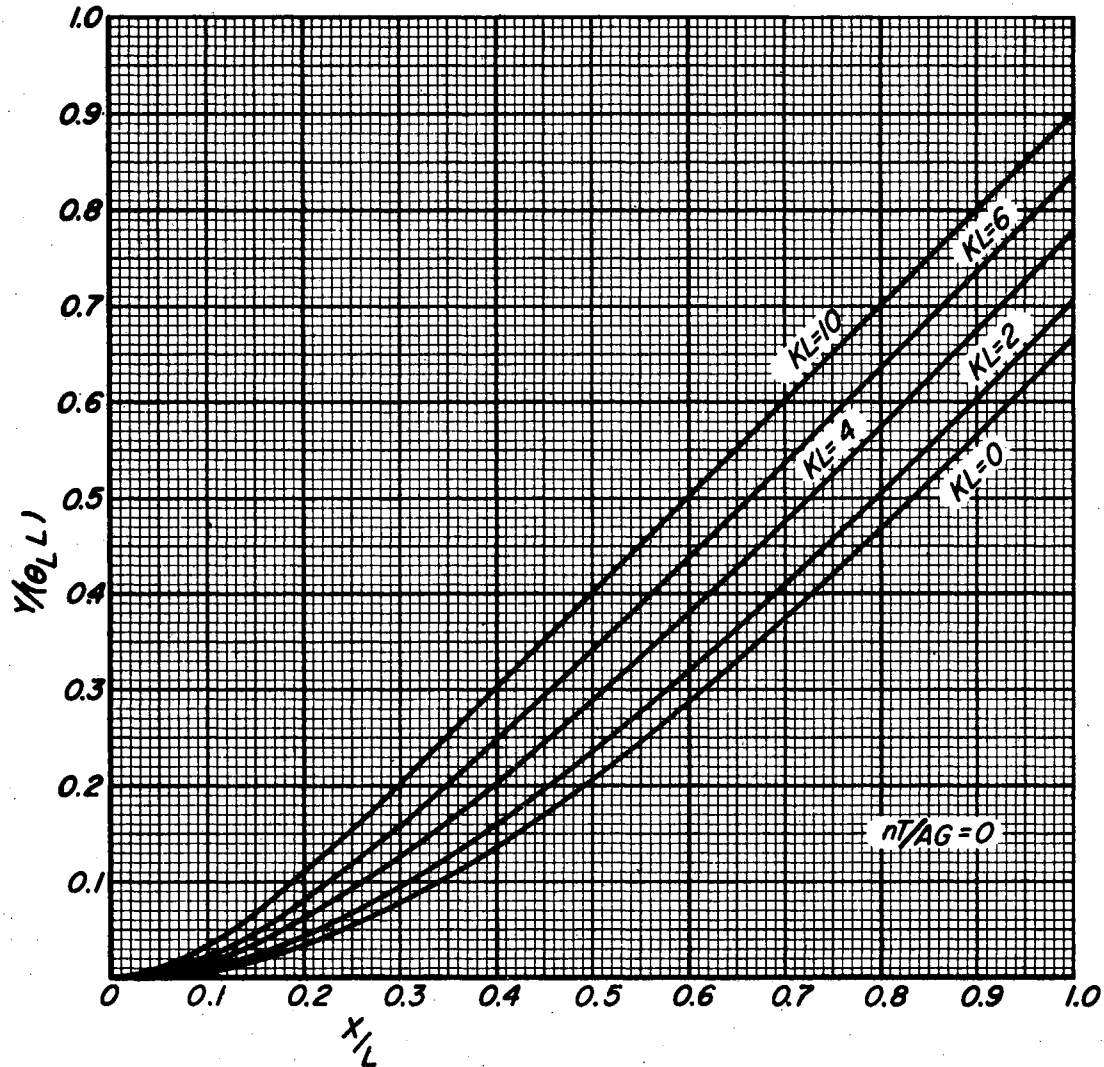
Figure 2.1.4. Elastic Curves of Webs Without Shear Deflection.

The maximum moment occurs at x = 0 and may be found from Equation 2.1.19

to be

$$M_o = - \frac{\sinh KL}{\cosh KL - 1} \left(\frac{TL}{KL} \theta_L \right).$$
(2.1.22)

$\dfrac{M_o}{Ty_L}$ is plotted in Figure 2.4.7, as $nT/AG = 0$. The validity of the assumption that

$nT/AG = 0$ (the shear deflection is negligible) is examined in Section 2.4.
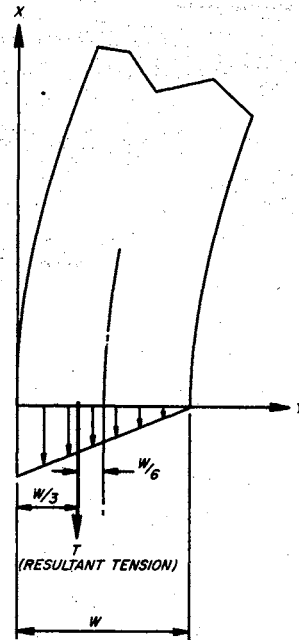
Figure 2.1.5. Critical Moment
Condition.

The "critical condition" is defined as the condition for which the inside edge
of the web at x = 0 has zero tension. Figure 2.1.5 shows the resultant tension for
the critical condition to be one-sixth of a web width from center. Therefore, the
critical moment is -TW/6. Note that, although previous drawings showed a central
tensile force and a superimposed moment, the tensile force system on a section of
the web is actually a distributed loading similar to that shown in Figure 2.1.5.

For the critical condition,

$$M_o\big)_{cr} = -\frac{TW}{6} = -\frac{TL}{KL} \frac{\sinh KL}{\cosh KL - 1} \theta_L$$

or

$$\theta_L\big)_{cr} = \frac{KL}{6} \frac{W}{L} \frac{\cosh KL - 1}{\sinh KL} \tag{2.1.23}$$

But $y_L = K_c \theta_L L$, so the maximum correction permissible before slackness occurs, expressed as a ratio of the web width, is

$$\left.\frac{y_L}{W}\right)_{cr} = \frac{KL}{6} K_c \frac{\cosh KL - 1}{\sinh KL}$$

or, from Equation 2.1.17

$$\left.\frac{y_L}{W}\right)_{cr} = \frac{1}{6} \frac{KL \cosh KL - \sinh KL}{\sinh KL} \quad . \tag{2.1.24}$$

This function is plotted in Figure 2.4.8 as the curve $nT/AG = 0$.

If θ_o, the slope of the elastic curve at $x = 0$, is not equal to zero because of a misaligned roller or because of circumferential creep of the web around the roller, the previous equations are slightly modified. Equation 2.1.16 becomes

$$\frac{y}{L} = \theta_L \left(1 - \frac{\theta_o}{\theta_L}\right)\left[\frac{\cosh KL}{\cosh KL - 1}\left(\frac{x}{L} - \frac{\sinh Kx}{KL}\right)\right.$$

$$+ \frac{1}{KL} \frac{\sinh KL}{\cosh KL - 1} \left(\cosh Kx - 1\right)\bigg] + \left(\frac{x}{L}\right)\theta_o \quad . \tag{2.1.25}$$

The correction at $x = L$ is given by the equation

$$\frac{y_L}{L\theta_L} = \left(1 - \frac{\theta_o}{\theta_L}\right)\left[\frac{KL \cosh KL - \sinh KL}{KL(\cosh KL - 1)}\right] + \frac{\theta_o}{\theta_L} \quad . \tag{2.1.26}$$

The slope equation is

$$\frac{dy}{dx} = \theta = \theta_L \left(1 - \frac{\theta_o}{\theta_L}\right)\left[\frac{\cosh KL}{\cosh KL - 1}(1 - \cosh Kx)\right.$$

$$+ \frac{\sinh KL}{\cosh KL - 1} \left(\sinh Kx\right)\bigg] + \theta_o \quad . \tag{2.1.27}$$

The moment and normal force equations are simply modified by the factor $(1-\theta_o/\theta_L)$:

$$M = \frac{TL}{KL}\left(1 - \frac{\theta_o}{\theta_L}\right)\theta_L\left[\frac{\cosh KL}{\cosh KL - 1}(\sinh Kx) - \frac{\sinh KL}{\cosh KL - 1}(\cosh Kx)\right] \quad (2.1.28)$$

and

$$N = T\theta_L\left(1 - \frac{\theta_o}{\theta_L}\right)\left[\frac{\cosh KL}{\cosh KL - 1}(\cosh Kx) - \frac{\sinh KL}{\cosh KL - 1}(\sinh Kx)\right] \quad . \quad (2.1.29)$$

The maximum moment (at $x = 0$) may be found from Equation 2.1.28 to be

$$M_o = -\frac{\sinh KL}{\cosh KL - 1}\left(\frac{TL}{KL}\theta_L\right)\left(1 - \frac{\theta_o}{\theta_L}\right) \quad . \quad (2.1.30)$$

The critical guide roller angle is

$$\theta_L\big)_{cr} = \frac{KL}{6}\frac{W}{L}\frac{\cosh KL - 1}{\sinh KL} + \theta_o \quad . \quad (2.1.31)$$

The critical correction can be found from the equation

$$\frac{y_L}{W}\bigg)_{cr} = \frac{1}{6}\frac{KL\cosh KL - \sinh KL}{\sinh KL} + \frac{L}{W}\theta_o \quad . \quad (2.1.32)$$

A comparison of Equations 2.1.16 through 2.1.24 with their corresponding equations with finite initial slope, Equations 2.1.25 through 2.1.32, reveals differences which are simple enough that separate plots of the latter equations are generally unnecessary.

If θ_L is equal to zero as, for example, in the exiting span of a guide whose plane of motion is not perpendicular to the exiting span, the error at the second roller relative to the first may be found from the equation

$$\frac{y_L}{L\theta_o} = 1 - \frac{KL \cosh KL - \sinh KL}{KL(\cosh KL - 1)} , \qquad (2.1.33)$$

which was derived from Equation 2.1.25. It may be noted from Equation 2.1.17 that Equation 2.1.33 may be written as,

$$\frac{y_L}{L\theta_o} = 1 - K_c . \qquad (2.1.34)$$

Equation 2.1.34 is valid even if K_c is calculated with the more general formula of Equation 2.4.17. The error at any intermediate point may be found by subtracting the value of the function $y/(L\theta_L)$ of Figure 2.1.4 from the value of x/L. If shear deflection must be considered, the error at an intermediate point may similarly be found from Figures 2.4.2 through 2.4.5.

A person familiar with the problem of lateral buckling of beams may feel that the analysis of this section neglects a stability problem. However, the lateral buckling problem as considered by Timoshenko and Gere (23), for example, cannot occur unless compressive stresses can be sustained, in contradiction to a basic assumption of this thesis. If the guide correction is great enough to cause M_o to be greater than TW/6 (a condition not considered in this thesis), slackness of one edge occurs but the tension in the web maintains the taut portion of the web in one plane. If the plane of guide roller motion is not parallel to the entering span, the taut portion of the web forms a helix, but no buckling of the taut portion occurs.

2.2. Tests and Justification of Boundary Conditions. Experimentation was necessary to provide direction for theoretical work and to verify certain important theories. The primary problem considered in this section is the determination of the boundary conditions at the downstream roller. The results are shown in Figure 2.2.7. A versatile web guiding test machine as shown in Figures 2.2.1 and 2.2.2
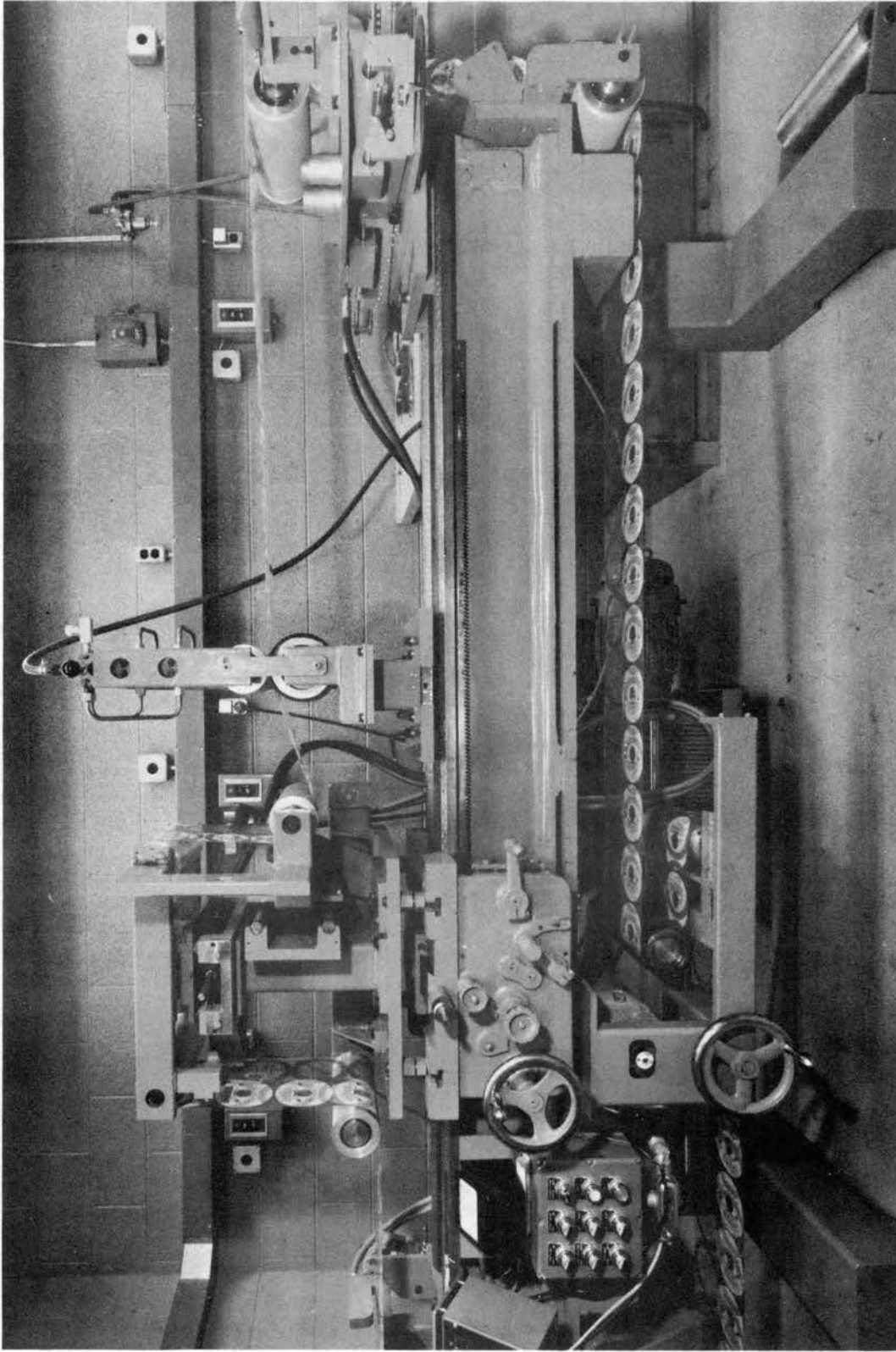
Figure 2.2.1. Side View of Web Guiding Test Machine.

DISPLACEMENT GUIDE FOR FINAL
CORRECTION OR ERROR INPUT
(ON MOVABLE CARRIAGE)

ADJUSTABLE AND
REMOVABLE
NIP ASSEMBLY

STEERING-TYPE
TEST GUIDE

WEB SPEED
INDICATOR

DRIVE MOTOR

CONTROLS

TENSIONING ROLLER

TENSION ADJUSTMENT WHEEL

DISPLACEMENT GUIDE
FOR ERROR CLEANUP
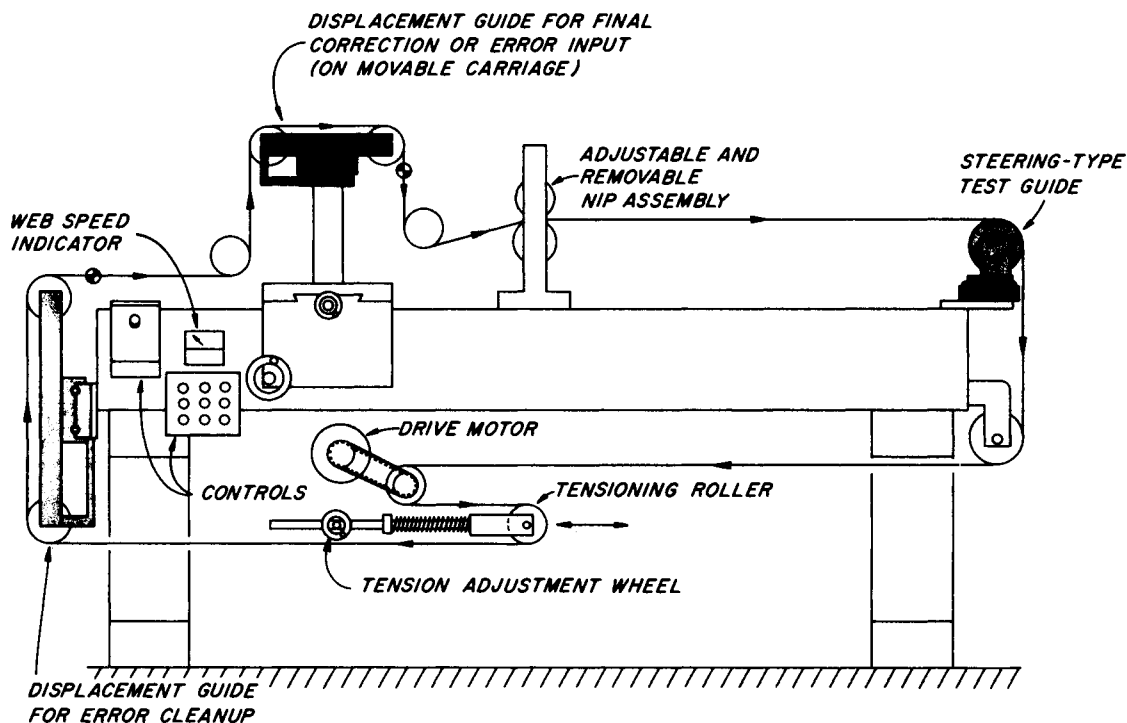
Figure 2.2.2. Schematic of Web Guiding Test Machine.

was constructed for testing of static and dynamic web behavior. The following discussion of the machine will aid in understanding and validation of the test results.

It was decided that the machine should handle an endless belt, so that it could run for long periods at a constant speed and so that tension control would be simple. The disadvantage of an endless belt is the disturbance caused by an imperfect splice. All necessary rollers were cantilevered so that the belt could be changed without disturbing the splice.

A "backbone" type of frame was chosen so that a straight reference would be available for precise alignment of components and for measurement of lateral web location, and so that certain components would be readily movable. An old lathe bed was re-planed and hand scraped to provide precision ways. New legs were necessary to make the belt changeable.

Figure 2.2.3. Drive and Tensioning Roller of Web Guiding Test Machine.

Power was provided by an SCR-controlled constant speed drive with tachom-
eter feedback. Speed was adjustable up to 1500 feet per minute. A speed
indicator was provided to read in feet per minute. The rubber-covered drive roller
and the drive motor are shown in the upper left of Figure 2.2.3.

The other roller in Figure 2.2.3 is the tensioning roller. Bevel gears from
the hand crank on the side of the machine drive a screw which loads two springs
against the floating tension roller. The tension roller is accurately aligned by tan-
dem ball bushings on hardened and ground rods. Tension is indicated by the pointer
and scale shown in the lower center of Figure 2.2.3. Figure 2.2.4 is the calibra-
tion curve for the tension indicator.

Three web guides with servo control systems were designed for the machine.
The guide on the rear of the machine was intended to be used at all times to correct
the errors which are introduced at the test guide or that accumulate thereafter. The
guide can be automatically centered for threading of the belt.
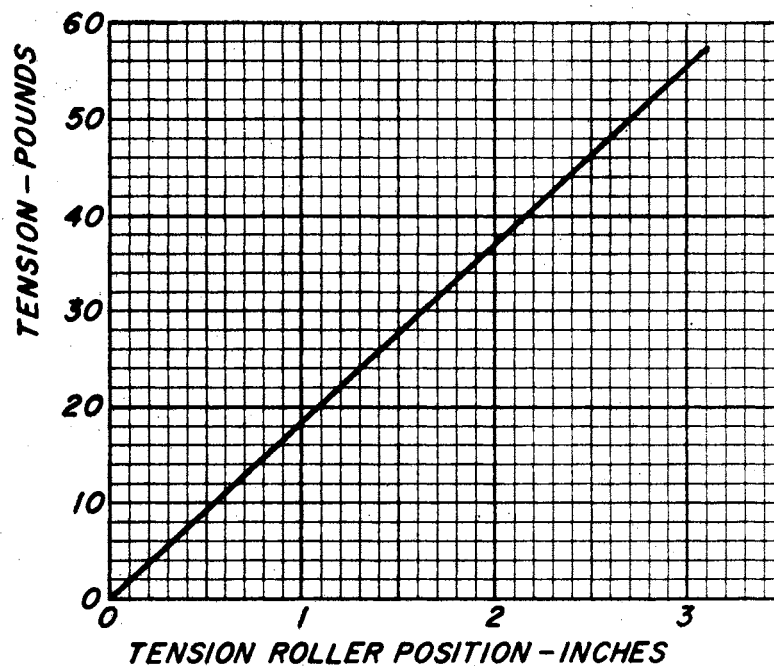
Figure 2.2.4. Calibration Curve for Tension Indicator
of Web Guiding Test Machine.

The error input guide on the lathe carriage may be used for introducing errors to the test guide, or may be used for final guiding for certain tests, such as the static tests of this chapter. The guide may be manually positioned with a selector switch and jog button.

The test guide on the front of the machine may be used for automatic guiding or may be manually positioned. For the tests of this chapter, it was manually positioned to give a certain roller angle. The mechanism of the guide is a double slider, with the ramp angles of the slider raceways and the slider displacement indicated as shown in Figure 2.2.5. A plan view of the guide mechanism is shown in Figure A.1.1. The roller angle was calculated from the raceway ramp angle and displacement from center, as outlined in Appendix A.

As was mentioned in Section 2.1, the assumption of zero moment at the guide roller was proved by verifying Equation 2.1.21 experimentally. Actually, the theory was formulated after experiments allowed no other conclusions. The normal side force was chosen to be measured because it was believed to be much easier to measure than the moment. But pitfalls existed for side force measurement. No measurements were taken near the splice. Unless the next roller after the guide was well aligned, a side force from the exiting span existed on the guide roller. If the web was cambered, the force in one direction would be greater than the force in the other direction. Readings taken with the guide displacement in both directions were averaged to minimize camber effects. Imperfections in the web caused considerable needle swing of the force scale. These variations were visually averaged. An aluminum web was yielded on its edges because of minor misalignment of rollers and it consequently gave a false area-moment-of-inertia effect. The final results were obtained with a web of much lower modulus to avoid yielding.

The apparatus for side-force measurement is shown in Figure 2.2.6. The roller was free to float endwise on ball bushings. The force was measured on the 10-pound
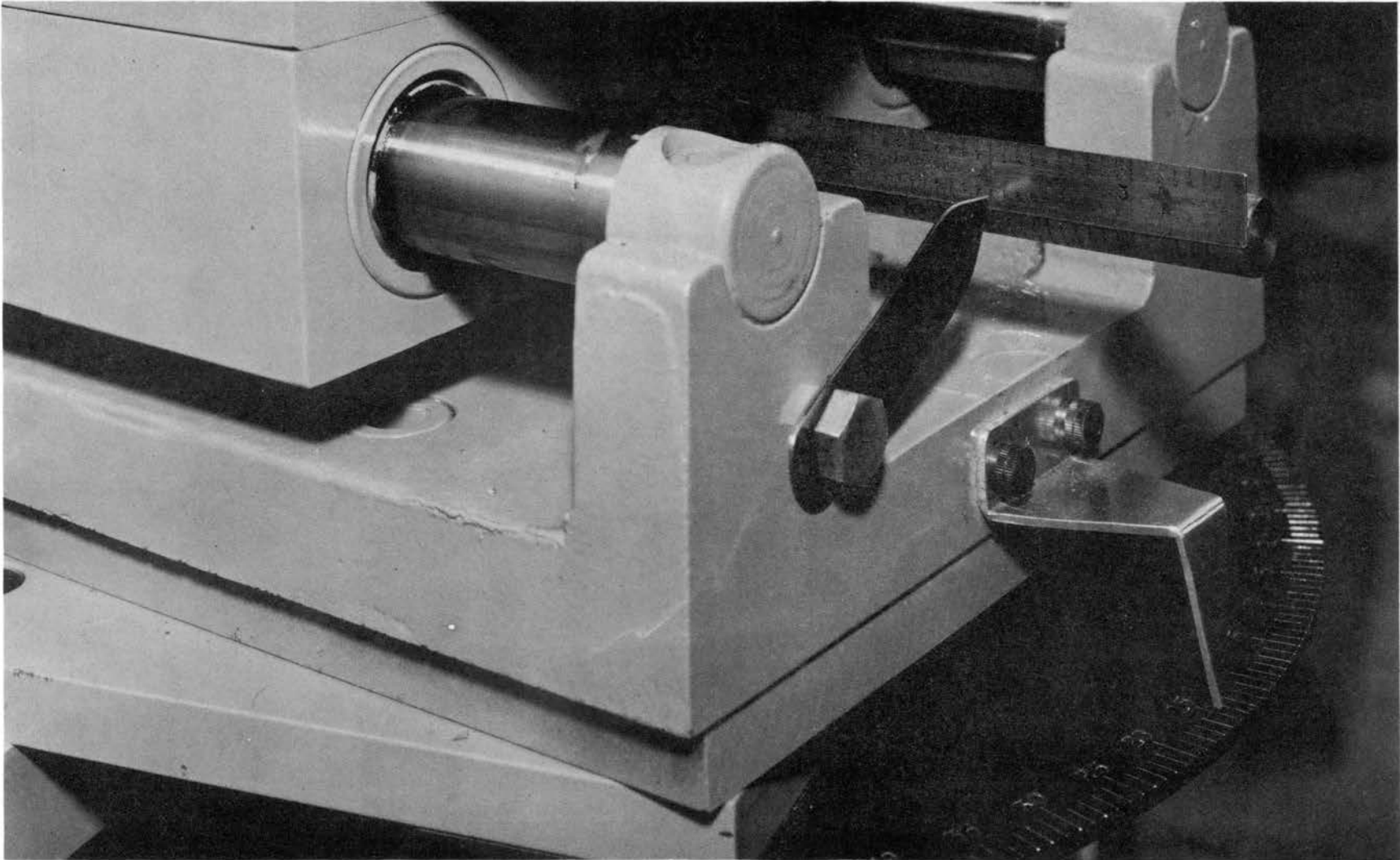
Figure 2.2.5. Raceway Angle and Slider Displacement Indicators.
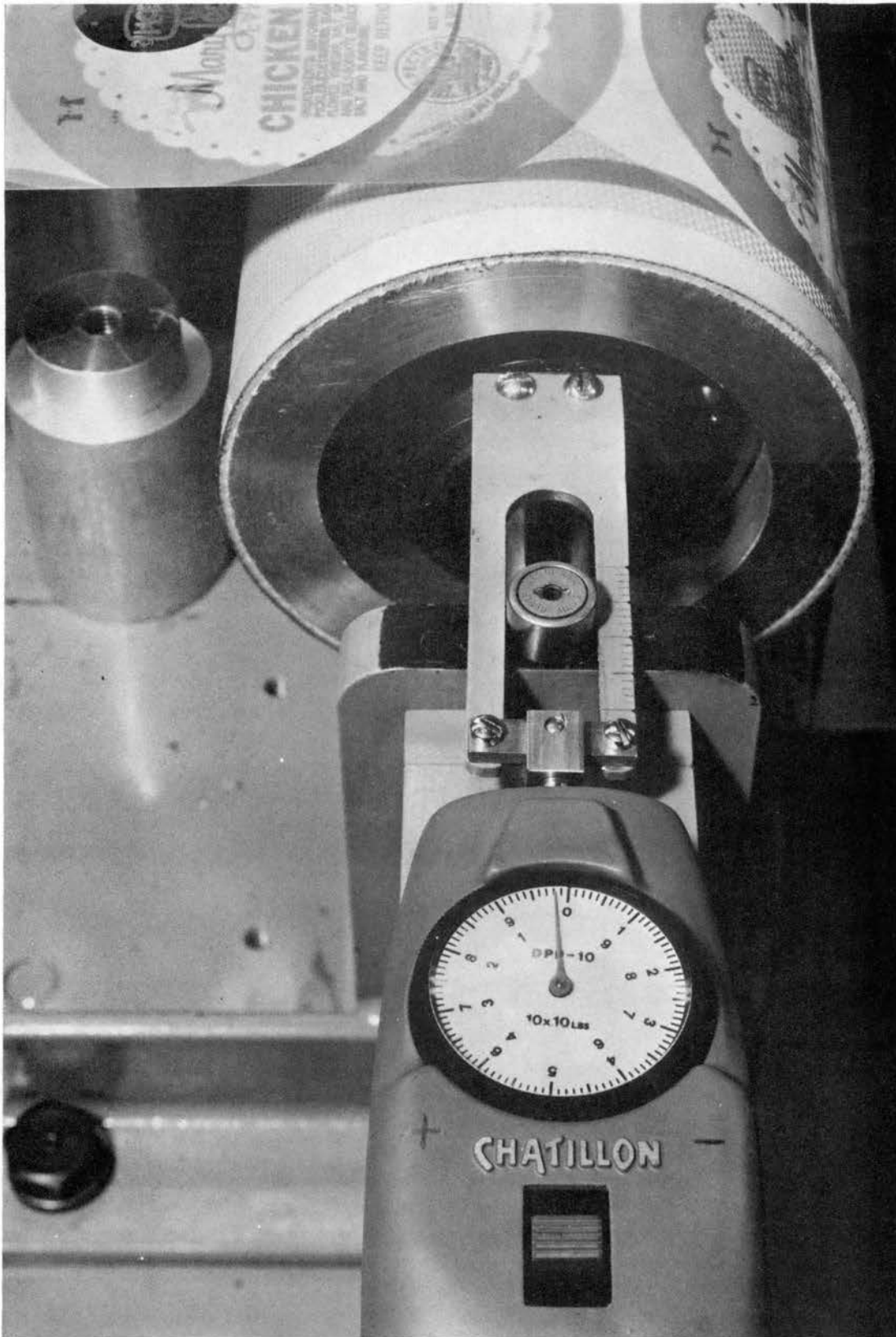
Figure 2.2.6. Apparatus for Web Normal Force Measurement.

scales. The amount of end float of the roller was unimportant in the steady state, because the angle determined the side force and the roller and web merely steered opposite directions until they reached equilibrium. The final test data is shown in Table I, and the data is plotted in Figure 2.2.7, in which the solid line is the plot of Equation 2.1.21.

In order to validate the significance of the test recorded in Figure 2.2.7, an analytical study of the sensitivity of the normal force N_L to the moment M_L was undertaken, as discussed in the following three paragraphs and summarized in Figure 2.2.8.

It can be observed that the tension is more evenly distributed (the moment in the web is less) at the guide roller than at the first part of the entering span. However, because of web imperfections and inexact methods of observation, it might be questioned if the moment has entirely disappeared at the guide roller. But the test of Figure 2.2.7 has been presented as proof that M_L is equal to zero. For this study, it is assumed that the uneven tension distribution at x_o is only partially redistributed in the entering span. The possibility is then examined of getting experimental data close enough to Equation 2.1.21 to lead to the belief that the condition of zero M_L was proved.

If C is the fraction of M_o that is present at x_L, the fourth boundary condition may be stated as $M_L = CM_o$. A derivation similar to that of Section 2.1 leads to the results:

$$\frac{y}{L} = \theta_L \left[\frac{\cosh KL - C}{(C+1)(\cosh KL - 1)} \left(\frac{x}{L} - \frac{\sinh Kx}{KL} \right) + \frac{1}{KL} \frac{\sinh KL}{(C+1)(\cosh KL - 1)} (\cosh Kx - 1) \right]$$

$$(2.2.1)$$

and

$$\frac{N_L}{T\theta_L} = \frac{1 - C \cosh KL}{(C+1)(\cosh KL - 1)} .$$

$$(2.2.2)$$

TABLE I

TEST DATA FOR PROOF OF ZERO M_L

Tension Pounds	L in.	W in.	θ_L Radians	Average Left & Right N_L Pounds	KL	$N_L/T\theta_L$
36.7	19.5	9.03	0.001885	2.375	0.2364	34.3
36.7	19.5	9.03	0.001885	2.45	0.2364	35.4
55.1	19.5	9.03	0.001885	2.40	0.2904	23.1
36.7	40	9.03	0.00377	1.10	0.485	7.95
55.1	40	9.03	0.00377	1.075	0.594	5.17
18.3	56.5	9.03	0.00377	0.575	0.484	8.34
55.1	56.5	9.03	0.00377	0.55	0.842	2.644
55.1	63	4.48	0.01884	0.15	2.684	0.1445
9.1	40	4.48	0.00377	0.125	0.694	3.64
36.7	40	4.48	0.00377	0.125	1.392	0.903
36.7	40	4.48	0.00941	0.325	1.392	0.941
36.7	20	4.48	0.00377	0.525	0.696	3.79
9.1	20	4.48	0.00377	0.55	0.346	16.0
18.3	20	4.48	0.00377	0.575	0.491	8.34
27.5	20	4.48	0.00377	0.625	0.601	6.03
36.7	20	4.48	0.00377	0.625	0.696	4.51
9.1	40	4.48	0.00377	0.125	0.694	3.64
36.7	40	4.48	0.00377	0.125	1.392	0.904
36.7	40	4.48	0.00941	0.325	1.392	0.941
36.7	56.5	4.48	0.01884	0.25	1.967	0.362
55.1	56.5	4.48	0.01884	0.20	2.408	0.1925

The theoretical curve is labeled:

$$\frac{N_L}{T\theta_L} = \frac{1}{\cosh KL - 1}$$
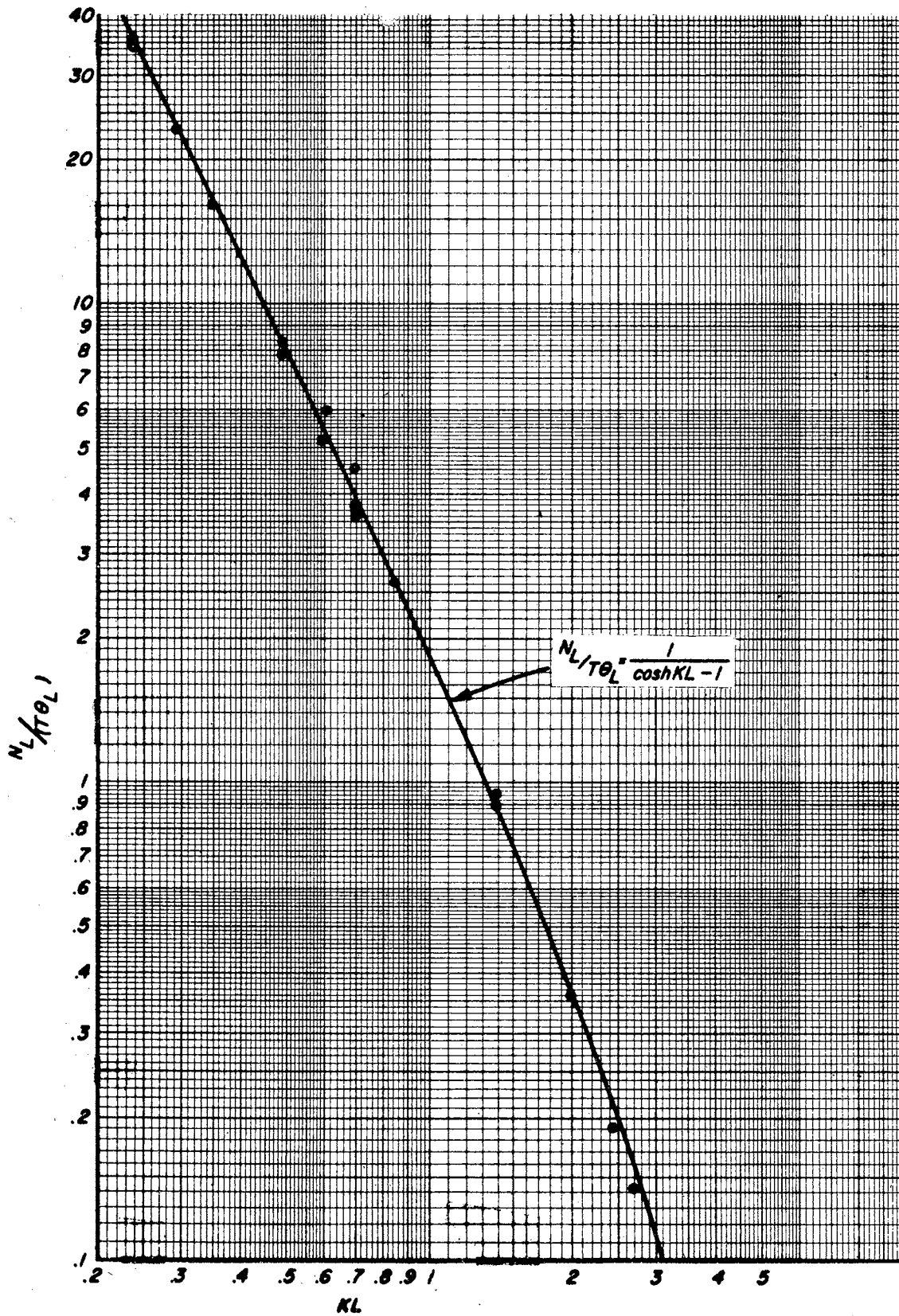
Figure 2.2.7. Experimental Data Compared to Theoretical Curve for Normal Force.
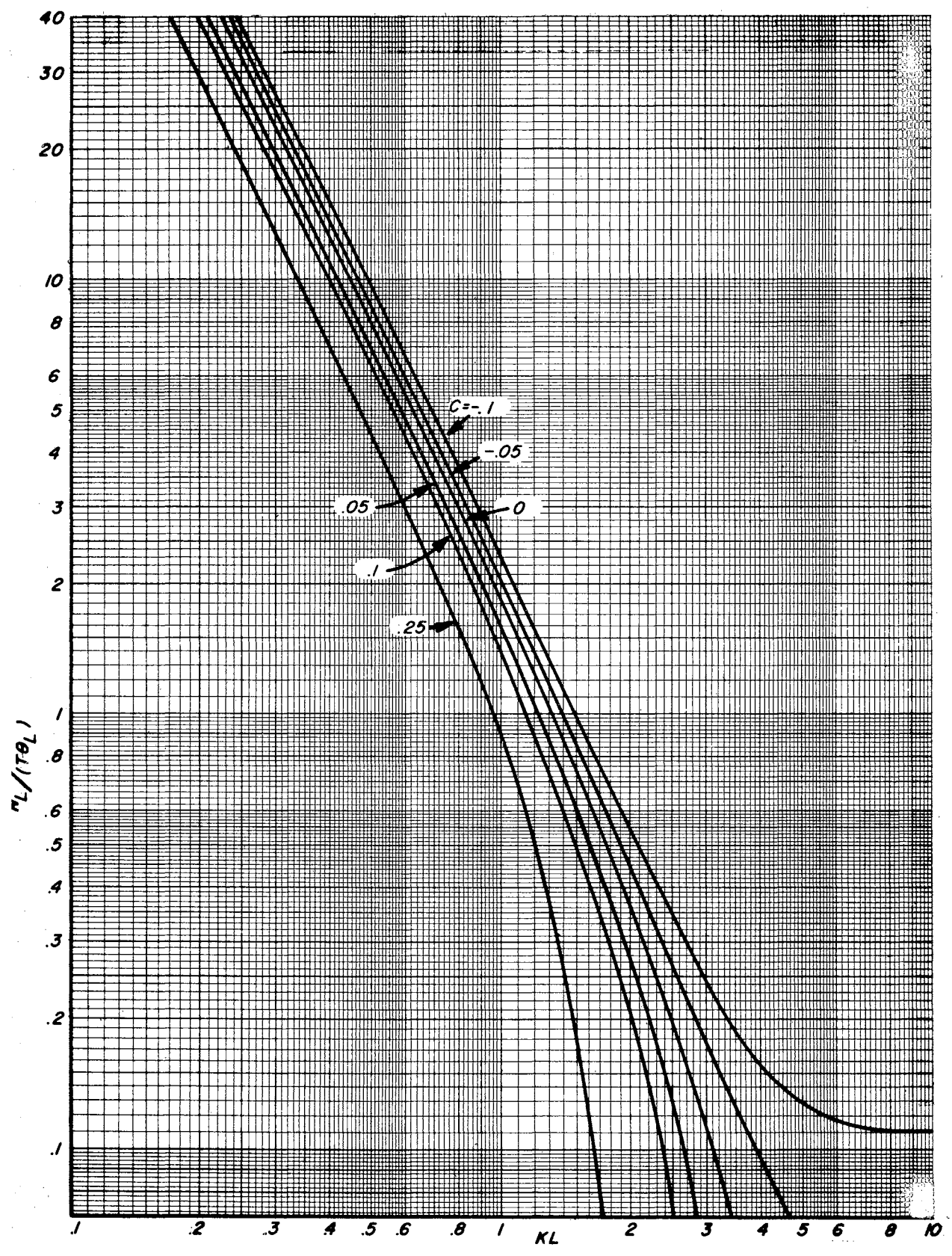
Figure 2.2.8. Study of Sensitivity of $N_L/T\theta_L$ to M_L.

Equation 2.2.2 is plotted in Figure 2.2.8. It is obvious that even if M_L is as small as five percent of M_o, $N_L/T\theta_L$ is somewhat different from that for zero M_L. The sensitivity of the chosen test is thus established, and Figure 2.2.7 is shown to be excellent experimental proof that the steady-state moment at the downstream roller is zero.

Tests were run of the shape of the static elastic curve. Some tests were run using a small visual comparator mounted to a movable base on the lathe bed. Readings at both ends of the web could not be conveniently made, however, and the most successful measurements were made with a simple scale calibrated in 0.010 inches and with a 0.003 inch diameter steel wire tightly stretched along the original position of the web edge. Typical sets of data are shown in Figures 2.2.9 and 2.2.10; the theoretical curves from Equation 2.1.16 are shown as solid lines. Figure 2.2.9 shows excellent correlation between theory and experiment. Figure 2.2.10 shows a slightly greater experimental deflection than the theory predicted. Deflection of
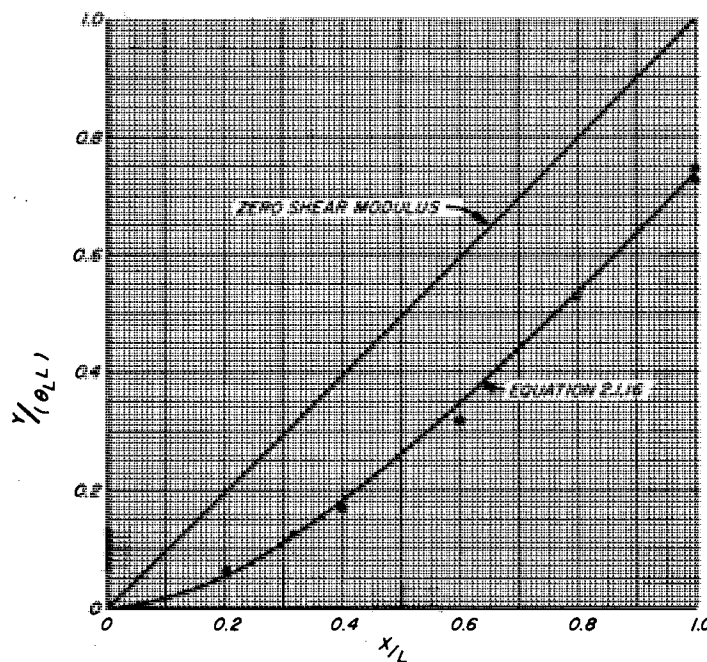
Figure 2.2.9. Experimental Data for KL=2.9 Compared to Theoretical Elastic Curve.
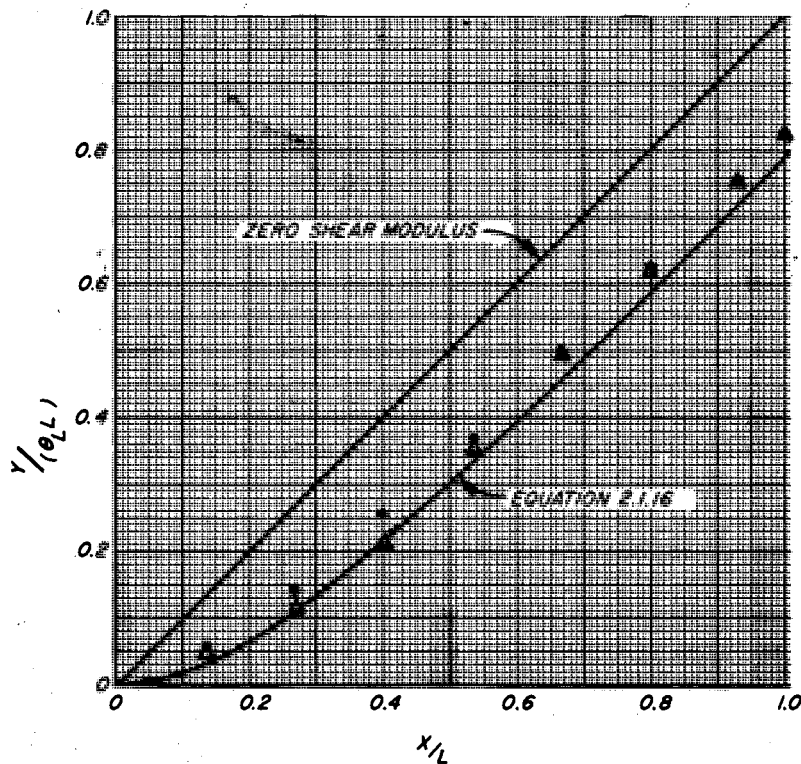
Figure 2.2.10. Experimental Data for KL=4.35
Compared to Theoretical
Elastic Curve.

the rubber covering on the lower roller and partial slippage on the steel upper roller
of the nip assembly at the entering roller may partially account for the discrepancy,
but the difference is probably within the range of experimental error for the test.

2.3. Tests of Web Properties. Many web materials, such as paper, textiles,
elastomers, and composites are quite variable in their physical properties. The
moduli of elasticity of many webs cannot be compactly and precisely documented,
because of significant nonlinearity, inelasticity, and long-term creep. Consequent-
ly, it was necessary to build a machine for testing of moduli of elasticity of webs
and coefficients of friction between webs and rollers. Friction data was not utilized
in this thesis, but would be needed for application of results and for an extension of
the study. Knowledge of moduli of elasticity was necessary for verification of the
theories of this thesis.

It was necessary to have web clamps which gripped the web uniformly across its width and which could be aligned perpendicularly to the web. It was also necessary that the web span length be well defined for elasticity testing. Figure 2.3.1 shows the web clamping arrangement. A long loose end of the web was folded over the bar and aligned with the test span to ensure perpendicularity of the web to the clamp.

Figure 2.3.2 shows the clamp on the carriage of the machine and the scale and dial indicator used for modulus of elasticity testing. The clamp was mounted on small ball bushings, which ensured that the scale reading was very nearly the force on the end of the web. The displacement of the end of the web was measured with a dial indicator, which measured clamp position. The dial indicator has been sufficiently sensitive for all materials, including metals, with a length of at least three or four feet. Web widths have been adequately measured with steel rules or tapes. Web thicknesses have been measured with a micrometer, but such a measurement is rather arbitrary for a woven material. The thickness measurement is of no importance in the calculations of this thesis, as long as a given measurement is consistently used, because E and I always appear as a product, and the calculated value of E is inversely proportional to the thickness measurement, whereas I is directly proportional. An error would thus be cancelled.

The friction test arrangement is shown in Figure 2.3.3. The web was wrapped 90 degrees around a locked roller which had the friction surface to be tested. The clamp was used as a weight and the friction forces, either static or dynamic, were read on the scale. The coefficient of friction was calculated with the belt formula from Spotts (22):

$$T_i = T_c e^{\mu\theta} \, . \tag{2.3.1}$$
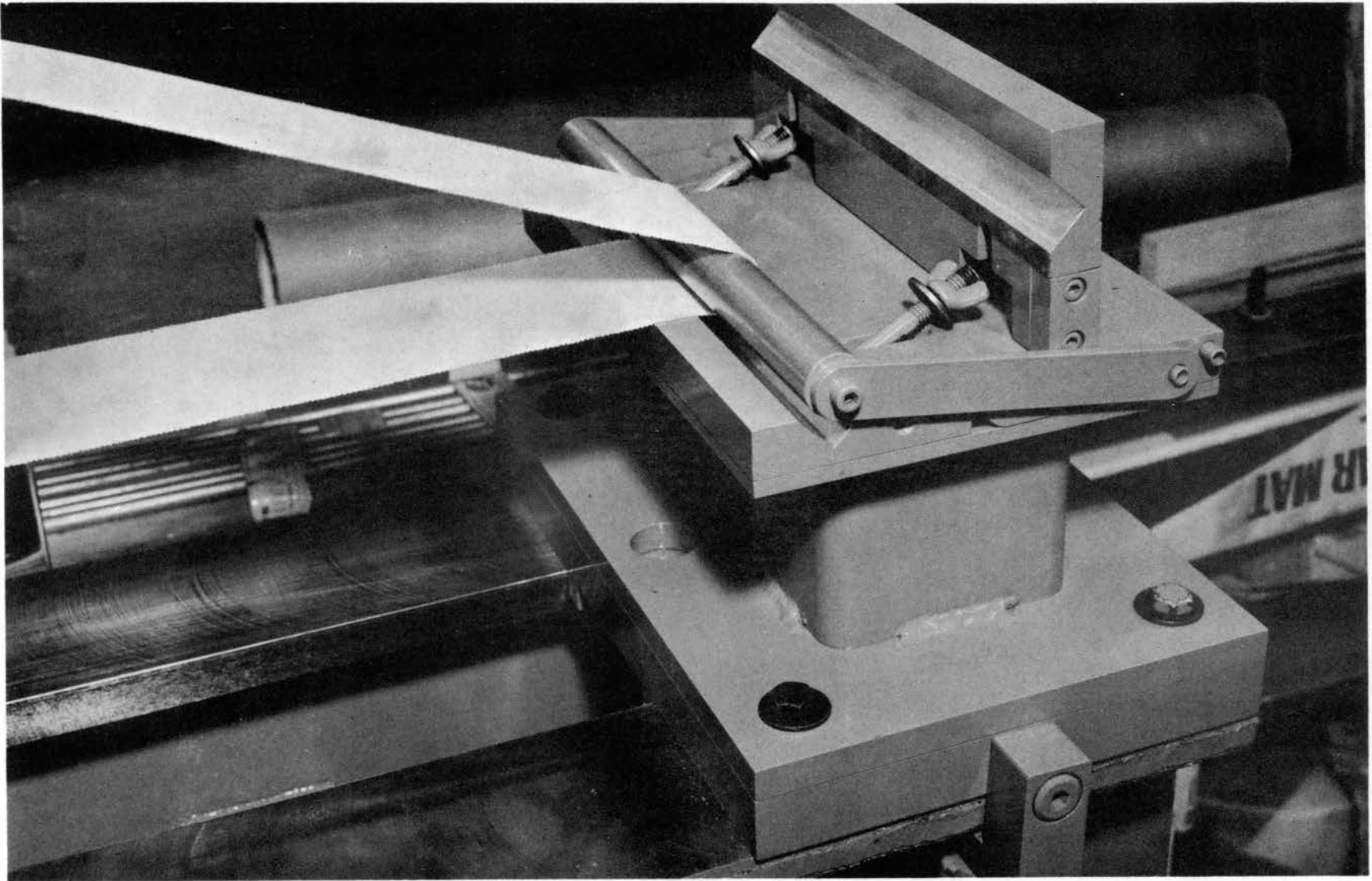
Figure 2.3.1. Web Clamping Method for Static Testing.
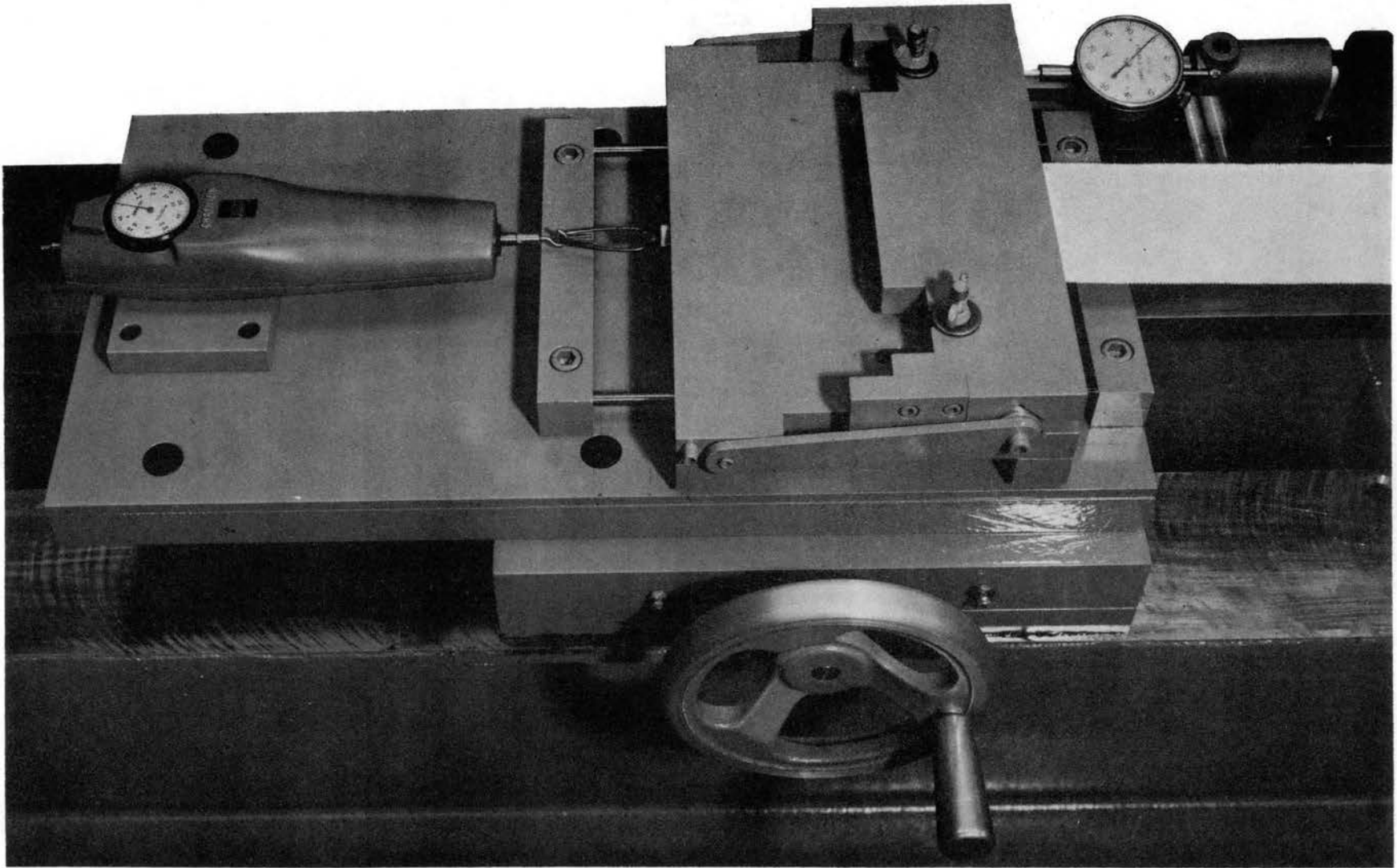
Figure 2.3.2. Clamp on Carriage, Scale, and Dial Indicator for Modulus of Elasticity Testing.
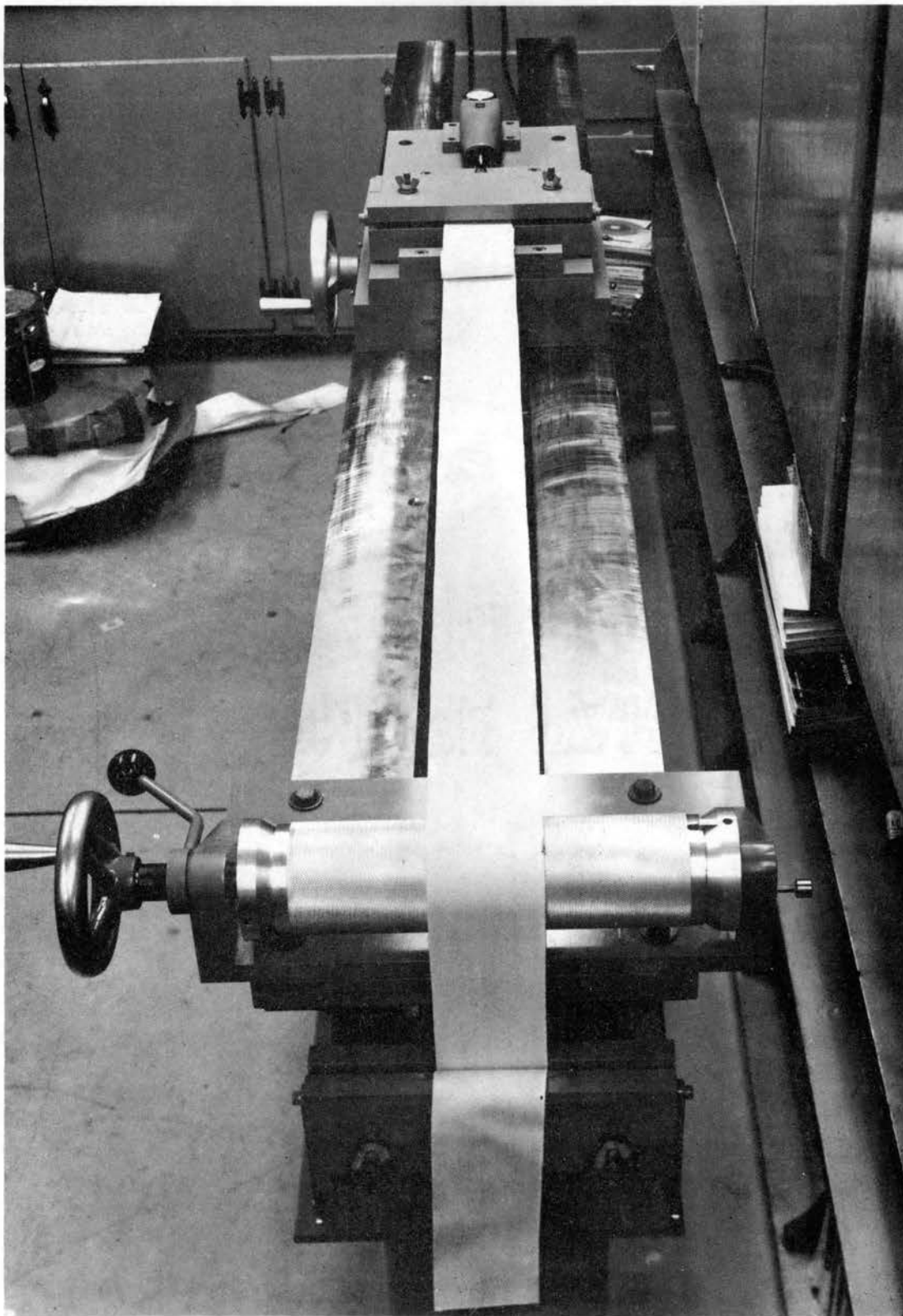
Figure 2.3.3. Test Arrangement for Measuring Friction Between Web and
Roller Surface.

In Equation 2.3.1, T_c is the constant weight, T_i is the indicated tension, θ

is the angle of web wrap in radians, and μ is the unknown coefficient of friction.

A test of the modulus of elasticity of the polystyrene used for most of the web

tests is shown in Figure 2.3.4. The test corresponded closely to the 450,000 psi

figure published by the manufacturer. Although hysteresis was measured, the modu-

lus of elasticity was the same for increasing and decreasing stress, except at the

extremes of the test. The hysteresis can be partially attributed to friction in the

force measurement scales.
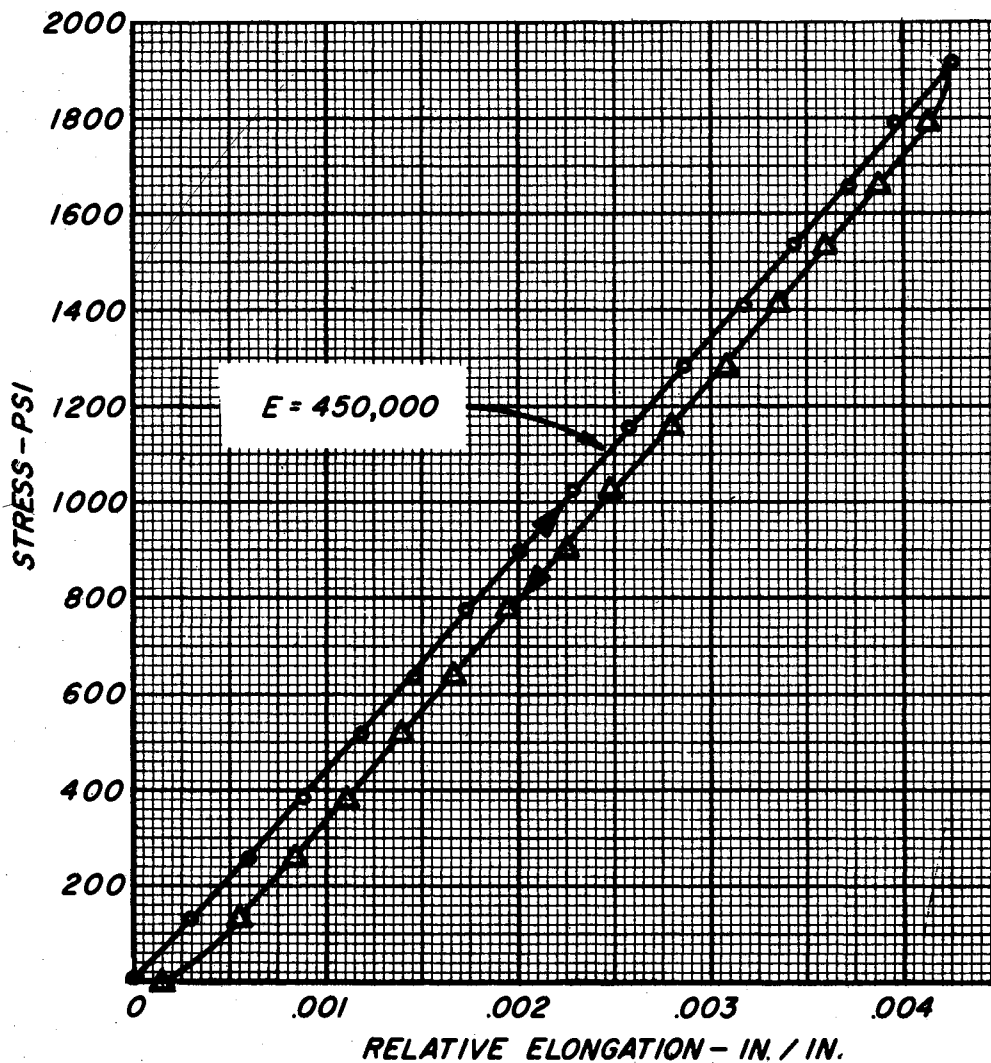
Figure 2.3.4. Stress-Strain Curve for Polystyrene Web.
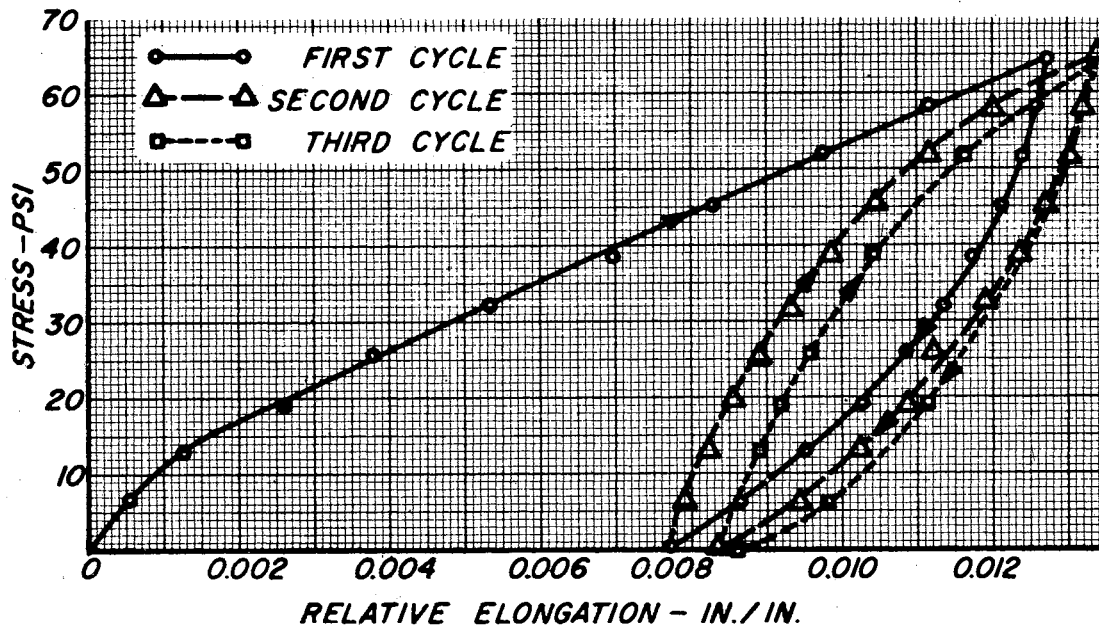
Figure 2.3.5. Stress-Strain Curves for Cloth Web.
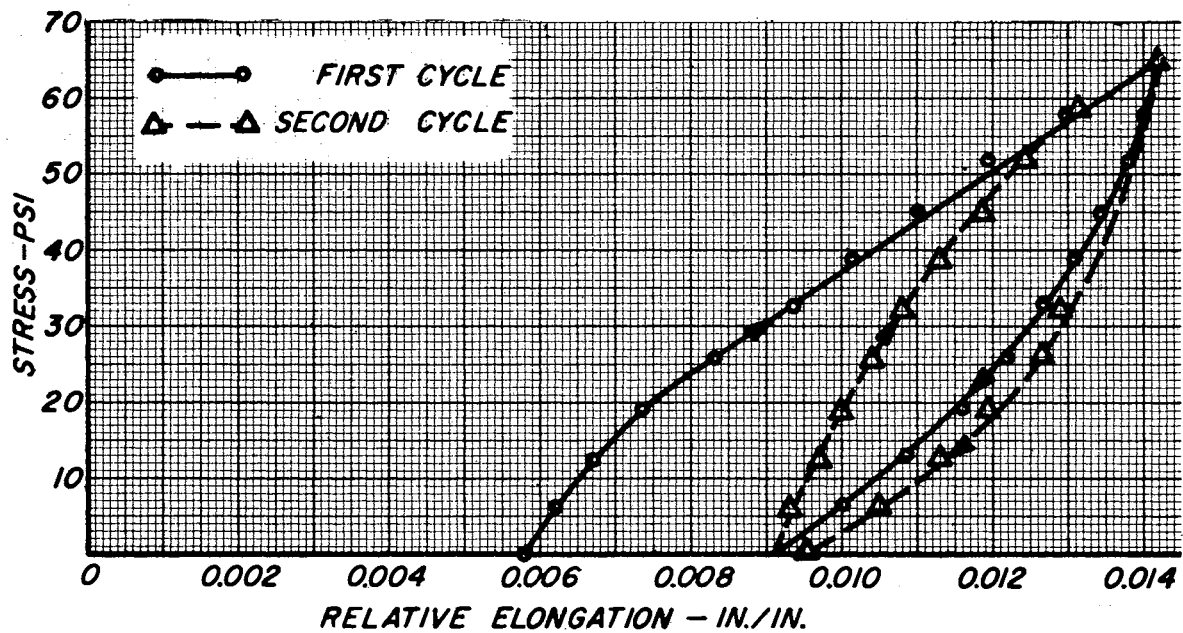
Figure 2.3.6. Stress-Strain Curves for Web of Figure 2.3.5 After Overnight Recovery.

A test of cotton cloth webbing is shown in Figures 2.3.5 and 2.3.6. The test of Figure 2.3.6 was run the day after the test of Figure 2.3.5, with the same zero points for stress and strain. Some dimensional recovery may be noted. The nonlinearity, hysteresis, and creep evident from the graphs are typical of textiles. Furthermore, textiles are generally anisotropic. It is obvious that elementary beam theory would be inexact for analysis of such a material. Section 2.6 discusses the possibility of considering the hysteresis, which is similar to that of a metal which is stressed beyond its yield point.

2.4. Shear Effect on Static Behavior. Thus far, only the deflection due to the moment in the web has been considered. The bending theory is sufficient for long web spans, but this section develops theory for shorter spans, for which the deflection due to shear stresses in the web are significant. An approximate method widely accepted, for example by Timoshenko and Gere (23), page 132, is used.

Figure 2.4.1 is used for the derivation. For this derivation, the subscript "b" means the bending effect, "s" the shear effect, and "t" the total or resultant effect.

The approximation consists of using the average shear stress instead of the actual parabolic shear stress distribution, and applying a correction factor n to give the actual deflection. A web has a rectangular cross section, so n is equal to 1.2, as published in many texts and handbooks. By definition of the shear modulus G, if the shear stress were evenly distributed, the angle of shear deflection would be N/AG. Therefore,

$$y_s' = \frac{dy_s}{dx} = \frac{nN}{AG} \tag{2.4.1}$$

where $A = tW$, the cross-sectional area of the web. Equation 2.4.1 may be differentiated twice to give
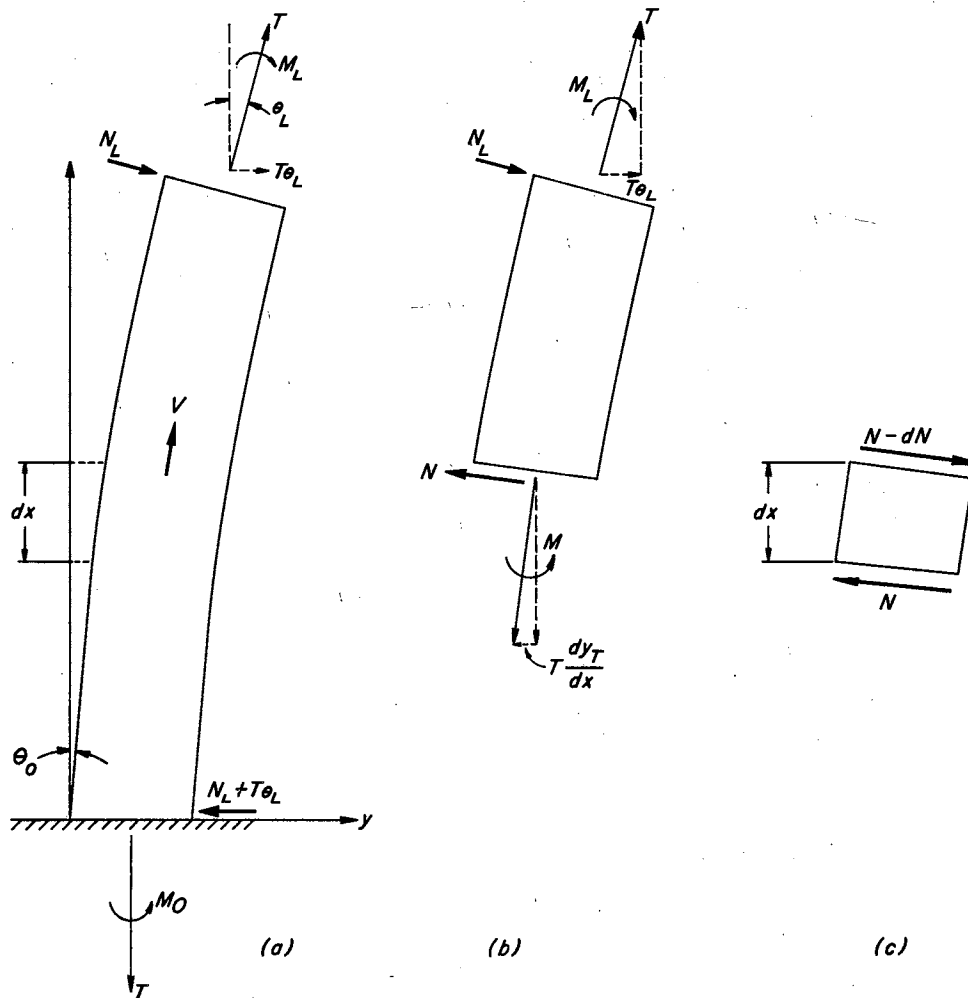
Figure 2.4.1. Freebodies and Symbols for Shear Analysis.

$$y_s''' = \frac{d^3 y_s}{dx^3} = \frac{n}{AG}\ \frac{d^2 N}{dx^2} \qquad . \tag{2.4.2}$$

From a summation of the horizontal forces on the freebody of Figure 2.4.1 (b),

$$N = T\left(\theta_L - \frac{dy_t}{dx}\right) + N_L \qquad . \tag{2.4.3}$$

Differentiation of Equation 2.4.3. twice gives the result

$$\frac{d^2N}{dx^2} = -T\frac{d^3y_t}{dx^3} \qquad . \tag{2.4.4}$$

Equation 2.4.4 combined with Equation 2.4.2 results in the equation

$$\frac{d^3y_s}{dx^3} = -\frac{nT}{AG}\frac{d^3y_t}{dx^3} \qquad . \tag{2.4.5}$$

Because $y_b''' = y_t''' - y_s'''$, Equation 2.1.2 may be written as

$$N = -EI\,(y_t''' - y_s''') , \tag{2.4.6}$$

which may be combined with Equation 2.4.5 to give

$$N = -EIy_t'''\left[1 + \frac{nT}{AG}\right] \qquad . \tag{2.4.7}$$

Equation 2.4.7 may be equated to Equation 2.4.3 and differentiated once to obtain:

$$-Ty_t'' = -EIy_t^{iv}\left[1 + \frac{nT}{AG}\right] \qquad . \tag{2.4.8}$$

Because the total effect is of interest for further work, and only derivatives of y_t are involved in the final equation, the subscript is subsequently omitted. If

$$K_e^2 = \frac{T}{EI\left[1 + \frac{nT}{AG}\right]} , \tag{2.4.9}$$

Equation 2.4.8 may be written as

$$y^{iv} - K_e^2\,y'' = 0 \qquad . \tag{2.4.10}$$

Equation 2.4.10 is identical to Equation 2.1.8 except for the substitution of K_e for K. Throughout this thesis the constant K_e identifies a solution which accounts for shear as well as bending.

The general solution of Equation 2.4.10 is:

$$y = C_1 \sinh K_e x + C_2 \cosh K_e x + C_3 x + C_4 . \qquad (2.4.11)$$

The boundary conditions for determining the four constants of Equation 2.4.11 are similar to those used in Section 2.1. However, the angle at the origin is not zero or any other explicit value, but must be written in terms of the normal force at $x = L$, which is initially an unknown. Consequently, five conditions are required, four for the differential equation and one for algebraic relationships.

The condition that $y = 0$ at $x = 0$ yields the result that $C_4 = -C_2$, so that the solution may now be written as

$$y = C_1 \sinh K_e x + C_2 (\cosh K_e x - 1) + C_3 x .$$

From a summation of horizontal forces on the entire free span of Figure 2.4.1, it may be seen that the normal shear force at $x = 0$, N_o, is $T\theta_L + N_L$. Two end conditions are established with this result. First, a consideration of the shear force at $x = 0$ from Equation 2.1.2 yields the result

$$N_L + T\theta_L = - TK_e C_1 / (1 + nT/AG). \qquad N = K_e^3 C_1$$

Secondly, Equation 2.4.1 relates N_o to the shear angle at $x = 0$, giving the result:

$$\frac{n}{AG} (N_L + T\theta_L) = C_3 + C_1 K_e .$$

Elimination of $(N_L + T\theta_L)$ by combining of the above two equations gives an expression for C_3 as a function of C_1:

$$C_3 = - C_1 K_e \frac{1 + 2nT/AG}{1 + nT/AG} \quad .$$

The boundary condition of zero moment at $x = L$, or equivalently that $y_L'' = 0$, as discussed in Section 2.2, establishes the condition

$$C_2 = - C_1 \frac{\sinh K_e L}{\cosh K_e L} \quad .$$

The last necessary boundary condition is that the slope of the downstream end of the web is equal to the roller angle θ_L. The constant C_2 is again given as a function of C_1:

$$C_2 = \frac{\theta_L - C_1 K_e \left[\cosh K_e L - \dfrac{1 + 2 nT/AG}{1 + nT/AG} \right]}{K_e \sinh K_e L} \quad .$$

The last two equations for C_2 may be equated to find C_1, after application of the identity $\cosh^2 K_e L - \sinh^2 K_e L = 1$:

$$C_1 = - \frac{\theta_L}{K_e} \left[\frac{\cosh K_e L}{\dfrac{1 + \dfrac{2nT}{AG}}{1 + \dfrac{nT}{AG}} \cosh K_e L - 1} \right] \quad . \tag{2.4.12}$$

C_2 and other constants may now be obtained by successive substitution into previous equations:

$$C_2 = \frac{\theta_L}{K_e} \left[\frac{\sinh K_e L}{\dfrac{1 + 2 \dfrac{nT}{AG}}{1 + \dfrac{nT}{AG}} \cosh K_e L - 1} \right] \tag{2.4.13}$$

$$C_3 = \theta_L \left[\frac{\cosh K_e L}{\cosh K_e L - \dfrac{1 + \dfrac{nT}{AG}}{1 + \dfrac{2nT}{AG}}} \right]$$ (2.4.14)

$$C_4 = \frac{-\theta_L}{K_e} \left[\frac{\sinh K_e L}{\dfrac{1 + \dfrac{2nT}{AG}}{1 + \dfrac{nT}{AG}} \cosh K_e L - 1} \right]$$ (2.4.15)

The solution to the differential equation 2.4.10 is:

$$\frac{y}{L} = \theta_L \left[\frac{\cosh K_e L}{\cosh K_e L - \dfrac{1 + \dfrac{nT}{AG}}{1 + \dfrac{2nT}{AG}}} \left(\frac{x}{L} \right) - \frac{1}{K_e L} \frac{\cosh K_e L}{\dfrac{1 + \dfrac{2nT}{AG}}{1 + \dfrac{nT}{AG}} \cosh K_e L - 1} \sinh K_e x \right.$$

$$\left. + \frac{1}{K_e L} \frac{\sinh K_e L}{\dfrac{1 + \dfrac{2nT}{AG}}{1 + \dfrac{nT}{AG}} \cosh K_e L - 1} (\cosh K_e x - 1) \right].$$ (2.4.16)

Equation 2.4.16 accounts for deflection due to shear stress. For normalization $K_e x$ may be replaced by its equivalent $(K_e L)(x/L)$. Note that Equation 2.4.16 reduces to Equation 2.1.16 if nT/AG is equal to zero, in which case K_e is equal to K.

Figures 2.4.2 through 2.4.5 are plots of Equation 2.4.16. These figures should be carefully studied to note the effect of shear deflection. The effect of shear decreases with increasing values of $K_e L$. If $K_e L = 0.1$ (Figure 2.4.2) a value of nT/AG
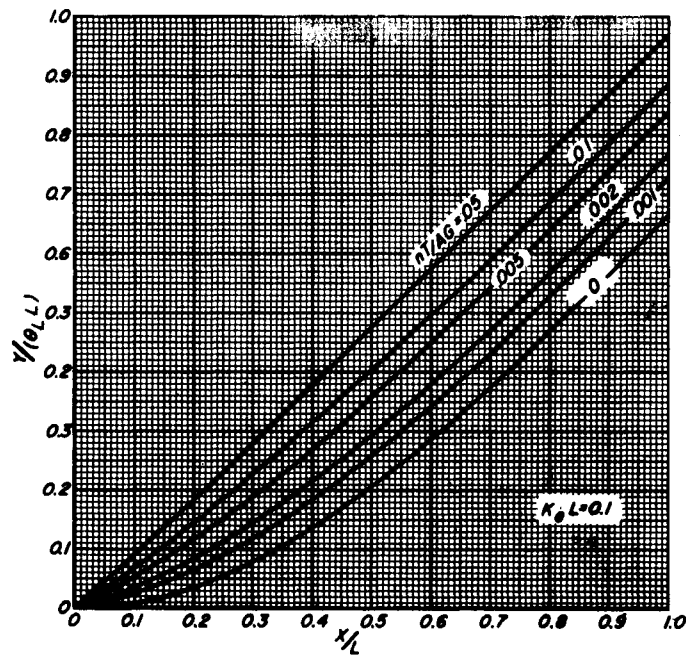
Figure 2.4.2. Static Elastic Curves
for $K_e L = 0.1$.
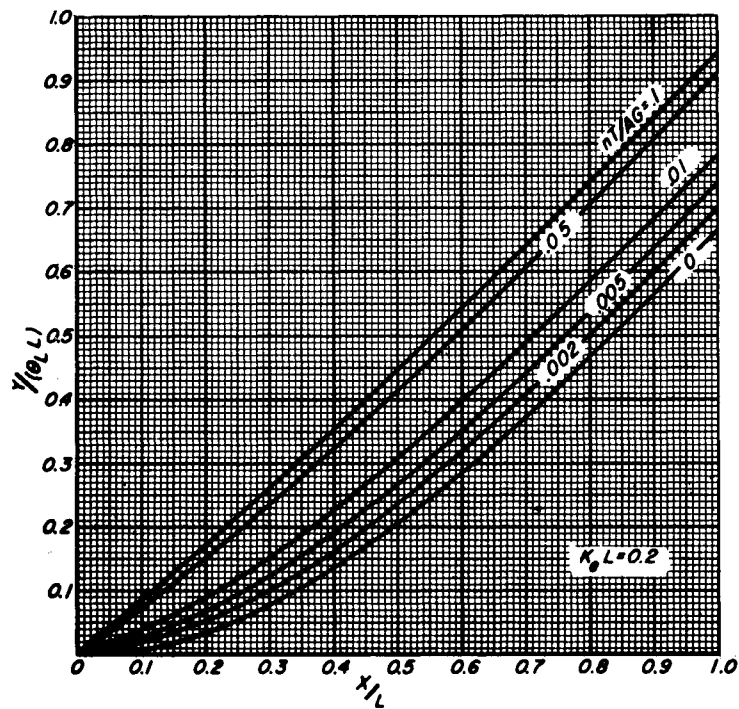
Figure 2.4.3. Static Elastic Curves
for $K_e L = 0.2$.
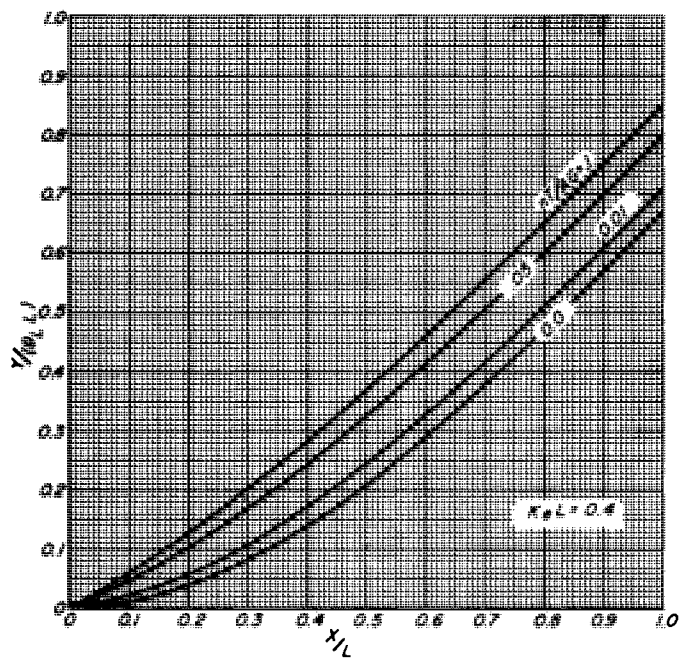
Figure 2.4.4. Static Elastic Curves
for $K_e L = 0.4$.
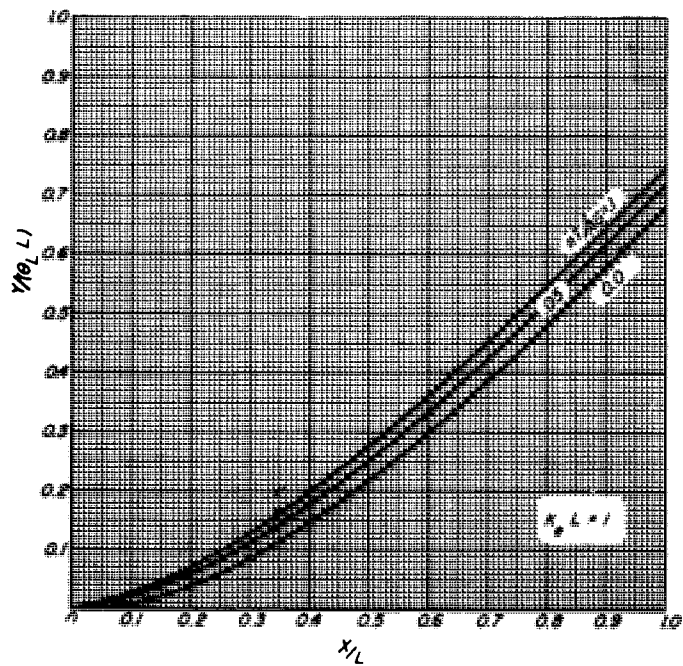
Figure 2.4.5. Static Elastic Curves
for $K_e L = 1$.

of 0.001 is significant, but if $K_e L = 1$ (Figure 2.4.5) a value of nT/AG of 0.05 has little effect. If $K_e L$ is greater than unity, the effect of shear is usually negligible.

Equations and relations of interest may be derived from Equation 2.4.16 exactly as their counterparts were derived from Equation 2.1.16.

The curvature factor K_c is

$$K_c = \frac{y_L}{L\theta_L} = \left[\frac{\cosh K_e L}{\cosh K_e L - \dfrac{1 + \dfrac{nT}{AG}}{1 + \dfrac{2nT}{AG}}}\right] - \frac{1}{K_e L}\left[\frac{\sinh K_e L}{\dfrac{1 + \dfrac{2nT}{AG}}{1 + \dfrac{nT}{AG}}\cosh K_e L - 1}\right] \qquad (2.4.17)$$

The effect of nT/AG on the curvature factor is shown in Figure 2.4.6.

The maximum moment M_o is $-EIy_o''$. Successive differentiation of Equation 2.4.11 and substitution of zero for x yield the result that $M_o = -EI\, C_2 K_e^2$, or from Equation 2.4.13:

$$M_o = -EI\theta_L K_e \left[\frac{\sinh K_e L}{\dfrac{1 + \dfrac{2nT}{AG}}{1 + \dfrac{nT}{AG}}\cosh K_e L - 1}\right] .$$

From Equation 2.4.9 and because $\theta_L L K_c = y_L$:

$$\frac{M_o}{Ty_L} = -\frac{1}{K_e L K_c}\left[\frac{\sinh K_e L}{\left(1 + \dfrac{2nT}{AG}\right)\cosh K_e L - \left(1 + \dfrac{nT}{AG}\right)}\right] . \qquad (2.4.18)$$

The negative of $M_o/Ty_L)$ is plotted in Figure 2.4.7. Consideration of shear is obviously much more important for low values of $K_e L$ than for high values.

K_C (CURVATURE FACTOR)

1.0

.95

.9

.85

.8

.75

.7

.65

$nT/AG = 25$

.1

.05

.01

.005

.002

.001

0

.1 .2 .3 .4 .5 .6 .7 .8 .9 1.0 $K_e L$ 2 3 4 5 6 7 8 9 10
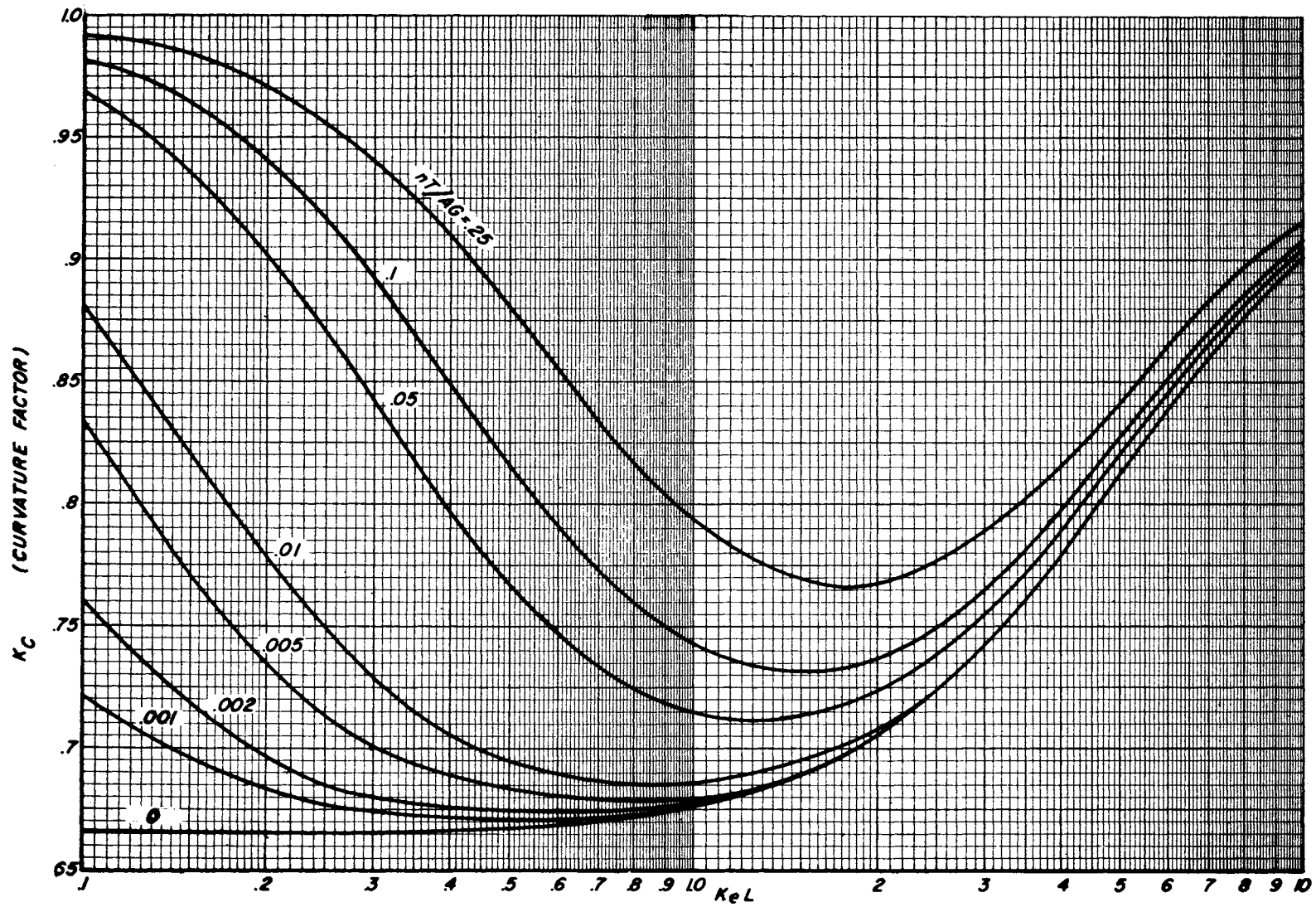
Figure 2.4.6. Effect of Shear and $K_e L$ on Curvature Factor.
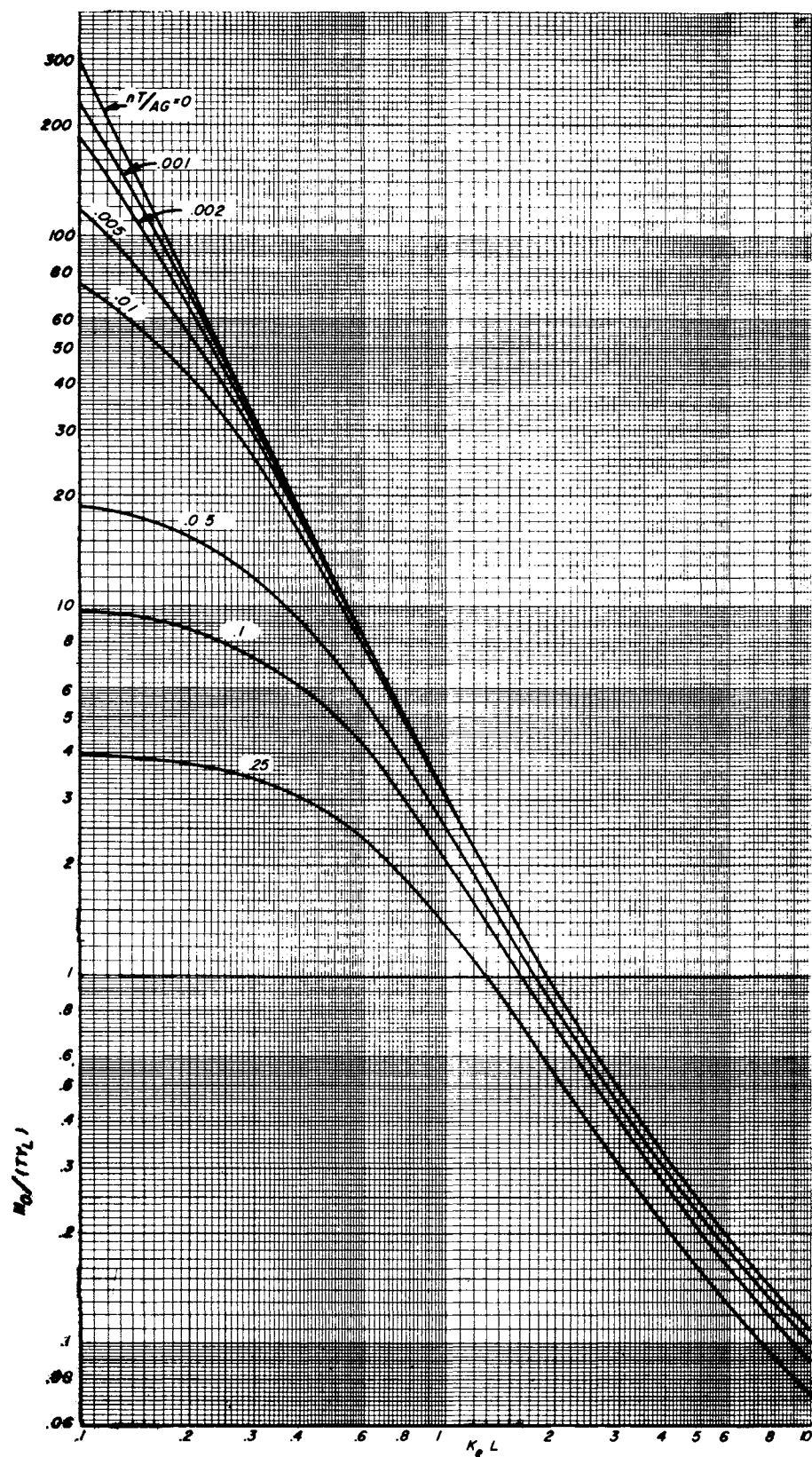
Figure 2.4.7. Effect of Shear and $K_e L$ on $M_o/(Ty_L)$.

Although no tests were run under conditions such that shear was significant, it is of interest to compare the steady-state normal force at the guide roller to that of Equation 2.1.21. Three differentiations of Equation 2.4.16, substitution of L for x, and application of the identity $\cosh^2 K_e L - \sinh^2 K_e L = 1$ yields the result:

$$\frac{N_L}{T\theta_L} = \frac{1}{\left(1 + \frac{2nT}{AG}\right)\cosh K_e L - \left(1 + \frac{nT}{AG}\right)} \qquad . \qquad (2.4.19)$$

Because nT/AG is usually less than 0.01, except for woven webs, the side force is determined quite accurately by Equation 2.1.21, the equation verified by experiment as reported in Section 2.2.

For the "critical moment" condition, M_o is equal to $-TW/6$, and $y_L)_{cr}$ is equal to $K_c L\theta_L)_{cr}$. Substituting these relations into Equation 2.4.18 and rearranging leads to the results:

$$\theta_L)_{cr} = \frac{K_e L}{6} \ \frac{W}{L} \ \left[\frac{\left(1 + \frac{2nT}{AG}\right)\cosh K_e L - \left(1 + \frac{nT}{AG}\right)}{\sinh K_e L}\right] , \qquad (2.4.20)$$

and

$$\frac{y_L}{W}\bigg)_{cr} = \frac{K_e L}{6} \ K_c \left[\frac{\left(1 + \frac{2nT}{AG}\right)\cosh K_e L - \left(1 + \frac{nT}{AG}\right)}{\sinh K_e L}\right] . \qquad (2.4.21)$$

These equations reduce to Equations 2.1.23 and 2.1.24 if nT/AG is equal to zero.

Equation 2.4.20 or 2.4.21 defines the conditions for which a web is taut over its entire width, which is the only condition studied in this thesis. Equation 2.4.21 specifies the maximum correction permissible by a steering guide without incurring slackness. Figure 2.4.8, a plot of Equation 2.4.21, shows that the permissible correction is hardly affected by values of nT/AG up to 0.01, if $K_e L$ is more than 0.5, but that at lower values of $K_e L$ the effect of small values of nT/AG is quite significant.
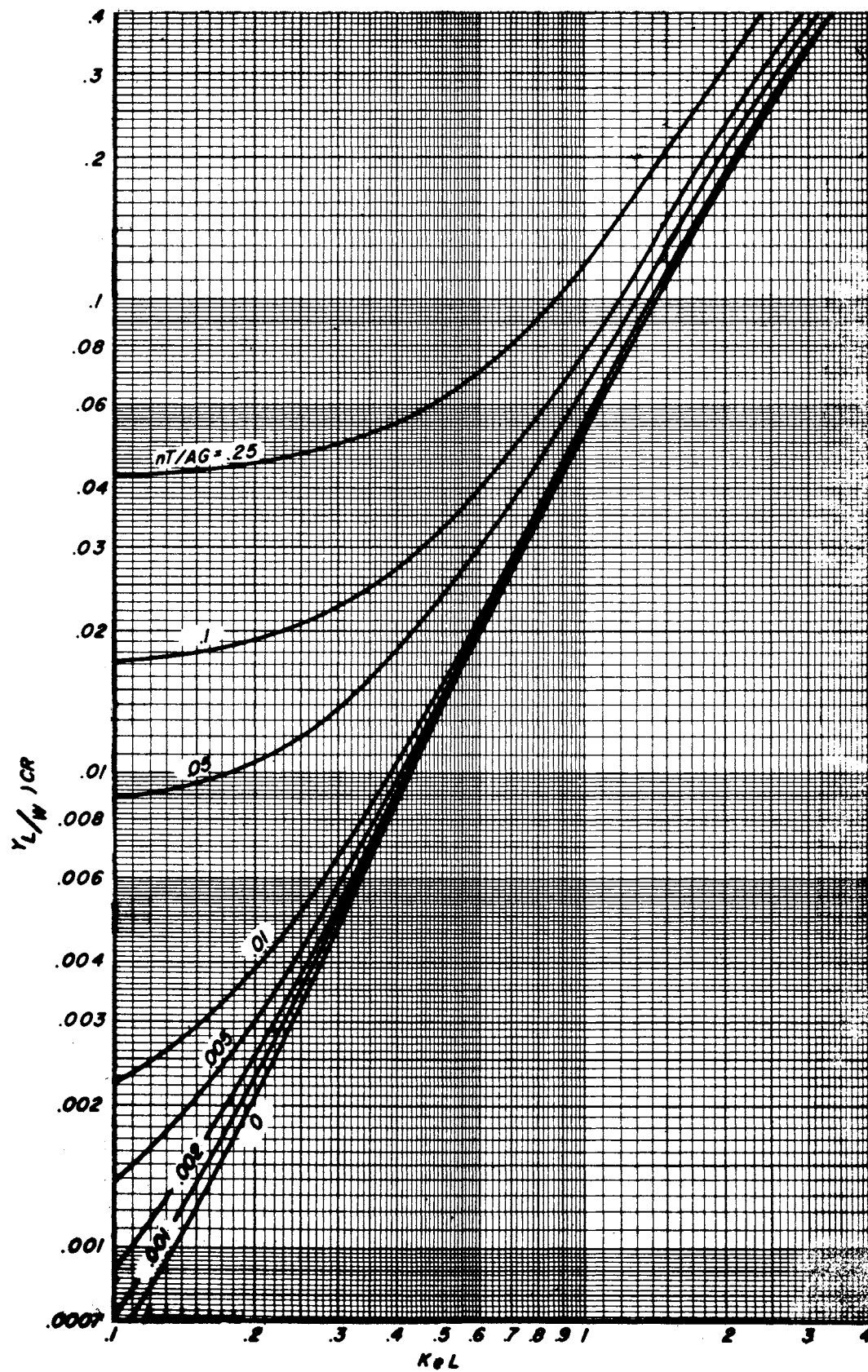
Figure 2.4.8. Effect of Shear and $K_e L$ on Critical Guide Correction.

The value of y_L/W required for satisfactory guiding varies widely in practice because of the great variations in material properties, web imperfections, process machine imperfections, line length and type of process encountered. However, for the sake of illustration, the error to be corrected is assumed to be plus and minus 5 percent of the web width; in other words, $(y_L/W)_{cr}$ must be equal to 0.05. Figure 2.4.8 shows that if nT/AG is less than 0.01, K_eL must be nearly equal to unity, but that if nT/AG were 0.1, K_eL could be as low as 0.72, and if nT/AG were 0.25 then K_eL could be as low as 0.31. Any larger value of K_eL would be permissible, but a smaller value would result in a slack edge when the maximum correction was attempted.

It is usually desired to build machines with web spans as short as possible. In other words, K_eL is usually as small as possible. The value of K_eL is probably seldom greater than three or four, even for a web span through an oven. But unless nT/AG is quite significant, K_eL must be larger than 0.6 or so in order to allow much correction by a steering guide. This section shows that if nT/AG is 0.05 or greater, somewhat smaller values of K_eL become practical, but such a large value of nT/AG is probably never encountered except with woven webs. It is suspected but not confirmed that values of nT/AG are commonly in the range of 0.01 to 0.10 for certain loosely woven webs.

Many web materials are stressed approximately at a given level regardless of the web dimensions. For example, steel is commonly run at 2000 to 3000 psi stress. The value of nT/AG for steel at 2500 psi tensile stress is 0.0003. A stainless steel belt has been known to be stressed at over 7000 psi, for which case nT/AG was approximately 0.001.

An unusual application was a titanium belt at a temperature of 400°F, stressed at 40,000 psi. The value of nT/AG was thus approximately 0.008.

Kouris (11) reported a mean curve for tension versus paper weight, based upon more than fifty paper and paper-board installations. The mean stress level was 600 psi. If the shear modulus of paper is assumed to be 180,000 psi, then nT/AG would be equal to 0.004 for a typical paper process machine.

2.5. Velocity Effect on Static Behavior. There is an effect of longitudinal velocity on the curvature of a web, whether the web behavior problem is steady state or dynamic. The reason for the effect is that the web negotiates a curve in its free span as it is guided. The mass of the web contributes a lateral inertia force proportional to its mass and lateral acceleration. The lateral (radial) acceleration of a point as it traverses a curve of radius R is V^2/R. The lateral force on a small element of length dx inches from a web of width W inches, thickness t inches, and density ρ pounds per cubic inch is

$$dF = \frac{V^2}{R} \frac{\rho W t}{386} dx \quad . \tag{2.5.1}$$

if V is measured in inches per second and R in inches. But R is the inverse of the curvature y", so Equation 2.5.1 may be rewritten as

$$\frac{dF}{dx} = \frac{V^2 \rho W t}{386} y" \quad . \tag{2.5.2}$$

A condition of side loading modifies Equation 2.1.8 only to the extent that the side load per unit length divided by EI appears on the right-hand side of the equation, as covered by Timoshenko and Gere (23). The side loading has an opposite sign to the curvature, as shown in Figure 2.5.1, so the differential equation of the elastic curve in the free span may be written as

$$y^{iv} - \frac{T}{EI} y" = - \frac{V^2 \rho W t}{386 \, EI} y"$$
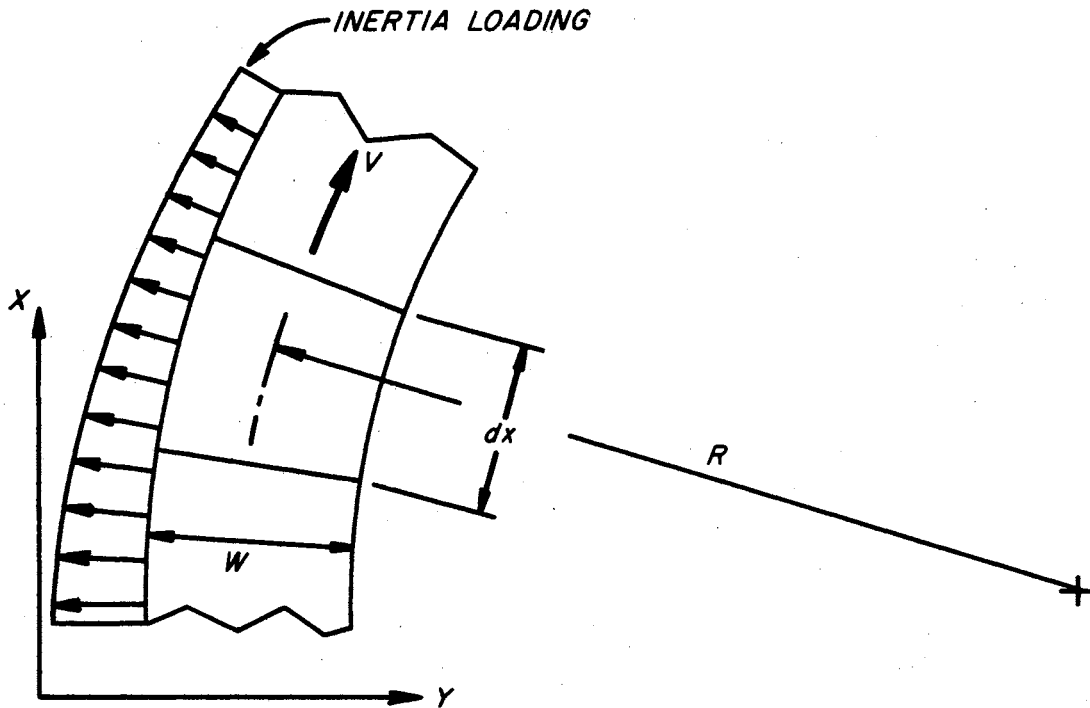
Figure 2.5.1. Inertia Loading Caused by Web Curvature.

which may be rewritten as a homogeneous equation

$$y^{iv} - \frac{T - V^2 \rho W t / 386}{EI} \, y'' = 0 \quad . \qquad (2.5.3)$$

If the symbol K_v is used to denote an equivalent K that allows for the effect of velocity, then

$$K_v^2 = \frac{T - V^2 \rho W t / 386}{EI} \qquad (2.5.4)$$

or equivalently

$$K_v^2 = \frac{A}{EI} \left(S_1 - \frac{V^2 \rho}{386} \right) \quad , \qquad (2.5.5)$$

where A is the cross-sectional area of the web, equal to tW, and S_1 is the average tensile stress in the web.

Equation 2.5.5 allows simple evaluation of the magnitude of the velocity effect. If a stress of 2500 psi is assumed for steel, the velocity effect amounts to 10 percent of the tensile effect if V^2 (0.283)/386 is equal to 250, or at a velocity of 584 inches per second or 2920 feet per minute. Such a speed is currently rare for steel process lines, but cold-rolling mills may go twice that fast, in which case the velocity effect would be 40 percent of the assumed tensile effect.

If the density of paper is assumed to be 0.02 pounds per cubic inch and the average tensile stress 600 psi, the velocity effect amounts to 10 percent of the tensile effect at a speed of 5400 feet per minute. However, special circumstances may sometimes arise in which a lighter tension is desired, so that the velocity effect would be more significant.

Although this chapter is concerned with static web behavior, it may be noted that the derivation of the velocity effect did not assume a static condition. Therefore, the K_v defined by Equation 2.5.4 or 2.5.5 could be substituted for K in the following chapters, if the web velocity is exceptionally high or the tension unusually low.

2.6. Static Behavior of Inelastic Materials. One might be tempted to apply the reduced modulus concept, originally derived by Theodore von Karman in his doctoral dissertation on inelastic buckling of columns, to the free span of a steered web; however, a careful study reveals that the von Karman reduced modulus would be incorrect.

The reduced modulus theory would apply to a material which is stressed into its inelastic range, as at Point 0 of Figure 2.6.1, and to which a moment is then applied. The moment would cause one side, denoted by A, to be stressed higher on the same curve, but the stress on the other side to be reduced. The reduction in stress follows a different curve, as shown by B.
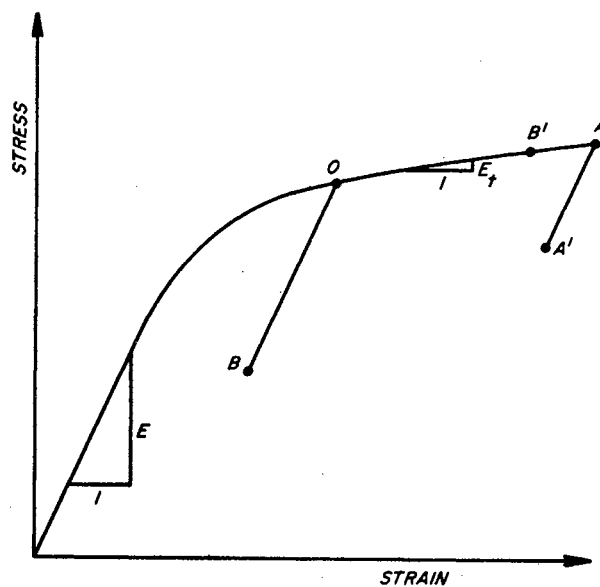
Figure 2.6.1. Inelastic Material Behavior of a Steered
Web in the Entering Span.

A guided web in its free entering span, however, has already had its sides

extended and contracted to Points A and B of Figure 2.6.1 as it traversed the con-

tact area of the entering roller. As it traverses the free span the material at Point

A goes to the condition of Point A' and that at B goes through Point 0 and to B'.

It is generally assumed that lines OB and AA' are parallel to the initial stress-strain

curve.

An exact analysis of the behavior of an inelastic guided web would be very

complicated, because the effective modulus would vary with x. Therefore, apparent-

ly no overall effective modulus could be used, and the differential equation would

have to be written in terms of a variable effective modulus. The effective modulus

would be greater than von Karman's reduced modulus because a greater portion of

the cross-section would exhibit the initial modulus than it does in the reduced modu-

lus theory.

Figure 2.6.2 shows a steady-state deflection curve of the inelastic web of

Figures 2.3.5 and 2.3.6. The inelasticity did not cause any drastic departure from

the shape of an elastic web, even though the inelastic behavior was extreme. The data points are shown, along with curves for moduli of elasticity assumed as E_t $(E_t = 4000, KL = 2.75)$, E_r $(E_r = 9250, KL = 1.8)$, and E (E = 40,000, KL = 0.87). As would be expected from the previous discussion, the curve which best fits the data points would lie between the two curves based upon E and E_r for most of the span. Note the great insensitivity of the elastic curves to changing values of the modulus of elasticity.

The gross inelasticity of the example would probably never be encountered in practice except for woven webs, where internal friction of the thread causes hysteresis.
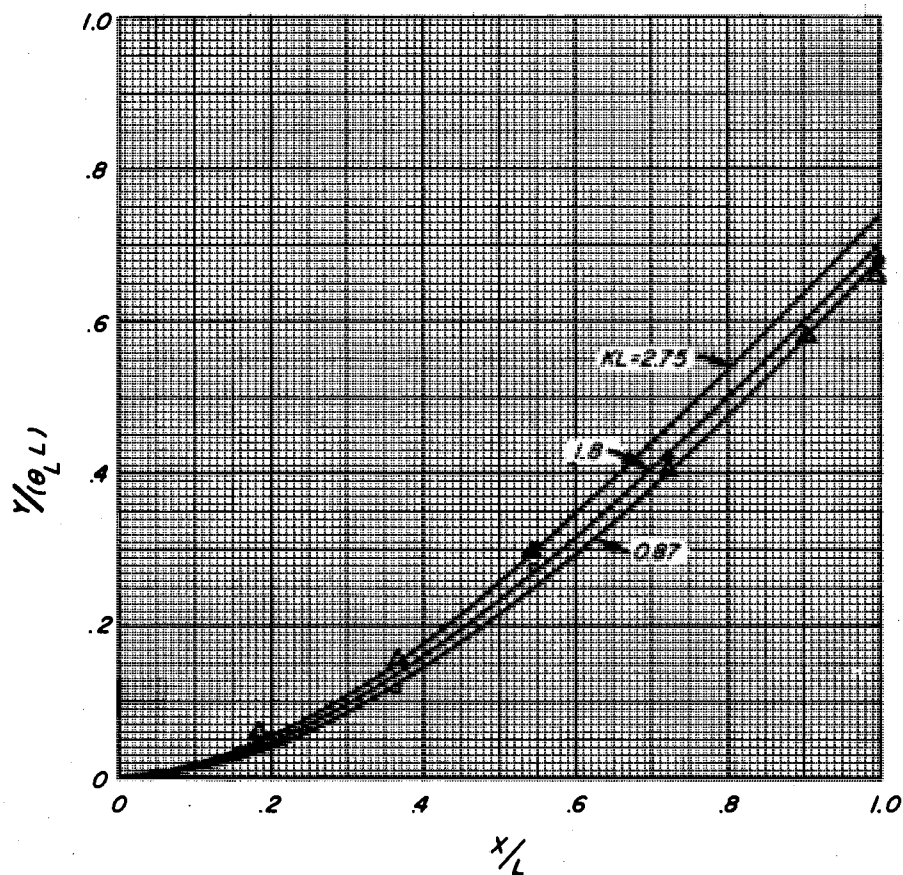
Figure 2.6.2. Comparison of a Test of an Inelastic Web to
Curves With Different Modulus Assumptions.

CHAPTER III

FIRST-ORDER DYNAMICS OF A MASSLESS WEB

This chapter considers lateral web dynamics under the idealizing assumption that the web has no shear strength and that it therefore stretches in a straight line between rollers. Changes in direction caused by non-parallel rollers occur as sharp angles at the rollers. The derivations are strictly kinematic; physical properties of the web are ignored.

With the notable exception of uncoated tire cord fabric, few webs approach the assumed behavior under all conditions. However, Chapter II showed that if nT/AG is relatively large and K_eL quite small, the web exhibits little curvature and makes a sharp break at the entering roller. Note, for example, the curve in Figure 2.4.2 for nT/AG of 0.05.

This chapter is included to provide a simple basis for the more complicated dynamics of Chapters IV and V and to demonstrate limiting conditions which the more complex dynamics approach as certain parameters become extreme. The theory is demonstrated for several practical combinations of guide rollers and stationary rollers.

3.1. Fundamental Theory. The fundamental law of static steering under the simplifying assumptions of this chapter is that the web in the entering span approaching any given roller aligns itself perpendicularly to the roller. The web therefore would make sharp angular breaks as it leaves each roller in a series of non-parallel rollers, as shown in Figure 3.1.1.
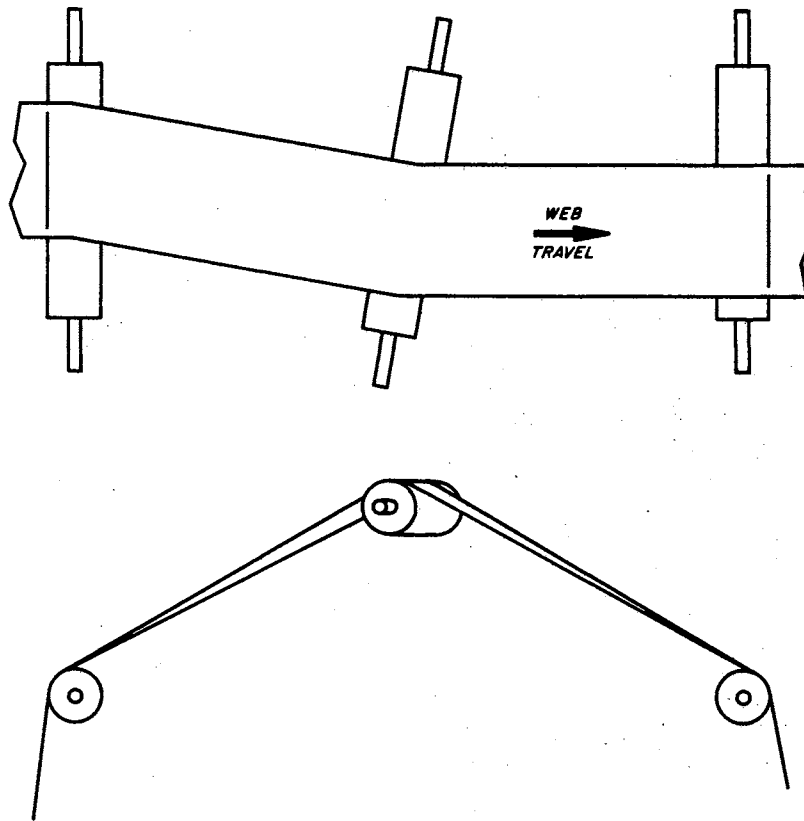
Figure 3.1.1. Web Passing Over a Series
of Non-Parallel Rollers.

The steady-state frictional force required to prevent lateral slippage of the

idealized web is obtained by taking components of the tensile force T along and

perpendicular to the upstream roller. The lateral force is equal to $T\theta$, where θ is

the total angle of nonparallelism of the rollers at each end of the web span of interest,

as viewed normal to the center line of the web. The pressure of the web on a single

roller is equal to T/WR, where W is the web width and R the roller radius. The pres-

sure multiplied by the circumferential length of lateral slippage in the contact area,

by the coefficient of friction, and by the width of the web must equal the side force.

If β is the angle of the arc of lateral slippage:

$$\frac{T}{WR} \; (\beta RW)(\mu) = T\theta \quad .$$

The arc of slippage is therefore equal to θ/μ, for the conditions assumed. A wrap angle of θ/μ is required to prevent complete lateral breakaway of the entire web on the upstream roller.

If the thinking of the previous paragraph is reversed and a transient relationship between the web and the downstream roller is considered instead of the steady-state relationship between the web and the upstream roller, the basis for the simplified theory of lateral web dynamics is established. If an error is assumed to displace the entering span out of perpendicularity to the downstream roller, slippage on the entering side of the contact area extends far enough into the contact area for the necessary friction force to be developed. Because of the assumed condition of zero shear strength, the web in the entire free span is straight. All points in and immediately preceding the contact area, such as Point A of Figure 3.1.2, are steered straight forward relative to the roller. Therefore the rate of lateral movement of the web edge is proportional to θ, the angle of deviation from perpendicularity between the web and roller, and to the velocity of the web.

If the roller is moving laterally, the total velocity of the web edge relative to the ground is equal to the sum of the velocity of steering of the web and the velocity of lateral transport of the web. In other words, the velocity of the web edge relative to the ground is equal to the velocity of the web edge relative to the roller plus the velocity of the roller relative to the ground.
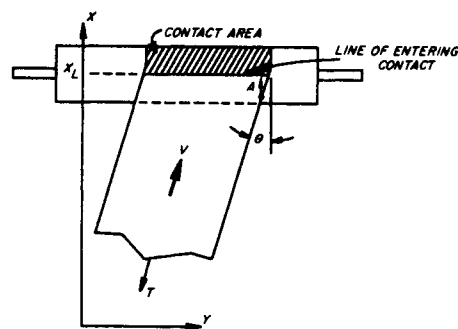
Figure 3.1.2. Steering Action of an Idealized Web.

The above two components of web velocity at the downstream roller may be expressed by the equation:

$$\frac{dy_L}{dt} = -V\theta + \frac{dz}{dt} \quad , \tag{3.1.1}$$

where z is the position of the downstream roller relative to the ground. The negative sign accounts for the fact that a positive angle as shown results in a negative velocity.

3.2. Response at Fixed Roller to Input at Previous Roller. The result of the derivation of this section was first reported by Campbell (3). However, the technique of derivation, which forms a basis for later derivations, has not been published.

The two rollers shown in Figure 3.2.1 are fixed and parallel to each other. The length of the free span is L. The web displacement at x_o is y_o, the input. The output is y_L, the web displacement at x_L. The angle of the web relative to the roller at x_L is $(y_L - y_o)/L$. The downstream roller is stationary. Therefore, from Equation 3.1.1,

$$\frac{dy_L}{dt} = -V\frac{y_L - y_o}{L} \quad , \tag{3.2.1}$$

or, taking the Laplace transform and assuming zero initial conditions,

$$SY_L(S) = -\frac{V}{L} Y_L(S) + \frac{V}{L} Y_o(S) \quad . \tag{3.2.2}$$

Rearrangement results in the transfer function:

$$\frac{Y_L(S)}{Y_o(S)} = \frac{1}{T_1 S + 1} \quad , \tag{3.2.3}$$
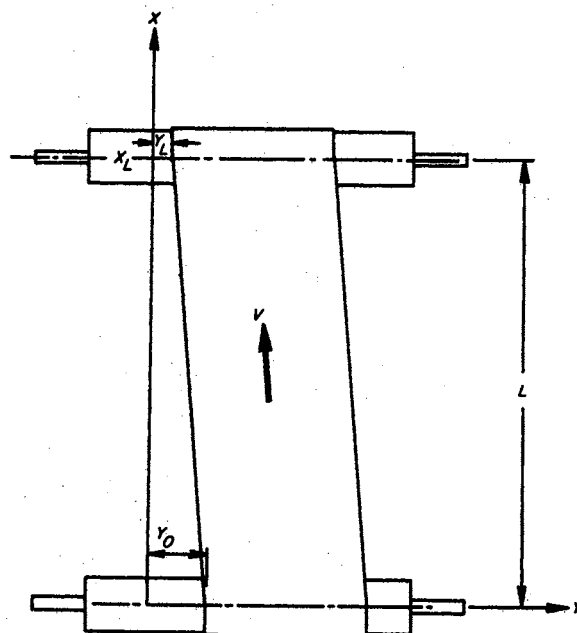
Figure 3.2.1. Symbols for Derivation of Response
at Fixed Roller.

where T_1 is the time constant:

$$T_1 = \frac{L}{V} \qquad .$$

<div style="text-align: right">(3.2.4)</div>

Equation 3.2.3 may be recognized as the transfer function of a first-order system, a simple lag. T_1 is the time required by a point on the web to traverse the free span. The frequency response of Equation 3.2.3 is shown in Figure 3.2.2. Note that the phase lag approaches 90 degrees and the amplitude ratio approaches zero at high frequencies.

Equation 3.2.3 may be used for the response of a web on a roller with the input being the position of the web at a point in the free span, if T_1 is considered to be the time constant of the web from the sample point to the next roller, not the time constant of the entire free span.
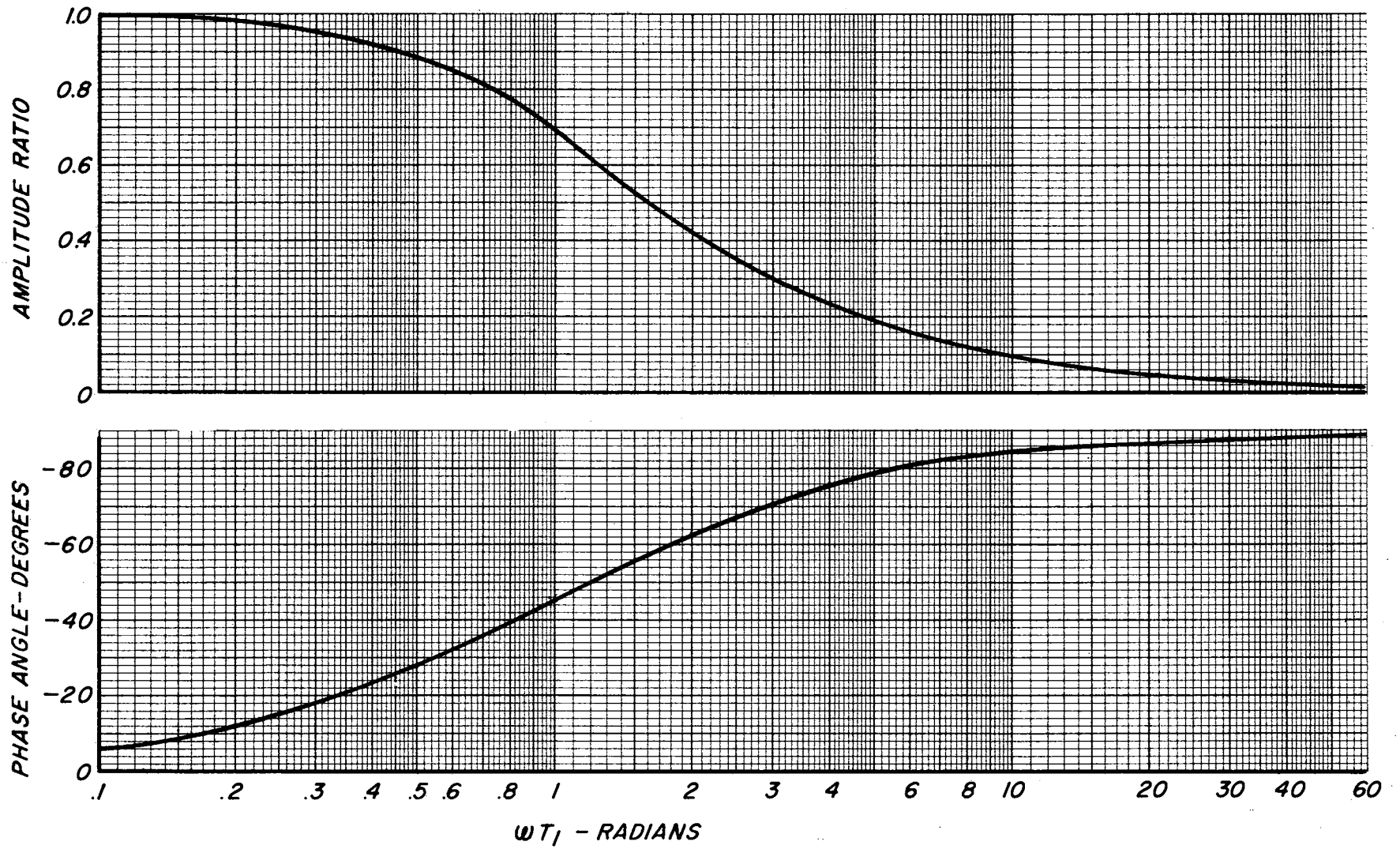
Figure 3.2.2. Frequency Response of Web at Fixed Roller to Input at Previous Roller.

3.3. Steering Guide Response. Figure 3.3.1 shows a steering guide with an instant center a distance L_1 upstream in the plane of the entering span. The entering span has a length of L, which may be greater or less than L_1. The lateral displacement of the roller at the downstream end of the free span is the input, z. The displacement of the web relative to the ground at the guide roller is the output, y_L.
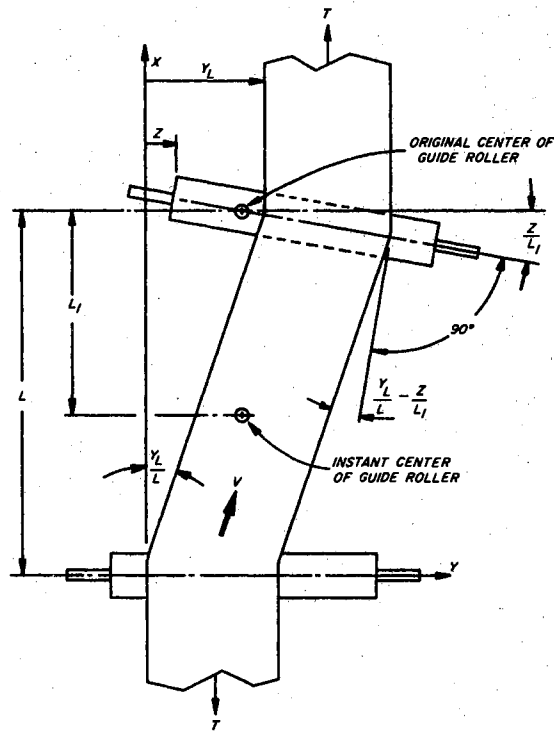
Figure 3.3.1. Symbols and Arrangement for
Derivation of Steering Guide
Response.

The angle of the guide roller is z/L_1 radians. The angle between the guide roller and the web is $(y_L/L) - (z/L_1)$. From Equation 3.1.1:

$$\frac{dy_L}{dt} = -V\left(\frac{y_L}{L} - \frac{z}{L_1}\right) + \frac{dz}{dt} \quad . \qquad (3.3.1)$$

The application of the Laplace transform for zero initial conditions yields the equation

$$SY_L(S) + \frac{V}{L} Y_L(S) = \frac{V}{L_1} Z(S) + SZ(S).$$ (3.3.2)

Note that for this idealized case the static steering factor is L/L_1, because the steady-state web angle is equal to the roller angle z/L_1, and the steady-state value of y_L is $(L)(z/L_1)$. The definition of the static steering factor is the ratio of the steady-state web position to the lateral roller position, or

$$S.S.F. = \frac{(L)(z/L_1)}{z} = \frac{L}{L_1} .$$ (3.3.3)

If L/V is replaced by T_1 (the entering time constant), Equation 3.3.2 may be written as the transfer function

$$\frac{Y_L(S)}{Z(S)} = \frac{T_1 S + (L/L_1)}{T_1 S + 1} .$$ (3.3.4)

Equation 3.3.4 is plotted in frequency response form in Figure 3.3.2 for the oversteering case (instant center between the guide roller and the entering roller) and Figure 3.3.3 for the understeering case (instant center upstream from the entering roller). Note that phase lag is associated with oversteering and phase lead with understeering, but that the amplitude ratio approaches unity at high frequencies regardless of the value of the static steering factor.

The phase characteristics of Figures 3.3.2 and 3.3.3 are identical to those of simple RC lead-lag networks. The amplitude characteristics are similar to those of the RC networks, but their gain levels differ.
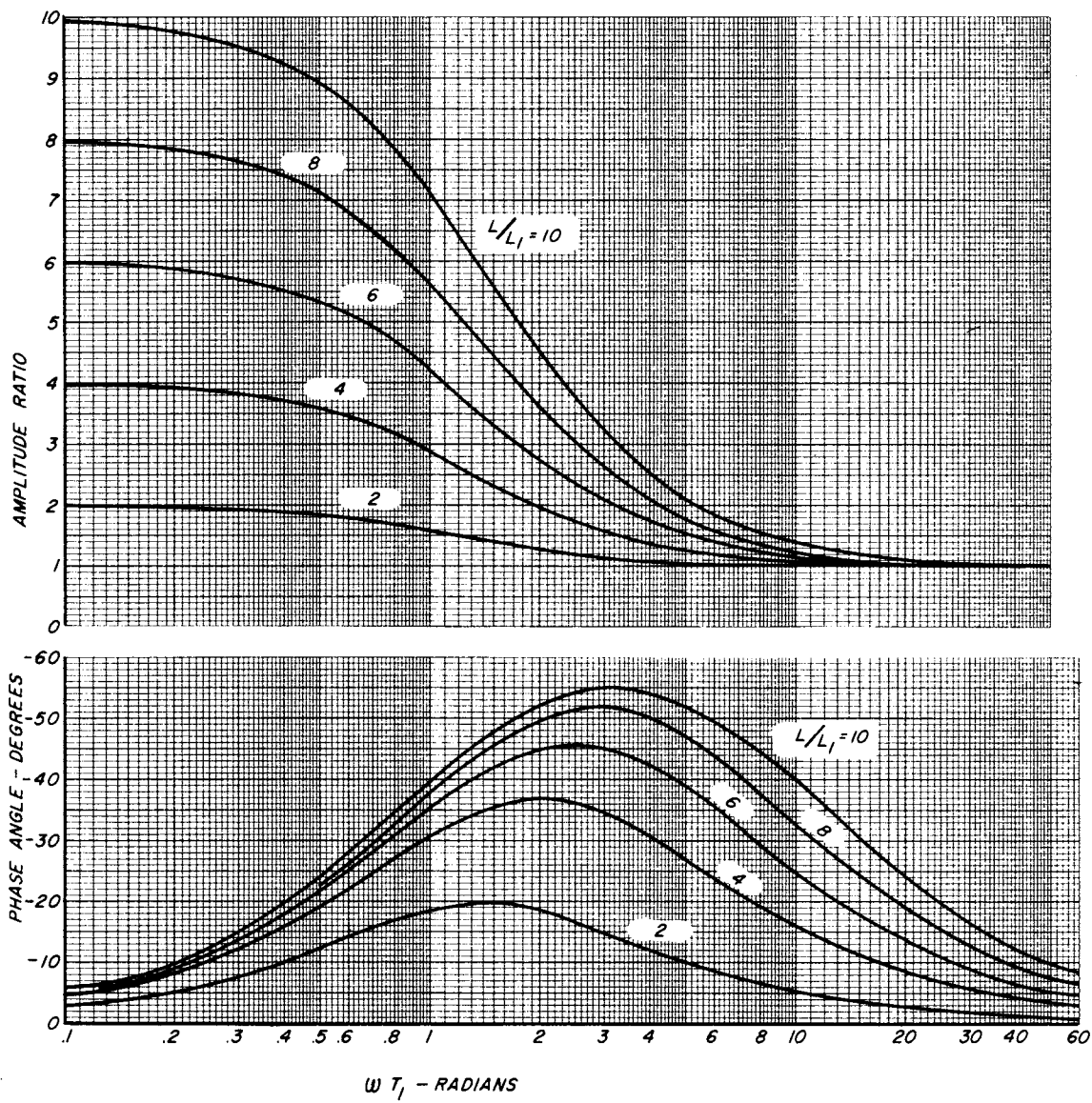
Figure 3.3.2. Frequency Response of an Oversteering Guide.
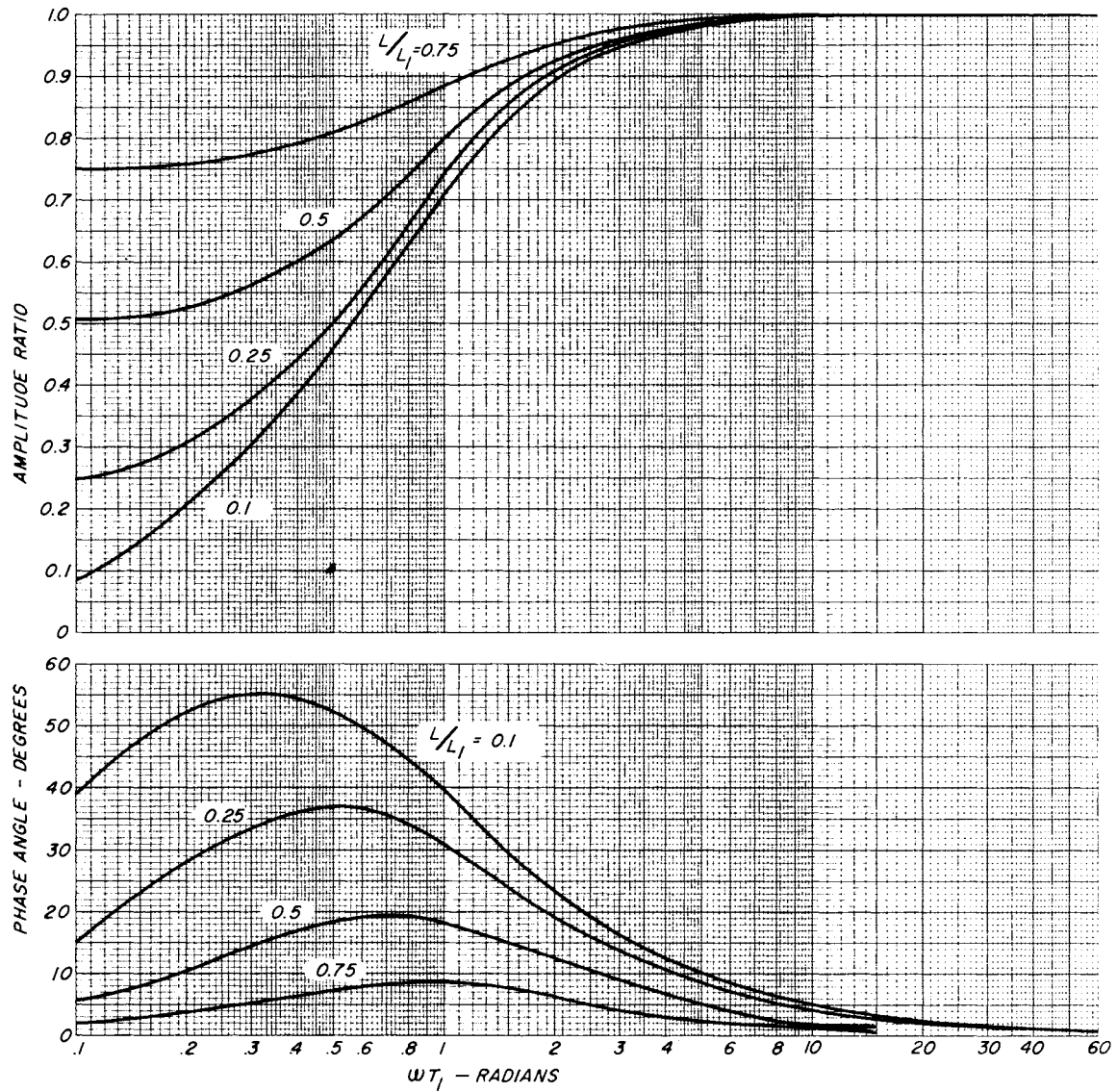
Figure 3.3.3. Frequency Response of an Understeering Guide.

3.4. Response at a Point Between Two Parallel Rollers.

Figure 3.4.1 shows a web between two rollers which are parallel when viewed perpendicularly to the centerline of the web as shown. The two rollers may be non-parallel in other views, because twisting of the web is assumed to have no effect on its behavior.
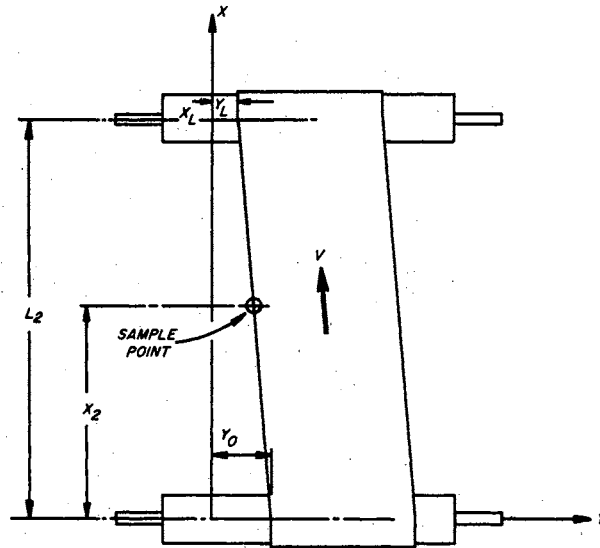
Figure 3.4.1. Symbols for Derivation of Response
Between Two Parallel Rollers.

The input is y_o, and there is no restriction upon the method of generation of y_o. For example, the first roller could be the guide roller considered in Section 3.3, with the output y_L of Section 3.3 being the input y_o of this analysis.

The second roller is assumed to be fixed. The response y_2 is to be found at a sample point a distance x_2 downstream from the first roller. The response at the downstream roller is y_L. From Equation 3.2.3:

$$Y_L(S) = \frac{Y_o(S)}{T_2 S + 1} \quad , \qquad (3.4.1)$$

where T_2 is the time constant of the free span under consideration. Because of the
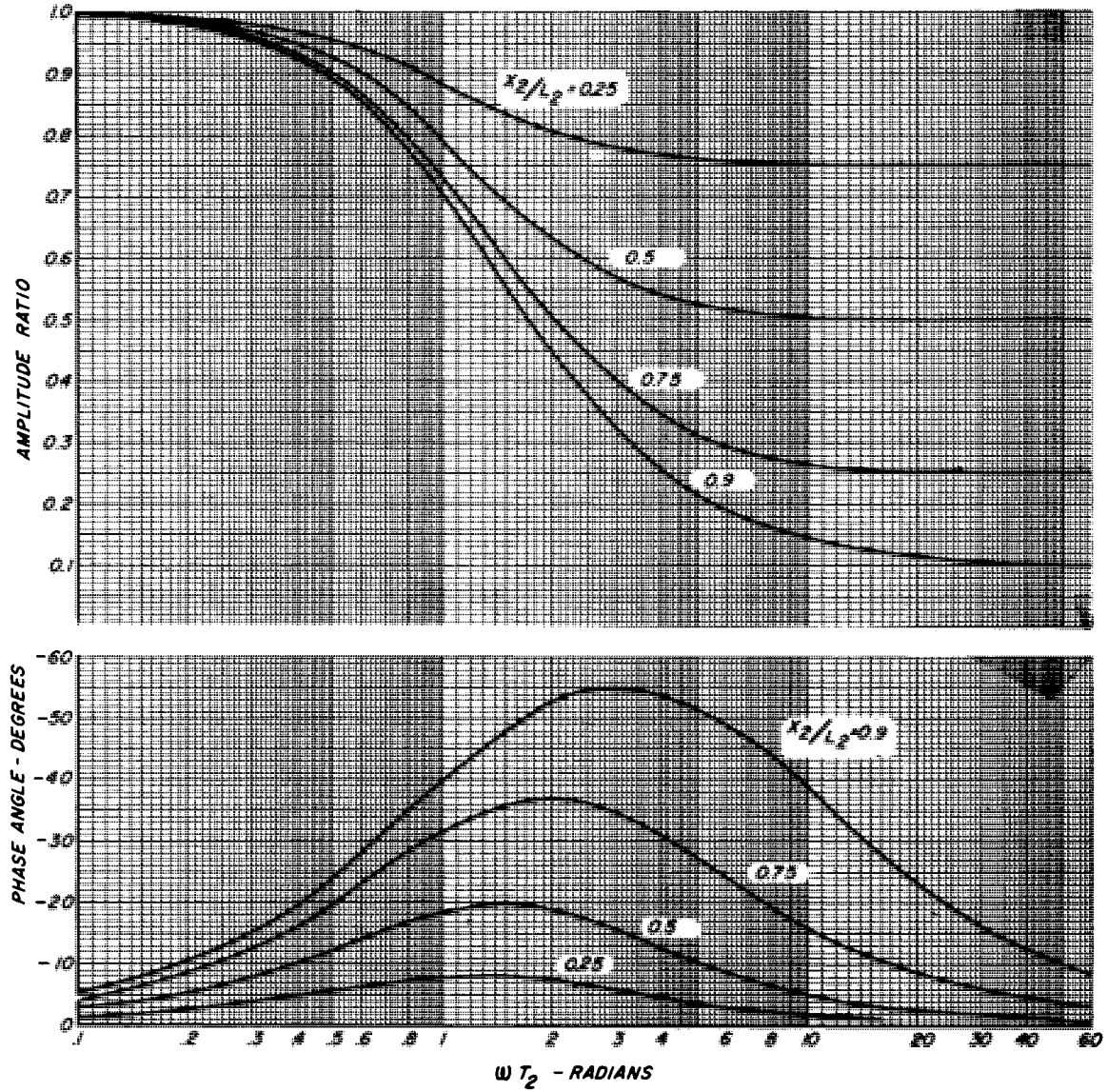
Figure 3.4.2. Frequency Response at a Point Between Two Parallel Rollers.

assumed straight web path:

$$Y_2 = Y_L \mp \left(\frac{Y_o - Y_L}{L_2}\right)(L_2 - x_2) \quad . \qquad (3.4.2)$$

Equation 3.4.2 may be reduced to the equation:

$$Y_2 = Y_o \left(1 - \frac{x_2}{L_2}\right) + Y_L \left(\frac{x_2}{L_2}\right) \quad . \qquad (3.4.3)$$

Applying the Laplace transform to Equation 3.4.3, substituting Equation 3.4.1, and simplifying gives the transfer function:

$$\frac{Y_2(S)}{Y_o(S)} = \frac{T_2 (1 - x_2/L_2) S + 1}{T_2 S + 1} \quad . \qquad (3.4.4)$$

The frequency response characteristics of Equation 3.4.4 are shown in Figure 3.4.2. Note that a sensing head in the exiting span always results in a phase lag, but the lag approaches zero as the sensing head is moved nearer the guide roller. The control system stability problem is generally less severe in this case than for the lagging response to an oversteering guide, because the gain of the oversteering guide is greater than unity, whereas the gain for the exiting span dynamics is less than unity.

3.5. First-Order Theory for Conventional Steering Guide. First-order theory covered thus far in this chapter may be summarized in the form of a transfer-function block diagram of a conventional steering guide system.

The dynamics of the controller, actuator and the machine structure are not within the scope of this thesis and will not be considered. The dynamics of hydraulic servo systems, electric servo motors, and mechanical structures, as well as techniques for system compensation are well known.
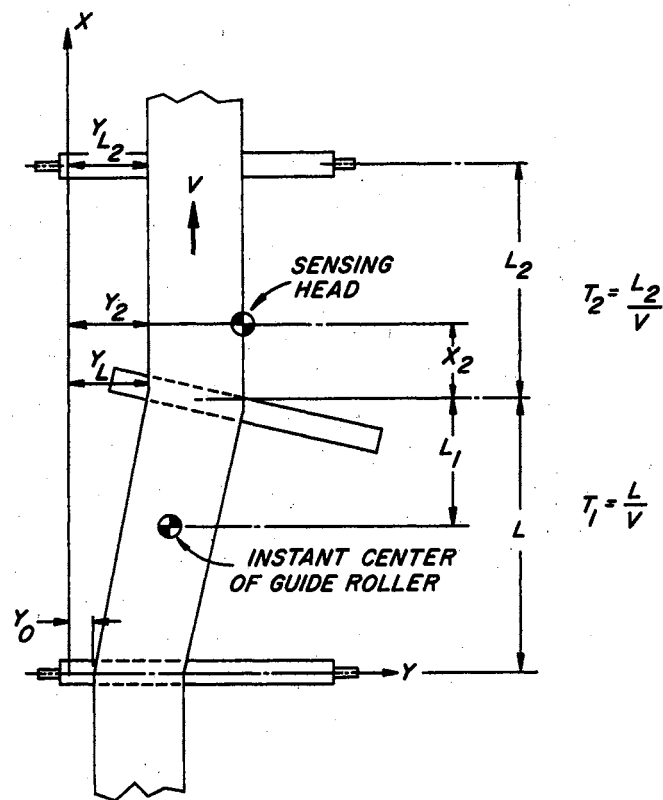
Figure 3.5.1. Schematic of Conventional
Steering Guide.

The common arrangement of a steering guide locates the sensing head in the exiting span. The schematic for such a system is shown in Figure 3.5.1, and the block diagram is shown in Figure 3.5.2. The transfer functions are obtained from Equations 3.3.4, 3.2.3, and 3.4.4. The dynamics in the exiting span beyond the sensing head are outside the control loop, but are a simple lag according to first-order theory. Neither attenuation nor phase lag is of great importance outside the control loop, so the post-guiding dynamics would be of little interest if the first-order theory were actually correct. Web curvature predicted by second-order theory, however, can adversely affect the accuracy of guiding at points beyond the sensing head.

According to the first-order theory, the entering span of the steering guide contributes no dynamics to the system if the axis of the instant center of the guide

ENTERING SPAN DYNAMICS

$$\frac{Y_0}{\quad}$$
ERROR AT
ENTERING
ROLLER

$$\frac{1}{T_1 S + 1}$$

ENTERING SPAN
DYNAMICS

EXITING SPAN
TO SENSING HEAD

EXITING SPAN
DOWNSTREAM
OF SENSING HEAD

R
DESIRED
GUIDE
POINT

CONTROLLER
AND
ACTUATOR

Z

$$\frac{T_1 S + \frac{L}{L_1}}{T_1 S + 1}$$

Y_L

$$\frac{(1 - X_2/L_2)T_2 S + 1}{T_2 S + 1}$$

Y_2

$$\frac{1}{(1 - X_2/L_2)T_2 S + 1}$$
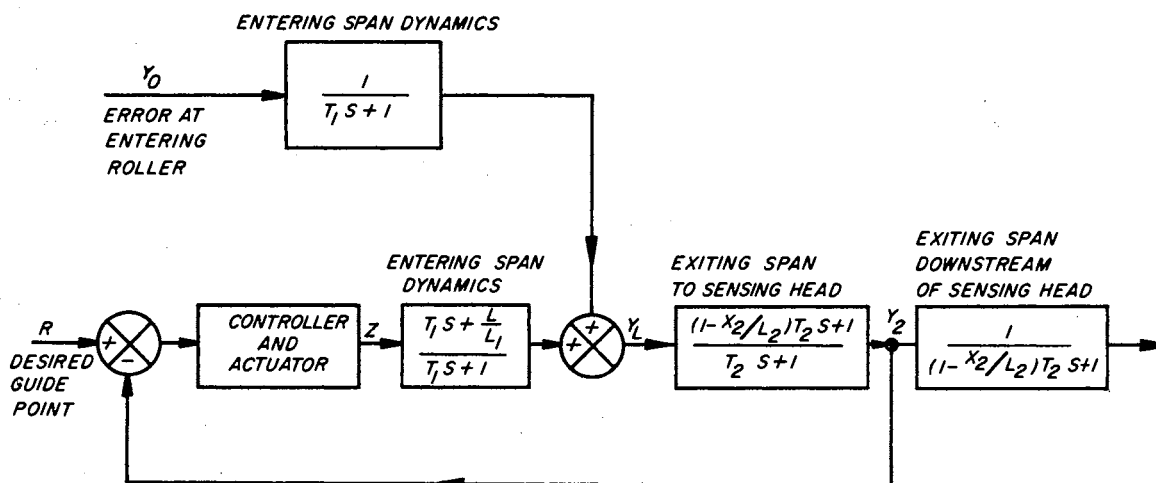
Figure 3.5.2. Block Diagram of Conventional Steering Guide.

passes through the center of the entering roller ($L = L_1$). The exiting span contributes no dynamics if the web is sensed just as it passes over the roller, as may be done with reflective photoelectric sensing. The temptation to utilize the phase lead characteristics of an understeering guide should be tempered with the knowledge that its dynamics vary with web speed.

3.6. Transport Lag Across Roller. If the shear strength of a web is low, or zero as assumed in this chapter, there may be a significant transport time lag across the contact area of a roller. This time lag is caused by the fact that if the friction is sufficient, the web cannot move relative to the roller as it traverses the contact area.

If the circumferential length of the contact area is very short in relation to the free web span, as is usually the case with steering guides, the transport lag may be neglected.

The Laplace transform of a signal delayed by time T is equal to e^{-ST} multiplied by the Laplace transform of the signal.

An example of a guide which may be significantly affected by the transport

lag is a single-roller displacement guide. The transport lag is outside the control

loop and is therefore no problem if the guide is pivoted about an axis in the enter-

ing span of the web, as displacement guides are commonly designed. In such a

case, the entering span is merely twisted and does not respond to guide roller

position. However, structural considerations may favor a center-pivoted displace-

ment guide, which is used as an example of a transport lag problem in the following

paragraphs.

Three views of the guide under consideration are shown in Figure 3.6.1. The

input z is considered to be the lateral motion of the roller at the downstream end of

the contact area. From Equation 3.1.1,

$$\frac{dy_L}{dt} = -V\left(\frac{y_L}{L}\right) - \frac{dz}{dt} \quad . \tag{3.6.1}$$
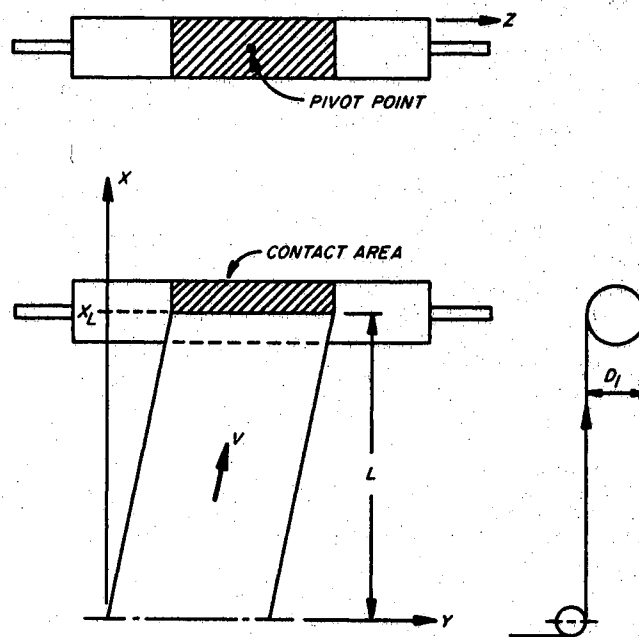
Figure 3.6.1. Schematic of Single-Roller
Center-Pivoted Displacement
Guide.

The negative sign on the $d\dot{z}/dt$ term is because of the fact that a positive dz/dt causes a negative dy_L/dt. The transfer function arising from Equation 3.6.1 is

$$\frac{Y_L(S)}{Z(S)} = \frac{-T_1S}{T_1S+1} \qquad . \qquad (3.6.2)$$

If friction is sufficient to effect the time lag across the roller, the web behavior across the roller may be expressed as

$$y_D(t) = y_L(t - \mathcal{T}) + z(t - \mathcal{T}) + z(t) \quad , \qquad (3.6.3)$$

where y_D is the web position relative to the ground at the point of departure from the contact area and $\mathcal{T}$ is the transport lag. The transport time is:

$$\mathcal{T} = \pi D_1/2V \qquad . \qquad (3.6.4)$$

The Laplace transform of Equation 3.6.3 is:

$$Y_D(S) = e^{-S\mathcal{T}}Y_L(S) + e^{-S\mathcal{T}}Z(S) + Z(S) \quad . \qquad (3.6.5)$$

If Equation 3.6.5 is divided by $Z(S)$, Equation 3.6.2 substituted, and the result algebraically rearranged, the transfer function for the web dynamics of the entire guide except for the sensing arrangement in the exiting span is found to be:

$$\frac{Y_D(S)}{Z(S)} = \frac{T_1S + 1 + e^{-(\pi/2)(D_1/L)T_1S}}{T_1S + 1} \qquad . \qquad (3.6.6)$$

The exiting span dynamics are covered in Section 3.4.

The frequency response characteristics of Equation 3.6.6 are shown in **Figures** 3.6.2 and 3.6.3 for values of D_1/L of one-fifth and unity. As L becomes **large** in relation to D_1, the low-frequency dynamics approach those of Equation 3.3.4 **for a**
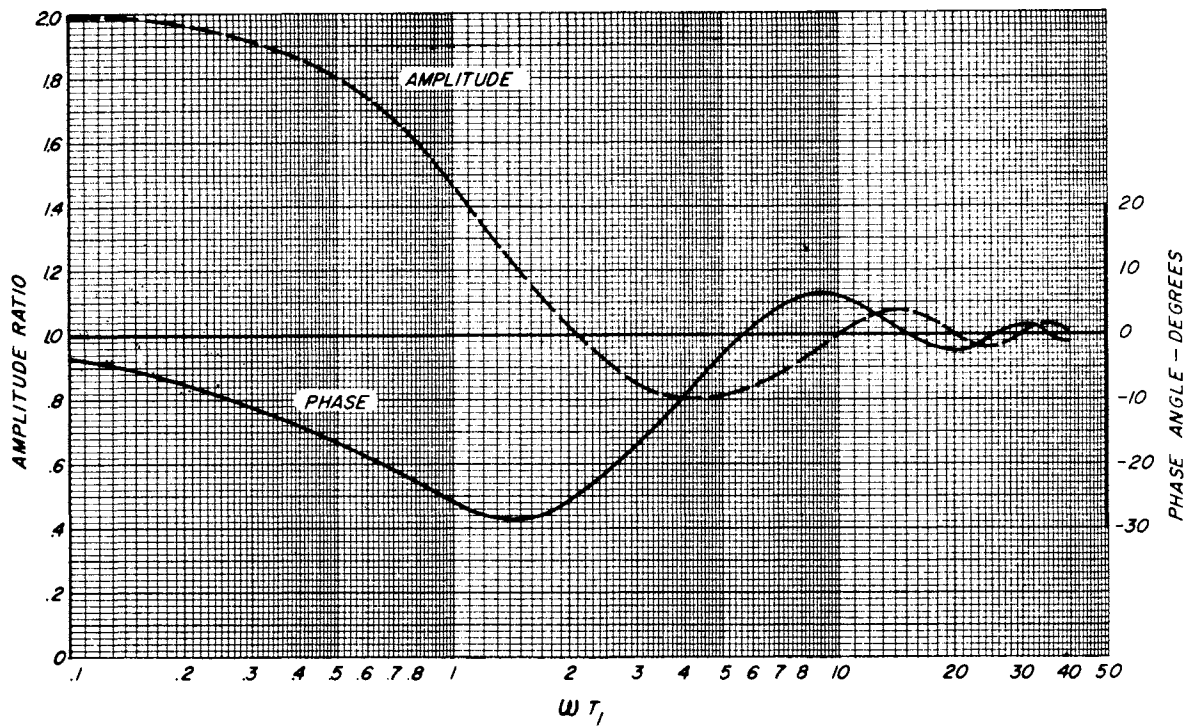
Figure 3.6.2. Frequency Response of Single-Roller Center-Pivoted
Displacement Guide for $D_1/L = 0.2$.
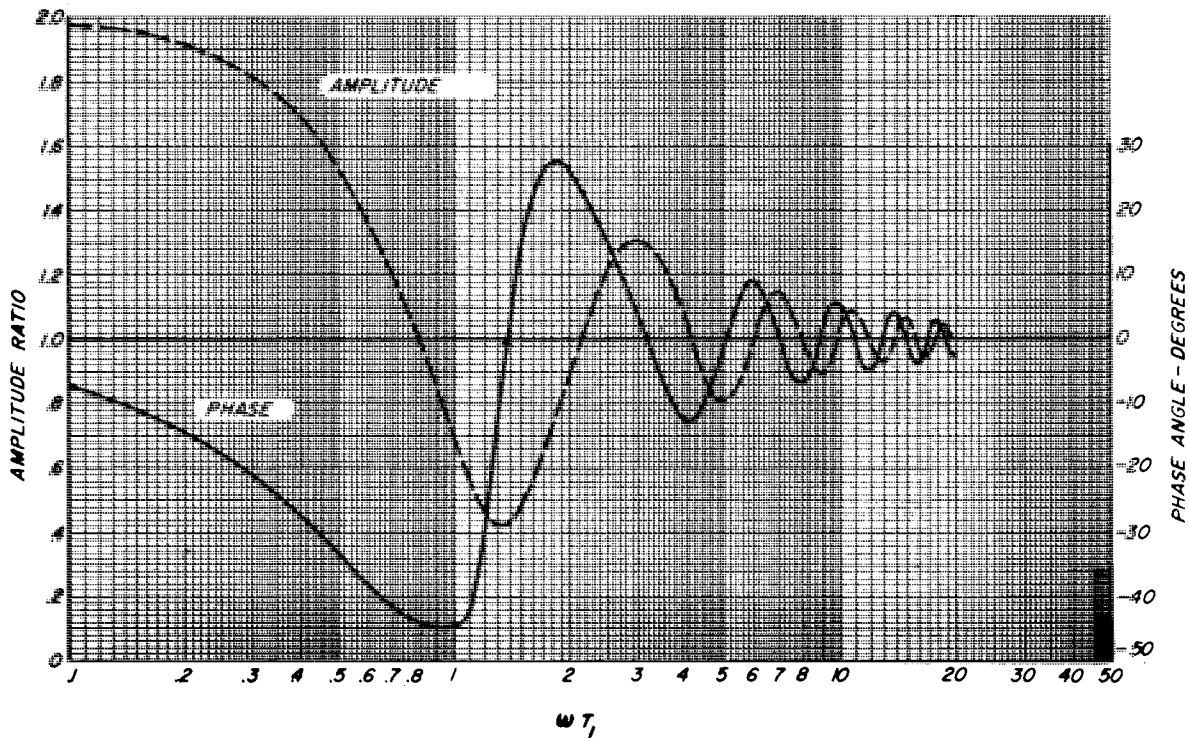
Figure 3.6.3. Frequency Response of Single-Roller Center-Pivoted
Displacement Guide for $D_1/L = 1$.

steering guide with a static steering factor of two. Figure 3.6.3 shows that the

response changes drastically with frequency if D_1 is equal to L.

3.7. Center-Pivoted or End-Pivoted Steering Guide Response. This section

is included to demonstrate the application of the fundamental dynamics of the pre-

vious sections to a specialized guide configuration.

A schematic of the center-pivoted guide under consideration is shown in

Figure 3.7.1. An understanding of the behavior of the guide requires more than

a passing glance. Section 3.3 shows that the static steering factor of a center-

pivoted guide is infinite, because L_1 is zero. The low-frequency gain relative to
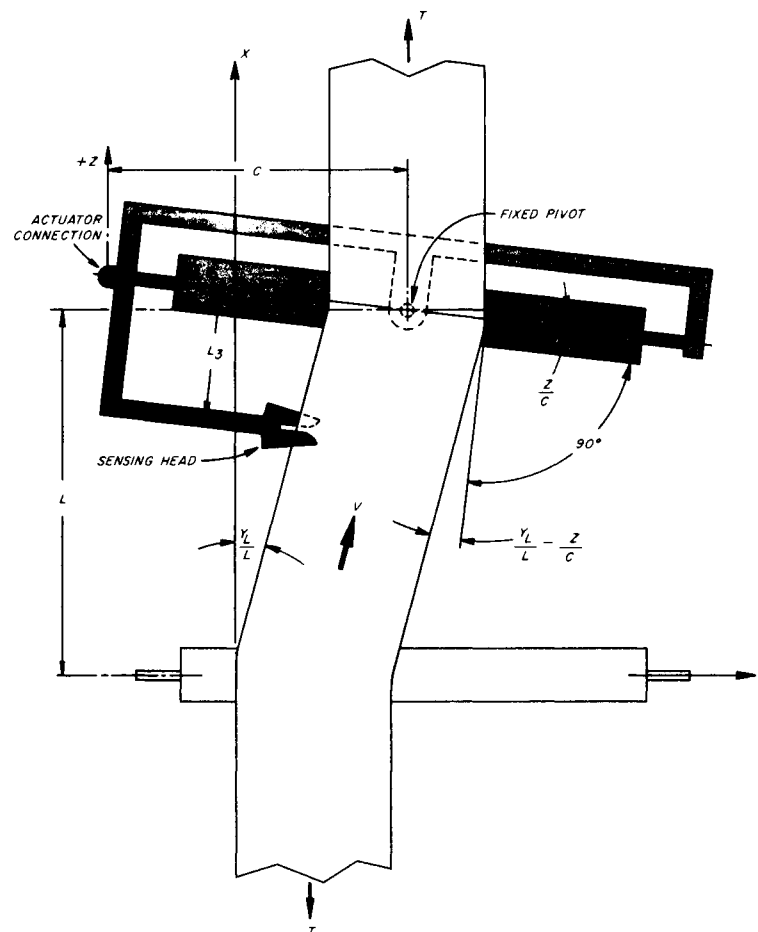
Figure 3.7.1. Schematic of Center-Pivoted Steering
Guide With Position Feedback.

lateral roller position would be infinite and the phase lag would approach 90 degrees. But with the sensing head mounted as shown in Figure 3.7.1, the response of Section 3.3 is not the response of ultimate interest. The motion of the sensing head creates position feedback from the guide roller as though it were a Type 0 system. However, the steady-state guide point change at the sensing head is exactly the correct amount to compensate for the web shift in the entering span, if curvature between the sensing head and the guide roller is neglected. The net result for the ideal web is exact steady-state positioning of the web on the guide roller.

The block diagram of the servo system of Figure 3.7.1 is shown in Figure 3.7.2. The controller-actuator combination usually contains an integrator, but the internal feedback loop, which is usually necessary for stability, destroys the integrating action. The response to web error between the sensing head and the guide roller is different from the response to roller position; therefore, the summation of signals in the block diagram occurs at the guide roller, not at the sensing head.
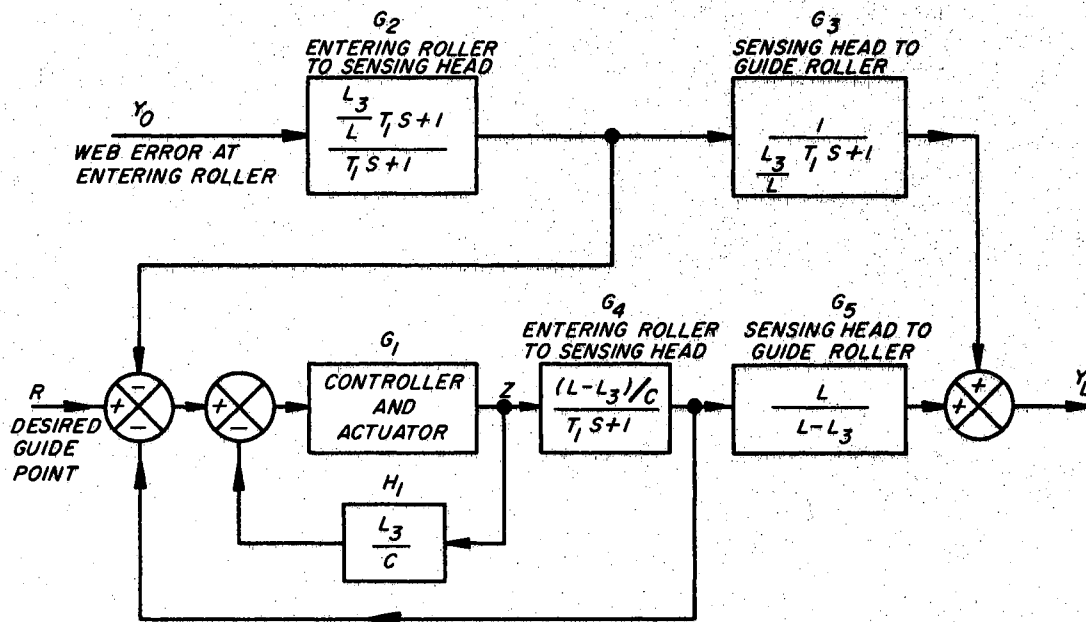
Figure 3.7.2. Block Diagram of Center-Pivoted Steering Guide With Position Feedback.

The derivation of the fundamental transfer function of a center-pivoted steering guide is similar to that of the steering guide of Section 3.3. Equation 3.1.1 in this case becomes

$$\frac{dy_L}{dt} = -V\left(\frac{y_L}{L} - \frac{z}{C}\right) ,$$

(3.7.1)

because there is no lateral motion at the guide roller. Note that the z of this section is different than the z of Equation 3.1.1. The Laplace transform yields the result

$$(S + \frac{V}{L}) \, Y_L(S) = \frac{V}{C} \, Z(S) ,$$

(3.7.2)

or in transfer function form:

$$\frac{Y_L(S)}{Z(S)} = \frac{L/C}{T_1 S + 1} .$$

(3.7.3)

The web in response to z moves at only one end, in contrast to the problem of Section 3.4, and behaves as a simple lever with its end dynamics given by Equation 3.7.3. Sensing at an intermediate point in the span necessitated the breakup of the dynamics of Equation 3.7.2 into G_4 and G_5. Equation 3.4.4, with minor changes in nomenclature, gives G_2, and Equation 3.2.3 leads to G_3. A simple lever consideration results in H_1.

The reference signal R is the lateral position of the sensing head on its shifting arm or the guide point position adjustment. Elementary closed-loop control theory confirms that the steady-state response of y_L to the input R is unity and that the steady-state response of y_L to the disturbance y_o is zero. Such response is characteristic of a Type I control system, but the system under consideration is not a true Type I system, because no pure integrator exists in its forward loop.

The dynamics of an end-pivoted steering guide would be the same as those derived in this section for the center-pivoted guide, if C is still the distance from the actuator to the pivot point. The end-pivoted guide would cause a transient change in average tension in certain installations.

3.8. General Two-Roller Displacement Guide Dynamics. It is sometimes inconvenient to locate the axis of rotation of a displacement guide in the entering web span. This section generalizes the location of the pivot axis. The rollers are assumed to be small in relation to the web spans, so that transport lags can be neglected.

The derivation is based upon Figure 3.8.1. The input is z, the lateral motion of the second roller of the guide. The static guiding factor is L/L_1. If L_1 is less than L the result is overguiding; if L_1 is greater than L the result is underguiding.
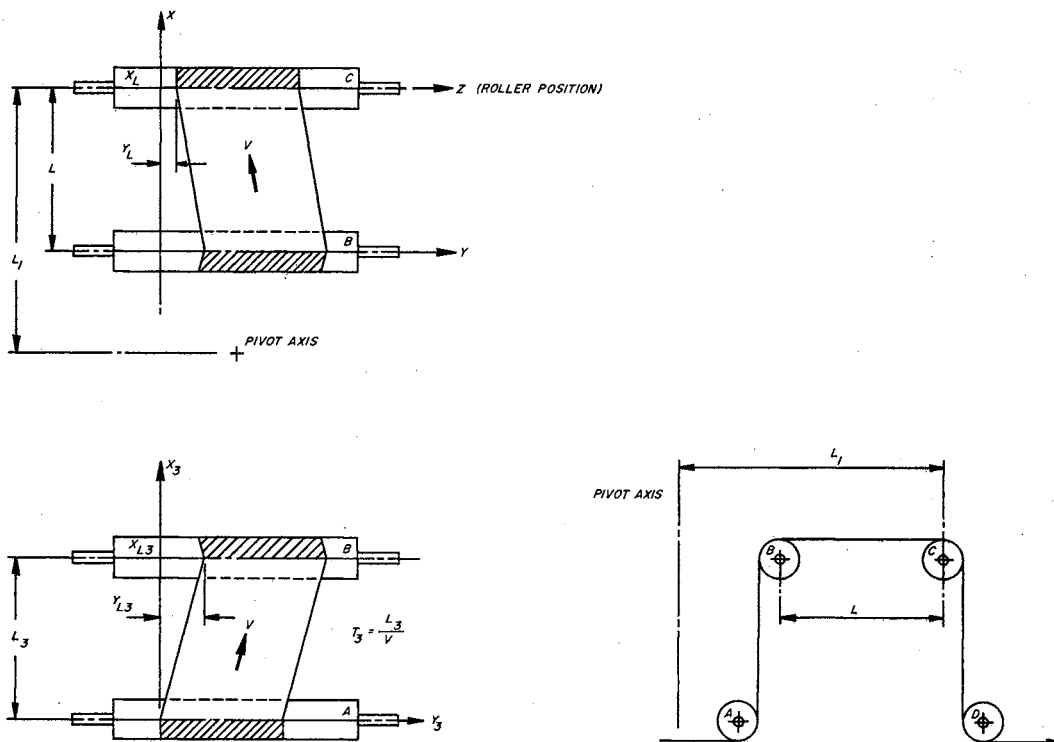
Figure 3.8.1. Schematic of General Two-Roller Displacement Guide.

The lateral motion of the first roller is $(1 - L/L_1)z$; therefore, its velocity is $(1 - L/L_1)(dz/dt)$. The differential equation of motion of the entering span, from Equation 3.1.1, is:

$$\frac{dy_{L3}}{dt} = -V\left(\frac{y_{L3}}{L_3}\right) + \left(1 - \frac{L}{L_1}\right)\frac{dz}{dt} \quad . \tag{3.8.1}$$

The differential equation for the span between the shifting rollers of the guide is:

$$\frac{dy_L}{dt} = -V\left(\frac{y_L - y_{L3}}{L} - \frac{z}{L_1}\right) + \frac{dz}{dt} \quad . \tag{3.8.2}$$

Equation 3.8.1 can be converted to the transfer function

$$\frac{Y_{L3}(S)}{Z(S)} = \frac{(1 - L/L_1)\,T_3 S}{T_3 S + 1} \quad . \tag{3.8.3}$$

Equation 3.8.3 may be substituted into Equation 3.8.2 after the Laplace transform has been applied to obtain the overall transfer function of the guide, except for exiting span dynamics:

$$\frac{Y_L(S)}{Z(S)} = \frac{T_3^2\,(L/L_3)\,S^2 + \left[1 + (L/L_3)\right]T_3 S + (L/L_1)}{T_3^2\,(L/L_3)\,S^2 + \left[1 + (L/L_3)\right]T_3 S + 1} \quad . \tag{3.8.4}$$

The "first order" theory thus results in a second-order transfer function. The reason for such a result is that two web spans are involved and they are both affected by guide motion. The denominator of Equation 3.8.4 may be factored into

$$\left[(T_3 L/L_3)\,S + 1\right]\left[T_3 S + 1\right] \quad ,$$

so the denominator roots are always real. The numerator roots may be real or complex.
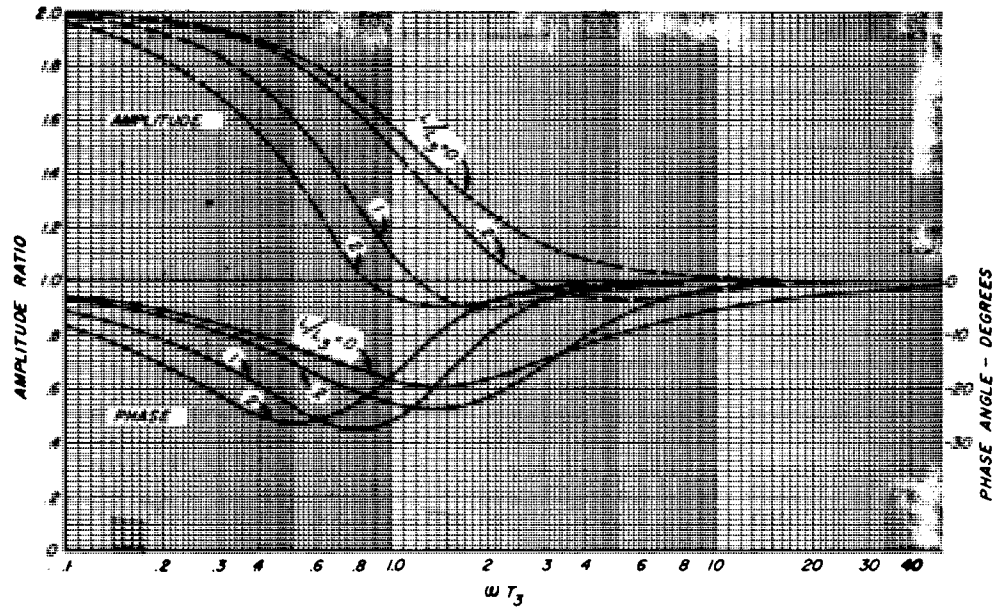
Figure 3.8.2. Frequency Response of Center-Pivoted Two-Roller Displacement Guide.

As L/L_3 approaches zero, the response approaches that of the steering guide of Equation 3.3.4.

The frequency response of Equation 3.8.4 is plotted in Figure 3.8.2 for the special case of a center-pivoted displacement guide (L/L_1 equal to 2), for different values of L/L_3. As with a steering guide, phase lag is associated with overguiding and phase lead with underguiding. The peak phase lag may be seen to be quite insensitive to variations in L/L_3, but the frequencies of the peak phase lag and the amplitude drop-off are significantly shifted.

3.9. Summary of First-Order Theory. Chapter III has presented a general technique for dynamic analysis under the simplifying assumption that the web has no shear strength. The validity of this assumption is examined in the following chapters. The basic equation for dynamic steering analysis is Equation 3.1.1.

Sections 3.2, 3.3, and 3.4 developed transfer functions for specific web handling situations. These transfer functions were manipulated and used for specialized web guide arrangements in the examples of Sections 3.5 through 3.8. The only

additional fundamental theory introduced in the latter four sections was the transport

lag theory of Section 3.6.

Although the web dynamics of an ideal displacement guide (with its pivot

axis in its entering span) are trivial, the dynamics of certain special displacement

guides were demonstrated in Sections 3.6 and 3.8 to be quite complex.

CHAPTER IV

SECOND-ORDER DYNAMICS OF A MASSLESS WEB

Chapter II showed that the steady-state boundary conditions at a guide roller are that the web is perpendicular to the guide roller and that the moment is zero. The dynamics that result from nonperpendicularity of the web to the roller and from a finite moment at the guide roller will be examined in this chapter. The analysis of web mechanics is similar to the static analysis of Chapter II for each of two components of web shape which are superimposed in the dynamic analysis. The web dynamic analysis is similar to the analysis of Chapter III.

Sections 4.2 through 4.6 develop transfer functions for specific web handling situations. The cases presented in Sections 4.3 and 4.5 consider shear deflection in addition to the bending deflection. The theory of Sections 4.2 and 4.4 was verified by experiment, as reported in Section 4.7.

Chapter V establishes the conditions for which the assumption of negligible web inertia is valid.

4.1. <u>Fundamental Theory</u>. The differential equation of the elastic web curve, Equation 2.1.8. or 2.4.10, applies to the web whether or not it is in its steady-state condition, if web mass is neglected; only the boundary conditions change. Because time and location are both variables in the dynamic condition, it is more correct to write the differential equation and all derivatives as partials. Equation 2.1.8 becomes:

$$\frac{\partial^4 y}{\partial x^4} - K^2 \frac{\partial^2 y}{\partial x^2} = 0 \quad . \tag{4.1.1}$$

The two independent variables, x and t, are considered separately, so it is often unnecessary to use partial derivative notation. Because primes and superscripts were used to denote differentiation with respect to x in Chapter II, derivatives with respect to time are written in full. Derivatives with respect to x continue to be denoted with primes.

The general approach of this chapter is the following: Partial differential equations relating the downstream end conditions of a web to its dynamics of steering at the downstream end are developed. The downstream end conditions necessary for evaluation of the dynamic equations are determined from static analysis of a generalized web condition. For simplicity of analysis, the static condition is broken into two components. The two components are superimposed when the equations of dynamic steering are converted to an ordinary differential equation for a specific web handling situation.

A static analysis of the web condition at any given time is satisfactory because the web mass is neglected in this chapter. Chapter V considers web mass and examines the validity of the assumption that the mass can be neglected.

Equations for Dynamic Steering

Figure 4.1.1 shows a shiftable roller with a curved web passing over it. The foundation hypothesis for the following derivation is that, within the limits of friction, every point on the web (such as A and B in the figure) which are in or immediately upstream of the contact area of a cylindrical roller move perpendicularly to the roller axis.

The roller and web angles as shown are positive in accordance with the previous sign conventions. It is obvious that as all web points of interest move perpendicularly to the roller, the lateral velocity of the web edge relative to the roller as Point A passes the line of ontering contact is equal to the slope of the web relative to the
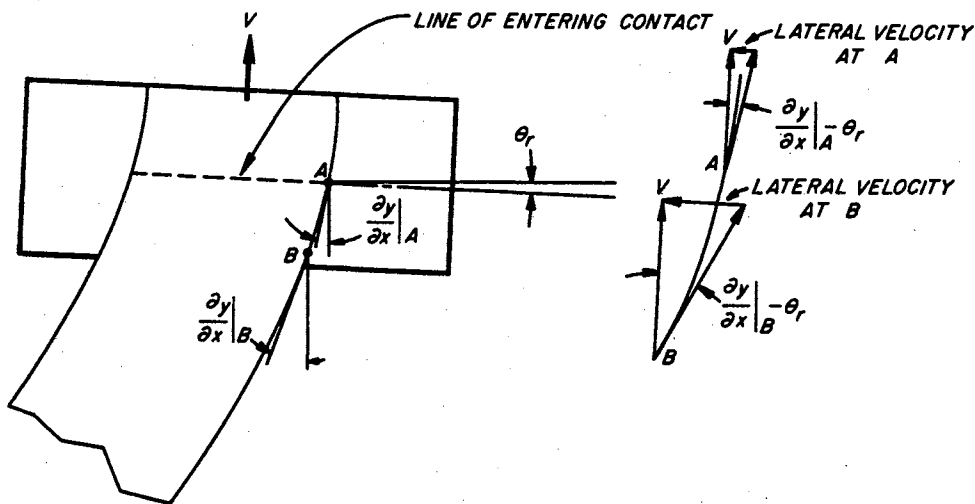
Figure 4.1.1. Steering Action of a Web
With Induced Curvature.

roller at Point A, multiplied by V, the longitudinal velocity of the web. Note that the lateral velocity of the edge is not the particle path of any one point on the edge, but is the position of a succession of points on the edge of the web as the web passes a given transverse line, such as the line of entering contact.

The lateral velocity of the web edge relative to the ground is equal to the velocity of the web edge relative to the roller plus the velocity of the roller relative to the ground. Because Point A is shown on the line of entering contact, the subscript L can be used to identify it as a point at the downstream roller, as consistently used in previous notation. The above reasoning can be expressed in equation form:

$$\frac{dy_L}{dt} = V\left(\theta_r - \frac{\partial y}{\partial x}\bigg|_L\right) + \frac{dz}{dt} , \qquad (4.1.2)$$

where y_L is the lateral web position at the downstream roller, θ_r is the roller angle, $(\partial y/\partial x)_L$ is the slope of the web evaluated at L, and z is the lateral position of the roller.

Equation 4.1.2 may be expressed as: The velocity of the web edge at the line

of entering contact is equal to the velocity of steering plus the velocity of lateral transport.

Similarly to the above argument, the lateral velocity of the web edge relative to the roller as Point B passes the line of entering contact is equal to the product of the slope of the web relative to the roller at Point B, and the longitudinal velocity V.

The difference in lateral velocity of the web edge relative to the roller between the time of passing of Points A and B may be expressed as

$$\frac{dy_L}{dt}\Big|_A - \frac{dy_L}{dt}\Big|_B = V\left(\frac{\partial y}{\partial x}\Big|_A - \frac{\partial y}{\partial x}\Big|_B\right). \qquad (4.1.3)$$

The left side of Equation 4.1.3 may be divided by Δt, the time required between the passing of Point A and B, and the right side by $\Delta x/V$, the equivalent of Δt:

$$\frac{\frac{dy_L}{dt}\Big|_A - \frac{dy_L}{dt}\Big|_B}{\Delta t} = \frac{V^2\left(\frac{\partial y}{\partial x}\Big|_A - \frac{\partial y}{\partial x}\Big|_B\right)}{\Delta x}. \qquad (4.1.4)$$

As Points A and B are moved infinitesimally closely together, the left side of Equation 4.1.4 becomes the lateral acceleration at $x = L$ and the right side becomes the product of V^2 and the web curvature at $x = L$. However, only the lateral acceleration due to web steering is considered in Equations 4.1.3 and 4.1.4. If the roller moves laterally, the total lateral acceleration of the web is equal to the sum of the acceleration due to steering and the acceleration due to lateral transport. Therefore, the equation for lateral acceleration of a web, without a consideration of shear deflection,

is

$$\frac{d^2 y_L}{dt^2} = V^2 \left.\frac{\partial^2 y}{\partial x^2}\right|_L + \frac{d^2 z}{dt^2} \quad . \qquad\qquad (4.1.5)$$

Equations 4.1.2 and 4.1.5 are used in Sections 4.2, 4.4, and 4.6 to write ordinary differential equations of web response for specific cases.

Note that Equation 4.1.5 is not merely the derivative of Equation 4.1.2; differentiation of the latter equation results in an extra term containing the velocity of roller swivelling, $d\theta_r/dt$. Because of the assumption that shear deflection is negligible, no acceleration can occur as an instantaneous result of roller swivelling, but only indirectly as the web curvature changes. A suddenly swivelling roller instantaneously swivels the downstream end of the web an equal amount, so that no instantaneous change in steering rate occurs, in contrast to the first-order theory of Chapter III.

If web deflection due to shear is significant, Equation 4.1.5 is modified, but Equation 4.1.2 is correct. The acceleration of the web at the downstream roller for the case of significant shear deflection is equal to the acceleration due to curvature and lateral transport as given by Equation 4.1.5, plus the acceleration due to the rate of change of the angle of shear deflection at the downstream roller. The lateral velocity due to the angle of shear deflection may be deduced from the discussion of Section 3.1 and Figure 3.1.1 to be equal to $-V\theta_{Ls}$, where θ_{Ls} is the slope due to shear deflection of the web at the downstream roller. The lateral acceleration due to a changing angle of shear deflection is found by differentiation with respect to time. The complete equation relating acceleration of the web at the downstream roller to web curvature, lateral transport, and rate of change of the angle of shear deflection is

$$\frac{d^2 y_L}{dt^2} = V^2 \left. \frac{\partial^2 y}{\partial x^2} \right|_L + \frac{d^2 z}{dt^2} - V \frac{d\theta_{Ls}}{dt} \quad . \tag{4.1.6}$$

Equations 4.1.2 and 4.1.6 are used in Sections 4.3 and 4.5 to write ordinary differential equations of web response for specific cases.

As an aid to systematic derivation and visualization, the principle of super-position is used in Chapters IV and V. The end of the web is considered to undergo pure translation and the result superimposed upon the effect of pure angular rotation of the end. A moment at x_L is associated with each component of deflection, so that Equation 4.1.5 or 4.1.6 must be considered for each component. The web and roller are not perpendicular to each other in the case of end rotation of the web, so Equation 4.1.2 must also be used for that component.

Web Mechanics Analysis for Bending

In this subsection, relations are derived which apply only if shear deflection is negligible. Figure 4.1.2 is used for the derivation of relations for pure translation of the end. Differential Equation 2.1.8 is valid, so its general solution is given by Equation 2.1.11. The first boundary condition, that y_o is zero, gives the result that C_4 is equal to $-C_2$. The condition that y_o' is zero gives the result that C_3 is equal to $-C_1 K$.

The fact that M_o is equal to $-M_L$, which may be observed from symmetry, may be restated by application of Equation 2.1.1 as

$$y_o'' = -y_L'' \, , \quad \text{or}$$

$$-C_2 K^2 = C_1 K^2 \sinh KL + C_2 K^2 \cosh KL, \quad \text{or}$$
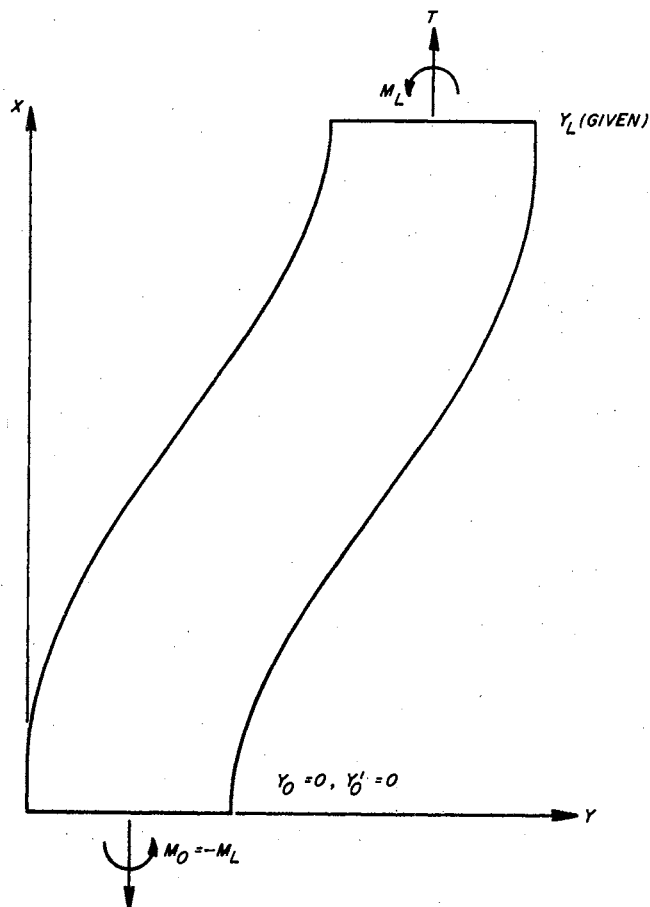
Figure 4.1.2. Boundary Conditions for Translation
of End of Web.

$$C_1 = - \frac{\cosh KL + 1}{\sinh KL} \, C_2 \quad .$$

Substituting the above conditions into Equation 2.1.11 and evaluating at x = L gives:

$$y_L = C_2 \left[-(\cosh KL + 1) + \cosh KL + KL \, \frac{\cosh KL + 1}{\sinh KL} - 1 \right]$$

or:

$$C_2 = \frac{y_L \sinh KL}{KL \, (\cosh KL + 1) - 2 \sinh KL} \qquad . \qquad (4.1.7)$$

Further substitution into previous formulas yields the other constants:

$$C_1 = - \frac{y_L (\cosh KL + 1)}{KL (\cosh KL + 1) - 2 \sinh KL} \quad , \tag{4.1.8}$$

$$C_3 = \frac{y_L K (\cosh KL + 1)}{KL (\cosh KL + 1) - 2 \sinh KL} \quad , \tag{4.1.9}$$

and

$$C_4 = - \frac{y_L \sinh KL}{KL (\cosh KL + 1) - 2 \sinh KL} \quad . \tag{4.1.10}$$

The primary parameter of interest for evaluation of Equation 4.1.5 is y_L''. M_L, which is equal to $-EIy_L''$, may alternatively be of interest. Because y_L'' is equal to $K^2(C_1 \sinh KL + C_2 \cosh KL)$ and EIK^2 is equal to T, simplification leads to the results:

$$y_L'' = -K^2 y_L \left[\frac{\sinh KL}{KL (\cosh KL + 1) - 2 \sinh KL} \right] \tag{4.1.11}$$

and

$$M_L = T y_L \left[\frac{\sinh KL}{KL (\cosh KL + 1) - 2 \sinh KL} \right] \quad . \tag{4.1.12}$$

It is convenient for later derivations to let

$$f_1(KL) = \frac{(KL)^2 \sinh KL}{KL (\cosh KL + 1) - 2 \sinh KL} \quad , \tag{4.1.13}$$

so that

$$y_L'' = - \frac{y_L}{L^2} f_1(KL) \tag{4.1.14}$$

and

$$M_L = \frac{T y_L}{(KL)^2} f_1(KL) \quad . \tag{4.1.15}$$
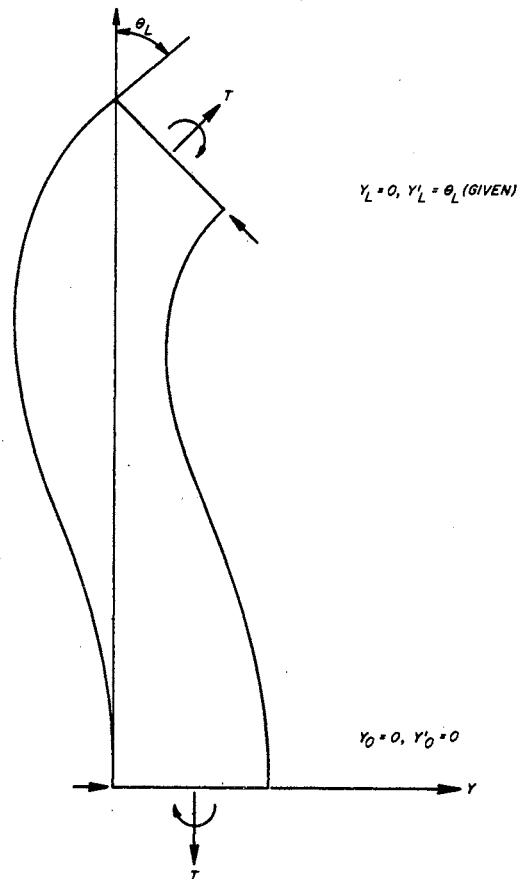
Figure 4.1.3. Boundary Conditions for Rotation of
End of Web.

A similar derivation for pure rotation of the end is necessary. Figure 4.1.3

shows the web and its boundary conditions. The details of the derivation are omitted.

The constants of Equation 2.1.11 are found to be:

$$C_1 = \frac{\theta_L}{K} \left[\frac{\cosh KL - 1}{KL \sinh KL - 2(\cosh KL - 1)} \right] , \qquad (4.1.16)$$

$$C_2 = \frac{\theta_L}{K} \left[\frac{KL - \sinh KL}{KL \sinh KL - 2(\cosh KL - 1)} \right] , \qquad (4.1.17)$$

$$C_3 = -\theta_L \left[\frac{\cosh KL - 1}{KL \sinh KL - 2(\cosh KL - 1)} \right] , \qquad (4.1.18)$$

and

$$C_4 = -\frac{\theta_L}{K}\left[\frac{KL - \sinh KL}{KL \sinh KL - 2(\cosh KL - 1)}\right] . \tag{4.1.19}$$

Equations of primary interest similar to those for end translation are:

$$y_L'' = K\theta_L\left[\frac{KL \cosh KL - \sinh KL}{KL \sinh KL - 2(\cosh KL - 1)}\right] \tag{4.1.20}$$

and

$$M_L = -\frac{T\theta_L}{K}\left[\frac{KL \cosh KL - \sinh KL}{KL \sinh KL - 2(\cosh KL - 1)}\right] , \tag{4.1.21}$$

or

$$y_L'' = \frac{\theta_L}{L} f_2(KL) \tag{4.1.22}$$

and

$$M_L = -\frac{TL\theta_L}{(KL)^2} f_2(KL) , \tag{4.1.23}$$

where

$$f_2(KL) = KL\left[\frac{KL \cosh KL - \sinh KL}{KL \sinh KL - 2(\cosh KL - 1)}\right] . \tag{4.1.24}$$

Web Mechanics Analysis for Bending and Shear

Derivations similar to those just completed are now undertaken to account for the additional effect of shear deflection. The derivations are quite parallel to the previous ones, but more complex. The conditions chosen for superposition for the sake of tidiness are pure translation and pure rotation of the end before shear deflection is taken into account. In other words, the translating end has its shear angle present at each end, and the rotating end has an angle of shear in addition to its angle of rotation.

Figure 4.1.4 shows the web with end translation and its boundary conditions. The differential equation was derived in Section 2.4, and its solution is given by
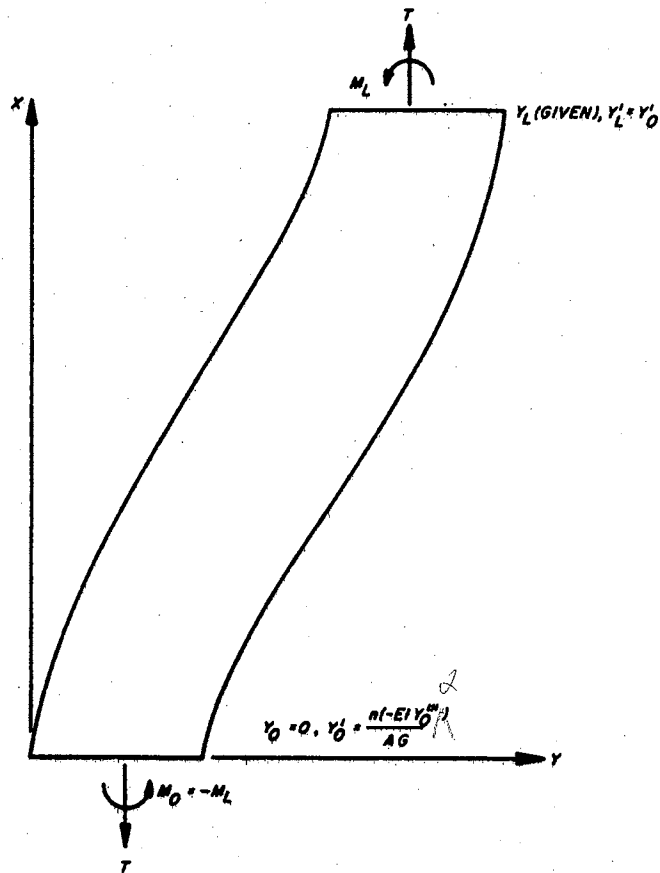
Figure 4.1.4. Boundary Conditions for Translation
of End of Web With Consideration
of Shear Deflection.

Equation 2.4.11 as

$$y = C_1 \sinh K_e x + C_2 \cosh K_e x + C_3 x + C_4$$

Five end conditions, shown in Figure 4.1.4, are required for evaluation of the

four constants because of an algebraic unknown, as in Section 2.4.

The evaluation of constants closely parallels previous examples and gives the

results:

$$C_1 = - y_L \left[\frac{\cosh K_e L + 1}{K_e L \left[\cosh K_e L + 1 + \dfrac{nT/AG}{1 + (nT/AG)} (\cosh K_e L + 1) \right] - 2 \sinh K_e L} \right]$$

$$(4.1.25)$$

$$C_2 = y_L \left\{ \frac{\sinh K_e L}{K_e L \left[\cosh K_e L + 1 + \dfrac{nT/AG}{1 + (nT/AG)} (\cosh K_e L + 1)\right] - 2 \sinh K_e L} \right\} , \quad (4.1.26)$$

$$C_3 = \frac{y_L}{L} \left\{ \frac{K_e L \left[\cosh K_e L + 1 + \dfrac{nT/AG}{1 + (nT/AG)} (\cosh K_e L + 1)\right]}{K_e L \left[\cosh K_e L + 1 + \dfrac{nT/AG}{1 + (nT/AG)} (\cosh K_e L + 1)\right] - 2 \sinh K_e L} \right\} , \quad (4.1.27)$$

and

$$C_4 = - y_L \left\{ \frac{\sinh K_e L}{K_e L \left[\cosh K_e L + 1 + \dfrac{nT/AG}{1 + (nT/AG)} (\cosh K_e L + 1)\right] - 2 \sinh K_e L} \right\} . \quad (4.1.28)$$

Equations for the moment and curvature at the end, which are necessary for the dynamic analysis are:

$$y_L'' = - K_e^2 y_L \left\{ \frac{\sinh K_e L}{K_e L \left[\cosh K_e L + 1 + \dfrac{nT/AG}{1 + (nT/AG)} (\cosh K_e L + 1)\right] - 2 \sinh K_e L} \right\} \quad (4.1.29)$$

and

$$M_L = \frac{T y_L}{1 + (nT/AG)} \left\{ \frac{\sinh K_e L}{K_e L \left[\cosh K_e L + 1 + \dfrac{nT/AG}{1 + (nT/AG)} (\cosh K_e L + 1)\right] - 2 \sinh K_e L} \right\} . \quad (4.1.30)$$

These equations reduce to Equations 4.1.11 and 4.1.12, respectively, if nT/AG is equal to zero.

It is also necessary to find the slope at x_L, which is the same as the slope at x_o:

$$y'_L = (K_e L)\left(\frac{y_L}{L}\right)\left\{\frac{\dfrac{nT/AG}{1+(nT/AG)}(\cosh K_e L + 1)}{K_e L\left[\cosh K_e L + 1 + \dfrac{nT/AG}{1+(nT/AG)}(\cosh K_e L + 1)\right] - 2\sinh K_e L}\right\}$$ (4.1.31)

If

$$f_1(K_e L) = (K_e L)^2\left\{\frac{\sinh K_e L}{K_e L\left[\cosh K_e L + 1 + \dfrac{nT/AG}{1+(nT/AG)}(\cosh K_e L + 1)\right] - 2\sinh K_e L}\right\}$$ (4.1.32)

then the equations may be written

$$y''_L = -\frac{y_L}{L^2}f_1(K_e L) \ ,$$ (4.1.33)

$$M_L = \frac{Ty_L}{(K_e L)^2(1+nT/AG)}f_1(K_e L) \ ,$$ (4.1.34)

and

$$\theta_L = y'_L = \left[\frac{nT/AG}{(1+nT/AG)K_e L}\right]\left[\frac{y_L}{L}\right]\left[\frac{\cosh K_e L + 1}{\sinh K_e L}\right]f_1(K_e L) \ .$$ (4.1.35)

The second component of the dynamic condition of the web with shear deflection considered is the rotation of the end at x_L. The necessary boundary conditions are shown in Figure 4.1.5. The general solution is again given by Equation 2.4.11. Note that θ_{L1} is the slope of the end of the web before shear deflection is taken into account. The evaluation of constants by steps similar to previous examples yields the results:

$$C_1 = \frac{\theta_{L1}}{K_e}\left[\frac{\cosh K_e L - 1 + (nT/AG)(\cosh K_e L - 1 - 2K_e L\sinh K_e L)}{K_e L\sinh K_e L - 2(\cosh K_e L - 1) + \dfrac{nT/AG}{1+(nT/AG)}K_e L\sinh K_e L}\right] \ ,$$ (4.1.36)
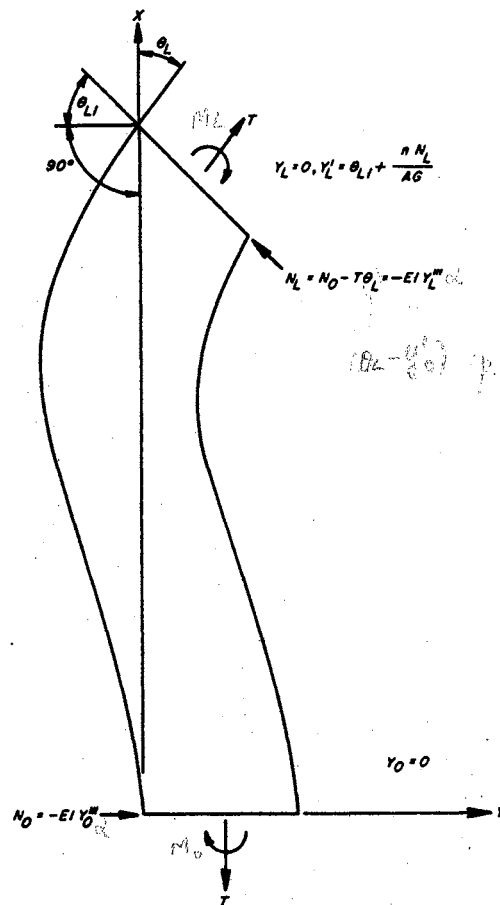
Figure 4.1.5. Boundary Conditions for Rotation of End
of Web With Consideration of Shear Deflection.

$$C_2 = \frac{\theta_{L1}}{K_e} \left[\frac{K_e L - \sinh K_e L + (nT/AG)(2K_e L \cosh K_e L - \sinh K_e L)}{K_e L \sinh K_e L - 2(\cosh K_e L - 1) + \dfrac{nT/AG}{1 + (nT/AG)} K_e L \sinh K_e L} \right] , \quad (4.1.37)$$

$$C_3 = -\theta_{L1} \left[\frac{[1 - (2nT/AG)] (\cosh K_e L - 1)}{K_e L \sinh K_e L - 2 (\cosh K_e L - 1) + \dfrac{nT/AG}{1 + (nT/AG)} K_e L \sinh K_e L} \right] , \quad (4.1.38)$$

and

$$C_4 = -\frac{\theta_{L1}}{K_e} \left[\frac{K_e L - \sinh K_e L + (nT/AG)(2 K_e L \cosh K_e L - \sinh K_e L)}{K_e L \sinh K_e L - 2(\cosh K_e L - 1) + \dfrac{nT/AG}{1 + (nT/AG)} K_e L \sinh K_e L} \right] . \quad (4.1.39)$$

Important equations for moment and curvature of the end of the web are:

$$y_L'' = K_e \theta_{L1} \left[\frac{K_e L \cosh K_e L - \sinh K_e L + (nT/AG)(2 K_e L - \sinh K_e L)}{K_e L \sinh K_e L - 2(\cosh K_e L - 1) + \dfrac{nT/AG}{1 + (nT/AG)} K_e L \sinh K_e L} \right] \quad (4.1.40)$$

and

$$M_L = \frac{T\theta_{L1}}{K_e(1 + \frac{nT}{AG})} \left[\frac{K_e L \cosh K_e L - \sinh K_e L + (nT/AG)(2 K_e L - \sinh K_e L)}{K_e L \sinh K_e L - 2(\cosh K_e L - 1) + \dfrac{nT/AG}{1 + (nT/AG)} K_e L \sinh K_e L} \right] . (4.1.41)$$

These equations reduce to Equations 4.1.20 and 4.1.21 if nT/AG is equal to zero.

For the dynamic analysis, it is necessary to know the actual slope of the end of the web, which may be found from the equation

$$y_L' = K_e(C_1 \cosh K_e L + C_2 \sinh K_e L) + C_3 \quad . \quad (4.1.42)$$

Combining Equations 4.1.36, 4.1.37, 4.1.38, and 4.1.42 yields

$$\theta_L = y_L' = \theta_{L1} \left[\frac{K_e L \sinh K_e L - 2(\cosh K_e L - 1) + (nT/AG)(\cosh K_e L - 1)}{K_e L \sinh K_e L - 2(\cosh K_e L - 1) + \dfrac{nT/AG}{1 + (nT/AG)} K_e L \sinh K_e L} \right] . \quad (4.1.43)$$

For simplification, let

$$h_1(K_e L) = \frac{K_e L \sinh K_e L - 2(\cosh K_e L - 1) + (nT/AG)(\cosh K_e L - 1)}{K_e L \sinh K_e L - 2(\cosh K_e L - 1) + \dfrac{nT/AG}{1 + (nT/AG)} K_e L \sinh K_e L} \quad (4.1.44)$$

then

$$\theta_{L1} = \frac{\theta_L}{h_1(K_e L)} \quad , \quad (4.1.45)$$

so that the parameter θ_{L1} can be eliminated from Equations 4.1.36 through 4.1.41.

The angle of shear deflection subtracts from the angle that would be present without shear deflection; therefore, the angle of shear deflection for a rotated end is $\theta_{L1} - \theta_L$, or:

$$\theta_{Ls} = \theta_L \left(\frac{1}{h_1(K_e L)} - 1 \right) .$$ (4.1.46)

If Equation 4.1.45 is utilized and if

$$f_2(K_e L) = K_e L \left[\frac{K_e L \cosh K_e L - \sinh K_e L + (nT/AG)(2 K_e L - \sinh K_e L)}{K_e L \sinh K_e L - 2(\cosh K_e L - 1) + (nT/AG)(\cosh K_e L - 1)} \right] ,$$ (4.1.47)

the curvature and moment equations can be written as

$$y_L'' = \frac{\theta_L}{L} f_2(K_e L)$$ (4.1.48)

and

$$M_L = - \frac{TL\theta_L}{(K_e L)^2 \left(1 + \frac{nT}{AG}\right)} f_2(K_e L) .$$ (4.1.49)

The fundamental derivations of this section are applied to special cases throughout the rest of Chapter IV.

4.2. **Response at Fixed Roller to Input at Previous Roller.** The response considered in this section is a refinement of that covered in Section 3.2, which neglected web curvature. Shear deflection is neglected here, but will be included in Section 4.3.

Equations 4.1.2 and 4.1.5 are the basis for the second-order theory of web steering if shear deflection is negligible.

For the case under consideration, the downstream roller is not moving laterally; therefore, dz/dt and d^2z/dt^2 are zero. Also, the downstream roller angle θ_r is zero,

so Equations 4.1.2 and 4.1.5 are greatly simplified:

$$\frac{dy_L}{dt} = -V \left.\frac{\partial y}{\partial x}\right|_L \tag{4.2.1}$$

and

$$\frac{d^2 y_L}{dt^2} = V^2 \left.\frac{\partial^2 y}{\partial x^2}\right|_L \quad . \tag{4.2.2}$$

In Section 4.1, the curvature of the web at the downstream end was considered as two components, expressed in Equations 4.1.14 and 4.1.22. In this section, y_o is considered the input. If y_o is finite, not zero as assumed in the derivation of Section 4.1, $(y_L - y_o)$ may be substituted for y_L in all the formulas. The total curvature of the web at x_L may then be expressed as:

$$\left.\frac{\partial^2 y}{\partial x^2}\right|_L = \frac{\theta_L}{L} f_2(KL) - \left(\frac{y_L - y_o}{L^2}\right) f_1(KL) \quad . \tag{4.2.3}$$

θ_L which is also denoted as y_L' , is identically equal to $(\partial y/\partial x)_L$, so that Equation 4.2.1 may be written as

$$\theta_L = -\frac{1}{V} \frac{dy_L}{dt} \tag{4.2.4}$$

and substituted into Equation 4.2.3 to obtain:

$$\left.\frac{\partial^2 y}{\partial x^2}\right|_L = -\frac{1}{VL} \frac{dy_L}{dt} f_2(KL) - \left(\frac{y_L - y_o}{L^2}\right) f_1(KL) \quad . \tag{4.2.5}$$

Substitution of Equation 4.2.5 into Equation 4.2.2 yields the second-order linear differential equation:

$$\frac{d^2 y_L}{dt^2} = -\frac{V}{L} \frac{dy_L}{dt} f_2(KL) - \left(\frac{V}{L}\right)^2 \left(y_L - y_0\right) f_1(KL) . \qquad (4.2.6)$$

Application of the Laplace transform to Equation 4.2.6, rearrangement, and substitution of T_1 for L/V gives the transfer function for the response of y_L to an input at y_0:

$$\frac{Y_L(S)}{Y_0(S)} = \frac{1}{\dfrac{T_1^2}{f_1(KL)} S^2 + \dfrac{f_2(KL)}{f_1(KL)} T_1 S + 1} . \qquad (4.2.7)$$

It can be shown that $f_2(KL)/f_1(KL)$ is equal to the curvature factor K_c (Equation 2.1.17), which was shown in Section 2.1 to approach two-thirds for small values of KL and unity for large values. Both $f_1(KL)$ and $f_2(KL)$ become large for large values of KL. Thus, if KL is very large (much greater than commonly encountered), the second-order term of Equation 4.2.7 drops out, the first-order coefficient reduces to T_1, and the equation becomes the same as Equation 3.2.3.

The frequency response of Equation 4.2.7 is plotted in Figure 4.2.1. A comparison to Figure 3.2.2 reveals that the second-order effects are quite significant, particularly at high frequencies. However, the phase lag and the attenuation at low and medium frequencies as given by the first-order theory is a fair approximation. Note that increasing KL causes the behavior to move closer to the first-order behavior except at very high frequencies, as discussed in the previous paragraph.

4.3. **Shear Effect on Response at a Fixed Roller.** For the case under consideration, Equation 4.1.6 simplifies to:

$$\frac{d^2 y_L}{dt^2} = V^2 \left.\frac{\partial^2 y}{\partial x^2}\right|_L - V \frac{d\theta_{Ls}}{dt} . \qquad (4.3.1)$$
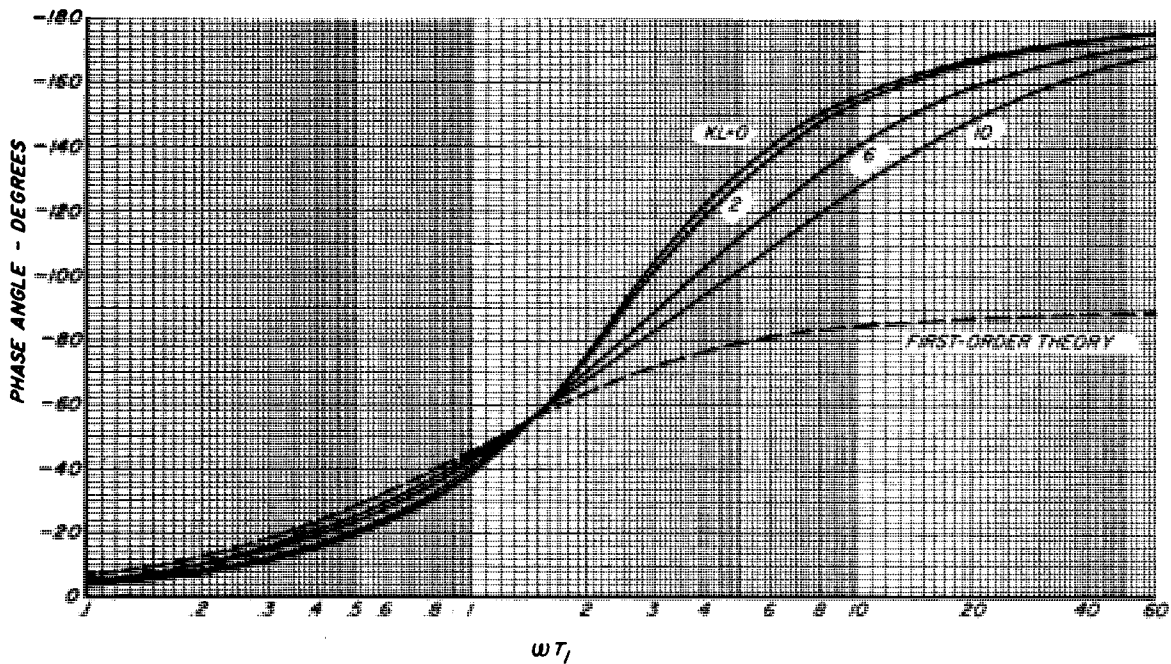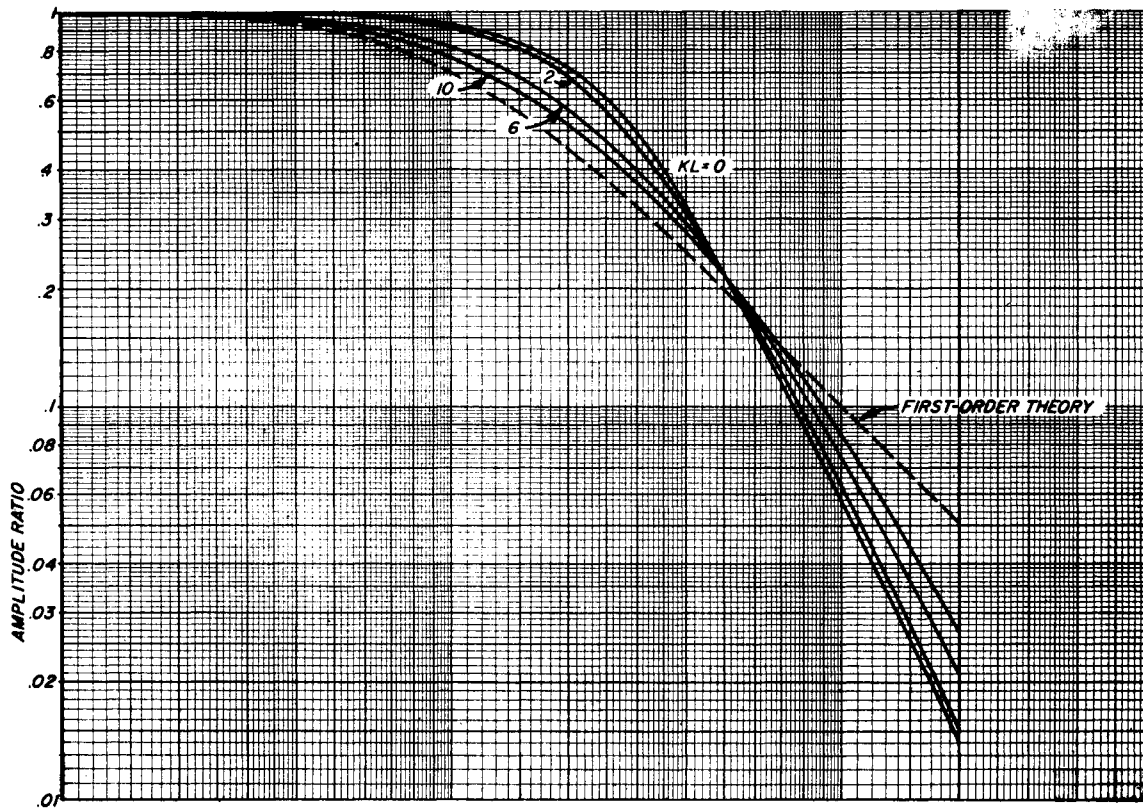
Figure 4.2.1. Second-Order Frequency Response of Web at Fixed Roller to Input at Previous Roller.

The d^2z/dt^2 dropped out as in the previous section because the downstream roller is stationary.

If the derivation considering shear effects on end translation in Section 4.1 had not considered y_o to be zero, Equations 4.1.25 through 4.1.35 would have differed only by the term $(y_L - y_o)$ instead of y_L. In this section, y_o is the input.

The angle of shear is obtained from Equations 4.1.35 and 4.1.46 and may be written as

$$\theta_{Ls} = \frac{y_L - y_o}{L} \, g_1(K_e L) - \theta_L \, g_2(K_e L) \tag{4.3.2}$$

where

$$g_1(K_e L) = \frac{nT/AG}{(1 + nT/AG)} \frac{\cosh K_e L + 1}{K_e L \sinh K_e L} f_1(K_e L) \quad , \tag{4.3.3}$$

$$g_2(K_e L) = \frac{1}{h_1(K_e L)} - 1 \quad , \tag{4.3.4}$$

and θ_L is identically equal to y_L'.

The total curvature of the web at x_L is obtained from Equations 4.1.33 and 4.1.48 as

$$\left.\frac{\partial^2 y}{\partial x^2}\right|_L = \frac{\theta_L}{L} f_2(K_e L) - \left(\frac{y_L - y_o}{L^2}\right) f_1(K_e L) \, . \tag{4.3.5}$$

Substitution of Equation 4.3.5 and the time derivative of Equation 4.3.2 into Equation 4.3.1 gives the result:

$$\frac{d^2 y_L}{dt^2} = V^2 \frac{\theta_L}{L} f_2(K_e L) - \frac{V^2}{L^2} (y_L - y_o) f_1(K_e L)$$

$$- \frac{V}{L}\left(\frac{dy_L}{dt} - \frac{dy_o}{dt}\right) g_1(K_e L) + V \frac{d\theta_L}{dt} g_2(K_e L) . \qquad (4.3.6)$$

Equation 4.2.1 applies to this case; therefore, θ_L may be substituted for its equivalent in Equation 4.2.4 to obtain:

$$\frac{d^2 y_L}{dt^2} = - \frac{V}{L} \frac{dy_L}{dt} f_2(K_e L) - \left(\frac{V}{L}\right)^2 (y_L - y_o) f_1(K_e L)$$

$$- \frac{V}{L}\left(\frac{dy_L}{dt} - \frac{dy_o}{dt}\right) g_1(K_e L) - \frac{d^2 y_L}{dt^2} g_2(K_e L) . \qquad (4.3.7)$$

Application of the Laplace transform to Equation 4.3.7, rearrangement, and substitution of T_1 for L/V gives the following transfer function, which is the equivalent of Equation 4.2.7 except that shear deflection is taken into account:

$$\frac{Y_L(S)}{Y_o(S)} = \frac{\left[g_1(K_e L)/f_1(K_e L)\right] T_1 S + 1}{\left[\dfrac{1 + g_2(K_e L)}{f_1(K_e L)}\right] T_1^2 S^2 + \left[\dfrac{f_2(K_e L) + g_1(K_e L)}{f_1(K_e L)}\right] T_1 S + 1} . \qquad (4.3.8)$$

The theory of Section 4.2 is precise if nT/AG is very small or if $K_e L$ is large, as was discovered for the static behavior of Chapter II. Generally, Equation 4.3.8 will yield results between those of Equations 3.2.3 and 4.2.7, for a given value of $K_e L$.

4.4. Steering Guide Response. The steering guide considered in Section 3.3 will now be analyzed with the second-order theory. Figure 3.3.1 shows the guide

(a) Translation   (b) Rotation
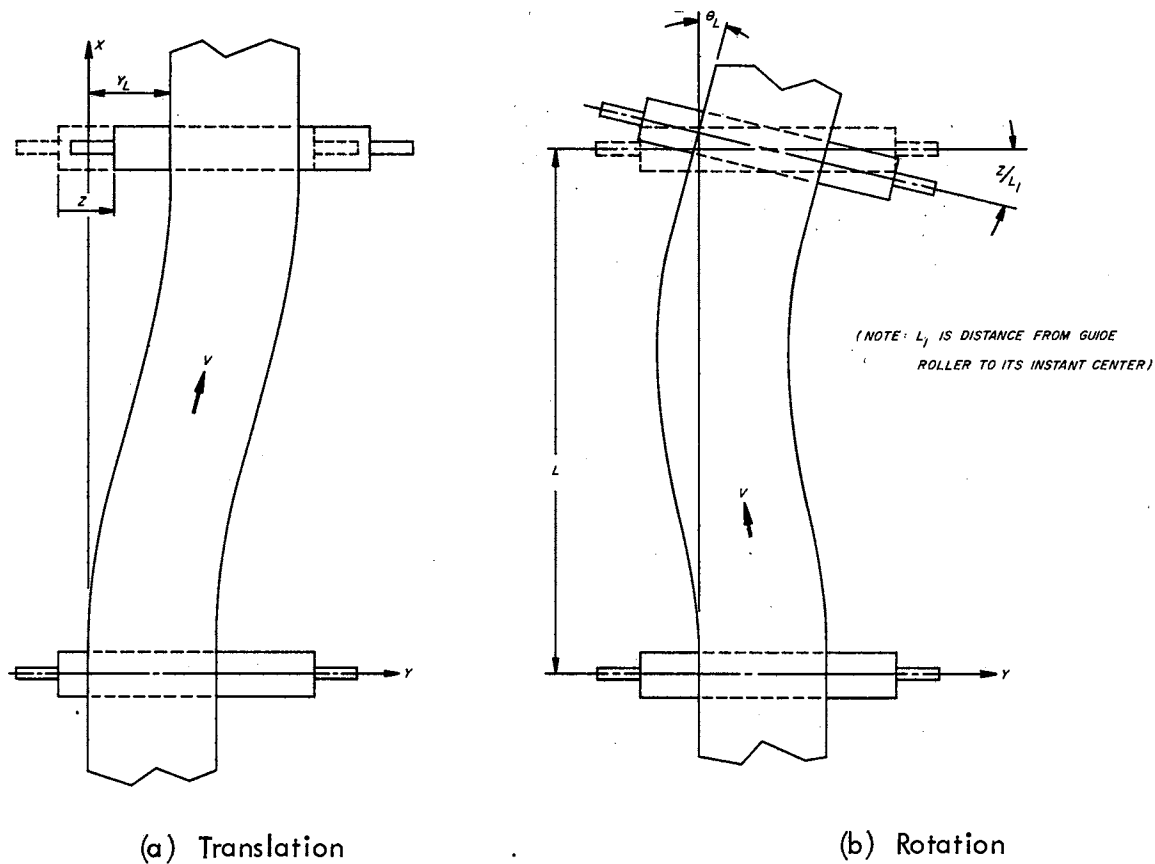
Figure 4.4.1. Two Components of Deflection of a Web Located by a Steering Guide.

arrangement and nomenclature. Figure 4.4.1 shows the scheme of superposition of translation and rotation of the end, as discussed in Section 4.1.

The roller angle θ_r in Equation 4.1.2 is equal to z/L_1. Therefore, the equation can be rewritten as

$$\left.\frac{\partial y}{\partial x}\right|_L = \frac{1}{V}\left(\frac{dz}{dt} - \frac{dy_L}{dt}\right) + \frac{z}{L_1} \quad . \tag{4.4.1}$$

The two components of end curvature given by Equations 4.1.14 and 4.1.22 may be substituted into Equation 4.1.5:

$$\frac{d^2 y_L}{dt^2} = V^2 \left(-\frac{f_1(KL)}{L^2} y_L + \frac{f_2(KL)}{L} \left.\frac{\partial y}{\partial x}\right|_L \right) + \frac{d^2 z}{dt^2} \quad . \tag{4.4.2}$$

The substitution of Equation 4.4.1 into Equation 4.4.2 yields the differential

equation of motion of the web at the steering guide:

$$\frac{d^2 y_L}{dt^2} = -\frac{V}{L} \, f_2(KL) \, \frac{dy_L}{dt} - \left(\frac{V}{L}\right)^2 f_1(KL) \, y_L$$

$$+ \frac{d^2 z}{dt^2} + \frac{V}{L} \, f_2(KL) \frac{dz}{dt} + \left(\frac{V}{L}\right)^2 \frac{L}{L_1} \, f_2(KL) z \qquad . \qquad (4.4.3)$$

Application of the Laplace transform to Equation 4.4.3, rearrangement, and

substitution of T_1 for L/V and K_c for $f_2(KL)/f_1(KL)$ results in the transfer function

of the steering guide:

$$\frac{Y_L(S)}{Z(S)} = \frac{\dfrac{T_1^2}{f_1(KL)} \, S^2 + K_c T_1 S + \dfrac{LK_c}{L_1}}{\dfrac{T_1^2}{f_1(KL)} \, S^2 + K_c T_1 S + 1} \qquad . \qquad (4.4.4)$$

The steady-state response of the guide, the static steering factor, is seen to

be LK_c/L_1 instead of L/L_1, as given by the linear theory. As KL becomes very large,

$f_1(KL)$ becomes large and K_c approaches unity, so that Equation 4.4.4 reduces to

Equation 3.3.4.

Equation 4.4.4 is plotted in Figures 4.4.2 through 4.4.5, for KL values of

zero and ten, and for a broad range of static steering factors. If KL is less than

unity, the response is very near to that given by the curves for KL of zero. At a

KL value of ten, the response is approaching that given by the first-order theory as

shown in Figures 3.3.2 and 3.3.3.

Figure 4.4.2. Second-Order Frequency Response of an Oversteering Guide
With KL = 0.
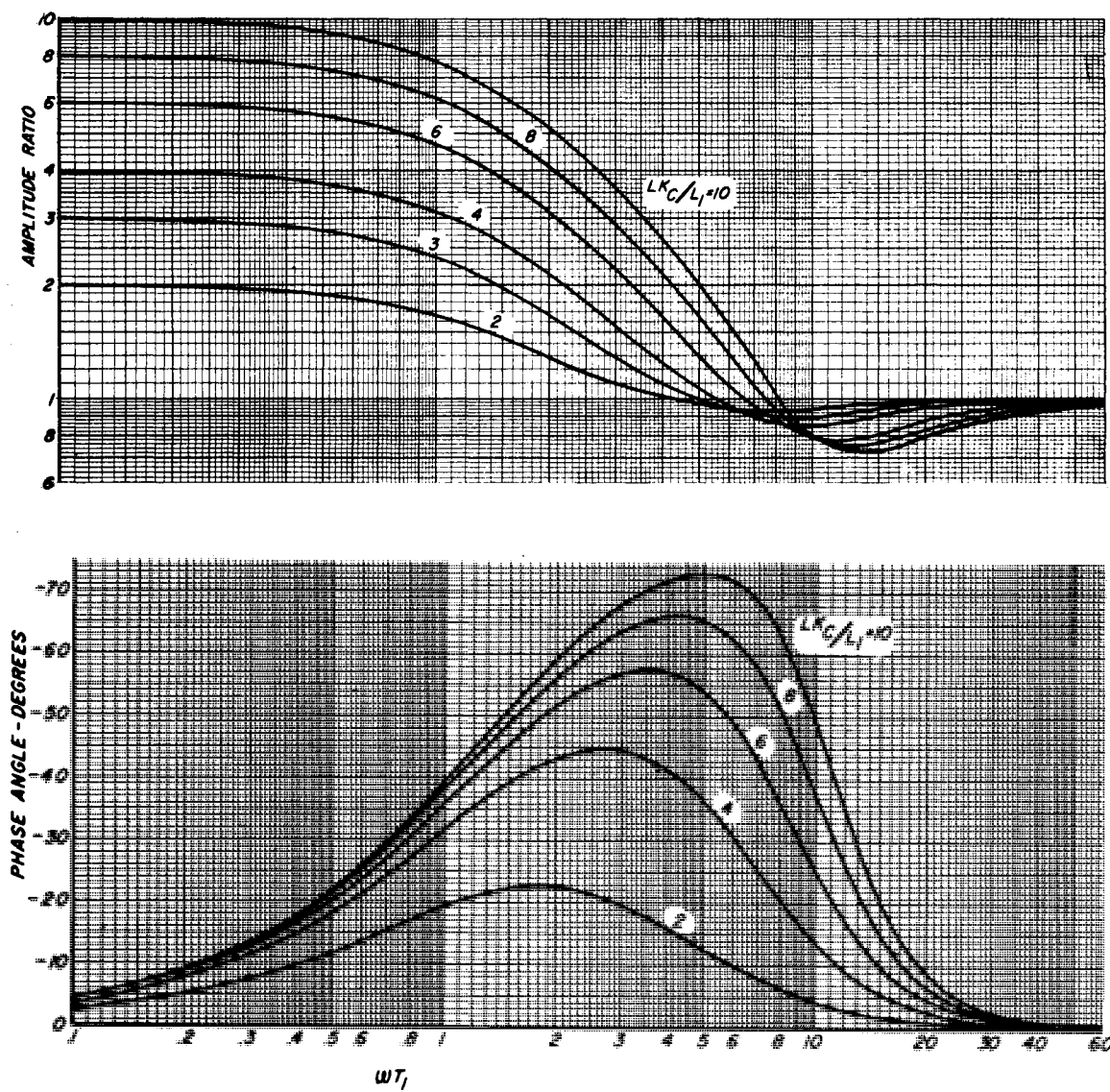
Figure 4.4.3. Second-Order Frequency Response of an Oversteering Guide With KL = 10.
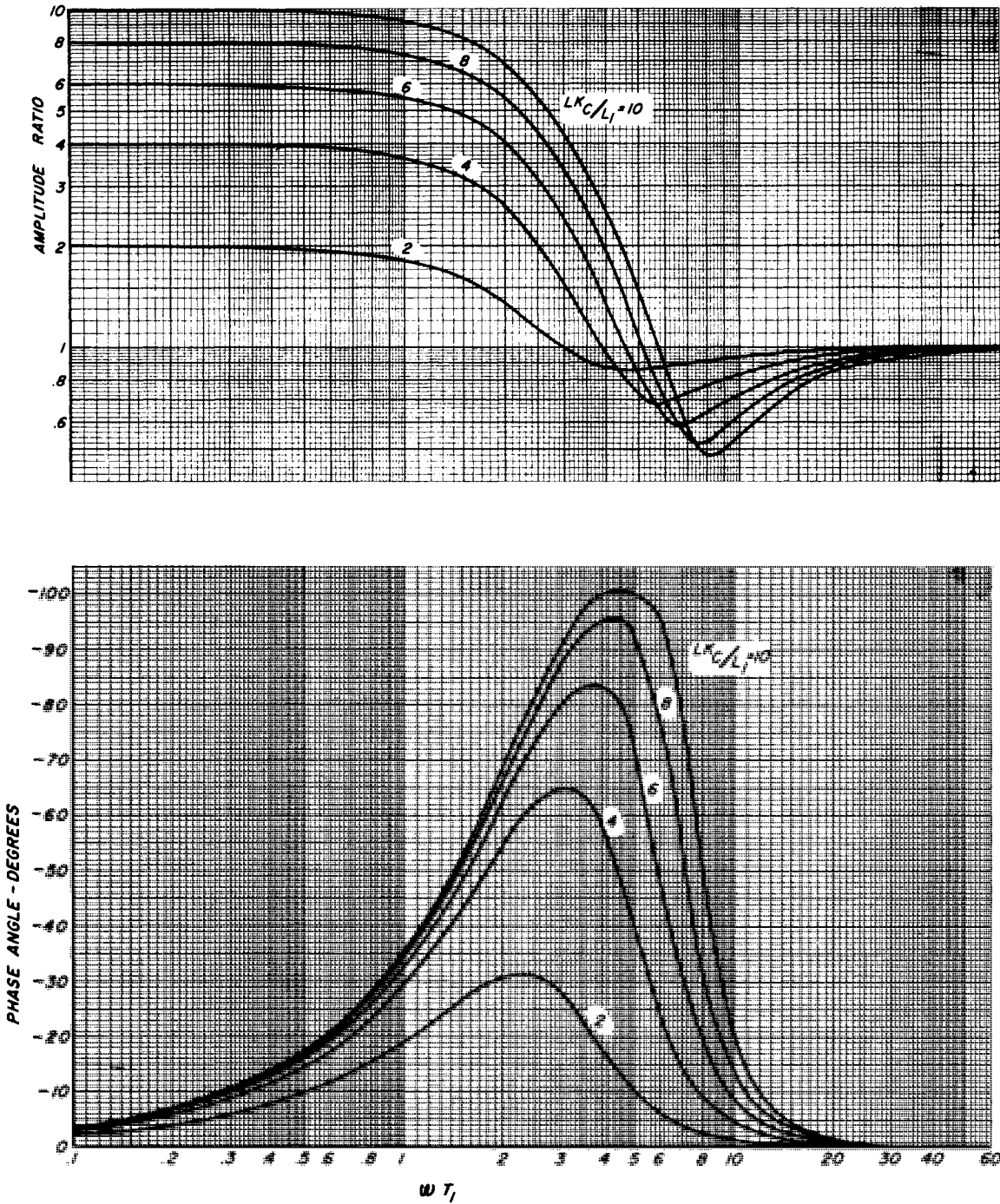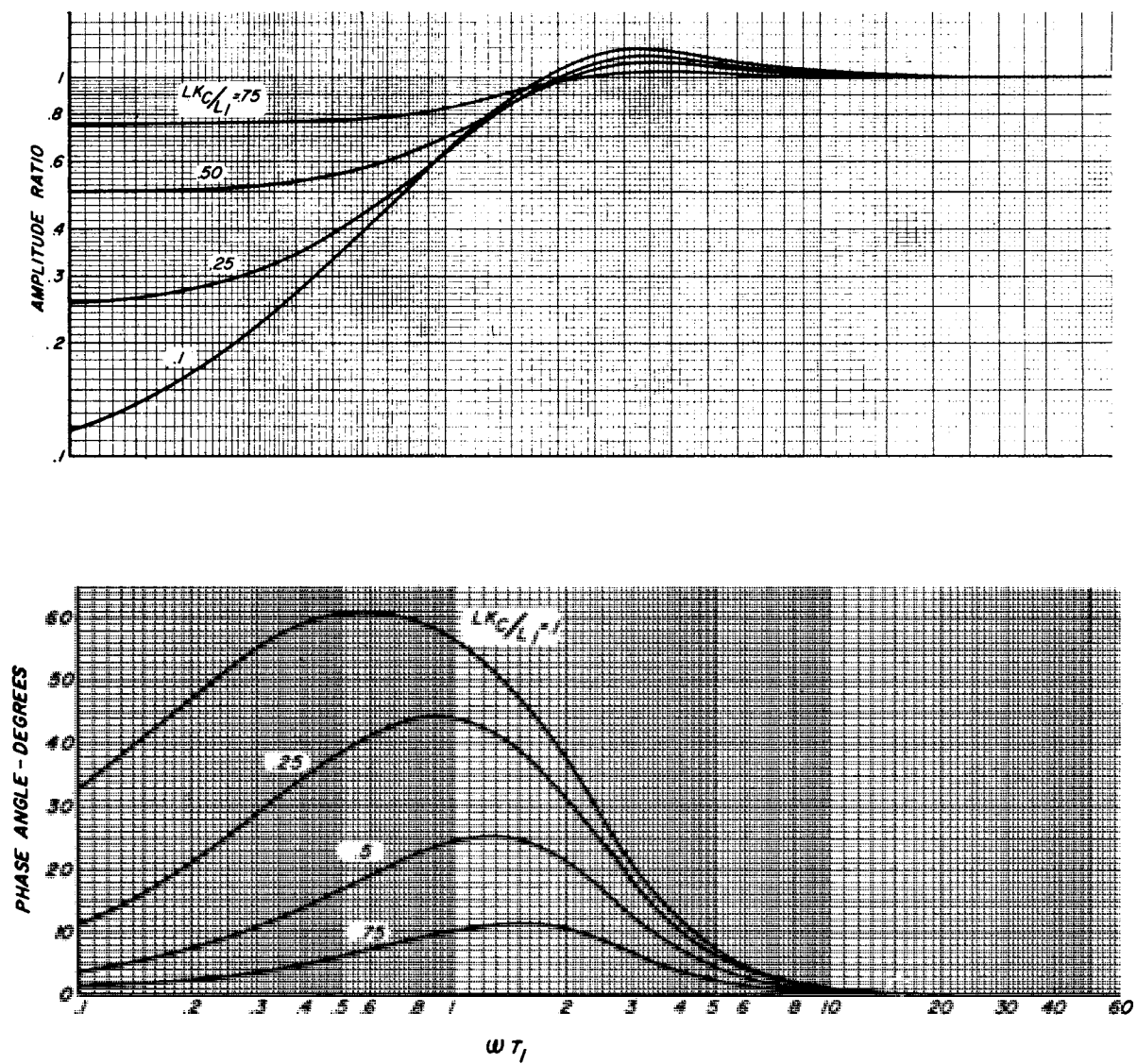
Figure 4.4.4. Second-Order Frequency Response of an Understeering
Guide With KL = 0.
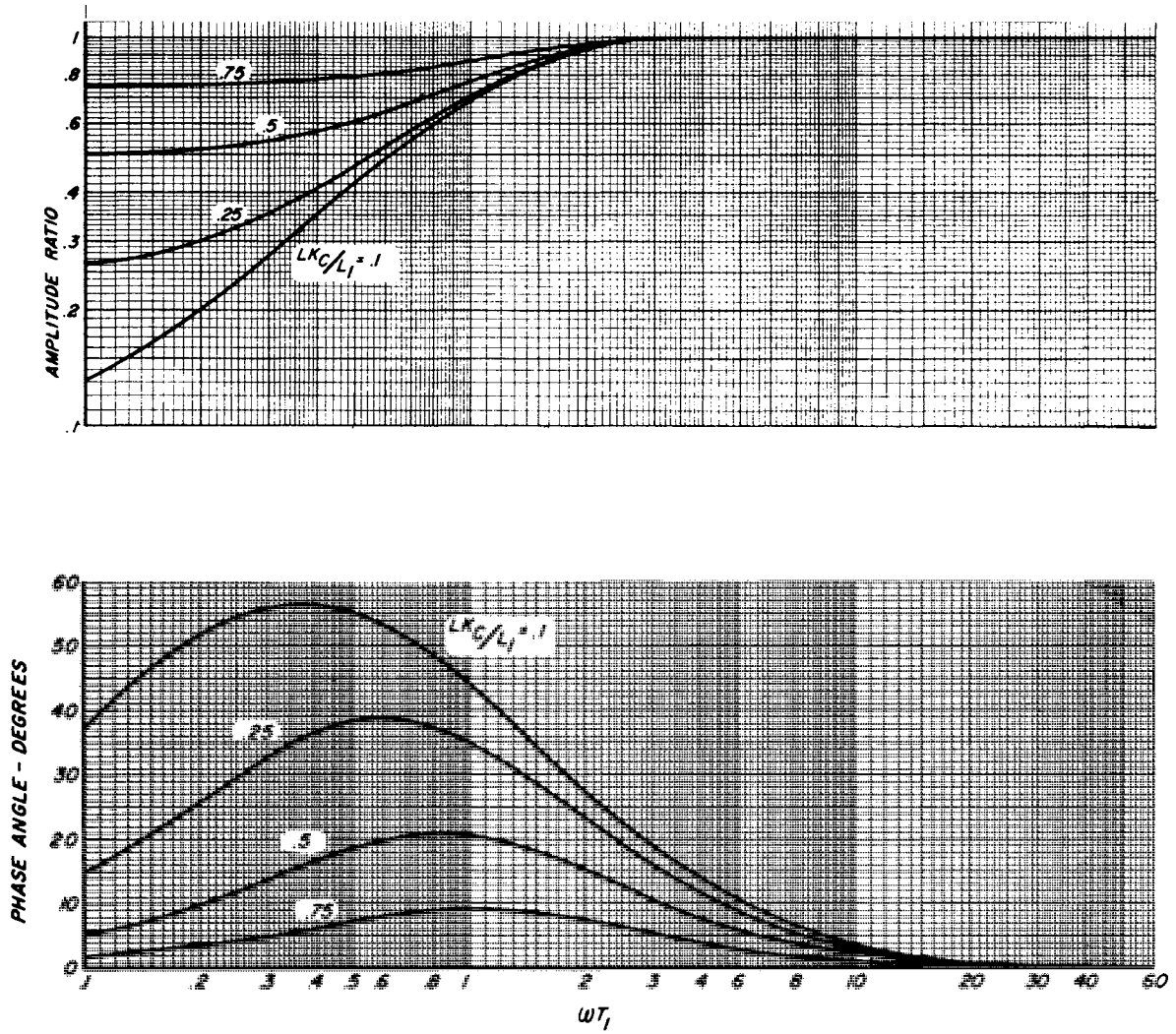
Figure 4.4.5. Second-Order Frequency Response of an Understeering
Guide With KL = 10.

4.5. Shear Effect on Steering Guide Response. If shear deflection is significant, the response of a steering guide will be between the extremes specified by Equations 3.3.4 and 4.4.4, for a given value of KL. This section analyzes the response of a web on a conventional steering guide, for the situation in which the shear deflection is significant.

Equation 4.1.6 applies to the case under consideration. θ_{Ls} is given by Equations 4.1.35 and 4.1.46. If we define $g_1(K_eL)$ and $g_2(K_eL)$ as in Equations 4.3.3 and 4.3.4, θ_{Ls} may be expressed as

$$\theta_{Ls} = \left(\frac{y_L}{L}\right) g_1(K_eL) - \theta_L\, g_2(K_eL) \quad , \tag{4.5.1}$$

where θ_L is identically equal to y'_L .

The total curvature of the web at x_L is given by Equations 4.1.33 and 4.1.48 as

$$\left.\frac{\partial^2 y}{\partial x^2}\right|_L = \frac{\theta_L}{L} f_2(K_eL) - \frac{y_L}{L^2} f_1(K_eL) \quad . \tag{4.5.2}$$

Equation 4.1.2 is applicable to the case under consideration. The roller angle θ_r is equal to z/L_1, so that rearrangement results in Equation 4.4.1.

Substitution of Equation 4.5.2 and the time derivative of Equation 4.5.1 into Equation 4.1.6 yields the result

$$\frac{d^2 y_L}{dt^2} = \frac{V^2}{L}\left.\frac{\partial y}{\partial x}\right|_L f_2(K_eL) - \left(\frac{V}{L}\right)^2 y_L f_1(K_eL) + \frac{d^2 z}{dt^2}$$

$$- \frac{V}{L}\frac{dy_L}{dt} g_1(K_eL) + V\frac{d}{dt}\left[\left.\frac{\partial y}{\partial x}\right|_L\right]\left[g_2(K_eL)\right] \quad . \tag{4.5.3}$$

Further substitution of Equation 4.4.1 and its time derivative into Equation 4.5.3 gives, after rearrangement, the following differential equation of motion of the web at the steering guide:

$$\left[1 + g_2(K_eL)\right]\frac{d^2y_L}{dt^2} + \frac{V}{L}\left[f_2(K_eL) + g_1(K_eL)\right]\frac{dy_L}{dt} + \left(\frac{V}{L}\right)^2 f_1(K_eL) y_L$$

$$= \left[1 + g_2(K_eL)\right]\frac{d^2z}{dt^2} + \frac{V}{L}\left[f_2(K_eL) + \frac{L}{L_1} g_2(K_eL)\right]\frac{dz}{dt} + \left(\frac{V}{L}\right)^2 f_2(K_eL)z. \quad (4.5.4)$$

Application of the Laplace transform to Equation 4.5.4 and substitution of T_1 for L/V and K_c for $f_2(K_eL)/f_1(K_eL)$ results in the transfer function for the steering guide:

$$\frac{Y_L(S)}{Z(S)} = \frac{\left[\dfrac{1 + g_2(K_eL)}{f_1(K_eL)}\right]T_1^2 S^2 + \left[K_c + \dfrac{L}{L_1}\dfrac{g_2(K_eL)}{f_1(K_eL)}\right]T_1 S + \dfrac{LK_c}{L_1}}{\left[\dfrac{1 + g_2(K_eL)}{f_1(K_eL)}\right]T_1^2 S^2 + \left[K_c + \dfrac{g_1(K_eL)}{f_1(K_eL)}\right]T_1 S + 1} \qquad . \qquad (4.5.5)$$

Equation 4.5.5 reduces to Equation 4.4.4 if nT/AG is negligible.

4.6. Response at a Point Between Two Parallel Fixed Rollers. The subject of this section was studied with first-order theory in Section 3.4. A study of the effect of shear deflection similar to the studies of Sections 4.3 and 4.5 could be undertaken, but is not covered in this thesis.

Figure 4.6.1 shows the two components of web shape used in the derivation. The slope of the web at x_o is assumed to be zero, but another derivation (not covered in this thesis) assuming y'_o as the input, with y_o equal to zero, could be useful.

Enough foundation has been built to solve this problem without recourse to the fundamental theory of Equations 4.1.2 and 4.1.5. The differential equations

of the elastic curves of the two components of deflection were solved in Section 4.1. The constants are given in Equations 4.1.7 through 4.1.10 and 4.1.16 through 4.1.19. The first four constants must have $(y_L - y_o)$ substituted for y_L to allow for the fact that y_o is unequal to zero.

The resultant elastic curve may be written as

$$y = y_o + \left[\frac{\theta_L}{KL \sinh KL - 2 (\cosh KL - 1)} \right] \left[(\cosh KL - 1)(\frac{1}{K} \sinh Kx - x) \right.$$

$$\left. - (\sinh KL - KL) (\frac{1}{K}) (\cosh Kx - 1) \right]$$

$$+ \left[\frac{y_L - y_o}{KL (\cosh KL + 1) - 2 \sinh KL} \right] \left[(\cosh KL + 1)(Kx - \sinh Kx) \right.$$

$$\left. + (\sinh KL)(\cosh Kx - 1) \right] \qquad . \qquad (4.6.1)$$

If the specific sampling point x_2 is substituted for the general x and $(KL)(x/L)$ for Kx, and if

$$f_4(KL, x_2/L) = \left[\frac{-1}{KL \sinh KL - 2 (\cosh KL - 1)} \right] \left[(\cosh KL - 1)\left(\frac{\sinh (KL)(x_2/L)}{KL} - \frac{x_2}{L} \right) \right.$$

$$\left. - \left(\frac{\sinh KL - KL}{KL} \right) \left(\cosh (KL) \left(\frac{x_2}{L} \right) - 1 \right) \right] \qquad (4.6.2)$$

and $f_5(KL, x_2/L) = \left(\frac{1}{KL(\cosh KL + 1) - 2 \sinh KL} \right) \left[\left[(\cosh KL + 1) \right] \left[(KL)(x_2/L) \right. \right.$

$$\left. \left. - \sinh (KL)(x_2/L) \right] + \left[\sinh KL \right] \left[\cosh (KL)(x_2/L) - 1 \right] \right] \qquad , \qquad (4.6.3)$$

(a) Translation   (b) Rotation
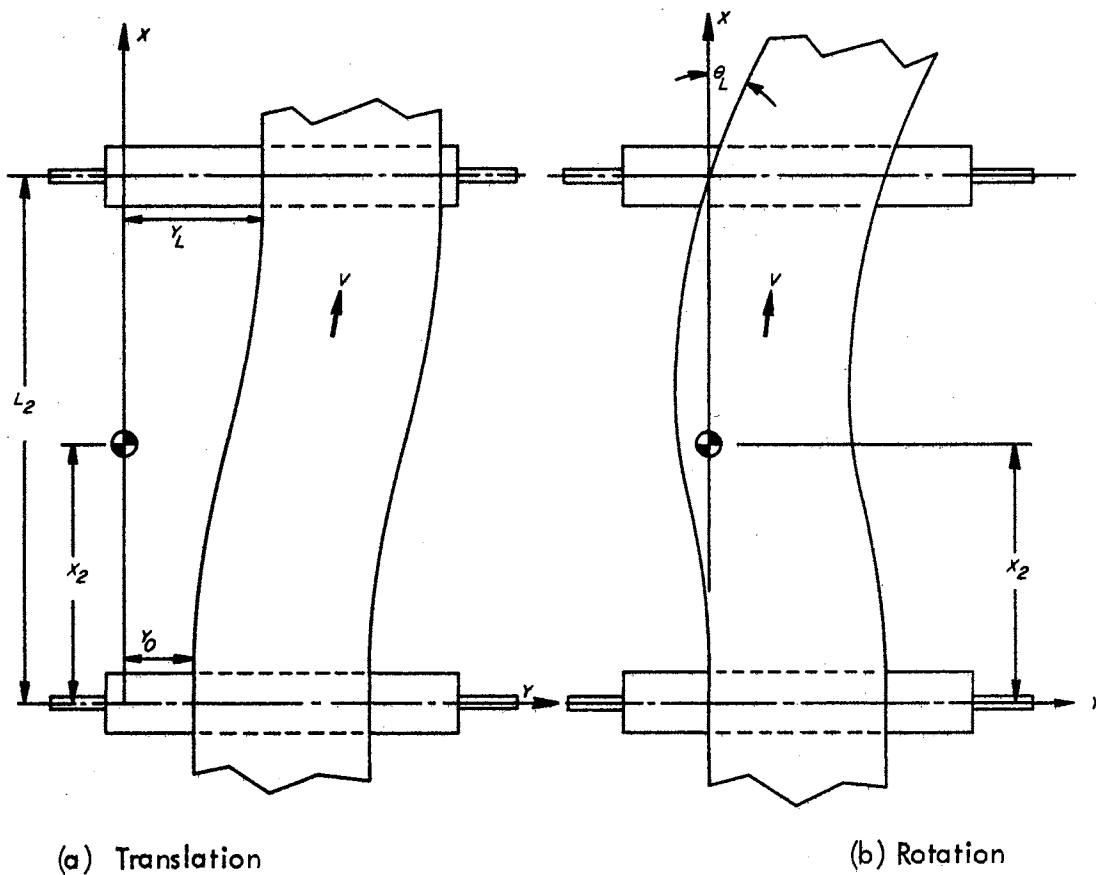
Figure 4.6.1. Two Components of Deflection of a Web Between Two Parallel Rollers.

then Equation 4.6.1 can be written as

$$y_2 = y_o - f_4 L \theta_L + (f_5)(y_L - y_o) \quad . \qquad (4.6.4)$$

Equation 4.6.4 may be converted to a relationship of transfer functions by using the Laplace transform and dividing the result by $Y_o(S)$:

$$\frac{Y_2(S)}{Y_o(S)} = 1 - f_4 L \frac{\theta_L(S)}{Y_o(S)} + (f_5)\left(\frac{Y_L(S)}{Y_o(S)} - 1\right) \quad . \qquad (4.6.5)$$

The unknown transfer functions will be derived from those found previously in this thesis.

From Equation 4.2.7:

$$\frac{Y_L(S)}{Y_o(S)} = \frac{1}{\dfrac{T_2^2}{f_1(KL)}\, S^2 + K_c T_2 S + 1} \quad . \qquad (4.6.6)$$

By simple algebraic manipulation of Equation 4.6.6:

$$\frac{Y_L(S)}{Y_o(S)} - 1 = -\frac{\left[T_2^2/f_1(KL)\right] S^2 + T_2 K_c S}{\left[T_2^2/f_1(KL)\right] S^2 + K_c T_2 S + 1} \quad . \qquad (4.6.7)$$

For the behavior of a web on the second of two parallel rollers, the Laplace transform of Equation 4.2.4 is

$$\theta_L(S) = -\frac{1}{V}\, S Y_L(S) \quad . \qquad (4.6.8)$$

If Equation 4.6.8 is divided by $Y_o(S)$ and Equation 4.6.6 substituted, the result is

$$\frac{\theta_L(S)}{Y_o(S)} = \frac{-(1/V)S}{\dfrac{T_2^2}{f_1(KL)}\, S^2 + K_c T_2 S + 1} \quad . \qquad (4.6.9)$$

Substitution of Equations 4.6.7 and 4.6.9 into Equation 4.6.5 and subsequent algebraic manipulation yields the transfer function for response at the sample point x_2 between parallel rollers, with position of the web at the first roller considered as the input:

$$\frac{Y_2(S)}{Y_o(S)} = \frac{\left[T_2^2/f_1(KL)\right](1-f_5) S^2 + T_2\left[K_c(1-f_5)+f_4\right] S + 1}{\left[T_2^2/f_1(KL)\right] S^2 + T_2 K_c S + 1} \quad . \qquad (4.6.10)$$

Figure 4.6.2. Second-Order Frequency Response at a Point Between Two
Parallel Rollers for KL = 0.

Figure 4.6.3. Second-Order Frequency Response at a Point Between Two
Parallel Rollers for KL = 10.

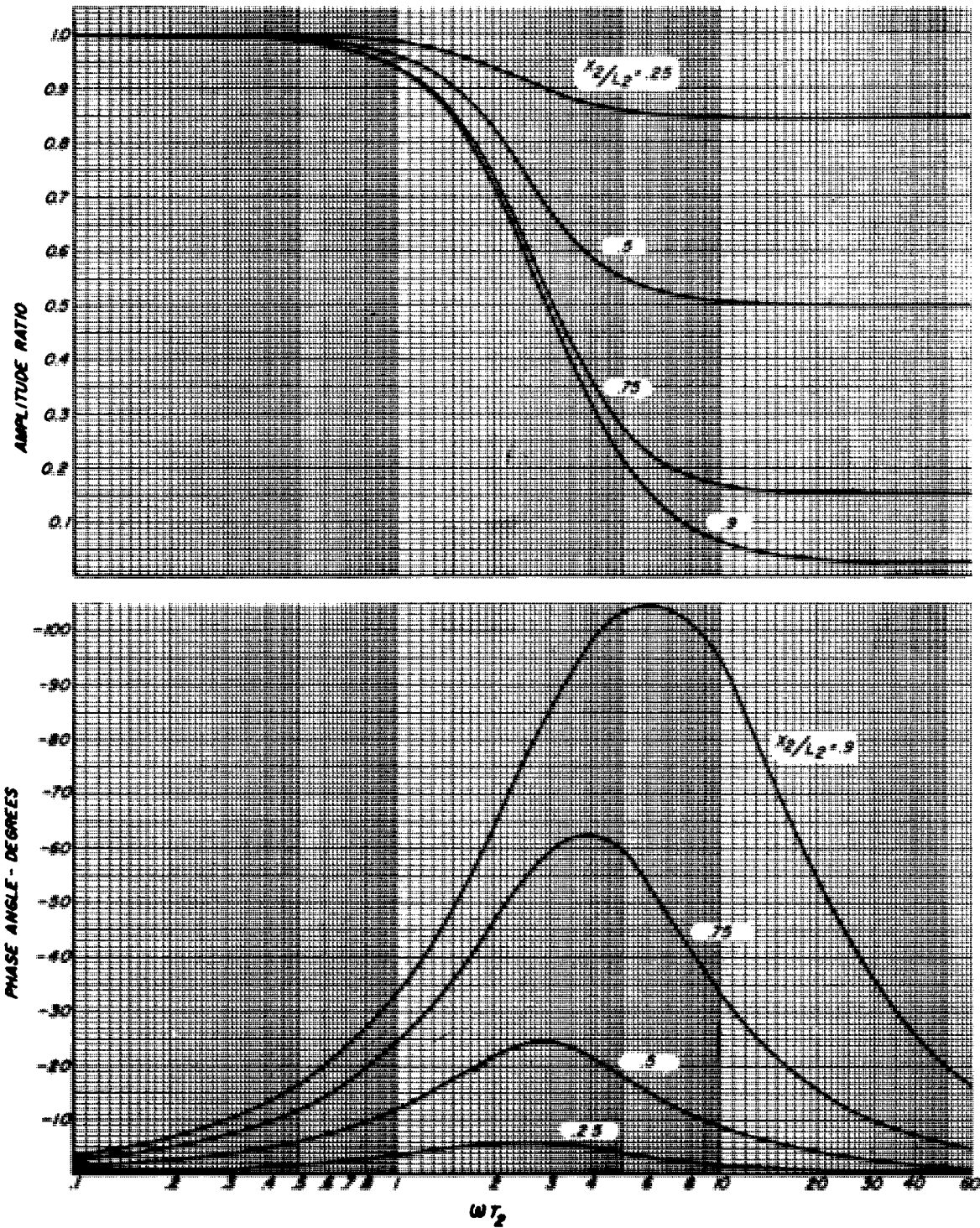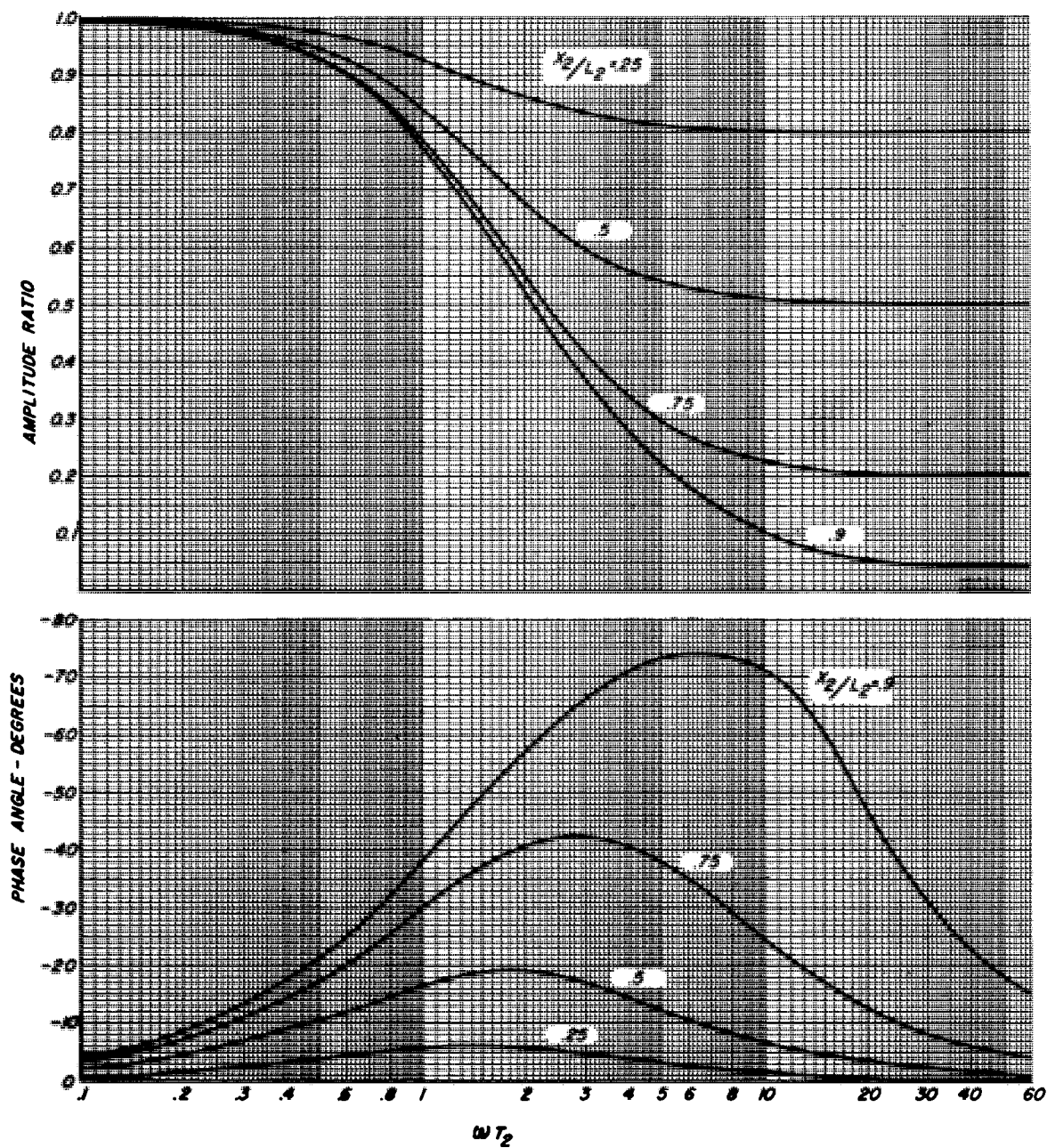The frequency response of Equation 4.6.10 is shown in Figure 4.6.2 for a KL value of zero, and in Figure 4.6.3 for a KL value of ten. It should be noted that both the amplitude ratio and the phase lag depart significantly from that given by the first-order theory shown in Figure 3.4.2. The response for values of KL up to unity is very near that for KL of zero.

4.7. Experimental Verification. The dynamic test machine described in Section 2.2 was used for verification of the second-order theory of this chapter. Figures 2.2.1 and 2.2.2 should be reviewed by the reader.

The primary problems encountered involved finding a stable, elastic, straight, flat web, and in sensing at the desired points. Because transmitted-light sensing was used for part of the testing, it was necessary that the web be opaque. It was desirable to use a web of low modulus of elasticity to permit the value of KL to be large enough that comparatively large inputs could be introduced, in order to improve the accuracy of measurement.

The webs used were polystyrene plastic 0.009 inches thick, painted with white latex paint. The modulus of elasticity before coating was 450,000 psi, and was 510,000 psi after painting, based upon the original thickness. The moment of inertia was also based upon the original thickness, so that the thickness error cancelled in all the equations of interest.

Whenever possible, sensing was done with special transmitted-light sensing heads with four inches of proportional band. When it was necessary to sense at the edge of the contact area, a reflected-light sensing head was used. The reflected-light sensing head had a very limited proportional band, so it was necessary to servo-position the sensing head. The position of the sensing head was measured with a linear potentiometer on the actuator. A servo motor with a corner frequency of 15 cps was used to drive a ball screw as an actuator. If the servo-positioner dynamics had been significant, the indicated readings could have been corrected

accordingly; however, no phase lag or amplitude error of the servo system could be detected at the test frequencies.

Signal recording was done on two channels of a Honeywell Visicorder, which had many times the frequency capability necessary.

Web irregularities caused difficulty even after great care in workmanship and technique. At low frequencies of oscillation, the splice caused errors in every cycle. At higher frequencies, the cycles which were disturbed by the splice could be discarded. Irregularities in the trace were visually smoothed with drafting curves and a pencil.

The sine-wave error input was introduced by "chasing" a small oscillating blade with one of the air-piloted hydraulic servo systems, which positioned one of the rollers of the test machine. The blade was oscillated by a crank driven through a gearbox by one of the rollers of the machine. A six-speed gearbox with ratios in geometric progression, with each ratio differing from the preceding one by a factor of two, drove the crank. If further frequency selection had been necessary, the drive gears or the driven roller size could have been changed, but the frequency range of interest was adequately covered with six data points. The amplitude of oscillation was readily changed with several selections of crank throw radius.

Because the oscillation frequency was proportional to web speed, ωT_1 was a constant regardless of the web speed. The speed control of the "constant-speed" drive was quite poor at low speeds, so that the chosen method of oscillation was highly desirable.

The sine-wave error input for the first test configuration was generated by the apparatus of Figures 4.7.1 and 4.7.2 and the response measured at the downstream roller shown in Figure 4.7.3. The theory which was to be verified is covered in Section 4.2.
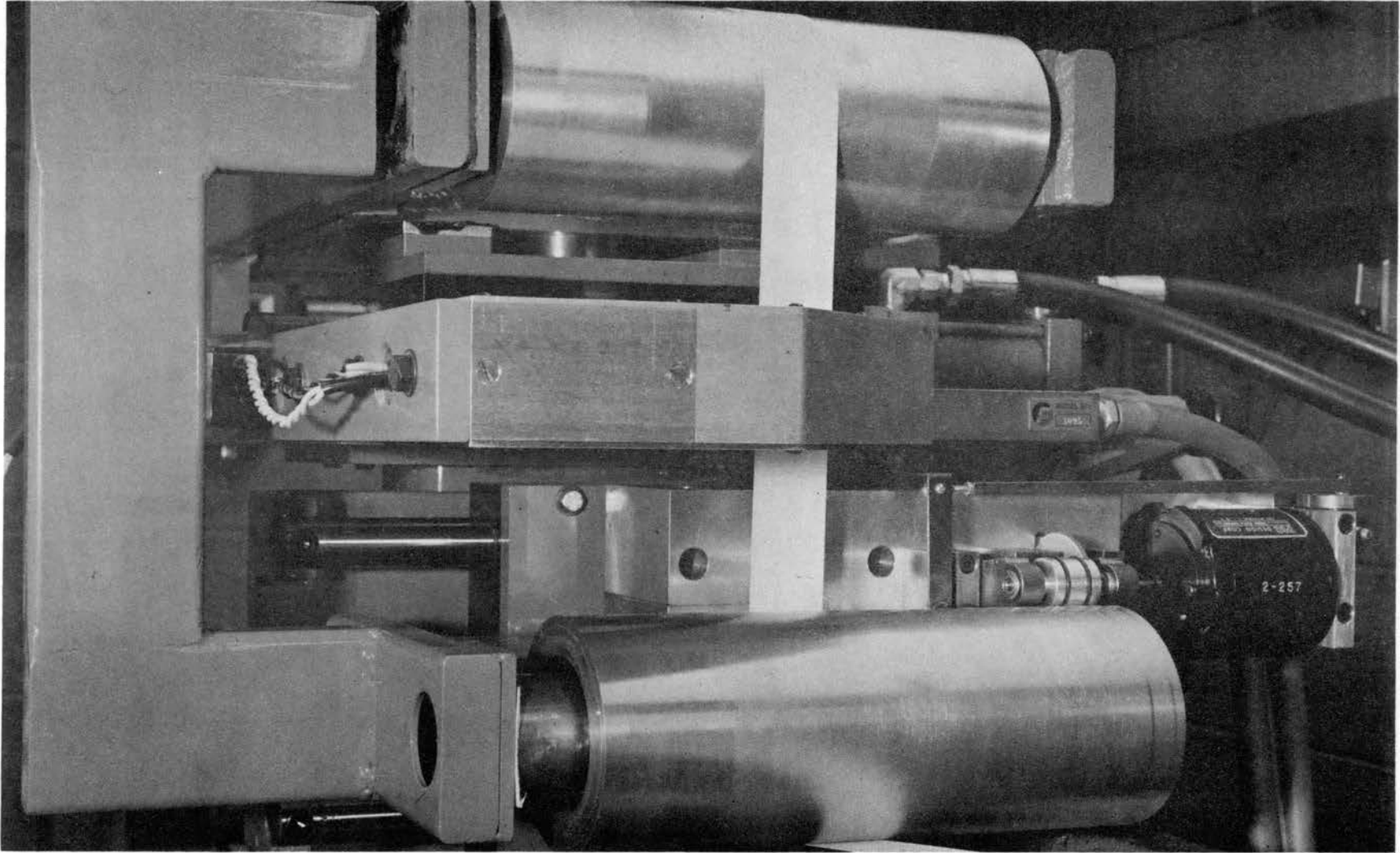
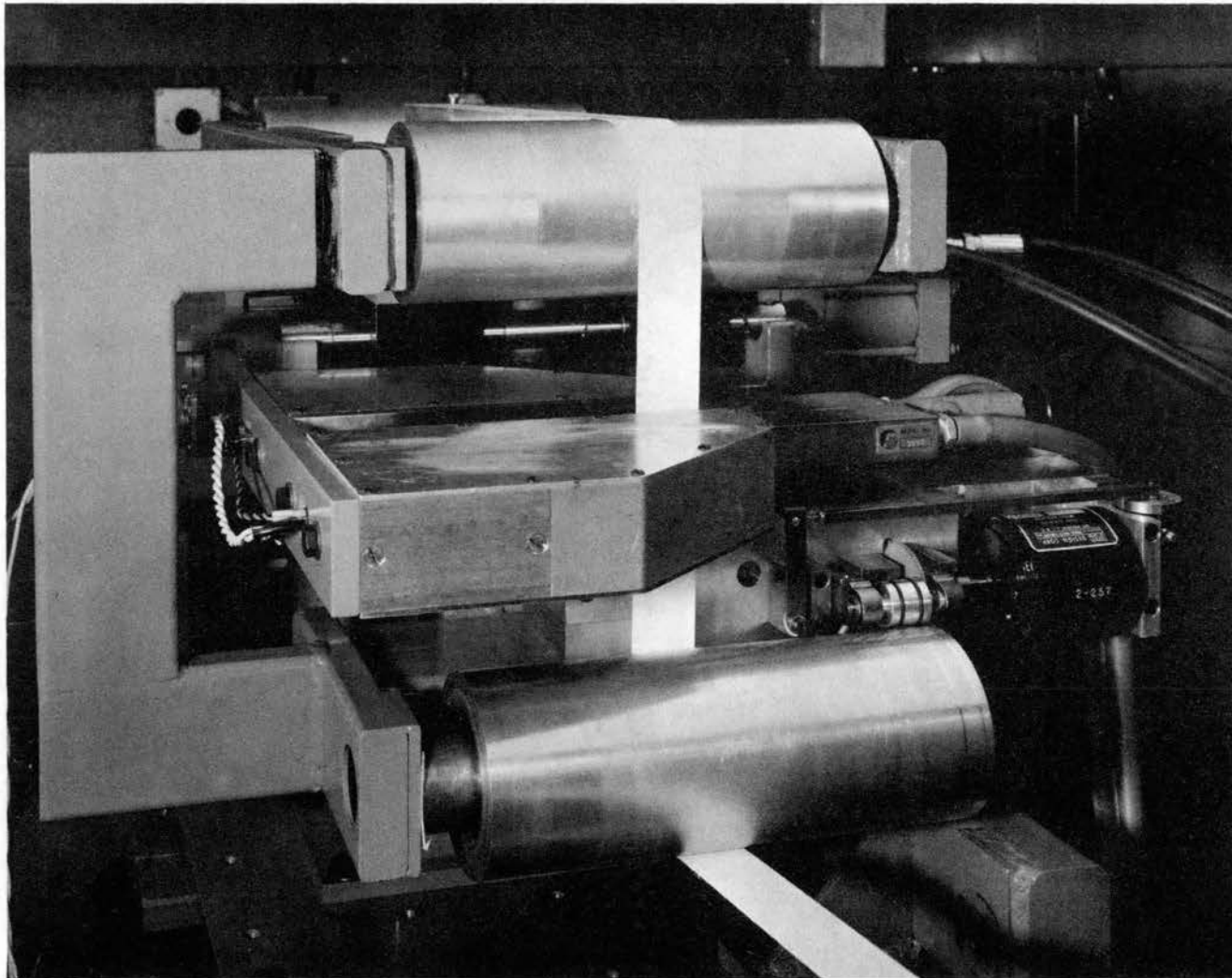Figure 4.7.1. Sine-Wave Generator on Displacement Guide.

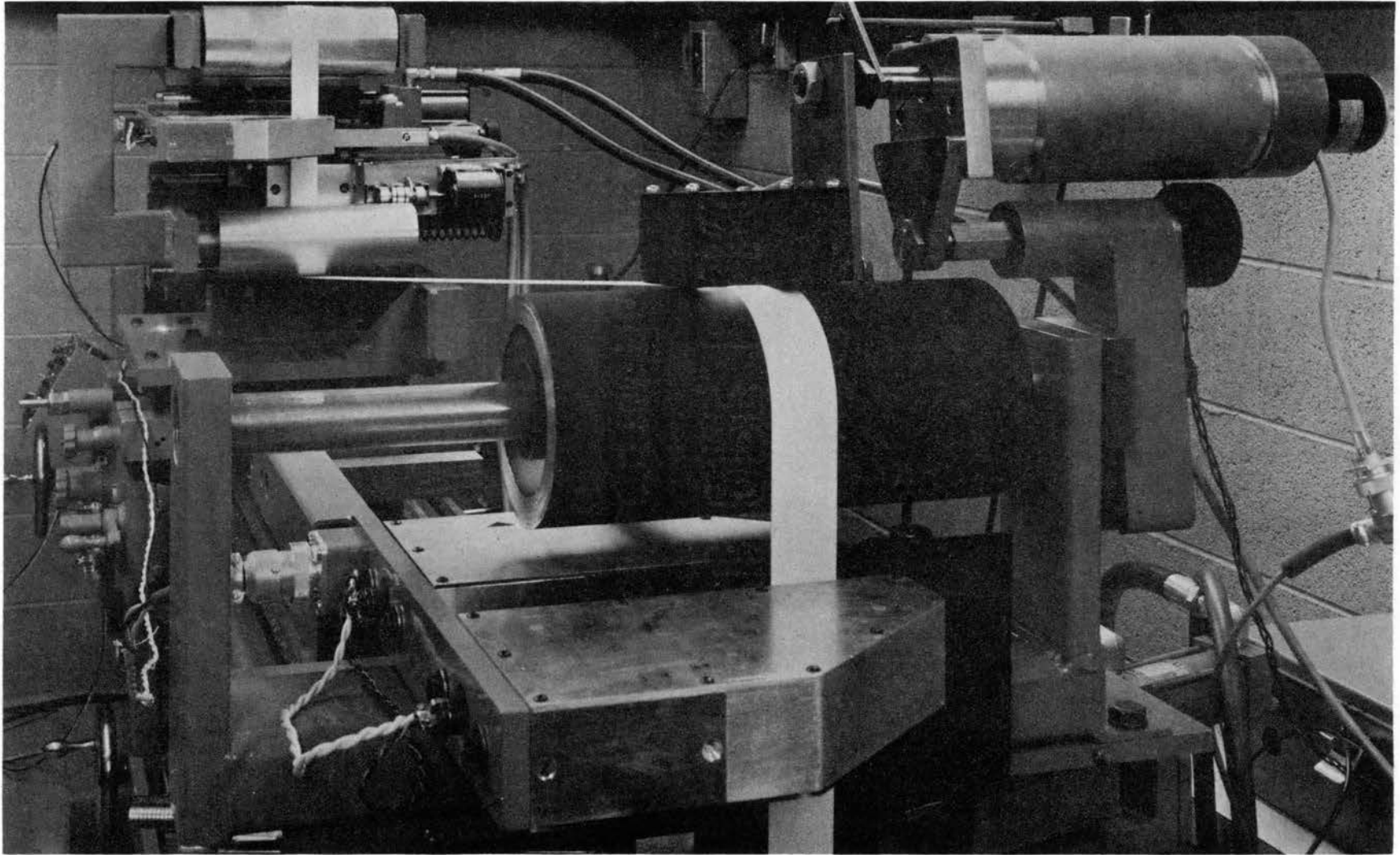Figure 4.7.2. Sine-Wave Generator on Displacement Guide.

Figure 4.7.3. Apparatus for Testing Response at a Fixed Roller to Input at Previous Roller.

Although the black roller of Figure 4.7.3 was part of a steering guide assembly, for the test under discussion it was centered and locked. The output response was measured with the electro-mechanical servo positioner shown in the top right of Figure 4.7.3.

The input oscillation was introduced by the displacement guide on the carriage of the test machine. The guide was servo-controlled by the mechanical oscillator shown on the right of Figures 4.7.1 and 4.7.2. The input position of the web was sensed by the large sensing head midway between the rollers of Figures 4.7.1 and 4.7.2.

The displacement guide shown in Figures 4.7.1 and 4.7.2 is unconventional, for the special needs of this test. The upper pivoting assembly of two rollers, seen best in Figure 4.7.2, follows normal practice, but the lower roller would normally be stationary. Figure 4.7.1 shows the rods, which are parallel to the roller axis, on which the lower roller assembly slides. The rigid arm attached to the lower roller assembly is held against the displacement guide assembly by a spring, which is visible below the oscillator gearbox in Figure 4.7.3. The lower roller thus moves laterally (relative to the web) the same as the front roller of the displacement guide. The web between the rollers moves laterally the same amount as y_o, the beginning of the free span, so y_o can be sensed with the sensing head between the rollers.

The experimental data for response at the downstream roller with the input at the first roller is shown in Figure 4.7.4. The theoretical response from Equation 4.2.7 is shown as solid and dashed lines. The polystyrene web described previously was 1.5 inches wide and under 30 pounds of tension, and with a free span length of 63 inches for the test of KL = 10. For KL = 2, the width was 3.0 inches, the tension 46 pounds, and the free span length was 30 inches.

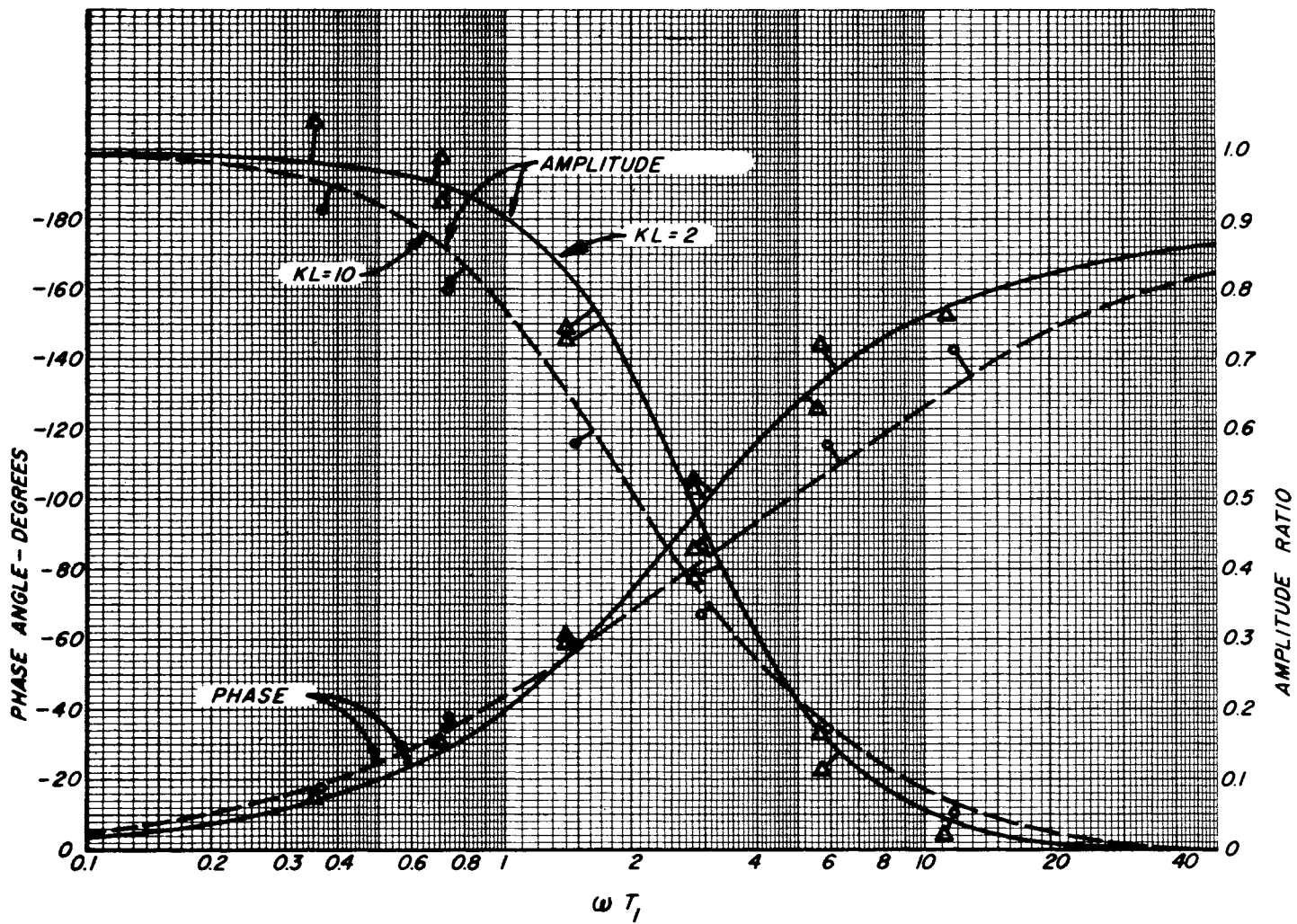The data scatter of Figure 4.7.4 is more than one might wish, but the theory

Figure 4.7.4. Comparison of Experimental Results to Theoretical Curves
for Response at a Fixed Roller.
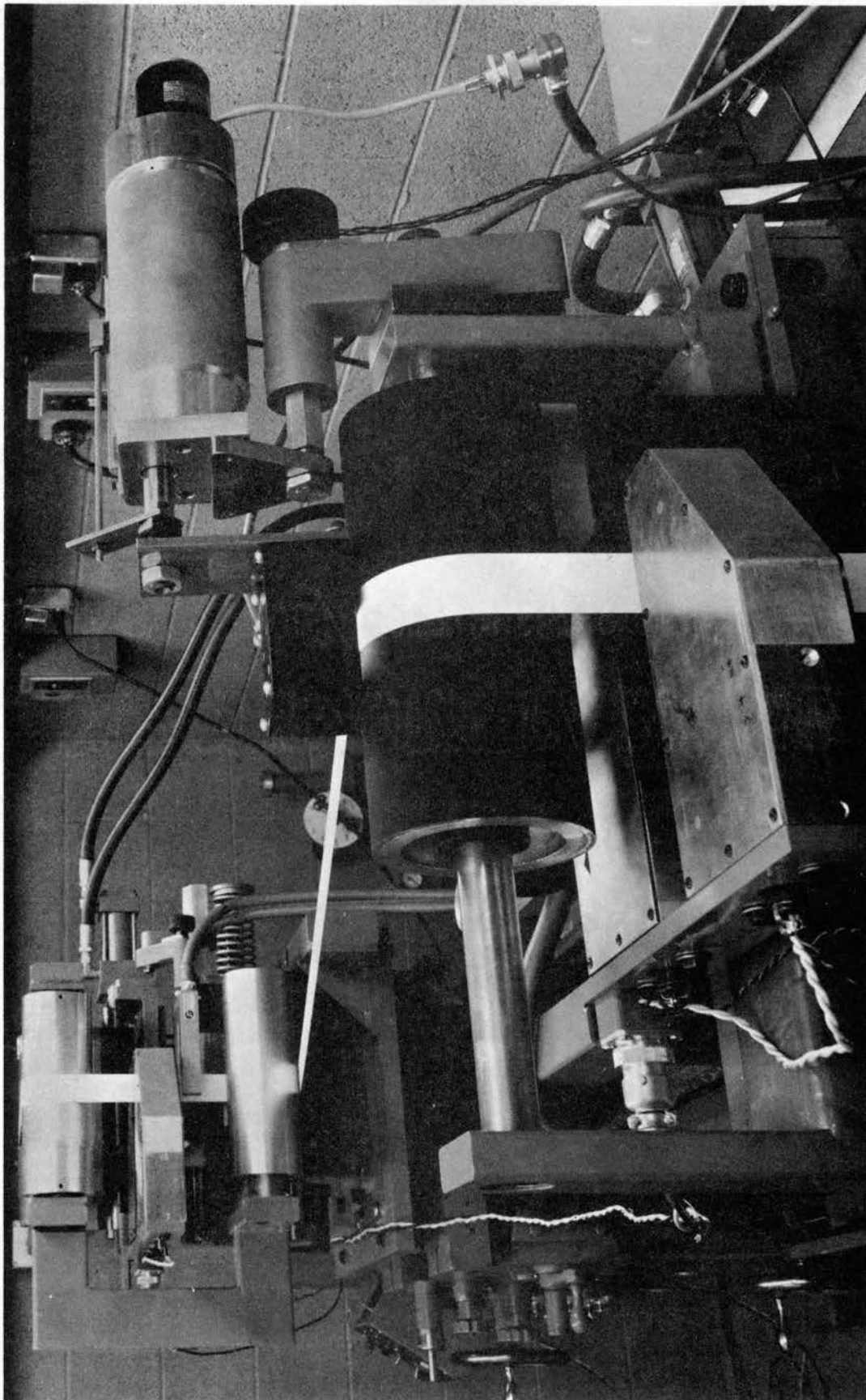
Figure 4.7.5. Apparatus for Testing Response to a Steering Guide Input.
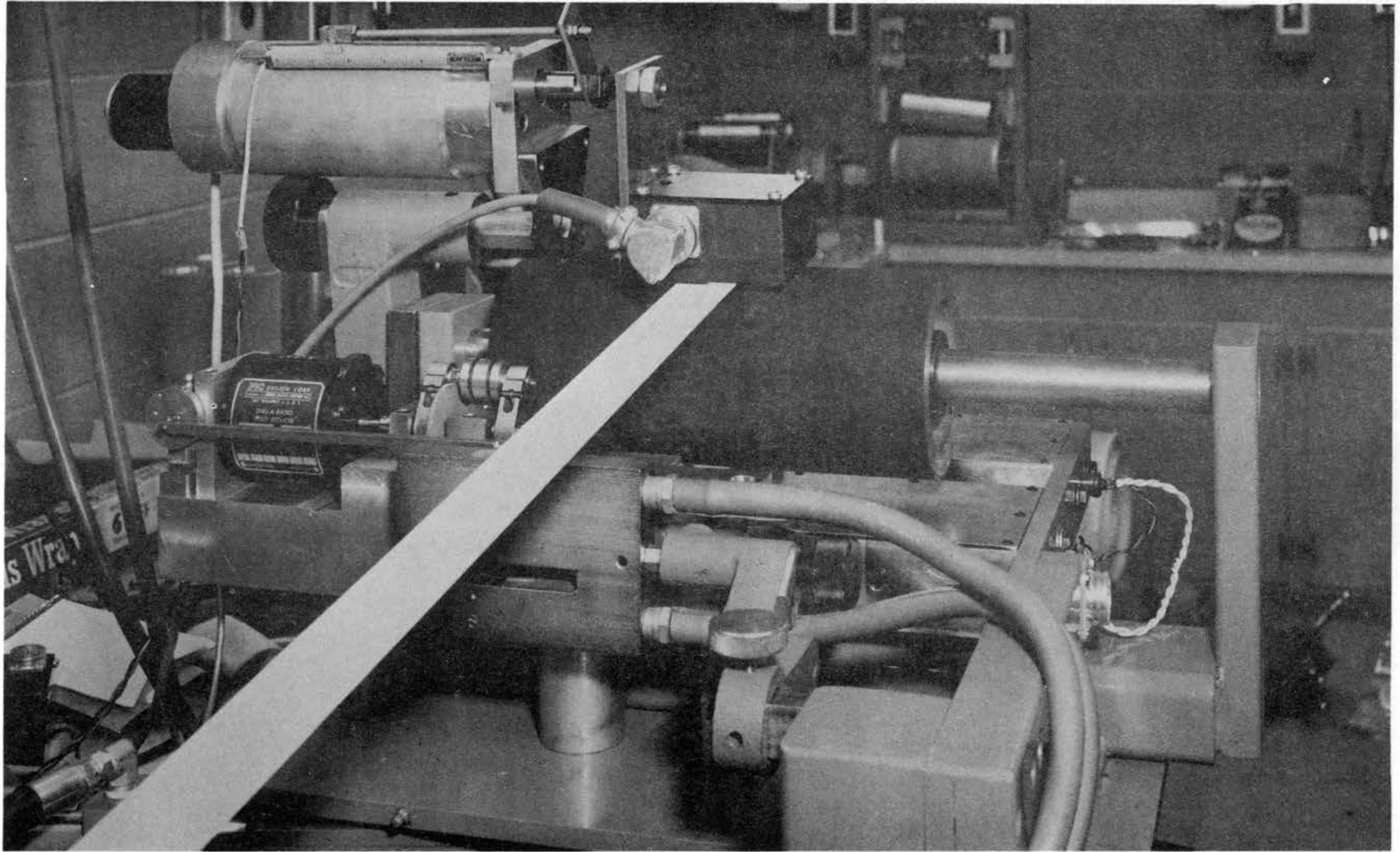
Figure 4.7.6. Sine-Wave Generator and Position Sensor on the Steering Guide.

is well supported. The relative levels of both amplitude and phase lag for the two values of KL are clearly indicated at all frequencies tested.

Another set of dynamic tests were run to verify the transfer function of a steering guide. The test arrangement is shown in Figure 4.7.5 and 4.7.6. The black roller is the roller of the guide under test. The displacement guide used for the input in the previous test was used as a final error-cleanup guide for this test. Incidentally, the ability to guide the web as it entered the test span contributed to better results than those of the previous test.

The large sensing head shown between the rollers of the displacement guide in the background of Figure 4.7.5 was not used in this test. The small air-jet sensing head on the right of the web below the large head automatically controlled the displacement guide.

The test guide position was sensed by the large sensing head in the foreground of Figure 4.7.5. The black metal plate in the gap of the sensing head was attached to the guide assembly and overhung the web enough that the web edge was never sensed. The sensing head, amplifier, and recorder combination was calibrated with the scale on the slider block, shown in Figure 2.2.5.

The position of the web relative to the guide roller was sensed by the electro-mechanical servo positioner shown above the black roller. The linear potentiometer for position measurement is shown at the top of the actuator in Figure 4.7.6. The oscillator previously described was moved to the steering guide, which it controlled as shown in Figure 4.7.6.

The data obtained from the test described above is not the desired data for confirmation of Equation 4.4.4. The measured output is relative to the roller and the desired output is relative to the ground. In transfer-function form, the measured data was $[Y_L - Z]$ $(S)/Z(S)$ and the desired data is $Y_L(S)/Z(S)$. A simple algebraic
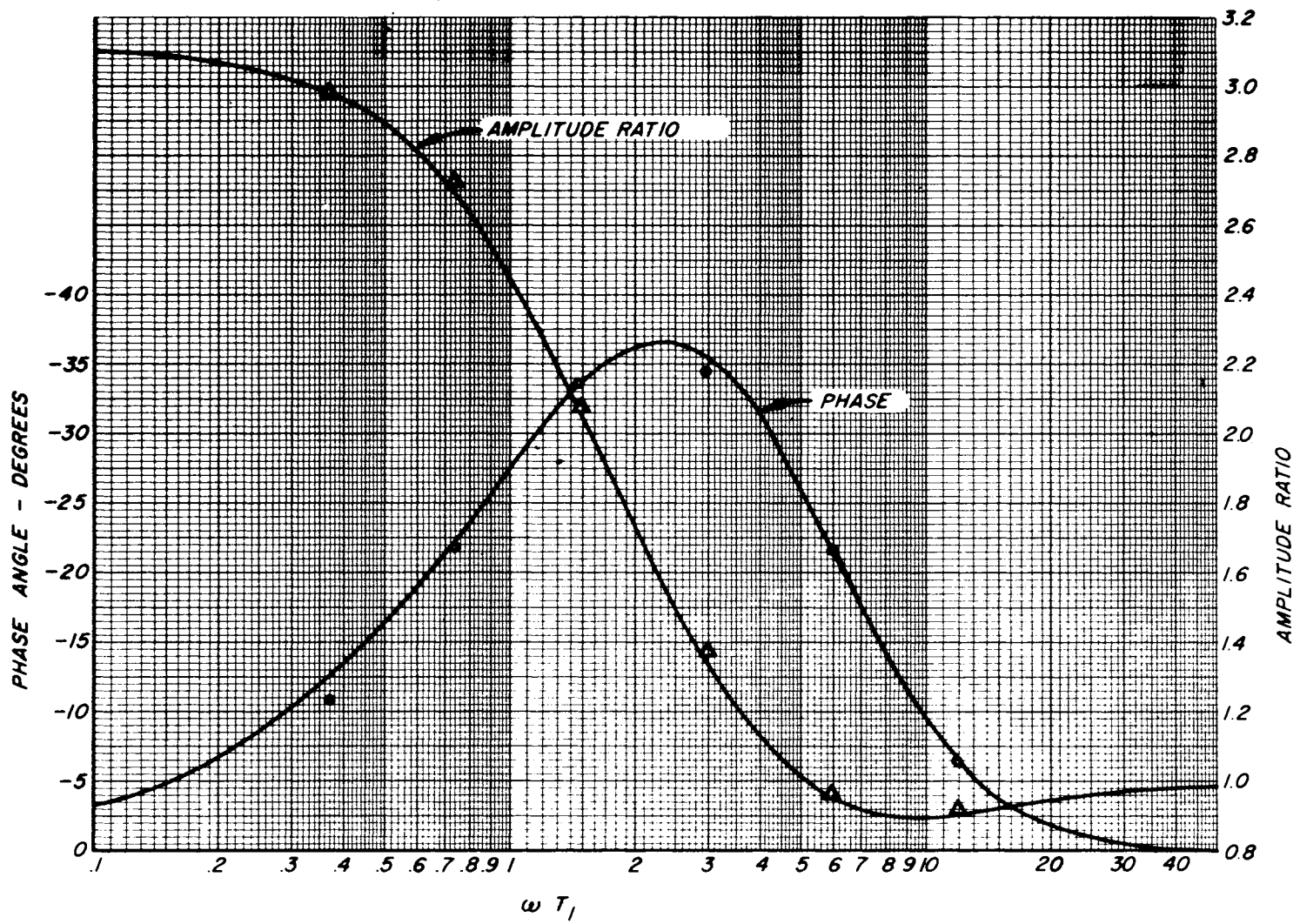
Figure 4.7.7. Comparison of Experimental Results to Theoretical Curves for Response to an Oversteering Guide (KL = 10, $K_c L/L_1$ = 3.12).
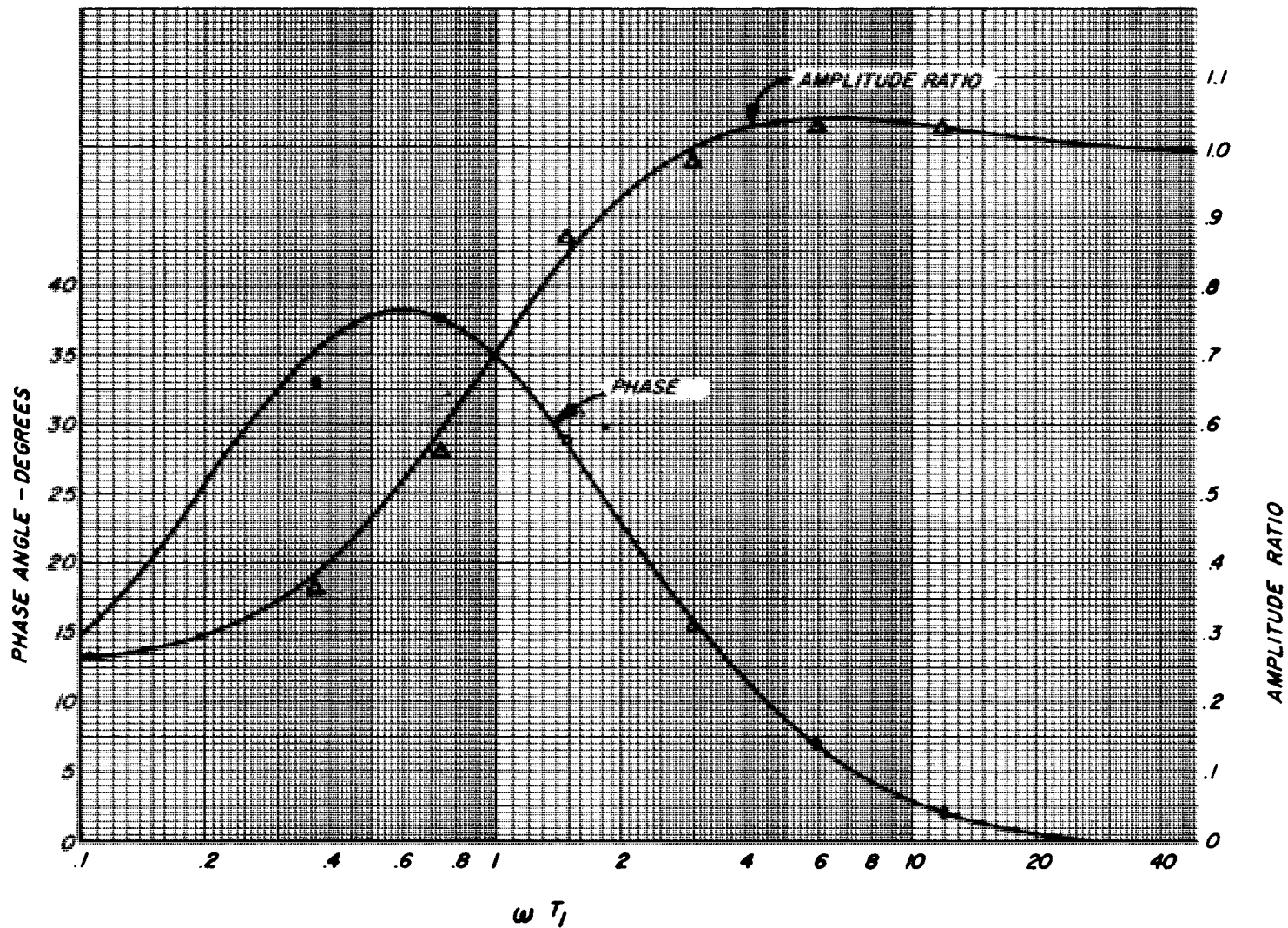
Figure 4.7.8. Comparison of Experimental Results to Theoretical Curves for Response to an Understeering Guide (KL = 10, $K_c L/L_1 = 0.25$).

manipulation gives the desired output:

$$\frac{Y_L(S)}{Z(S)} = \frac{[Y_L-Z](S)}{Z(S)} + 1 = \frac{[Y_L-Z](S) + Z(S)}{Z(S)} \quad . \qquad (4.7.1)$$

Vector arithmetic then yields the desired data.

For this test, the painted polystyrene web was 1.5 inches wide, the tension was 30 pounds, and the length of the free span was 63 inches, to make KL equal to ten.

The test data for the steering guide in an oversteering condition is shown in Figure 4.7.7. The solid curves are theoretical, from Equation 4.4.4. A similar set of data is shown in Figure 4.7.8 for an understeering guide. The test data gave superb confirmation of the theory.

CHAPTER V

SECOND-ORDER DYNAMICS WITH CONSIDERATION OF WEB MASS

All previous analysis except for the study of Section 2.5 has assumed that the mass of the web has a negligible effect on lateral web behavior. This chapter considers the effect of web mass for a web undergoing a steady-state sinusoidal disturbance. The transfer function for response of a web to the motion of a conventional steering guide is developed from the fundamental theory for consideration of mass. The region of validity of the massless theory is examined in Section 5.3.

5.1. Fundamental Theory. The general partial differential equation of the free span of the web if the mass of the web is considered is:

$$EI \frac{\partial^4 y}{\partial x^4} - T \frac{\partial^2 y}{\partial x^2} = -\frac{w}{g} \frac{\partial^2 y}{\partial t^2} , \qquad (5.1.1)$$

where w is the weight per unit length and g is the acceleration of gravity.

In vibrations studies, it is customarily assumed that all points on the web undergo sine-wave motion of a given frequency. The time variable is then eliminated by studying only the shape at the condition of maximum deflection. The nodes and antinodes are given by the points of zero and maximum deflection. Such an approach is compatible with the frequency-response approach to automatic controls analysis, which likewise assumes a steady-state sine-wave input.

Damping which in a real web would be contributed by internal friction and by air friction is neglected. As a result of the assumption of zero damping, all

147

points on the web are either in phase with the input sine wave or 180 degrees out of phase.

The web span will be analyzed with a sine-wave translation of the end, then with a sine-wave rotation of the end. The two results can then be superimposed for specific cases.

It is assumed that

$$y = y_m \sin(\omega t + \phi) \quad , \tag{5.1.2}$$

where the subscript m denotes the maximum value of the deflection at any given point and ϕ is a phase angle, either zero or 180 degrees for the case of no damping. The partial differential equation may now be written as an ordinary differential equation of the elastic curve of maximum amplitude:

$$EI \frac{d^4 y_m}{dx^4} - T \frac{d^2 y_m}{dx^2} - \omega^2 \frac{w}{g} y_m = 0 \quad . \tag{5.1.3}$$

If

$$n^4 = \frac{1}{EI} \frac{\omega^2 w}{g} \tag{5.1.4}$$

and

$$K^2 = T/EI \quad , \tag{5.1.5}$$

then Equation 5.1.3 may be written as

$$\frac{d^4 y_m}{dx^4} - K^2 \frac{d^2 y_m}{dx^2} - n^4 y_m = 0 \quad . \tag{5.1.6}$$

The roots of the characteristic equation of Equation 5.1.6 are

$$r = \pm \sqrt{(1/2)(K^2 + \sqrt{K^4 + 4n^4})} \quad , \qquad \pm i \sqrt{(1/2)(-K^2 + \sqrt{K^4 + 4n^4})} \quad ,$$

which may be written as $r = \pm p, \pm iq$ if

$$p = \sqrt{(1/2)(K^2 + \sqrt{K^4 + 4n^4})} \qquad (5.1.7)$$

and

$$q = \sqrt{(1/2)(-K^2 + \sqrt{K^4 + 4n^4})} \quad . \qquad (5.1.8)$$

The general solution to Equation 5.1.6 may be written as

$$y_m = A \sinh px + B \cosh px + C \sin qx + D \cos qx. \qquad (5.1.9)$$

For the boundary conditions shown in Figure 5.1.1, the constants can be
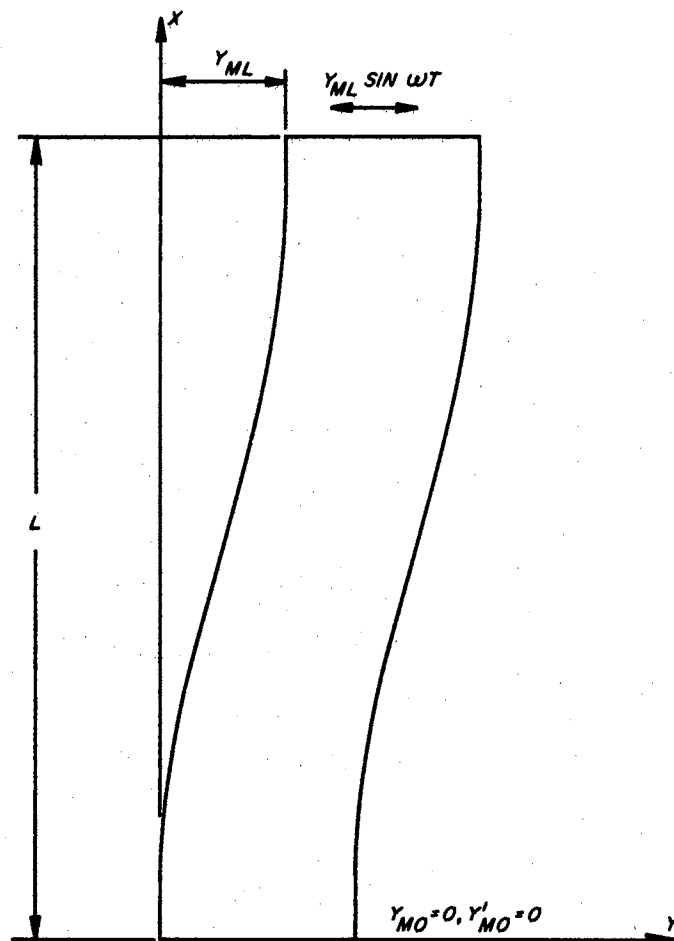
Figure 5.1.1. Boundary Conditions for Maximum Translation of the Web End.

found to be:

$$A = \frac{-y_{mL}(\sinh pL + \frac{q}{p}\sin qL)}{2(1 - \cosh pL \cos qL) + \left(\frac{p}{q} - \frac{q}{p}\right)\sinh pL \sin qL} \quad , \tag{5.1.10}$$

$$B = \frac{y_{mL}(\cosh pL - \cos qL)}{2(1 - \cosh pL \cos qL) + \left(\frac{p}{q} - \frac{q}{p}\right)\sinh pL \sin qL} \quad , \tag{5.1.11}$$

$$C = \frac{y_{mL}(\frac{p}{q}\sinh pL + \sin qL)}{2(1 - \cosh pL \cos qL) + \left(\frac{p}{q} - \frac{q}{p}\right)\sinh pL \sin qL} \quad , \tag{5.1.12}$$

and

$$D = \frac{-y_{mL}(\cosh pL - \cos qL)}{2(1 - \cosh pL \cos qL) + \left(\frac{p}{q} - \frac{q}{p}\right)\sinh pL \sin qL} \quad . \tag{5.1.13}$$

If

$$K_1 = \frac{1}{2(1 - \cosh pL \cos qL) + \left(\frac{p}{q} - \frac{q}{p}\right)\sinh pL \sin qL} \quad , \tag{5.1.14}$$

then the elastic curve may be written as:

$$y_m = y_{mL}K_1 \left[(\sinh pL + \frac{q}{p}\sin qL)(-\sinh px + \frac{p}{q}\sin qx) \right.$$

$$\left. + (\cosh pL - \cos qL)(\cosh px - \cos qx) \right] \quad . \tag{5.1.15}$$

The moment at x_o is:

$$M_{mo} = Ty_{mL}K_1 \left[\cosh\left(\frac{p}{K}\right)(KL) - \cos\left(\frac{q}{K}\right)(KL) \right]\left[\left(\frac{p}{K}\right)^2 + \left(\frac{q}{K}\right)^2\right] \quad , \tag{5.1.16}$$

and the moment at x_L is:

$$M_{mL} = Ty_{mL}K_1 \left\{ \left[\left(\frac{q}{K} \right)^2 - \left(\frac{p}{K} \right)^2 \right] \left[1 - \cosh\left(\frac{p}{K} \right)(KL)\cos\left(\frac{q}{K} \right)(KL) \right] \right.$$

$$\left. + 2\left(\frac{p}{K} \right)\left(\frac{q}{K} \right)\sinh\left(\frac{p}{K} \right)(KL)\sin\left(\frac{q}{K} \right)(KL) \right\} \qquad . \qquad (5.1.17)$$

Note that the moment equations have been non-dimensionalized by use of the terms:

$$\frac{p}{K} = \sqrt{(1/2)(1 + \sqrt{1 + 4(n/K)^4})} \qquad (5.1.18)$$

and

$$\frac{q}{K} = \sqrt{(1/2)(-1 + \sqrt{1 + 4(n/K)^4})} \qquad . \qquad (5.1.19)$$

The second component of the maximum deflection and the boundary conditions are shown in Figure 5.1.2. The constants of Equation 5.1.9 in this case are found to be:

$$A = \frac{\theta_{mL}(\cosh pL - \cos qL)}{2p(1 - \cosh pL \cos qL) + (\frac{p^2}{q} - q)\sinh pL \sin qL} \qquad , \qquad (5.1.20)$$

$$B = \frac{-\theta_{mL}(\sinh pL - \frac{p}{q}\sin qL)}{2p(1 - \cosh pL \cos qL) + (\frac{p^2}{q} - q)\sinh pL \sin qL} \qquad , \qquad (5.1.21)$$

$$C = \frac{-\theta_{mL}(p/q)(\cosh pL - \cos qL)}{2p(1 - \cosh pL \cos qL) + (\frac{p^2}{q} - q)\sinh pL \sin qL} \qquad , \qquad (5.1.22)$$

and

$$D = \frac{\theta_{mL}(\sinh pL - \frac{p}{q}\sin qL)}{2p(1 - \cosh pL \cos qL) + (\frac{p^2}{q} - q)\sinh pL \sin qL} \qquad . \qquad (5.1.23)$$

If $K_2 = \dfrac{1}{2pL(1 - \cosh pL \cos qL) + (\frac{p^2}{q} - q)L \sinh pL \sin qL}$,   (5.1.24)

then the elastic curve of maximum deflection can be written as:

$$y_m = K_2 \theta_{mL} L \left[(\cosh pL - \cos qL)(\sinh px - \frac{p}{q} \sin qx) \right.$$

$$\left. - (\sinh pL - \frac{p}{q} \sin qL)(\cosh px - \cos qx) \right]$$.   (5.1.25)
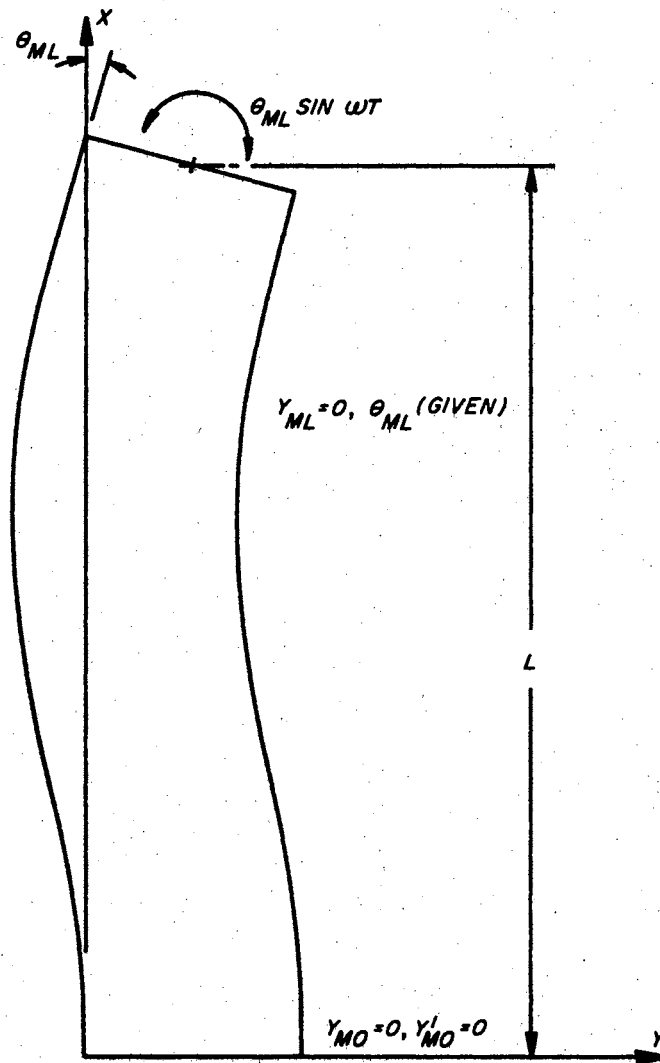
Figure 5.1.2. Boundary Conditions for Maximum Rotation
of the Web End.

The moment at x_o is:

$$M_{mo} = K_2 T \theta_{mL} L \left[\sinh\left(\frac{p}{K}\right)(KL) - \left(\frac{p}{K}\right)\left(\frac{K}{q}\right) \sin\left(\frac{q}{K}\right)(KL) \right]\left[\left(\frac{p}{K}\right)^2 + \left(\frac{q}{K}\right)^2\right] , \quad (5.1.26)$$

and at x_L the moment is:

$$M_{mL} = K_2 T \theta_{mL} L \left[\left(\frac{p}{K}\right)^2 + \left(\frac{q}{K}\right)^2\right]\left[\sinh\left(\frac{p}{K}\right)(KL)\cos\left(\frac{q}{K}\right)(KL)\right]$$

$$- \left[\left(\frac{p}{K}\right)\left(\frac{q}{K}\right) + \left(\frac{p}{K}\right)^3\left(\frac{K}{q}\right)\right]\left[\cosh\left(\frac{p}{K}\right)(KL)\sin\left(\frac{q}{K}\right)(KL)\right] . \quad (5.1.27)$$

Note that the non-dimensionalizing scheme of Equations 5.1.18 and 5.1.19 has been applied to the moment equations.

The factor $(n/K)^4$ in Equations 5.1.18 and 5.1.19 can be expressed in familiar terms. From Equations 5.1.4 and 5.1.5:

$$\left(\frac{n}{K}\right)^4 = \frac{\omega^2 w}{g} \frac{EI}{T^2} . \quad (5.1.28)$$

If ρ is the density of the web in pounds per cubic inch, W the web width, T_1 the time constant of the free web span, and S_1 the average tensile stress in the web, the equation may be expressed as

$$\left(\frac{n}{K}\right)^4 = (\omega T_1)^2 W_4 , \quad (5.1.29)$$

where

$$W_4 = \frac{\rho W^2 E}{(12)(386)T_1^2 S_1^2} , \quad (5.1.30)$$

Equations 5.1.18 and 5.1.19 show that (p/K) and (q/K) are functions only of $(n/K)^4$, which is a function only of W_4 and ωT_1. A comparison of the moment equations of this chapter with the moment equations of the massless web, Equations 4.1.12 and 4.1.21, reveals that ratios of corresponding moments can be expressed as functions of KL, p/K, and q/K if θ_L can be substituted for θ_{mL} and y_L for y_{mL}. Therefore, if the substitutions are permissible, the moment ratios can be expressed as functions of KL, ωT_1, and W_4.

Although the elastic curve of maximum amplitude was used for the derivations of this chapter, the results apply to the web at any time. Equation 5.1.2 assumed that any given point on the web would vibrate sinusoidally. For each of the two components of deflection, the moment varies sinusoidally, either in phase with or 180 degrees out of phase with the input. Therefore, the substitution of θ_L for θ_{mL} and y_L for y_{mL} is permissible.

If the symbol MR_{tr} denotes the moment ratio for end translation and MR_{ro} for end rotation:

$$MR_{tr} = \frac{\text{Equation } 5.1.17}{\text{Equation } 4.1.12} \tag{5.1.31}$$

and

$$MR_{ro} = \frac{\text{Equation } 5.1.27}{\text{Equation } 4.1.21} \; . \tag{5.1.32}$$

The curvature ratio is equal to the moment ratio; therefore, the equations of web dynamics of Chapter IV may be modified to account for the mass of the web, as in the example of the next section.

5.2. Steering Guide Response With Consideration of Web Mass. Only one example will be given of the consideration of the effect of web inertia on lateral web dynamics. This example corresponds to the massless analysis of Section 4.4.

Equations 4.1.2 and 4.1.5 still apply, but the curvature $(\partial^2 y/\partial x^2)_L$ of

Section 4.1 is modified by the ratios of Equations 5.1.31 and 5.1.32. Equation 4.4.1

is the desired specialized form of Equation 4.1.2. The two components of end cur-

vature given by Equations 4.1.14 and 4.1.22 must be modified by multiplying by

Equations 5.1.31 and 5.1.32, respectively. Further substitution exactly as in

Section 4.4 results in the differential equation of motion of the web at the steering

guide:

$$\frac{d^2 y_L}{dt^2} = -\left(\frac{V}{L}\right)(MR_{ro})f_2(KL)\frac{dy_L}{dt} - \left(\frac{V}{L}\right)^2 (MR_{tr}) f_1(KL)y_L + \frac{d^2 z}{dt^2}$$

$$+\left(\frac{V}{L}\right)(MR_{ro}) f_2 (KL)\frac{dz}{dt} + \left(\frac{V}{L}\right)^2 \left(\frac{L}{L_1}\right)(MR_{ro}) f_2 (KL) z \qquad . \qquad (5.2.1)$$

The above equation can be transformed to its transfer function form:

$$\frac{Y_L(S)}{Z(S)} = \frac{\dfrac{T_1^2}{(MR_{tr})f_1(KL)}S^2 + \dfrac{MR_{ro}}{MR_{tr}} K_c T_1 S + \dfrac{MR_{ro}}{MR_{tr}}\dfrac{L}{L_1} K_c}{\dfrac{T_1^2}{(MR_{tr})f_1(KL)}S^2 + \dfrac{MR_{ro}}{MR_{tr}} K_c T_1 S + 1} \qquad . \qquad (5.2.2)$$

Equation 5.2.2 should be quite accurate except for frequencies very close to a

resonance. It must be remembered that the moment ratios are functions of ωT_1, as

well as W_4 and KL. For most situations currently encountered, the moment ratios

are near unity for frequencies of interest, and Equation 5.2.2 reduces to Equation

4.4.4.

    5.3. Region of Validity of Massless Theory. For a given value of W_4, the

moment ratios (Equation 5.1.31 and 5.1.32) approach unity at low frequencies.

When the moment ratios are close to unity until the frequency is somewhat higher

than the cutoff frequency of the control system, the massless theory is valid.

Cases in which the mass of the web is not negligible are rarely encountered

in current practice, but are most likely to be found as steering guides in the metals

industry because of the high density, the long spans required, and the high modulus

of elasticity.

An example of a practical value of W_4 for a steel strip will give an idea of

the significance of the mass. Assume the average stress S_1 of a 60-inch-wide steel

strip to be 2500 psi and its error to be plus or minus three inches. For the value of

nT/AG of 0.0003, Figure 2.4.8 shows that KL must be 0.98 if a slack edge is to be

avoided, for the given y_L/W of 0.05. The required free span is calculated from

the formula for KL:

$$KL = \frac{L}{W} \sqrt{\frac{12\,S_1}{E}} \quad .$$

For this case: $\qquad\qquad KL = 5.32(10)^{-4}L$

or $\qquad\qquad L = 1840 \text{ in.} = 153.5 \text{ ft.}$

If the web speed is 1500 feet per minute (25 feet per second) and the entering

span is 153.5 feet, the entering time constant T_1 is 6.14 seconds. From Equation

5.1.30:

$$W_4 = \frac{(0.283)(60)^2(2.9)(10)^7}{(4632)(6.14)^2(2500)^2} = 0.0271$$

Figure 5.3.1 shows that the moment ratios depart significantly from unity within

the frequency range of interest, because the frequency in radians per second is equal

to $\omega T_1/6.14$ for this case and web guide control systems commonly have cutoff
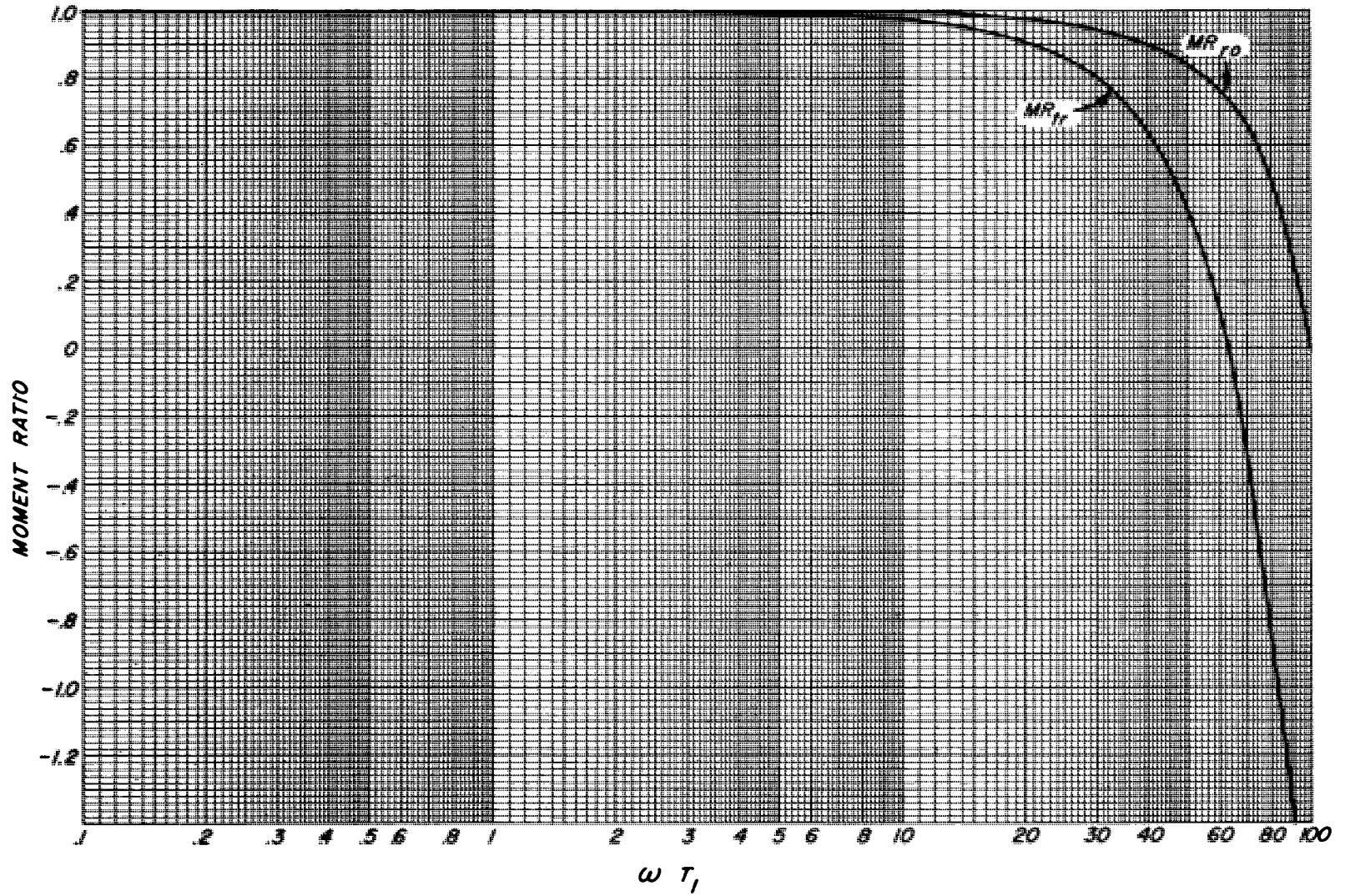
Figure 5.3.1. Moment Ratios for $W_4 = 0.0271$ for Example Problem.

frequencies of around 25 radians per second. Equation 5.2.2 was solved for the special case of a static steering factor LK_c/L_1 of unity. The transfer function for the massless analysis (Equation 4.4.4) is unity at all frequencies for this special case. For the example problem, the transfer function with consideration of mass is also very close to unity for all values of ωT_1 up to 100. Higher frequencies were not studied.

The example demonstrates that the massless theory can be valid even when the moment ratios depart drastically from unity, because of the slow response (compared to the lateral web vibration frequency) of the steering action of the web. No parameter study of Equation 5.2.2 has been undertaken to further establish the conditions of validity of Equation 4.4.4.

Figures 5.3.2 through 5.3.5 show the moment ratios as functions of ωT_1, for different values of KL and W_4. A high modulus of elasticity raises the value of W_4 and lowers the value of KL, while the reverse is true of stress and span length, so that a high value of both W_4 and KL probably would not be encountered in practice. Therefore, the graphs do not show high KL values when W_4 is high.

Moment ratios are shown until they leave the graphs at 100 radians per second or until they become large negative numbers. To avoid confusion, values of the moment ratios which would be on the graphs as the moment ratio goes from negative infinity to positive infinity are not shown. Higher-frequency moment ratios alternately go to negative infinity and positive infinity.
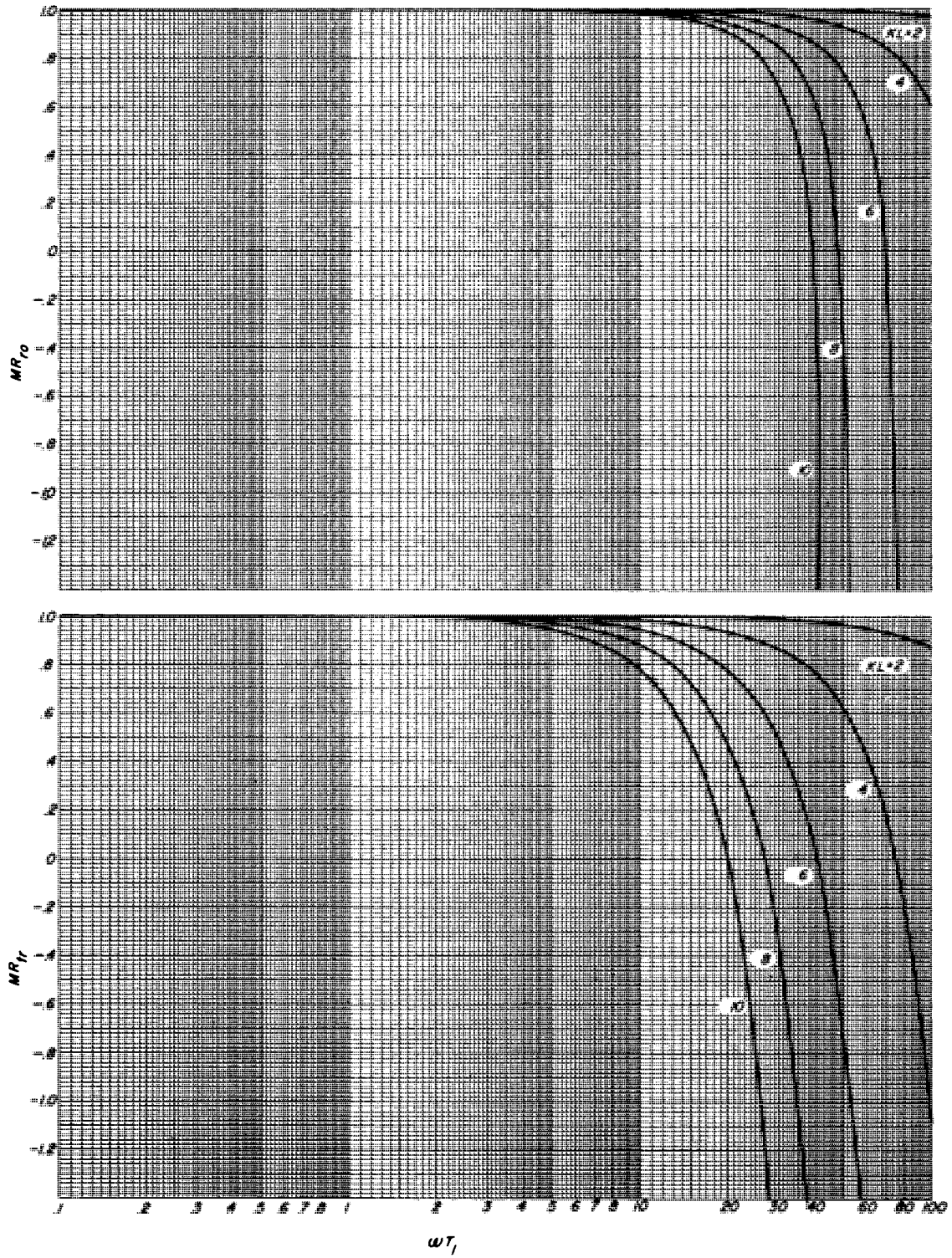
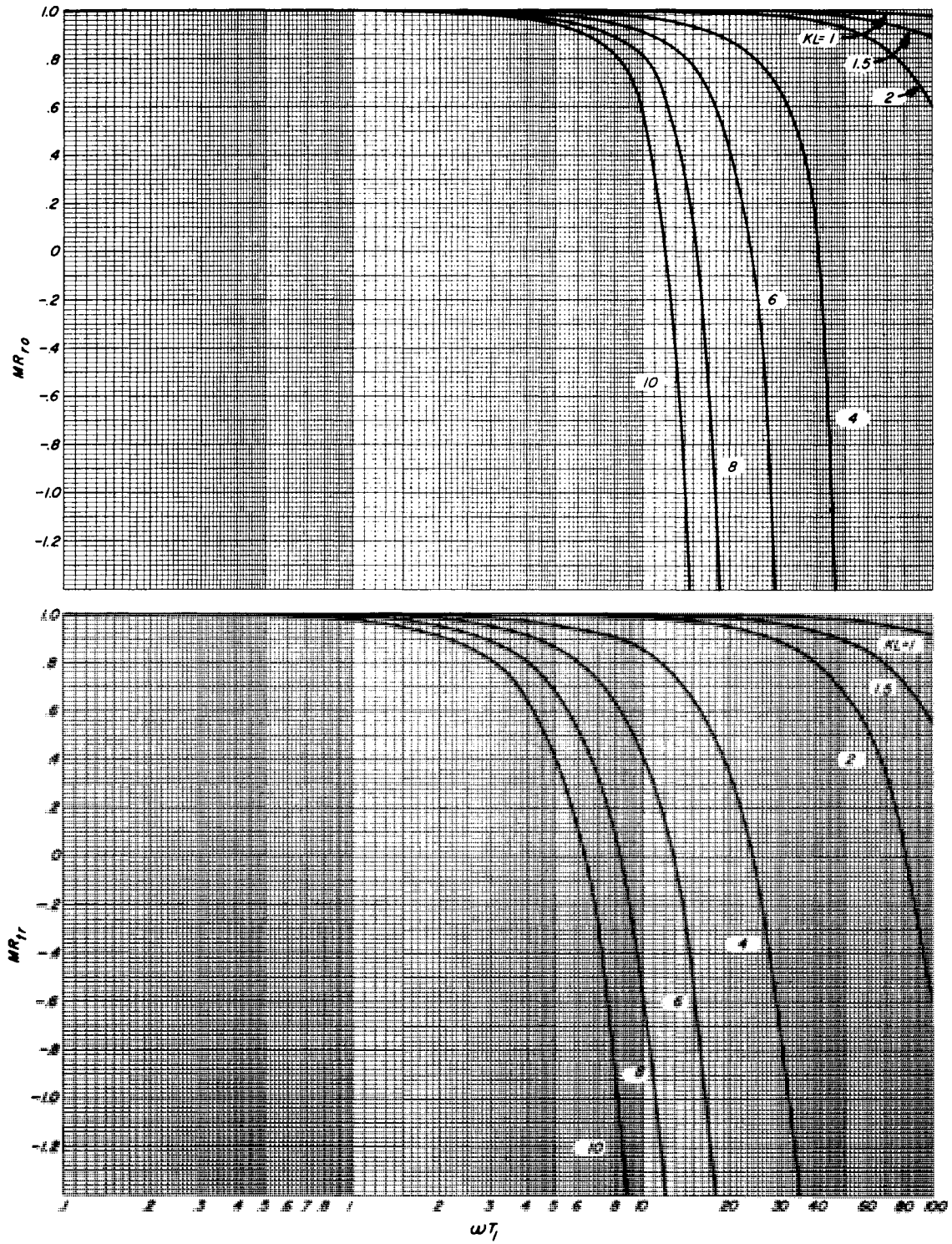Figure 5.3.2. Moment Ratios for $W_4 = 0.0001$.

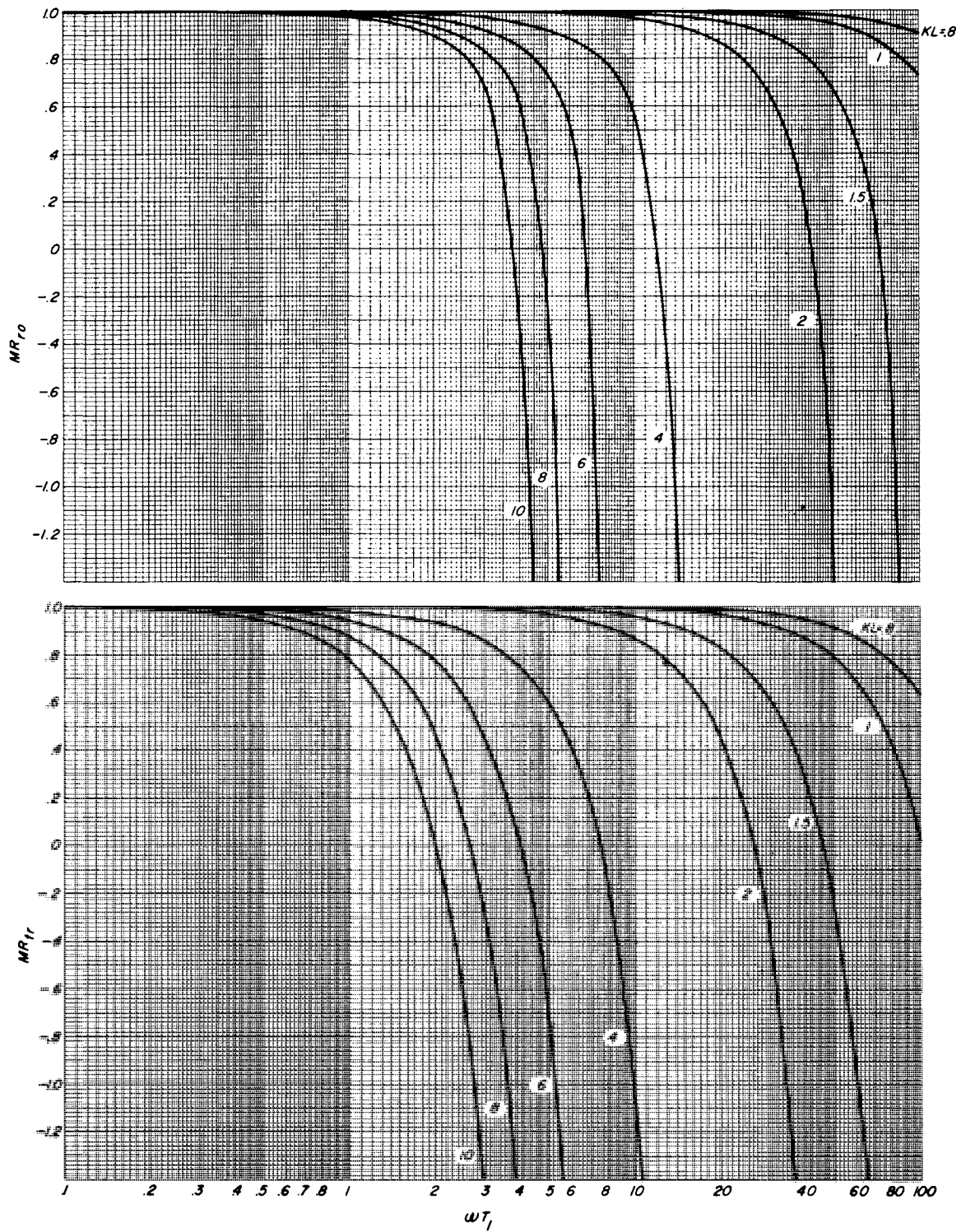Figure 5.3.3. Moment Ratios for $W_4 = 0.001$.

Figure 5.3.4. Moment Ratios for $W_4 = 0.01$.

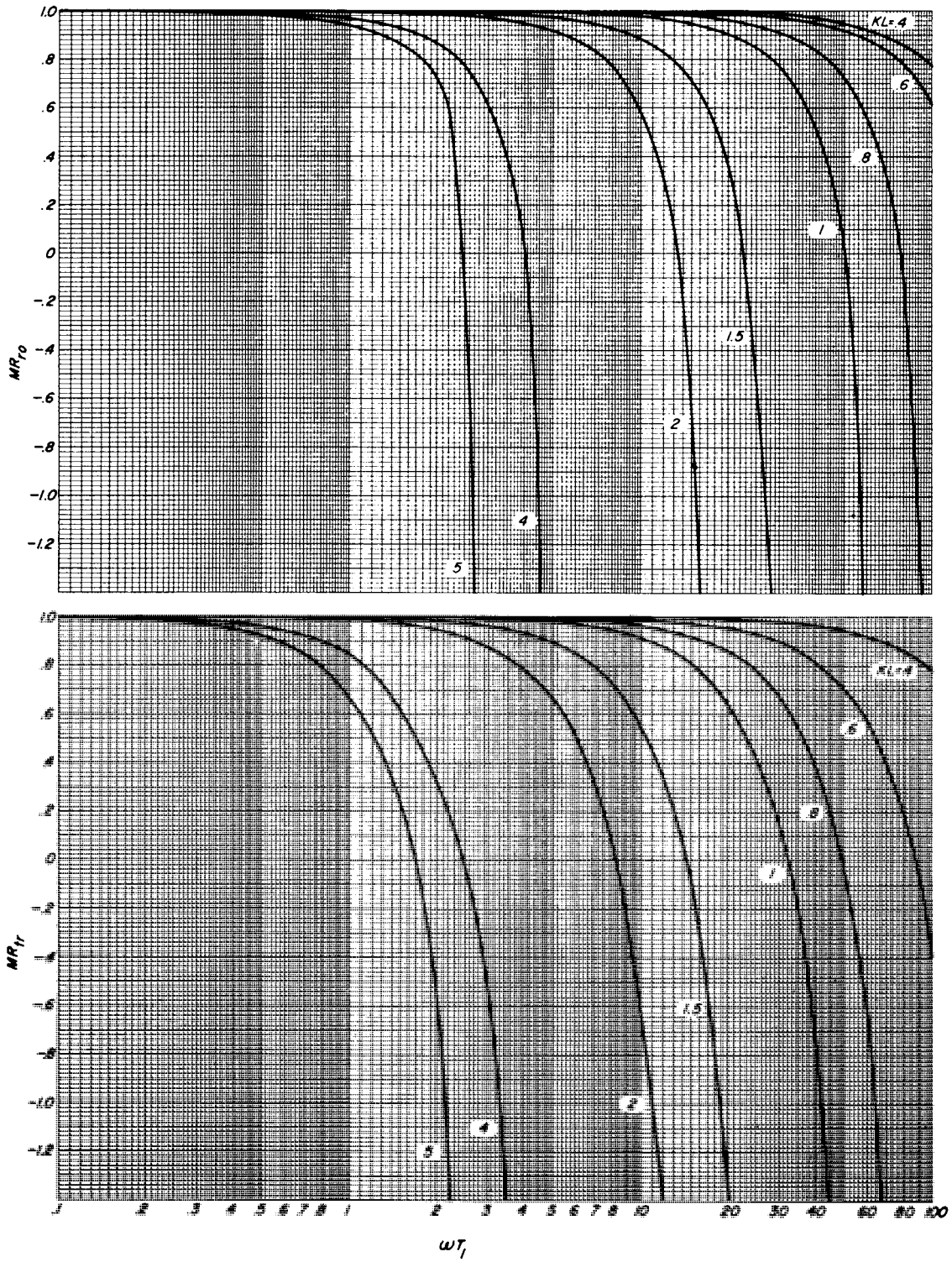Figure 5.3.5. Moment Ratios for $W_4 = 0.1$.

CHAPTER VI

SUMMARY AND CONCLUSIONS

This thesis, because of the extremely limited previous theory, has necessarily been broad. Some subjects, such as the fundamental static theory of Chapter II, have been covered in considerable depth. Certain other subjects have been lightly covered because of limited time or apparent minor importance. But essentially all the thesis after the introduction is completely new material - the foundation of a science which did not previously exist.

The static behavior of a taut moving web between non-parallel rollers was analyzed in Chapter II. Methods were developed for considering a broad range of operating conditions and materials, including anisotropic materials with low shear moduli. Web behavior was found to depend upon the dimensionless parameter KL (or $K_e L$). If $K_e L$ is small (less than unity or particularly if less than 0.6) and the shear modulus low, the static behavior was found to be quite dependent upon the shear deflection parameter nT/AG. Only woven webs are commonly affected significantly by shear deflection in the entering span of a steering guide.

The curvature factor, which is important because it is a factor in the static gain of a web guide, was found to be relatively insensitive to $K_e L$. Figure 2.4.6 shows the curvature factor to lie between two-thirds and unity. The maximum moment, which is necessary for static stress calculations, is shown in Figure 2.4.7 to be quite sensitive to $K_e L$.

The maximum correction permissible if a slack edge is to be prevented is shown in Figure 2.4.8 to also be quite sensitive to $K_e L$. The amount of correction

commonly needed dictates a value of K_eL of near unity. This value of K_eL requires that, for common operating conditions, the entering span of a steering guide for strip steel must often be more than 100 feet long, too long to commonly be practical. Paper and other relatively stiff materials also often demand more span than is available. Therefore, displacement guides must often be used.

The effect on curvature of inertia of a high-speed web was considered in Section 2.5. The effect is negligible in most current practical applications.

Chapter III presented a systematic method of analysis of the dynamics of webs for which the shear stiffness is negligible. The transfer functions of several practical web handling components and configurations were derived. Phase lead was shown to be associated with an understeering guide and phase lag with oversteering. Phase lag occurs between stationary rollers and between a roller and sampling point downstream in the free span.

The more accurate method of dynamic analysis of Chapter IV confirmed the trends found in the simplified analysis of Chapter III, and showed the simplified analysis to give a fair approximation at values of ωT_1 of less than two. The cutoff frequency was found to be well established by the simplified theory. But if K_eL is less than unity and nT/AG is less than 0.001, as is commonly the case, the second-order theory of Chapter IV was found to be necessary for accurate dynamic analysis.

The effect of shear was considered in two sections of Chapter IV. The effect of shear on the dynamic behavior is significant at approximately the same combinations of K_eL and nT/AG as for the static analysis.

In Chapter V a method was developed for modifying the second-order theory of Chapter IV for cases in which the mass of the web cannot be neglected. The conditions for which the massless theory is valid can be determined from the results of Chapter V. In most current practical applications, the mass can be neglected.

6.1. Contributions of Most Significance. From a scientific viewpoint, the significant contributions of this thesis were the establishment of the boundary conditions of a free web span in its static condition, and the subsequent formulation of the theories of dynamic web steering of Chapter IV. These theories should lay a foundation for the solution of problems not covered in this thesis, such as the problem of behavior of a cambered web.

From a practical engineering standpoint, the most significant contribution is probably the analysis of the static behavior of a web, covered in Chapter II. Until this analysis was done, there was no method for predicting the stress induced in the web by a steering guide, the amount of correction possible before a slack edge ensued, the amount of side force required to effect a given correction, or the shape of the guided web. Furthermore, accurate dynamic analysis was impossible until the static behavior was established.

The stress increase in a web due to guiding, which must be known in order to avoid stress conditions that would yield or tear the web, can be found from the static analysis. The maximum induced moment in the web is given, for example, by Equation 2.4.18. The ratio of the actual stress on the outside to the average stress is equal to $(6M + WT)/(WT)$, if a slack edge does not exist.

Figure 2.4.8 shows the amount of correction possible before slackness occurs, if there is no circumferential slippage around the entering roller. The amount of correction possible without causing edge slackness must be known in order to know whether or not the theory of this thesis applies, and in order to avoid buckles and wrinkles caused by slackness.

The normal force at the guide roller caused by the steering of the entering span is given by Equation 2.4.19. The normal force determines the required coefficient of friction between the web and guide roller, and the force required of the guide actuator to steer the web.

The static shape of the guided web is important in certain guide arrangements wherein curvature of the web occurs after the sensing head. Figure 6.1.1 shows an S-wrap or nip guide, which has an angle between the guide roller and the next roller as viewed into the exiting span. The actual web has a residual guiding error which can be found from Equation 2.1.34.

It was once a common belief that the plane of guide roller motion should be perpendicular to the bisector of the angle of the web across the guide. The exiting span would then appear as the exiting span of Figure 6.1.1, with the guide roller and the next roller nonparallel as viewed into the exiting span. This thesis clearly establishes the error of such a practice, because the stress in a proper installation would be evenly distributed at the guide roller, but for the "bisected angle"
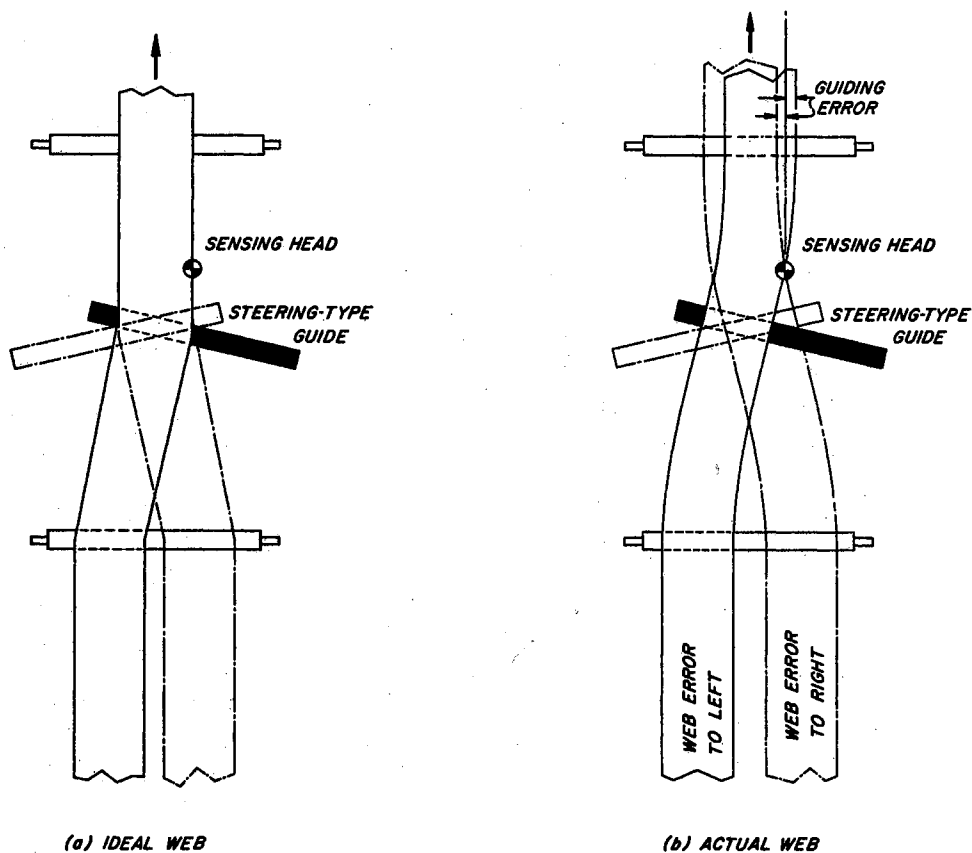

(a) IDEAL WEB   (b) ACTUAL WEB

Figure 6.1.1. Guiding Action on an S-Wrap, Nip, or
"Bisected Angle" Guide.

installation, curvature and stresses would be re-introduced into the exiting span. A guide should satisfactorily effect its correction, then transport the web downstream with no non-symmetrical tension distribution. If the friction is sufficient, such a goal can be achieved with a steering guide with its plane of motion perpendicular to the exiting span, or with a displacement guide.

The static theory can be used to establish tolerances of parallelism between stationary rollers on a process machine, with criteria of stress, edge tautness, or amount of steering, for the given material and operating conditions.

The practicing controls system engineer will probably apply the first-order theory of Chapter III more often than the more complex theory. The first-order theory clearly establishes trends and fairly accurately pinpoints values of ωT_1 of interest in dynamic analysis. The theory is relatively easy to apply to specialized circumstances, as demonstrated in several examples of Chapter III. The comparisons of this thesis between the first-order and second-order theory will provide an idea of the magnitude of the errors involved in the simpler theory.

Use of the second-order theory may become necessary as control systems become more complex. For example, a Type II system, which is quite intolerant of careless dynamic design, might be used advantageously for web guiding. The location of the sensing head in the exiting span, the transfer function for which is given by Equation 4.6.10, and the geometry of a steering guide, which could be analyzed with Equation 4.4.4, could be vitally important.

6.2. Suggestions for Further Study. Several important problems are left unsolved. One problem is the analysis of the static behavior of a guide which experiences more error than the critical correction of Figure 2.4.8. The normal force, maximum moment, and deflection would be obtained from the static analysis. The variable moment of inertia would probably necessitate a numerical solution on a digital computer. An iterative process would probably be necessary, because

it is a boundary value (not an initial value) problem.

The dynamics of a web with a slack edge would be more difficult than most of the problems of this thesis, because of its nonlinear nature. The need for such an analysis is presently questionable, because the slack edge would cause behavior between the second-order theory and the first-order theory of this thesis.

A second important problem which needs study concerns the circumferential friction around rollers, in order to quantify the conditions of moment transfer from one free span to another. Some worthwhile work has been done, following the theory of belt behavior, as presented by Spotts (22), but more exact analysis is needed.

A third important problem is a study of cambered web behavior. The theories of this thesis should be quite helpful in such a study. It is believed that camber is the primary source of error on a metal strip line, and it is important to know how much error reappears at a certain point beyond a guide. Or, stated differently, it is important to know how many guides will be required before the process line is designed and built.

Another problem which should be pursued is the problem of web wrinkling. The edge slackness criteria of this thesis should be helpful, but additional factors are involved. The span length of thin, highly flexible webs is limited because of "necking" and consequent wrinkling. Many factors not yet quantified affect wrinkling.

Special studies are needed of guiding out of a free loop, guiding a web with a sagging entering span, and guiding a web which is partially supported on rollers, such as the example of Figure 1.3.3.

BIBLIOGRAPHY

(1) Adams, D.P., E. R. Schwarz, and Stanley Backer. "The Relationship Between the Structural Geometry of a Textile Fabric and its Physical Properties." Textile Research Journal, Vol. 26 (1956).

(2) Amos, Stephen E. "Web Guiding Control." Machine Design, September, 1951.

(3) Campbell, Donald P. Process Dynamics. John Wiley and Sons, Inc., New York, N.Y. (1958).

(4) Crafts, Curtis S. Lateral Registration Devices for Printing Presses. Canadian Patent No. 474,415 (1951). (Filed December 7, 1949).

(5) Deering, Joseph M. "New Concepts for Automatic Strip Guiding for the Metals Industry." Iron and Steel Engineer Year Book. (1965), pp. 975 - 982.

(6) Dickhaut, Charles A. Sheet Straightener. United States Patent No. 1,634,984 (1927). (Filed December 29, 1925).

(7) Feiertag, Bruce A. "Intermediate Guiding on Steel Strip Processing Lines." Iron and Steel Engineer, September, 1967.

(8) Fife, Irwin L. Web Shifting Apparatus. United States Patent No. 2,797,091 (1957). (Originally filed April 28, 1950).

(9) Ham, C. W., and E. J. Crane. Mechanics of Machinery, Third Edition. McGraw-Hill Book Company, Inc., New York, N.Y. (1948).

(10) Kellogg, Robert M., and Frederick F. Wangaard. "Influence of Fiber Strength on Sheet Properties of Hardwood Pulps." TAPPI Technical Section. Vol. 47 (1964), pp. 361 - 367.

(11) Kouris, Michael, ed. "Winder Drive Power Requirements." TAPPI Special Report No. 432. Technical Association of the Pulp and Paper Industry, New York, N.Y. (1962).

(12) Lorig, E. T. "Automatic Self-Centering Rolls and Pulleys." (Paper presented before 1950 AISE convention in Cleveland, Ohio).

(13) Marhauer, Hans H. "The Dynamics of Web-Tension Measurement." ISA Transactions. Vol. 5, No. 3 (1966), pp. 242 - 247.

(14) Markey, Frank J. "Edge Position Control for the Steel Strip Industry." Iron and Steel Engineer, February, 1957.

(15) Müller, Rudolf. Roll Shifting Device. United States Patent No. 1,982,685 (1934). (Filed December 2, 1932).

(16) Murphy, Glenn. Advanced Mechanics of Materials. McGraw-Hill Book Company, Inc., New York, N.Y. (1946).

(17) Peirce, F. T. "The Geometry of Cloth Structure." Journal of the Textile Institute. Vol. 28 (1937), pp. T45 - T96.

(18) Shelton, John J. "Web Guiding Terminology and Concepts." (Unpublished Fife Corporation Engineering Bulletin E64-8, 1964).

(19) Shelton, John J. "Lateral Dynamics of a Moving Web." (Unpublished M.E. 610 research proposal, Oklahoma State University, 1966).

(20) Snyder, Harvey, Alexander V. Alexeff, and Howard R. Richards. Web Guiding Means. United States Patent No. 3,156,396 (1964). (Filed October 8, 1962).

(21) Sorsen, Spencer L. "Basic Techniques for Controlling Web Position." Automation, April, 1966, pp. 105 - 110.

(22) Spotts, M. F. Design of Machine Elements, Second Edition. Prentice-Hall, Inc., Englewood Cliffs, N.J. (1953).

(23) Timoshenko, Stephen P., and James M. Gere. Theory of Elastic Stability, Second Edition. McGraw-Hill Book Company, Inc., New York, N.Y. (1961).

(24) Wood, George B., Jr. Sheet Guiding Apparatus. United States Patent No. 2,722,415 (1955). (Filed October 25, 1950).

(25) Wright, Gerard C. "How to Make Belts Track." Machine Design, May 11, 1967.

(26) Younger, John E. Advanced Dynamics. The Ronald Press Company, New York, N.Y. (1958).

APPENDIX A

KINEMATICS OF A DOUBLE-SLIDER MECHANISM

A double-slider mechanism is one of the most compact and versatile mech-
anisms for a steering guide. It provides easy adjustment of the instant center of
the guide and its nonlinearity is usually not severe. Its natural adaptability to a
linear actuator is usually an advantage.

A double-slider steering guide as shown in Figure A.1.1 was used for all
tests of steering guides reported in this thesis. Because of the difficulty of direct
measurement of the very small roller angles, the lateral displacement of the slider
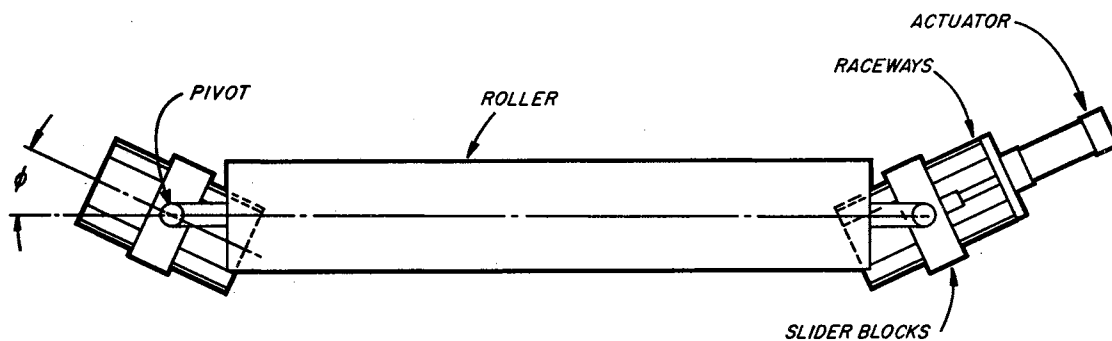was measured and the roller angle was calculated from the double-slider geometry.

Figure A.1.1. Plan View of a Double-Slider Steering Guide.

A.1.1. Relation Between Actuator Position and Roller Angle. The trigonom-
etry and symbols for the derivation are shown in Figures A.1.2 (a) and (b). The
actuator displacement is denoted by d, the ramp angle of the sliders by $\emptyset$, and the
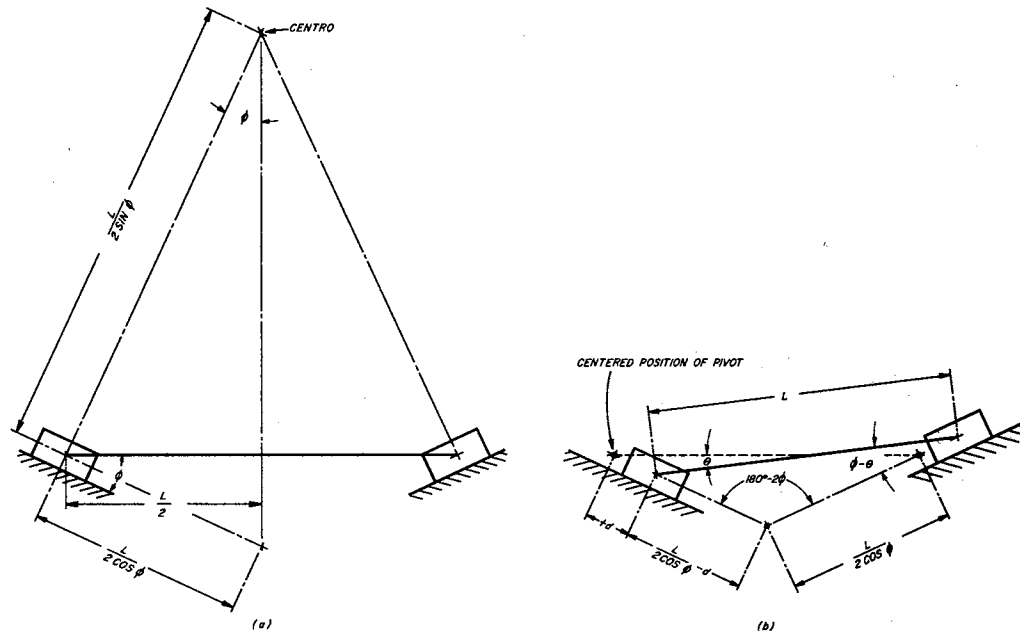roller angle by θ.

171

Figure A.1.2. Geometry for Derivation of Characteristics of a Double-Slider Steering Guide.

The triangle of Figure A.1.2(b) with corners at the slider pivots and the point of intersection of the paths of motion of the slider pivots may be studied with the law of sines:

$$\frac{\dfrac{L}{2 \cos \emptyset} - d}{\sin (\emptyset - \theta)} = \frac{L}{\sin (180° - 2\emptyset)} \quad . \qquad (A.1.1)$$

Because sin (180° - 2∅) is equal to sin 2∅, Equation A.1.1 may be rearranged as

$$\sin (\emptyset - \theta) = \left(\frac{1}{2 \cos \emptyset} - \frac{d}{L} \right) \sin 2 \emptyset \quad , \qquad (A.1.2)$$

or

$$\theta = \emptyset - \arcsin \left[\left(\frac{1}{2 \cos \emptyset} - \frac{d}{L} \right) \sin 2 \emptyset \right] \quad . \qquad (A.1.3)$$
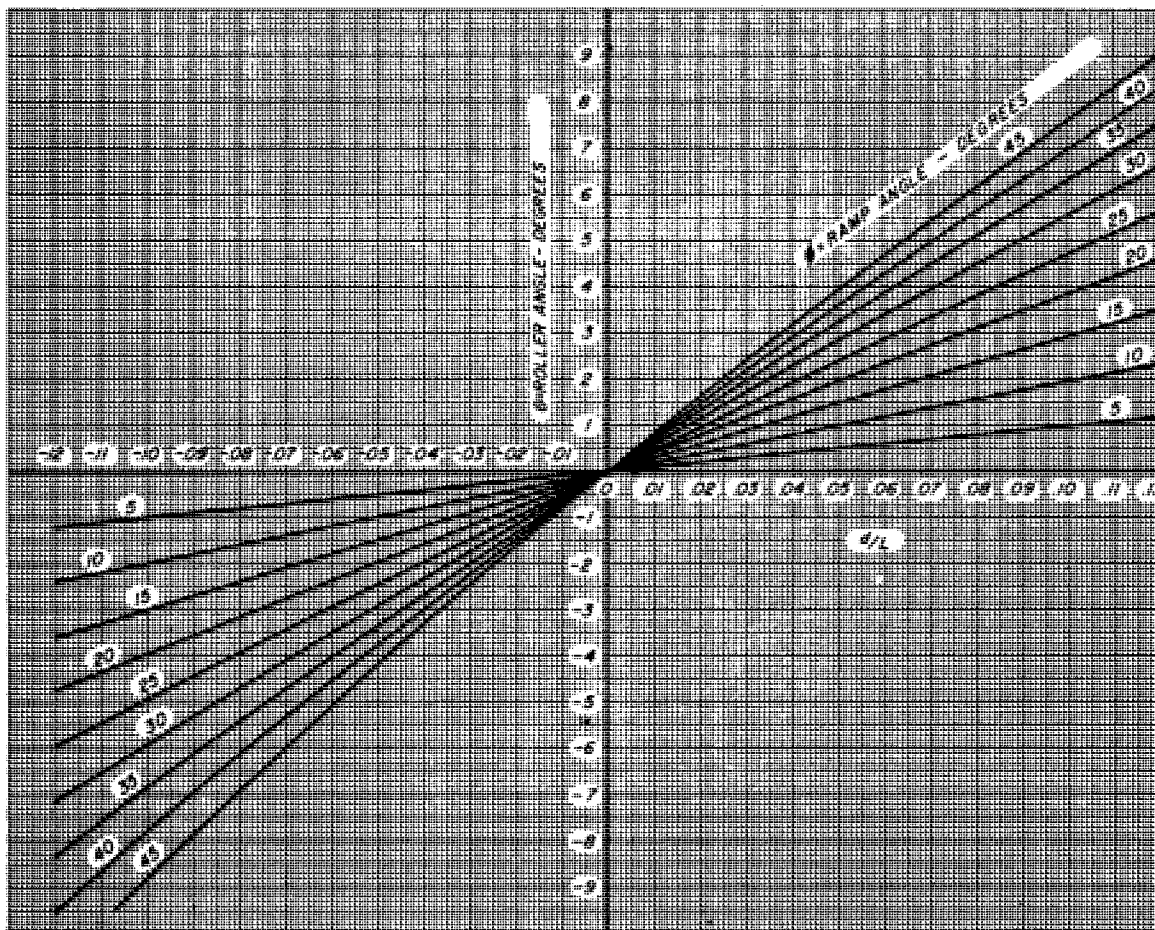
Figure A.1.3. Characteristics of a Double-Slider Steering Guide.

The identity sin 2 $\emptyset$ = 2 sin $\emptyset$ cos $\emptyset$ gives the result

$$\theta = \emptyset - \text{arc sin}\left[(\sin \emptyset)(1 - 2\frac{d}{L}\cos \emptyset)\right] .$$ (A.1.4)

Equation A.1.4 is plotted in Figure A.1.3. Note the nonlinearity at large ramp angles.

The gain, or the slope of a curve defined by Equation A.1.4, is

$$\frac{d\theta}{d(d/L)} = \frac{\sin \emptyset \,(2 \cos \emptyset)}{\sqrt{1 - \sin^2 \emptyset \,(1 - 2\frac{d}{L}\cos \emptyset)^2}} .$$ (A.1.5)

The gain near the center of the stroke of the actuator may be obtained by letting

d/L be zero in Equation A.1.5 and applying the identity $(1 - \sin^2 \emptyset)=\cos^2 \emptyset$:

$$\left.\frac{d\theta}{d(d/L)}\right|_{o} = 2 \sin \emptyset \qquad . \qquad\qquad (A.1.6)$$

Table II shows solutions of Equation A.1.4 for the steering guide used for

tests reported in Section 2.2. The spacing of the slider pivots, L in Equation

A.1.4, was 13.75 inches. The raceway angle $\emptyset$ was 15 degrees.

TABLE II

ROLLER ANGLES OF TEST STEERING GUIDE FOR
L = 13.75 INCHES AND $\emptyset$ = 15 DEGREES

d – inches	θ – radians
-1.50	-0.05697
-1.00	-0.03787
-0.50	-0.01892
-0.25	-0.00945
-0.10	-0.00378
-0.05	-0.00189
+0.05	0.00188
+0.10	0.00375
+0.25	0.00937
+0.50	0.01876
+1.00	0.03737
+1.50	0.05604

VITA

John Jarvis Shelton

Candidate for the Degree of

Doctor of Philosophy

Thesis: LATERAL DYNAMICS OF A MOVING WEB

Major Field: Mechanical Engineering

Biographical:

Personal data: Born near Elmore City, Oklahoma, May 16, 1935, the son of Marvin C. and Ruth E. Shelton.

Education: Attended grade school at the rural schools Love and Liberty in Garvin County, Oklahoma; graduated from Pauls Valley High School in 1953; received the Bachelor of Science degree from the University of Oklahoma, with a major in Mechanical Engineering in June, 1957; received the Master of Science degree from the Chrysler Institute of Engineering, with a major in Automotive Engineering, in June, 1959; received the Master of Science degree from the Oklahoma State University, with a major in Mechanical Engineering, in May, 1966; completed requirements for the Doctor of Philosophy degree in July, 1968.

Professional experience: Worked in the Central Engineering Division of Chrysler Corporation from June, 1957, through July, 1959, principally on suspension kinematics and stability and control theory; worked for Fife Corporation in Oklahoma City from September, 1959, to the present, primarily on hydraulic and mechanical components for control systems, analysis and testing of control systems, and web handling theory; presently Manager of Research and Development for Fife Corporation.

Professional societies and achievements: Member of the American Society of Mechanical Engineers; holder of two United States patents for web guiding equipment.